Más allá del prototipado rápido: automatización robótica de impresión 3D para la construcción

Beyond Rapid Prototyping: automation of robotic 3D printing for construction

TESIS DOCTORAL

Adolfo Nadal Serrano

Departamento de Ingeniería del Software e Inteligencia Artificial
Facultad de Informática
Universidad Complutense de Madrid

Febrero 2017

Más allá del prototipado rápido: automatización robótica de impresión 3D para la construcción

Beyond Rapid Prototyping: automation of robotic 3D printing for construction

Memoria que presenta para optar al título de Doctor en Informática
A dissertation submitted in partial satisfaction of the requirements for the degree Doctor in Computer Engineering

Adolfo Nadal Serrano

Dirigida por los Doctores
Directed by Doctors

Juan Luis Pavón Mestras
Óscar Liébana Carrasco

Departamento de Ingeniería del Software e Inteligencia Artificial
Facultad de Informática
Universidad Complutense de Madrid
Febrero 2017

Acknowledgements

This thesis has been a long, winding road that I have been lucky enough not to travel alone. This adventure began more than five years ago, during my stay at Columbia University. There, I had the chance to meet countless people of different origins, backgrounds, and interests, who influenced me in a way that I was still unable to even grasp. I became increasingly interested in emergent systems and the underlying logic behind social and group behaviors and dynamics. I came to understand the interrelated importance of both the individual and their social environment, and how each influences one another. From a technical point of view, I developed inestimable programming skills that allowed me to experiment and simulate such behaviors from a design point of view, in an attempt to understand the formal implications of such a strong underlying logic structure. Thanks to my architectural background, I was familiar with urban dynamics, and how small technological devices or advancements modify our behaviors, and mediate our environment in unforeseeable fashions. Although my first approach to the present study was initiated by simulating an agent-based urban system, I finally realized that holistic systems or global approaches are based upon very small, almost invisible factors and elements which have the beauty to intertwine and tangle with one another in unpredictable ways. As a result, I began to look deeper into these objects, realities, elements, and devices. I understood that, despite my initial reluctance to admit it, probably an ATM machine or a sign would condition our use and perception of the space more importantly than urban planning as such. Whether top-bottom approaches are strongly embedded in our current DNA system, it is obvious that the dynamics that rule our behavior cannot be thereby reduced or simplified. I decided to look into new ways to influence the system from within by offering a relatively insignificant contribution to the architectural and construction field. Modifying the way we build would indeed shake the state of things in the Real Estate market and probably force a different industrial approach to a certain degree. Looking into new ways to utilize the 3D printing technology and its applications seemed a perfect way to do it.

This process could not have taken place without the many people that have collaborated in different ways, supported by diverse means, and given incredibly creative suggestions, insightful comments and useful ideas without which this thesis would have been impossible. I would like to thank Mitchell Joachim for being especially patient and providing eloquent thoughts on the appropriateness –or not- of tackling issues in holistic ways. Mitchell has been crucial at letting me understand the influence of small devices in the behavior of whole systems in a bottom-up approach, an issue that has become essential to the development of the present work. I would also like to thank Edward Keller and Roland Snooks for their inspirational and enlightening work regarding multi-agent systems and their architectural and design intent.

Juan Pavón has been my patient, organized and demanding Director since the very beginning. Juan tried –unsuccessfully- to lead me to complete my thesis on the Self-Organizing City –a work that I would like to develop further as a life hobby, and that you are not reading because of its complexity and reach. Despite the fact, Juan has been a consistent support, and managed to re-orient the work to what it is today, a complete re-interpretation of one of the thousands of close-to-insignificant issues that constituted the first thesis on the city. I would also like to thank Juan for his support, comments, and help in writing articles, an aspect that he has helped me improve. Oscar Liébana has been also partially responsible for the thesis as it is. Oscar joined the Thesis as a co-director nearly one year ago, when 3D printing became one of its main issues. Indeed, Oscar has been also an outstanding Director, colleague, and friend.

Although the Thesis would have benefited from even more complex and expensive devices, materials, and developments, none of the current work would have been possible without the financial support from Naotech Solutions, S.L. Naotech is a small start-up based in Cantabria, Spain, that aims at the development of new technological solutions for large-scale 3D printing. Mainly focusing on R&D projects, Naotech founded the OS3D Chair at the Universidad Europea, where most of the work was developed and owns the copyright of some of the work hereby included. I would like to thank Daniel Bustamante and Guillermo Baraja for their constant support, understanding, and interest. Guillermo Baraja has become a very good partner and a better friend. I am looking forward to keeping the good work and I am sure that we will obtain important results in the near future.

Working on such an interesting project is indeed an every-day challenge, time investment, and personal bet. Being surrounded by the best team is thus crucial to the successful fulfillment of the labor. Again, the present Thesis can only exist thanks to the hard work, resilience, and persistent good mood of the human team behind the scenes. I cannot thank Hugo Cifre and Eduardo González enough for their priceless contribution and their unconditional involvement in the Thesis' project. Hugo has, in addition, developed the majority of the Processing applet for the material optimization algorithm. Eduardo has provided exceptional expertise in FDM printing and has contributed to the adaptation of the technology to robotic arms for the proof of concept herein presented. Also, I would like to show my appreciation to Vicente Soler for making me push my technical boundaries to limits I would not have explored otherwise. I would have probably not gotten into industrial robotics without his meaningful influence.

It is hard to describe the importance of my family at all levels. They are not only responsible for what I am today, but keep pushing me to become a better version of myself. There are simply no words to say what they mean to me. Jose Mari, you are a guiding light for me and anyone around you. You are kind, smart, and pleasant, and have always the correct solution. Carmen and Mercedes, thank you for your impulsiveness, patience, and jolliness; they are indeed a balance for my stubbornness and harshness. Mum and Dad, thanks for bringing me to life and supporting me unconditionally each and every day of my entire life. I cannot express enough my gratitude for what you have done for me. Grandma Milagros, I can finally tell you that I am done with the Thesis, so that you do not have to worry anymore. Thank you for your love and care all these years, I hope you are proud of what you have initiated.

I would also like to put into words my immense gratitude to Cristina de Cea and her family, who have embraced me from the first day we met. Cristina has suffered the process of writing the Thesis probably more than anyone else, and has always done so with a precious, enthusiastic smile on her face. I want to thank you for the long writing days and even longer nights, and for giving me the distance and perspective I needed so many times, and that I was unable to get. Thank you also for being the harmonic counterpoint to my numerous eccentricities.

Abstract

Additive Manufacturing was first developed more than 20 years ago. Despite this fact, it has remained encapsulated as a Rapid Prototyping technique until its eruption and subsequent exponential growth, which it has experienced in the last 10 years, being considered, as a consequence, one of the most disruptive technologies to shape the future of fabrication.

Rapid prototyping techniques have already reached the general public, causing new fabrication and distribution models to arise at many levels. Nonetheless, many professional applications of 3D printing stay unexplored. The thesis focuses on 3D printing for construction, which is stagnated at an early stage of development, especially regarding materials and oversized final products. Some efforts have been carried out in this direction, aiming at increasing size, speed, or materials. The current research discusses all three, within a globally interrelated systemic framework that serves as basis for the development of industrial, robot-based Additive Manufacturing applications. Thus, it is possible to overcome the current limitations of 3D printing technology in terms of its applications in the AEC industries, accounting for tool versatility, materials, finish quality, and environmental issues.

The thesis has a two-fold approach: on the one hand, it offers a comprehensive summary of the architecture and construction industries, where the proposed technology and methods would acquire their outmost relevance. Sufficient data is provided as to demonstrate the need for innovation in the AEC sector, especially regarding solutions related to optimized construction techniques and material usage. A more in-depth perspective of the Spanish market is provided, as a context for the industrial scope of the methods and apparatus provided in the present thesis. On the other hand, the document presents an innovative methodology that aims at overcoming the aforementioned limitations, involving an approach for the use of materials and their influence on real-scale products through easy-to-use software that allows for the control of six-axis robotic arms in order to print big-scale parts. In this sense, a series of test cases showing the integration of a design-to-fabrication process combining Integrated Robotic Systems (IRS) and Additive Layer Manufacturing (ALM) techniques are discussed and demonstrated through mock-up production models. A structure-based approach to material optimization and smart infill patterning is introduced and integrated within the main software component.

Still today, the design to fabrication workflow implies a series of well-differentiated, quasi-independent steps. Design, vastly reduced down to modelling operations at early conceptual stages, needs to constitute an early binding of ideas, form, and functionality, which may compromise the full fabrication process. Although not thoroughly described as such, modelling plays a crucial role in manufacturing, and must be tackled successfully in order to ensure the appropriateness of the resulting design's object. Furthermore, models need to comply with fabrication standards in terms of their form, shape, and geometrical properties, which utterly relate to the way in which they will be physically produced. Finally, the fabrication process itself has a series of requirements that need to be taken into account, as well as limitations and restrictions. These three steps are normally detached from one another, causing erroneous designs or failure during the production process, yielding undesired situations at both industrial and end-user levels. 3D printing does not differ from other fabrication processes in this sense, making it necessary to study a compelling process that combines all stages of the design-to-production process. These processes are studied and analyzed prior to the presentation of a solution that aims at the standardization of layer-based 3D printing. The present thesis offers a cohesive solution to this specific problem through a series of algorithms, validated through a plugin for the wide-spread 3D modelling application Rhinoceros –which allows to take advantage of its geometry kernel in order to empower, inform, and automate oversized additive fabrication with industrial, six axis robotic arms in an iterative manner.

From the perspective of the architectural implications of the use of 3D printing technologies for construction purposes, the thesis emphasizes technical aspects rather than speculative design solutions, which are meticulously explored in the state of the art section. It is thus preferred to take a pragmatic viewpoint from where to justify and explain the need for innovative construction solutions, as well as their possible application fields, advantages, disadvantages and economic and societal consequences in order to provide a theoretical disciplinary discourse. The software introduced previously marks the technological instance to this discussion. More specifically, the software implies a revolutionary construction workflow

through a potential robotic automation of construction procedures –such as raising structural components, walls, or inner partitions- thanks to a safe, controlled, and foreseeable methodology. As a consequence, construction labour would eventually be re-qualified, and the construction sector would benefit from the ability of adding extra value at no extra cost –from a geometrical point of view, this possibility would enable new management and control solutions. Additionally, safety would also be positively affected, as well as the environmental aspects of traditional construction through the introduction of decrease material consumptions, the use of local and renewable energy to feed machine operation, and a renewed energy in material science. In summary, the AEC industries could potentially gain new inertia and experience an unexpected growth through the cascading effect produced by the irruption of this new methodology and its underlying technology.

Resumen

La fabricación aditiva se desarrolló por vez primera hace más de 20 años. A pesar de este hecho, se ha mantenido encapsulada y aislada como una técnica de prototipado rápido hasta su eclosión y su crecimiento exponencial subsiguiente, experimentado en los últimos 10 años. Como consecuencia, la fabricación aditiva se considera una de las tecnologías más disruptivas del siglo, capaz de dar forma al futuro de la fabricación.

Las técnicas de prototipado rápido ya han llegado al público en general, permitiendo la emergencia de nuevos modelos de fabricación y distribución a muchos niveles. No obstante, muchas aplicaciones profesionales de la impresión en 3D están aún por explorar. La tesis se centra en la impresión 3D para la construcción, que se encuentra estancada en una etapa temprana de desarrollo, especialmente en lo relativo a materiales y productos finales de gran tamaño. Algunos esfuerzos se han llevado a cabo en esta dirección, con vistas a aumentar la capacidad de la tecnología en cuestiones de tamaño, velocidad, o variedad de materiales. En la presente investigación se analizan los tres ámbitos, dentro de un marco sistémico y que sirve como base para el desarrollo de aplicaciones de fabricación aditiva con fines industriales, basados en el empleo de robots de seis ejes. Por lo tanto, es posible superar las limitaciones actuales de la tecnología de impresión 3D en términos de sus aplicaciones en la industria de la arquitectura, ingeniería y la construcción (AEC), lo que representa la versatilidad de la herramienta, materiales, calidad de acabado, y las cuestiones ambientales que dicha tecnología implica.

Por tanto, la tesis tiene un doble enfoque. Por un lado, ofrece un amplio resumen de las industrias de arquitectura y construcción, en las cuales la tecnología y los métodos propuestos adquieren su mayor relevancia. Se proporcionan datos concluyentes para demostrar la necesidad de innovación en el sector AEC, especialmente con respecto a soluciones relacionadas con la optimización de las técnicas constructivas y el consumo de material. Asimismo, se proporciona una perspectiva más profunda del mercado español, como un contexto para el análisis y la aplicación de ámbito industrial de los métodos y herramientas descritos en la presente tesis. Por otra parte, el documento presenta una metodología innovadora que pretende superar las limitaciones mencionadas anteriormente, la cual implica un enfoque sobre el uso de materiales y su influencia sobre los productos a escala real a través de un software fácil de usar que permite el control brazos robóticos de seis ejes con el fin de imprimir piezas de gran escala. En este sentido, una serie de casos de prueba muestra la integración del proceso de diseño a la fabricación mediante la combinación de los sistemas robóticos integrados y la manufactura por estratificación; técnicas que se discuten y se manifiestan a través de modelos de producción. Un enfoque basado en la estructura para la optimización de materiales y patrones de relleno inteligente es introducido e integrado en el componente principal del software propuesto.

Todavía hoy, el diseño del flujo de trabajo de fabricación implica una serie de etapas bien diferenciadas, cuasi-independientes en la práctica. El diseño, reducido en gran parte a las operaciones de modelado en etapas tempranas conceptuales, tiene que constituir un primer enlace de ideas, forma y funcionalidad, lo que puede comprometer el proceso de fabricación completo. Aunque no se describe a fondo en el documento como tal, el modelado juega un papel crucial en la fabricación, y debe ser abordado con éxito con el fin de garantizar la idoneidad de objeto del diseño resultante. Por otra parte, los modelos tienen que cumplir las normas y requisitos de fabricación en cuanto a su forma y las propiedades geométricas, que se relacionan de modo coherente con la manera en que van a ser producidos físicamente. Por último, el proceso de fabricación en sí tiene una serie de requisitos que deben tenerse en cuenta, así como sus limitaciones y restricciones. Estos tres pasos normalmente se tratan separadamente, causando diseños erróneos o fallos durante el proceso de producción, y produciendo situaciones no deseadas, tanto a nivel industrial como para el usuario final. La impresión en 3D no se diferencia de otros procesos de fabricación en este sentido, por lo que es necesario un estudio de un proceso que obliga a combinar todas las etapas del proceso de diseño a la producción. Estos procesos se estudian y se analizan para proponer una solución que tiene como objetivo la normalización de la impresión 3D estratificada para la construcción. La presente tesis ofrece una solución coherente a este problema específico a través de una extensión de la aplicación de modelado 3D Rhinoceros, aprovechando su núcleo de geometría con el fin de

capacitar, informar y automatizar iterativamente la fabricación aditiva de gran tamaño con brazos robóticos industriales de seis ejes.

Desde la perspectiva de las implicaciones arquitectónicas de la utilización de tecnologías de impresión 3D para fines de construcción, la tesis hace hincapié en los aspectos técnicos en lugar de soluciones especulativas de diseño, las cuales son exploradas meticulosamente en el estado de arte. Así pues, se toma un punto de vista pragmático, desde donde justificar y explicar la necesidad de soluciones innovadoras de construcción, así como sus posibles campos de aplicación, ventajas, desventajas y consecuencias económicas y sociales con el fin de ofrecer un discurso disciplinar teórico coherente. El software introducido previamente constituye la vertiente tecnológica para esta discusión.

Más específicamente, el software implica un revolucionario flujo de trabajo de construcción a través de una potencial automatización robótica de procedimientos rutinarios de construcción –tales como levantar componentes estructurales, paredes o tabiques interiores, u otros elementos de relevancia dentro de la "obra gruesa"- gracias a una metodología segura, controlada y previsible. Como consecuencia, la mano de obra de la construcción se beneficiaría eventualmente de una recualificación, y el sector de la construcción ganaría la capacidad de agregar valor añadido sin costo adicional. Por ejemplo, desde un punto de vista meramente geométrico, esta posibilidad permitiría nuevas soluciones de gestión de la complejidad y control en obra relacionadas tanto con el replanteo como con la propia ejecución. Además, la seguridad también se vería afectada positivamente, así como los aspectos ambientales de la construcción tradicional a través del descenso en el consumo de material, la introducción de energía local y renovable para alimentar el funcionamiento de la máquina y un renovado impulso en la ciencia de los materiales. En resumen, las industrias AEC podrían potencialmente ganar nueva inercia y experimentar un crecimiento inesperado a través del efecto en cascada producido por la irrupción de esta nueva metodología y su tecnología subyacente.

Index

Chapter 1

Introduction

This chapter explains briefly the overall thesis' context, establishing its main focus. The chapter ends with a description of the document's structure and content.

1.1. Context

The thesis arises from the combination of two main interests: architectural design and technology. After some years devoted to the research and development of an increasing interest in complex architectural forms, I realized the need for a more formal agenda and an approach focused on pure construction issues. My personal experience working at a variety of non-standard projects for Toyo Ito & Associates raised the question of the importance of a system-oriented methodology for the ideation and development of design projects. These first notions were then supported by the numerous projects that I had the chance to work on and direct at UNStudio van Berkel & Bos, where the awareness of diagram-driven architecture was increasingly present. The systematic work carried out at the Netherlands-based office turned out to crystalize through a number of issues. In the first place, it became clear that setting up an underlying structure for the guidance of projects were not only a necessity, but an extraordinary tool for increasing project quality both in the initial analysis phases and towards the full deployment of the architectural design within the urban context. Second, it made clear that the current modus operandi in architecture lacks consistency and principles that could be directly implemented as guidelines throughout different projects and in order to achieve a systematic holistic approach. Finally, these whole system needed to be translated into actual, design "objects" or "realizations". The design had to communicate all the previously analyzed matters as well as a large amount of thereby related information, such as societal implications, economic issues, sustainability aspects, geometry constraints, and construction concerns.

The present research finds its place precisely at the intersection of the last two. On the one hand, the thesis aims to respond to a need for understanding architectural geometry from a computational and design point of view. On the other, it intends to find an answer to the intricate questions that arise when dealing with the physical realization of complex architectural objects from an innovative perspective that ultimately seeks to question the adequacy and appropriateness of current construction methods –especially when dealing with a world-wide scenario of exponentially increasing complexity. To a certain extent, the thesis emerges from the continuous investigation of rare and complex architectural forms and the impossibility to successfully address their fabrication or construction by traditional means or the most common available tooling. Especially in the Spanish construction market, which remains stagnated in a hindered state due to the pressure of vendors', fabricators', and developers' lobbies alike, it seems right to propose new design and fabrication means with the potential to radically affect its current status quo. The

so-called “construction bubble” triggered an unprecedented growth of the real estate market, which in turn resulted in a diminished quality of the building product as such –in other words, the incredibly active market would be able to sell almost any product, regardless of its quality, qualification, and location. As a consequence, the wealth created by the vast monetary flow stemming from the market’s star product –mortgage- would not only not help, but paradoxically have a negative impact on the product quality itself.

The scarcity of innovation at a construction level is plausible in the housing stock built in the last 15 to 20 years in Spain, especially since this country was set to enter the Euro in a globalized European market. Spain, while being one of the most industrialized countries in the world, needed to boost its macroeconomic figures to comply with the strict and restrictive European demands. Although the real estate crisis has certainly had unpredictable consequences of unparalleled magnitude, it might be argued that it is an opportunity for research and development of new, previously unforeseen approaches to the construction industry as a whole. In fact, several developers and construction companies are beginning to look into new construction methods, inhabitation models, and design paradigms. Concepts such as prefabrication are beginning to not only gain wide acceptance, but to be considered of increasing relevance to the market itself. In fact, many companies deem prefabrication to be the one and only way to become competitive in the new post-crisis paradigm, where construction times, efficiency, safety, and pre-construction control are mandatory requirements for a successful business model.

In addition to the real estate market, we have witnessed a boost in the creativity of architects regarding non-standard projects. Possibly fostered and maintained by East-Arabic countries, architects have been able to arise new geometrical and building management methods, such as algorithmic design and BIM (Building Information Modeling). Computational design methods and parametric methodologies shape intensely the body of the present thesis on the geometry and algorithmic side. On the contrary, the influence of the proposed work on BIM and construction management is considered as a side-effect that would eventually need to be incorporated into the whole workflow.

As a consequence, the business needs to respond to a complex network of relationships ranging from economic and financial issues to technical or social facts, including all sorts of aspects, namely construction and fabrication methods, new materials, design software, automation capabilities, and many others. The building industry needs to tackle an augmented level of information while achieving the highest quality standards within a highly constraint time frame. 3D printing has a certain potential to respond to a significant number of these issues, as it combines the ability to create otherwise unachievable results in terms of geometry, as well as a high degree of automation and versatility.

As explained in the following sections, the thesis exposes the benefits of 3D printing for construction, a method for its standardization, and a software-hardware apparatus that would enable such solution. Furthermore, a technological demonstrator is provided in form of a software package that merges the whole design-to-production workflow into a single process. Finally, material tests are exposed that look at demonstrating the benefits of smart infill pattern designs and the possibilities of integrating structural capacities into the whole fabrication system. The thesis covers, thus, a whole method and apparatus for a comprehensive 3D printing model for construction in an attempt to rethink the construction market from a technological point of view. The introduction of this technology would have clear positive effects in terms of construction forms, financial feasibility, risk management, material and waste sustainability, not to mention an exceptional innovation vector. Design proposals of speculative nature are intentionally left aside. It is not the purpose of the author to provide ideas or thoughts about possible implementations of the technology at a building design level or similar, although some are mentioned throughout the text. These are left for the reader’s imagination and are considered a sheer consequence of the development of the technology exposed in the thesis.

1.2. Objectives

The thesis pursues a very bold aim: to demonstrate the need and possibility for an innovative approach towards the democratization of real scale 3D printing processes as fabrication methods and their implication for real-scale applications, especially in the AEC sector. As a response to both the theoretical aspects and practical experiences gathered above, the thesis aims to offer a compelling solution to various issues, which are listed here for convenience:

- Propose critical thoughts and definitions of a new architectural and construction paradigm, as well as their implications for the construction sector, as explained in chapter 3.
- The development of a system that includes and responds to the lessons learnt from the case studies and the critical aspects of the construction sector:
    - The definition of an integrated AM method for construction towards the standardization of 3D printing construction processes.
    - The integration of platforms and their implications on the model definition mentioned above.
    - The development of a technological demonstrator that implements a software-hardware integration showcasing the mentioned examples of integration.
    - Proposals for a smarter use of geometry and the optimization of material and the consideration of systemic environmental issues through structural infill patterns.
    - Opportunities for material sustainability regarding:
        - The use of local materials and derived energy savings
        - The development of new materials, composites, and bio-materials
        - The use of local and/or renewable energy sources.

1.3. Methodology

As said above, the democratization process proposed in the thesis can relatively easily be applied to construction in a near future. Hence, current fabrication methods are carefully studied, then conclusions are thereby portrayed as to what technologies and methodologies may be implemented. Both theoretical and practical arguments are provided, drawing attention to a critical analysis of the overall context of the proposed methodology and its consequences on the industry it affects. A technological demonstrator is presented in order to prove both the proposed methodology as systemic background and its actual implementation as hardware and software. As a result, actual tests are completed in order to engage in each aspect of the overall design: (i) the method is proven through a software platform developed ad-hoc for this specific purpose; (ii) the materiality aspects are verified by means of both an innovative algorithm and destructive material tests; (iii) and hardware is developed to comply with the need to confront actual printing requisites.

These engage in a two-fold manner with (i) a novel integrative design-to-production approach that seeks to prove the feasibility and pertinence of a standardization process in automated construction on the one hand; and (ii) with a broader spectrum of construction technologies and solutions in order to enable further design capabilities and fabrication techniques that seek to put the excessive use of “traditional” means into question. The method is described as follows:

- First, an operational framework for the use of advanced fabrication techniques involving design-to-production automation is proposed. This framework sets out the employment of robotic arms for construction, and their appropriateness as convenient tools for large-scale 3D printing. In short, a paradigm shift is proposed.
- Second, this framework is tested through an ad-hoc development of a plugin for the control of 6-axis robotic arms within the Rhinoceros environment. This software development is, as said above, an innovative, nonexistent tool in the market. The software eases the employment of robotic arms and intends to penetrate the building industry through a standardized workflow.
- Third, an ad-hoc printing end effector is provided for the FDM printing process implied in the previous step. The tool is used as a proof of concept for the design of an affordable, open-source, off-the-shelf plastic nozzle. Hardware and software are specific developments using standard, yet reliable electronic components.

- Fourth, big parts are produced as proof of concept and tested against various stress types using different materials. Materials include regular PLA and ABS, as well as composites using plastic matrices with various glass-fiber densities.
- Finally, the introduction to a possible material optimization technique is discussed together with its implications in sustainability issues. A ground-breaking approach for the algorithmic optimization of material through a structural approach involving the analysis of solid geometry as a finite-element model is presented.

1.4. Chapter structure

The thesis is divided into a series of Chapters, which constitute its main structure and build up its arguments in a non-linear way. Ideally, the reader can either embark his journey throughout the thesis document from Chapter 2, or simply find an answer to his interests at any given chapter without necessarily reading the whole thesis body. Both ways are equally valid, provided each Chapter contains sufficient background information and a battery of results and conclusions as to become an independent piece of work. Nonetheless, should the reader be interested in reading the whole development, the thesis allows for a standard, linear argumentation, which follows a logical structure as well.

- **Chapter Two. State of the art: current trends in 3D printing.**

Chapter Two presents the most current innovations and the state of the art of the 3D printing technology related to the following aspects: (i) methodology, (ii) materials, (iii) software, and (iv) hardware. The methods and portrayed in the state of the art become the basis for the innovation of the presented approach, system, and experiments, and allow for a rich understanding of the 3D printing ecosystem at a variety of levels. The chapter covers current solutions for several industries and applications, methodologies and technologies, scales and materials.

- **Chapter Three: 3D printing in construction: a comprehensive methodological framework.**

Chapter Three explains briefly the main focus of the thesis and provides a theoretical, technical, and practical background. This chapter focuses mainly on the architectural possibilities of 3D printing for construction in general, and the proposed implementation in particular. General considerations regarding the construction sectors are made, especially those concerning its very particular nature and the current trends in building technologies at a global scale –mainly when comparing this sector to other possible target industries, such as the automotive or aerospace. Furthermore, a brief analysis of the foreseeable difficulties for the implementation of 3D printing for the construction sector is provided. The advantages and disadvantages of such solutions are discussed.

- **Chapter Four. Towards the standardization of real-scale, robotic 3DP. Software integration.**

Chapter Four exposes the main body of the thesis argument in the form of an innovative methodology of 3D printing in the context of construction within the overall field of AEC industries. As said above, it discusses the current situation of the construction market in terms of process automation regarding large 3D printing techniques and presents a design-to-production strategy that is exemplified in a software development in the form of a plugin In addition to that, this chapter introduces and explains the proof-of-concept development consisting of a software package that aims at demonstrating the possibility of a real industrial implementation of a global design-to-fabrication workflow regarding robotics and oversized fabrication for construction purposes. The chapter provides relevant information about the CAD-robot integration, as well as a significant amount of evidence of the embodiments and tests carried out to demonstrate it.

- **Chapter Five. Designing an off-the shelf, affordable AM end effector.**

Chapter Five aims primarily at describing the development of the technological demonstrator at a hardware level. A method and apparatus for adapting Fused Deposition Modeling (FDM) to robotic arms is provided, as well as a comprehensive depiction of the electronic system and devices thereby implied. This chapter illustrates a whole printing apparatus that is eventually used for testing and demonstration purposes, as it is an easy-to-use and affordable solution. Furthermore, the extrusion hardware could easily

be substituted by a more expensive, industrial, clay or concrete extruder to pursue more accurate results. Such substitution would only prove the adaptability of the whole software integration depicted in Chapter Four, minimizing operational changes. In fact, both extruders would not affect the system at a controller level. Annex I complements this chapter by emphasizing project development issues.

The FDM-like extruder is an adaptation of existing plastic extruders, exhibiting a number of improvements and differentiations. On the one hand, the electronics and programming have been completely redesigned from scratch to become more user-friendly and open-source. On the other hand, all its components have been customized for 3D printing purposes exclusively. Furthermore, and adaptor for the IRB 120 robot series from ABB is provided. The design of these parts engages in Rapid Prototyping techniques and Parametric Modeling, thus contributing to the flexibility and adjustability of the whole project.

The layout of the electronics is conceived following the preconditions listed here:

- The design must be open-source at this stage, as it intends to reach the general public and disseminate knowledge in non-related sectors such as architecture and construction. In order to achieve this, Arduino boards are used alongside other commercial electronic components.
- The hardware should be easy to standardize in order for the mock-up to eventually become an industrial development easy to adapt by fabricators and vendors alike.
- The Arduino code should be easily accessible for the manipulation of the variable printing conditions keeping the adjustability of its electronic components.
- The end effector and the electronics should be replicable by using straightforward, interchangeable electronic components.

Reliability, as the end effector needs to operate uninterruptedly for long periods of time.

- **Chapter Six. Material usage optimization through structure-oriented infill patterns.**

Chapter Six describes a method for enhancing the structural behavior of printed pieces in order to assure their viability for construction purposes and large-scale objects. A method and algorithm for creating smart infill patterns for 3D printed objects is described, alongside a number of tests in order to prove its viability and advantages. Additionally, a comparison between standard, space-packing algorithms and the proposed optimization is examined for future developments. As a consequence, a software for finite element structural analysis is described, resulting in lighter, yet more rigid, pieces. Further lines of research are set out in order to obtain a minimum viable product for industrial purposes. This chapter responds to the questions arisen both in Chapter Four and Five, as well as to the material tests documented in Annex II.

- **Chapter Seven: Conclusions and future work.**

The last Chapter completes the document by providing a comprehensive set of conclusions to every aspect discussed throughout the thesis. This chapter encompasses and validates the results of previous chapters and endorses a compelling summary of the realized works, their relationship with the thesis subject, and with the relevance of the matter, alongside a justification of the thereby resulting advancements in the field. Future lines of work are thereby presented as well.

- **Annex I. Test development. Process and improvements.**

Annex I covers the design process of the hardware and software involved in the thesis through a series of printed parts which are used as samples to expose diverse development issues. The section is conceived to emphasize the relationship between material and software as well as to provide compelling indications of the project development in the form of a walk-through. The project is divided into three main milestones: (i) the definition of the requisites and part hardware, (ii) routine-related issues and improvements, and (iii) overcoming the limitations inherent to the robot's controller.

- **Annex II. Material tests.**

This Annex provides a complete set of material tests that demonstrate not only the material properties of PLA and composites, but also –and more importantly- the distinct influence and of printing setups on the behavior of printed parts. In addition to actual test, a framework for concrete parts is provided,

pointing out the most relevant characteristics of the material in terms of usability and printability. The lessons learned from these test features are used to inform the implementation of the material optimization algorithm described in Chapter Six. These results may easily be extrapolated to actual real-scale production parts for the construction industry.

The thesis uses standard plastic printing materials as basis for its production development. This is due to two main reasons: on the one hand, the development of new materials is just far too complex and too financially demanding as to be able to be seriously addressed by the present work. On the other hand, the spectrum of materials is sufficiently broad already, giving very little or no space for individual undertakings to succeed.

PLA and ABS are used for demonstration purposes, although less explored materials are also studied. Cement-like materials are discussed for reference as to provide an overall reference for the studies included herein.

Chapter 2

State of the art: current trends in 3D printing.

This chapter introduces a comprehensive analysis of current 3D technologies, focusing both on small-scale and real-scale products, looking especially at literature and technology being currently developed. This analysis is used as starting point to define the focus of the current research from hardware, software, and procedural points of view. In order to illustrate the thereby following discussions with relevant examples, a comprehensive methodology has been selected. This chapter introduces as well both the methodology and the tooling.

2.1. Introduction

Since 1970 3D printing has experienced a great interest and an outstanding technological improvement. The birth of technology dates from 1976, where the first SLA-like, ink printer is created. Nonetheless, it is not until 1983 when more appropriate materials for 3D printing are used for these purposes. In 1983, Charles Hull creates the SLA printing system for rapid prototyping (RP) applications (*Wu, Wang, & Wang, 2016*). Five years later, Charles Hull creates 3DSystem, a firm which constitutes a milestone in the history of this particular technology.

In 1988, S. Scott Crump developed a technique called Fused Deposition Modeling (FDM), which allowed to create three-dimensional objects by the successive sequence of layers of fused material (*Stratasys, Inc., 1992*). FDM is arguably the most known and extended 3D method worldwide; in fact, it can be said that FDM has enabled further research due to the democratization of the hardware as a consequence of its affordable price, especially compared to SLA or SLS technologies. Moreover, FDM has been made available to the general public, thus creating a network of researchers specialized in the field.

During the 1990s many projects emerged simultaneously to the above mentioned industrial efforts to foster and promote the technology. The Massachusetts Institute of Technology (MIT) developed a 3D printer by modifying a standard ink printer. This project was carried out by two of their students, to be commercialized through 3DSystem, Crump's firm two years later.

As early as 1999, the biomedical sector printed the first organ from live tissue cells, becoming another landmark in the history of medical research. This event marked the starting point for many successful applications yet to come. Just three years later, researchers from the Wake Forest Institute in Regenerative Medicine crafted the first 3D printed kidney capable of filtering blood and produce animal urine.

Doctor Adrian Bowyer, a Senior Lecturer from Bath University (United Kingdom) invented in 2005 the first self-replicating 3D printer, in an attempt to create an affordable model that could compete with standard commercial printers. At the same time the RepRap community is given birth as a non-profit community (*Guerrero & Espinosa, 2014*) that aims at creating and sharing 3D printing related contents, such as hardware designs, software improvements, or 3D virtual models of all kinds. The RepRap project was an open design, and as such all of the designs produced by the project are released under the GNU general Public License (*Bogue, 2013; Pearce & Mushtaq, 2009*). Open Software Appropriate Technology (OSAT) has the potential to harness the capacities of distributed peer review, software transparency, and the culture from the open source movement, the academic world, and the contextual development of Appropriate Technologies (ATs) all at once. Thus, rather than programming code, the "source code" for these technologies are rather material lists, directions, specifications, designs, 3-D Computer Aided Design (CAD) techniques, and scientific theories needed to build, operate, and maintain AT. In this particular ecosystem, users are free to use and modify the source from any shared AT and, via the internet, engage in a parallel world-wide peer review process to determine the best practices and solutions, which tend to self-organize and standardize. One of the key impediments to the more rapid development of OSAT is the lack of means of production of open source technologies beyond a specific technical complexity, due to the intrinsic limitations of the open-source community, many times constituted by amateurs without the required technical background. This barrier is currently being challenged by open source, affordable 3D replicator versions (*Pearce, et al., 2010*).

Following this open-source logic, Josef Prusa developed the first low-cost, self-replicating 3D printed, which design was disclosed with the only condition that anyone receiving parts had to replicate them further for a 3rd party. The so-called Prusa printer was created in 2008 and has become a reference for the teaching community across the globe. Makerbot is given birth only one year later, 2009. The foundation of the company is a turning point in the history of desktop-oriented 3D printers and the fabrication ecosystem as such. Makerbot started as an open-source project nurtured by the *maker's community* and fostered by the advancements of the RepRap society. The placement of an Ikea-like mountable 3D printer assembly kit in the market by Bot Industries –founded by Bree Pettis, Adam Mayer, and Zach Smith- was the first commercial approach of the company, who decided to black-box its technology with the commercialization of its MakerBot Replicator 2 in 2012.

2009 became the year of the definitive settlement of social communities and forums related to 3D printing contents, although they emerge years earlier –see above. Thingiverse, also by Makerbot and Bot Industries, is still today the largest 3D printing exchange gateway in the world, where thousands of users upload and share their models on a daily basis. As of today, Thingiverse receives more than 173000 unique visits per day, generating roughly 400k dollars a year in income. Nonetheless, the research required to develop open source 3-D printers to the point where they are reliable for AT is non-trivial and is a barrier to OSAT's success. As reviewed here, open source 3-D printing is currently in the hacker/development stage and does not have the reliability nor the testing and verification needed to deploy in the field in developing countries. Consequently, the technology is being developed further by large corporations and small research-based startups alike (*Pearce, et al., 2010*).

3D printing also became present in many industries, such as aerospace design and engineering. *Sulsa*, the first fully 3D printed unmanned aircraft, arrived in 2011. All parts of the aircraft, except for the mechanical and electrical components, were 3D printed by sintering nylon fibers with laser.

The present Chapter intends to summarize these and other developments in the realm of 3D printing, paying special attention to the very diverse and broad range of models and possibilities. As seen above, the technology in itself deals with various aspects that integrate the realms of software, hardware, and procedures. All these are dealt with throughout the present thesis.

2.2. Current digital fabrication methods: main concepts and relevant technologies

2.2.1. Main fabrication concepts

Traditionally, fabrication procedures have been classified according to the treatment of the material or materials involved in the fabrication process. Both additive and subtractive processes involve material transformations, which can be defined and classified according to the following two groups:

- Subtractive fabrication or manufacturing (SM) is a process in which the final form or object is obtained from a whole piece of raw material. This material must account for a total volume that contains the final piece and is normally presented as a standard box-shaped piece. Techniques that are broadly considered subtractive include, but are not limited to, carving, milling, sanding, traditional sculpting, and many others.
- Additive fabrication or manufacturing (AM), as opposed to subtractive methods, includes every technique in which the process involves addition of material in different forms. This is, the resulting form, piece, part, or object is fabricated by adding parts or material to the model at the different stages of the process. The latest additive fabrication techniques include 3D Printing and robotic assembler arms, which constitute the main focus on the hardware studied in the thesis.

Although additive and subtractive methods haven been traditionally treated as such, they have experienced a substantial renovation due to the implementation of digital fabrication techniques and the affordability of industrial machinery since the beginning of the present century.

2.2.2. CNC definitions and common digital fabrication machines

CNC stands for Computer Numeric Control, and is used to define machines commonly involved in fabrication, particularly when high precision is at stake. These machines mount high-precision motors and robust hardware, specially conditioned to work under the most demanding conditions. The most common CNC machines are:

- Milling machines of different forms. Milling machines generally consist of a drill mounted on a moving head. 3 axis milling machines –commonly named 2.5D machines as well- are able to drill merely on the Z axis direction, thus having certain geometric constraints or limitations as to what sorts of geometry can be obtained. The head is normally attached to a rail system responsible for its movement on the XY plane and a motor that controls its height. As a result, these machines have a vertical orientation, which makes it impossible to orient the milling head for improved performance or to achieve certain holes in the final part. 5 axis milling machines, on the contrary, mount a more complex head, which allows for enhanced surface conditions and the proper orientation of the drill when necessary. The former are widely used for molding in construction related industries, while the latter are more oriented towards the modelling and fabrication of vessels or molds for the aerospace industry.

  According to actual design needs or part geometry, the mill software defines the so-called toolpath. The machine follows this toolpath –a sequence of points in space- to “navigate" through space, hence generating the final product out of a whole piece of material which is normally laid on a planar, stable surface called bed.

  Milling machines can be very expensive and require an extensive cleaning apparatus and careful maintenance, making them suitable for special equipment, such as laboratories or fabrication hubs. These machines may also require special foundations due to their weight and the inertia of the milling head when reaching high speeds.

- Laser (beam) cutters are in fact quite similar to ink printers, at least conceptually. In this case, the “printing head” is a laser that moves in 2D at a certain height from the bed, where the raw material is placed. The laser intensity can be adjusted to work with different materials in order to cut them or to create patterns or other effects on their surface –normally wood boards, plastics or similar. Laser cutters are used to automate tedious part fabrication in two-dimensional space. Although they do not offer any significant advantage as far as the construction of three-dimensional parts is concerned, these machines are used to create complex space frames consisting of rib-like structures, or volumetric objects with successive layers of either mechanically or chemically fixed material.
- Water jets can be compared to laser cutters in their operational aspects and machine architecture. They consist of a water impulsion system and a nozzle, which controls the flow

intensity of the water. High-pressure water is capable of cutting hard materials, such as metal plates and steel.

- Benders are machines used to, rarely enough, bend material. Although there are many different benders for many different purposes –some of them quite specific, such as bending steel profiles-, these machines are widely used for industrial production.
- 3D printers are the newest and most broadly known technological addition to the CNC fabrication ecosystem, especially those built as gantry-like systems –regardless the scale. As explained in future sections, 3D printers work with quite diverse techniques and materials, including laser sintering, fused deposition, and many more, meticulously described in the following sections throughout the present chapter. The apparently ever-expanding 3D printing market still allows for inventions and research opportunities, particularly in the fields of software and oversized parts alongside custom or tailor-made applications or solutions. Furthermore, the technology is experiencing an outstanding drop in costs and pricing. The most common printing techniques are described in the following section.

Despite some significant differences, industrial robots may be conceptually considered CNC machines. As explained later, robots have a completely diverse approach to movement control and orientation, and consist of a two-layer hardware structure: on the one hand, the so-called manipulator (n-axis arm); and the controller -a computer where actual inverse kinematics calculations are performed, on the other.

All above-mentioned machines have largely evolved from their initial models and are nowadays relatively easily to control through specific fabrication software relying on certain, widely used file standards. These standards allow for the use of a variety of design tools, which are studied throughout this section for future reference.

2.2.3. Digital fabrication applied to architecture and construction. 3D printing.

Architecture as a discipline is undergoing a quite deep process of transformation heavily influenced by the democratization of parametric design and fabrication software and the increasingly relevant use of complex geometries for design, which require high levels of control and rationalization.

On the other hand, as technologies spread, fabrication becomes more affordable, resulting in easy-to-use desktop machines that are rapidly approaching the quality and finishes of high-end, professional products.

Although explained further in section 2.5, it is worth looking at two particular matters in regards to the use of fabrication methods in architecture. On the one hand, Building Information Modeling (BIM) allows for the management and control of 3D models, whereby a whole geometrical and database is created. On the other, the creation of a dense network of fabrication laboratories, workshops, and ateliers –more commonly named FabLabs- has fostered the use and integration of digital fabrication tools. The ability to combine both has allowed for an unprecedented advancement of both design and construction technology, main drivers of the present thesis.

2.2.3.1. Professional and desktop 3D printers

As mentioned above, professional and desktop 3D printers are additive fabrication machines. The most common 3D fabrication types are powder-based composite materials and plastic extrusion through Fused Deposition Modeling (FDM).

3D printing is a form of additive manufacturing where a three dimensional object is created by laying down successive layers of material. 3D printers are generally faster, more affordable and easier to use than other additive manufacturing technologies –e.g. injection- and offer product developers the ability to print parts and assemblies made of several materials with different mechanical and physical properties in a single build process. Advanced 3D printing technologies yield models that can serve as product prototypes or final parts.

As it has been pointed out above, the cost of 3D printers has declined and is undergoing a deep process of constant evolution. This technology finds use in jewelry, footwear, industrial design, architecture, engineering and construction (AEC), automotive, aerospace, dental and medical industries, education, GIS, civil engineering, and more fields.

The democratization of fabrication technologies has brought a 3D printing revolution to the house-printer markets. There are unaccountable desktop, non-professional printers, many of which use open-source hardware and software. This fact has been facilitated as well by the expiration of many relevant patents, a topic that is discussed later in this chapter.

Some of the most relevant desktop 3D printers include the Pwder open source, processing-based 3D printer (*Pwder, 2012*); Makerbot replicator models (1, 2, 2x, and others); RepRap printers (such as Mini Kossel, Prusa), especially suitable for self-fabrication; Afinia 3D printers, focusing on ready-to-use models; Snap together; Cubify Cube 3D Printer; and Stratasys' Mojo. Other models include the Solidoodle 3D Printer, XYZ's Da Vinci 3D Printer, Hyrel 2 Hobbyist, Robo X 3D Printer, and Pegasus Touch. This list merely considers some of the most relevant choices while most of them are suitable for self-assembly or educational purposes. It is also important to consider the rapid development of desktop 3D printers, as today's models may be quickly outdated.

On the professional side, it is important to account for the following production models:

- **Powder technologies**. In the context of rapid manufacturing (RM), include (i) Selective Laser Sintering (SLS), (ii) Selective Laser Melting (SLM) and (iii) Electron Beam Melting (EBM) technologies. Other techniques use binding material to construct the desired object, especially related to oversized techniques –explained further in the following sections.

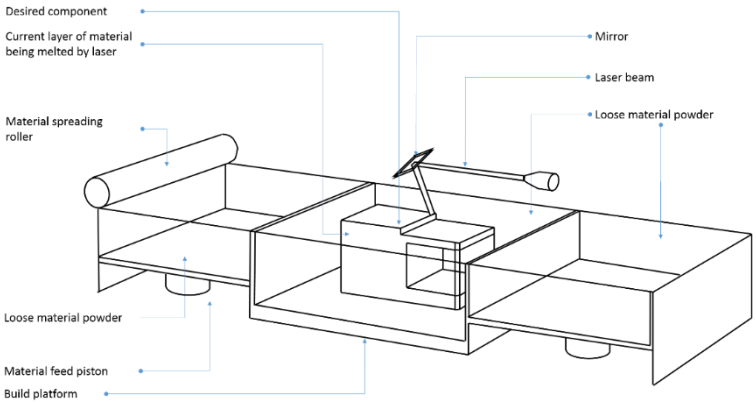

Fig. 1. Powder SLS technology (*New Zealand Rapid Prototyping Association, 2014*)

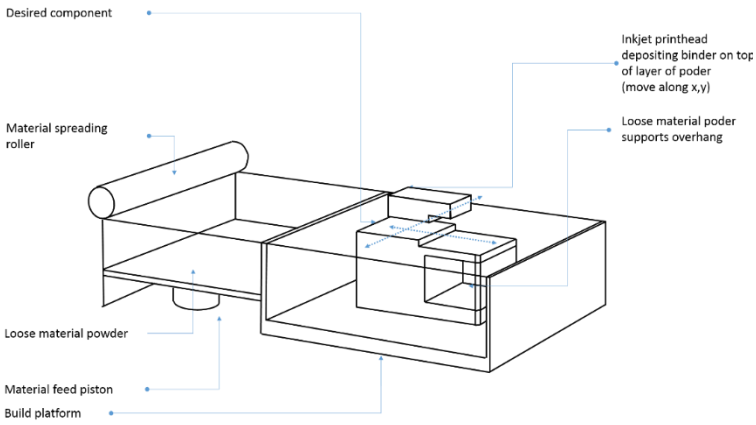

Fig. 2.Powder SLA technology (*New Zealand Rapid Prototyping Association, 2014*)

This means that powder 3D printers use powder as base material and a binder that glues it together where necessary. Though SLA and SLS will be explained further in the text, suffice it to say that material is "solidified" by different means in both techniques. SLS generally utilizes laser beams to synthesize material, whereas SLA normally uses special adhesives for the same purpose. Either case, the user designs the object using almost any 3D program, and exports the desired result as a *.STL file, which is read back by the machine's specific controller software. The binding material is then placed following a layer by layer logic until the final object is finished. An important feature of this technology is that it allows for the creation of movable parts and mechanisms.

3DSystems, Z-Corporation (zCorp) and Stratasys are currently the top three 3D printer manufacturers leading the so-called 3D printing revolution *(Goldman Sachs, 2013)*. These firms offer a variety of high-end products and materials. Normally, the systems consist of 2 machines which work in parallel: the actual binding machine -where the object is produced-, and a cleaning set -where the remaining of the raw material is removed. The object must then be infiltrated in order to increase its physical resistance and properties.

Fig. 3. zCorp's z460 Plus printer: building and cleaning sets –left and right. (*3D Systems, 2014*)

- **Plastic printers** work according to either of the following ways: on the one hand, certain printer models place cut-to-shape layers on top of one another (plastic layering); on the other hand, most printers extrude plastic filament through a high-temperature extrusion device, commonly named nozzle (plastic extrusion or Fused Deposition Modeling).

  In the FDM paradigm, thermoplastic, plastic-like, or composite materials of plastic matrix are heated until they reach a semi-fluid state and extruded in thin material layers that build up to the final shape of the object. Plastic then solidifies back as it cools down in a controlled atmosphere and coheres with previous layers in a relatively short time. ABS, PP, PLA, Nylon, and other plastics can be used to implement FDM technologies. In addition to these materials, there is also space for composites or bio composites, where the plastic composition may vary.

  As a consequence of the above, a whole new range of materials become available for experimenting rapid-prototyping.
- **Wax printers**: Solidscape's thermal inkjet method uses a single inkjet nozzle to jet a plastic build material and a wax-like support material which are held in a melted liquid state in reservoirs. The liquids are fed to individual nozzles which squirt tiny droplets of material as they are moved in an X-Y fashion in the required pattern to form a single layer of the final object. The materials harden as they are deposited and form a solid base for the next layer to come.

  After a layer of the object is formed by jetting, a milling head is passed over the layer to give it a uniform thickness. Particles are vacuumed away and captured in a filter as the milling head cuts the excess of material. The process is repeated to form the entire object. After the object is completed, the wax support material is dissolved away.

  The most outstanding characteristic of the Solidscape system is the ability to produce extremely fine resolution and surface finishes, almost equivalent to CNC machines.

Moreover, wax printers can print movable parts and intricate geometries, as was the case of powder printers. This technology is, however, slow for the production of large objects.

3D Systems produces an inkjet machine called the ThermoJet Modeler. This machine utilizes several hundred nozzles in a wide head configuration. It uses a hair-like matrix of build material to provide support for overhangs which can be easily brushed off once the object is complete. This machine is much faster than the Solidscape approach, although it is unable to reach the former's surface finish and resolution.

- **Tissue printers:** although these printers are at a very early stage of development, research involving tissue or other living materials are becoming increasingly important. Terreform One's live house project *(Joachim, Tan, Medvedik, & Aiolova, 2011; Luebkman, 2015; LeManager, Hiltner, & Shewry, 2012)* widely published in different media alongside many other project by the same firm, shows how it is possible to create 3D printed forms out of living material. According to Terreform's founder and director, Mitchell Joachim, this type of materials are incredibly energy efficient, as well as structurally solid. In addition to this, living houses could self-repair, grow, and expand, as well as adapt to several forms and shapes if controlled by adequate scaffoldings. Section 2.4.5 expands further on this subject.

Normally, the maximum production capacity for both professional and desktop 3D printers does not exceed a total of 20cm x 20cm x 20cm in size. This volume is limited in most cases by the bed calibration issues, which is difficult to achieve and maintain beyond that size. In addition to calibration difficulties, guaranteeing a proper planarity of the printing bed becomes gradually problematical and challenging with the increase in size.

2.2.3.2. Industrial robots

Robots are versatile machines that are widely used in industries like car manufacturing, heavy material processing, packaging, painting, coating, cleaning, assembling, sealing, water jet cutting, laser cutting, welding operations and many others. Robots are very good at repetitive tasks, but need to be tested and calibrated every time a different task involving a different tool and/or movement is programmed.

There are two basic robot types:

- Articulated robotic arms: They usually contain six axis, connected in chain, in a similar manner as a human arm. This allows to position the head of the mounted tool in almost any possible orientation within the building envelope of the robot.
- Parallel robots: The linkages work in parallel rather than as a chain. They are more precise but have a more limited building envelope.

Besides their industrial applications, robots are currently used in architecture schools around the world, including some of the most advanced and renowned institutions, such as ETH Zürich, Bartlett (UCL), University of Technology Sidney, and many others. In Spain, very few universities have robots available. To our best knowledge at the date of printing this thesis, merely the IAAC, UEM, and CEU have this equipment. These schools employ articulated robots in order to explore different architectural or engineering applications, which normally result in small-scale constructions.

Although customizable, robotic arms are not normally designed for a particular or specific fabrication method. According to their payload capacity and reach distance, robots can host different tools -such as heat wires, milling heads, saws, material extruders, and others, so that they may adapt to various project types. This versatility comes at the cost of the end user having to program the robot's tool path.

As it happens with milling machines, robotic arms are operated through a device called controller. A controller usually contains the drivers for the different robot axis and a computer that hosts the robot programs and allows for manual manipulation of the robot. It is common to have multiple robots working together on the same task. A single controller can be connected to multiple robots in order to synchronize their movements. Each robotics manufacturer develops its own programming language to control the robot (RAPID, KUKA language, and many others). The main robot vendors supply custom software packages that allow writing advanced and abstract robot programs. Furthermore, it is possible to automate program writing directly in the proprietary languages of the top robot manufacturers.

Some of the major manufacturers of industrial robots are:

- ABB: ASEA Brown Boveri is a Swedish-Swiss multinational corporation devoted to science and boosting productivity in the manufacturing realm. Engaged in both the automation and power technologies, ABB provides solutions for manufacturing chains through a variety of possibilities, including Discrete Automation and Motion, Low Voltage Products, Process Automation, Power Product, and Power Systems. The most commonly used ABB robot models are IRB 120 (payload = 3kg, distance = 0.58m) and IRB 1600 ID or similar (payload = 4kg, distance = 1.5m). This range of reach may vary according to the tool employed by the robot.
- KUKA AG is a Germany–based company focused on automating manufacturing process using robots. Unlike ABB, KUKA's business model comprises only two divisions: Systems and Robotics. The Robotics division supplies industrial robots. The company offers customized solutions based on a series of standard products with payloads, therefore classifying its robots according to their bearing capacity. As in the case of ABB Robots, a payload capacity between 5 and 16 kilograms is normally enough for architectural processes. The KR 6 to KR 16 cover various robots and configurations.
- Universal Robots is also a company devoted to automate processes with robotic arms. The vendor pledges to have the most easily programmable, reliable, and safe robots in the market, and are proud of their collaborative robotic arms. These robots have a peculiar alignment of the 6 axis chain allowing higher freedom of movement at the expense of load capacity and accuracy. They can be used in an office environment since they are safer to use than the more common industrial robots.

Other vendors include Fanuc, 3D Robotics, Aethon, Carbon Robotics, Foxconn Technology group, Ekso Bionics, Open Bionics, Rethink Robotics, ReWalk Robotics, Robotiq, SCHUNK, Siasun, Softbank Robotics Corporation, UCL Robotics, Toyota, and Yaskawa. These companies supply robots for the most diverse applications and sectors. Although the previously listed companies focus on productivity robots and automation, the use of collaborative robots and bionics is increasing in a significant manner. This becomes more obvious when analyzing the main robotic companies in the world: approximately 17 out of the 50 biggest robot companies relate their services to the development of medical, bionics, or autonomous machines (*Robotic Business Review (RBR), 2016*).

The use of robotics in architecture is constrained by how difficult it is for the designer to actually program the robot. A preferred alternative to using the software developed by the robot manufacturer is using plugins that can generate a robot program inside a CAD solution the designer is already familiar with. This way they can develop both the design and tool path using the same software. Information on existing software or applications is described more thoroughly in following chapters.

2.2.3.3. Autonomous machines

Autonomous or unmanned machines are not purely within the scope of the thesis. Despite this fact, it is still worth briefly looking at these machines, specifically regarding those being currently explored for construction, architecture, or 3D applications for inhabitation or similar functions.

Drones and autonomous flying machines, are increasingly being used for non-military applications. Quadcopters, for instance, perform properly thanks to their stability and power, besides being inexpensive to build. As said, ongoing research on their application for construction focuses both on traditional and non-traditional construction materials. In this sense, architects Gramazio and Kohler used quadcopters in 2011 (*Helm, Selen, Gramazio, & Kohler, 2012*) in order to assemble a structure made out of bricks and are currently using drones to deploy tensile structures. Nevertheless, these machines still need to be pre-programmed for such purposes. In order for them to carry out their tasks properly, most drones are still not environment-aware, which complicates their operation and shrinks their application scope. Further explorations (*Augugliaro, et al., 2014*) seek to put the potential self-orientation capabilities of drones into practice (*ETH Zürich, 2014*).

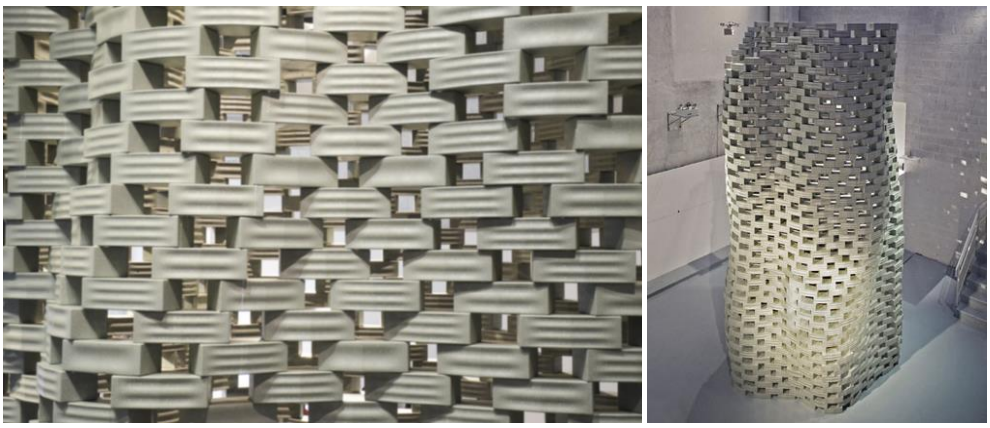

Fig. 4. The Flight Assembled Architecture/Flying Machine Enabled Construction (*ETH with Professors D'Andrea and Gramazio + Kohler, 2014*). Photo courtesy from: Francois Lauginie.

Similarly, there are attempts to use autonomous robots using infrared sensors to align themselves with respect to the desired construction geometry and capable of recognizing existing objects in their near surroundings or environment. These experiments aim at developing autonomous construction systems for building separated artifacts with simple blocks (*Ardiny, Witwicky, & Mondada, 2015*)

2.3. Small-scale, product-oriented printing

As said before, different materials require different technological approaches to 3D printing. Small scale, product-oriented printing focus primarily on rapid prototyping for industrial parts or emergent design study phases.

Although they will be explained thoroughly in the following sections, it is worth to point out the following 3D printing technologies classified by the relating material groups:

- Thermoplastics:
    - Polylactic Acid (PLA)
    - ABS
    - Nylon
    - Polycarbonate (PC)
    - Polyphenilsulfone (PPSF and PPSU)
    - ULTEM resin and Polyethermide Resins
- Composites:
    - Composite Filament Fabrication
    - Fused Filament Fabrication
    - Reinforced Filament Fusion
    - Biocomposites
    - Cement and glass fibers
    - Bioplastics and concrete assemblies
- Concrete
- Glass
- Ceramics
- Metals

- Direct Metal Laser Sintering (DMLS)
- Selective Laser Melting (SLM)
- Electro Beam Melting (EBM)

- Mixed materials and processes
  - Laminated Object Manufacturing (LOM)
  - Stereolitography (SLA)
  - Selective Laser Sintering (SLS)

2.3.1.1. Thermoplastics

Table 1. FDM properties

Abbreviation:	FDM
Material type:	Solid (Filaments)
Materials:	• Thermoplastics such as ABS, Polycarbonate, and Polyphenylsulfone; • Elastomers
Max part size:	914.4 x 609.6 x 914.4 mm (36.00 x 24.00 x 36.00 in.)
Min feature size:	0.127 mm (0.005 in.)
Min layer thickness:	0.0127 mm (0.0050 in.)
Tolerance:	0.0127 mm (0.0050 in.)
Surface finish:	Rough
Build speed:	Slow
Applications:	Form/fit testing, Functional testing, Rapid tooling patterns, Small detailed parts, Presentation models, Patient and food applications, High heat applications

Fused Deposition Modeling (FDM) was developed by Stratasys in Eden Prairie, Minnesota. In this process, a plastic or wax material is extruded through a nozzle that traces the parts cross sectional geometry layer by layer. The build material is usually supplied in filament form, but some setups utilize plastic pellets fed from a hopper instead. The nozzle contains resistive heaters that keep the plastic at a temperature just above its melting point so that it flows easily through the nozzle and forms the layer. The plastic hardens immediately after flowing from the nozzle and bonds to the layer below. Once a layer is built, the platform lowers, and the extrusion nozzle deposits another layer. The layer thickness and vertical dimensional accuracy is determined by the extruder die diameter, which ranges from 0.3 to 0.125 millimeters. In the X-Y plane, a 0.1 mm resolution or higher is achievable. A range of materials are available including ABS, polyamide, polycarbonate, polyethylene, polypropylene, and investment casting wax.

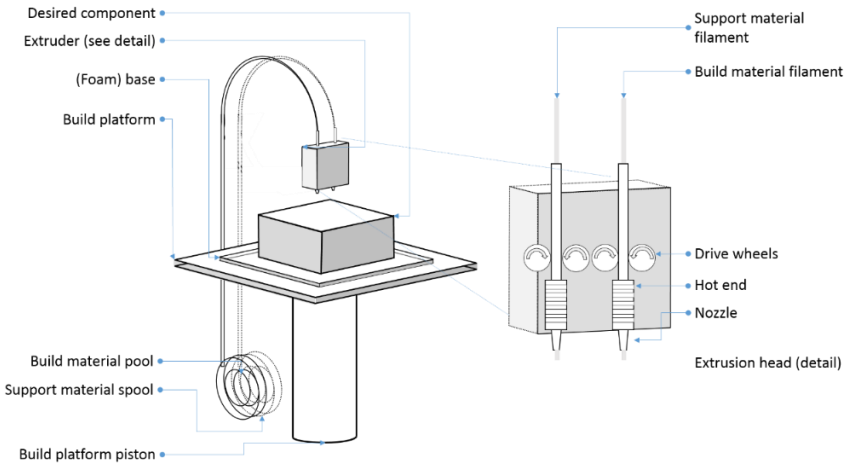

Fig. 5. FDM extrusion technology diagram showing nozzle

2.3.1.2. Polylactic Acid (PLA)

PLA is a thermoplastic aliphatic polyester derived from renewable resources, such as corn starch -in the United States, tapioca roots, chips or starch -mostly in Asia. Sugar cane is also a source for PLA in the rest of the world. In 2010, PLA had the second highest consumption volume of any bio-plastic of the world *(Ceresana, 2011*).

There are many advantages associated to the use of PLA plastic. First, PLA does not give off fumes like ABS does, or warp nearly as much. Furthermore, PLA is harder than ABS, but more brittle. It also stays flexible for a short while as it cools, which can be handy, especially for large prints. Finally, it does not warp and crack on larger objects the way ABS can, which, combined with the previously named feature, makes it a great candidate for real-scale objects.

Many companies work with PLA as primary printing material. Makerbot Industries' products, for instance, were designed to be built by anyone with basic technical skills and were described as about as complicated as assembling IKEA furniture. The first printers were sold as do it yourself kits, requiring only minor soldering, but later models were designed as closed-box products, with little or no user customization or construction. MakerBot printers print with ABS, high-density polyethylene (HDPE), PLA, and polyvinyl alcohol (PVA).

Stratasys' Fortus 3D Production systems are also worth mentioning. Stratasys are worldwide leading manufacturers quickly gaining presence in the fast growing field of Direct Digital Manufacturing (DDM). DDM is a process that uses additive fabrication technologies, such as FDM, to manufacture parts. This company use the same thermoplastics as traditional injection-molded parts, fact that has accompanied by the explosion in 3D printers using filament technology caused by the expiration of the patents on the original FDM version by Stratasys.

Fig. 6. A FDM MakerBot Replicator 2X

2.3.1.3. ABS (Acrylonitrile butadiene styrene)

This material is a terpolymer of acrylonitrile, butadiene and styrene. Usual compositions are about half styrene with the balance divided between butadiene and acrylonitrile. Meaningful variations in this proportions are, of course, resulting in many different grades of acrylonitrile butadiene styrene with a wide range of features and applications. In addition to this, many blends with other materials such as polyvinylchloride, polycarbonates and polysulfones have been developed.

ABS polymer was first discovered during World War II when its basis, styrene butadiene rubber (SBR), was used for alternatives to regular rubber. Commercially acrylonitrile butadiene styrene polymers first became available in the early 1950s in an attempt to obtain the best properties of both polystyrene and styrene acrylonitrile.

Some of the most important features of this material are related to that property optimization search. Thanks to its thermal stability, ABS is flame retardant, and has a high heat resistance. Moreover, it displays good mechanical behavior, which yields a particularly high resistance to impacts, plus a significant dimensional stability. ABS can be processed easily, which makes it a great material for general purposes, and offering a good finish quality with a high degree of glossiness.

As a result of the above mentioned features, ABS is a material widely used in automotive applications –both exterior and interior parts, electrical and electronic applications, appliances, cases and housings, and computer components. Nevertheless, it has also a number of disadvantages that is important to point out, especially for high-end parts or objects subject to use by end-clients. The most relevant are its limited weathering resistance, and its moderate heat, moisture and chemical resistance. Moreover, its production costs are still relatively high despite its use, and it becomes flammable with high smoke generation.

2.3.1.4. Polyamides: Nylon

Nylon was the first commercially successful synthetic thermoplastic polymer and one of the most commonly used polymers. Nylon is a generic designation for a family of synthetic polymers known generically as aliphatic polyamides, made of repeating units linked by amide bonds. Nylon is quite well known for its tensile strength.

2.3.2. PC (Polycarbonate)

This material is formed by a condensation polymerization resulting in a carbon that is bonded to three oxygen atoms. The most common system for this polymerization is formed by a reaction of bisphenol A and phosgene. Applications of polycarbonate are almost always those which take advantage of its uniquely high impact strength –although low scratch-resistance- and its exceptional clarity. These unique properties have resulted in applications such as bulletproof windows, break resistant lenses, compact discs, etc. More recently however, additional interest has resulted because of the low flammability of polycarbonate and its chemical stability, thus becoming a valuable asset for construction purposes of water-related uses in the industry.

Polycarbonates used in engineering are strong materials, and some degrees might become transparent. Polycarbonate has a glass transition temperature of about 147ºC, and flows at about 155ºC and higher temperatures. It is easily thermoformed and molded, since its upper working temperature ranges between 115 and 130 ºC approximately. The downside of this property is, naturally, that it can be used almost exclusively in low-temperature applications. Unlike other thermoplastics, PC can withstand significant plastic deformations without cracking or breaking (*Parvin & Williams, 1975*).

This material was first prepared by Alfred Einhorn in 1898 and extensively researched until 1930 where they were discarded. Research was then re-started in the mid-1950s by General Electric and Bayer. In 1958 the Polycarbonate popularity expanded to a global community. Today, approximately 75% of the Polycarbonate market is held by Sabic Innovative Plastics and Bayer Material Science.

Some of its more important features include its ease for mold release, good UV resistance, high flow, high impact resistance, and its capacity to maintain its mechanical properties when exposed to high temperatures for long periods of time. PC shows, among other handy properties, good dimensional stability, high heat resistance, good impact resistance, and outstanding ease for being processed. It is also a good flame retardant.

Polycarbonate can be used, as it was the case of ABS, for generic electrical and electronic applications, and many automotive, medical and healthcare purposes. Due to its low electric conductivity, it is also employed in housing appliances, industrial applications, and electrical parts. Its outstanding mechanical properties and durability make it suitable for sports.

However, PCs are subject to stress cracking, and degrades upon extended residence time in processing equipment. It is required a fairly high processing temperature for its molding and is merely fair chemically stable. Finally, it might be unsuitable for high-end uses on the client side due to its aromatic sensitivity.

2.3.3. PPSF or PPSU (Polyphenylsulfone)

PPSF/PPSU (polyphenylsulfone) material has the greatest heat and chemical resistance of all Fortus materials. Proper for aerospace, automotive and medical applications. PPSF parts are dimensionally

accurate, to better predict end-product performance. Users can also sterilize PPSF via steam autoclave, EtO sterilization, plasma sterilization, chemical sterilization and radiation. PPSF to manufacture conceptual modeling, functional prototyping, manufacturing tools, and end-use-parts.

2.3.4. ULTEM™ RESIN thermoplastic polyetherimide (PEI) resins

The ULTEM Resin family of amorphous C polyetherimide (PEI) resins offers outstanding elevated thermal resistance, high strength and stiffness, and broad chemical resistance. Plus, ULTEM copolymers are available for even higher heat, chemical and elasticity needs. ULTEM resins balance mechanical properties and processability.

Fig. 7. ULTEM parts

Table 2. Mechanical properties of some materials used in FDM printing

	ABS plus P430	ABSi	ABS-M30	ABS-M30i	ABS-ESD7	PC-ABS	PC-ISO	PC	NYLON 12	ULTEM™ 9085	PPSF
Tensile Strength (MPa)	37	37	36	36	36	41	57	68	48	72	55
Tensile Elongation (%)	3.0	4.4	4.0	4.0	3.0	6.0	4.3	4.8	30	5.9	3.0
Flexural Strength (MPa)	53	62	61	61	61	68	90	104	60	115	110
IZOD Impact, notched (J/m)	106	96	139	139	111	196	86	53	200	106	59
HDT (°C)	96	87	96	96	96	110	133	138	82	167	189

Table 3. Features of some ABS, PC, PP, and ULTEM variations

Material	Features
ABS-M30, ABSplus-P430 (acrylonitrile butadiene styrene)	• Greater tensile, impact, and flexural strength than standard Stratasys ABS • Layer bonding is significantly stronger for a more durable part than standard Stratasys ABS • Versatile Material: Good for form, fit and functional applications
ABS-ESD7 (acrylonitrile butadiene styrene - static dissipative)	• Static dissipative with target surface resistance of 107 ohms (typical range 109 – 106 ohms) • Makes great assembly tools for electronic and static sensitive products • Widely used for functional prototypes of cases, enclosures and packaging
ABS-M30i (acrylonitrile butadiene styrene - ISO 10993 USP Class VI biocompatible)	• Biocompatible (ISO 10993 USP Class v1) material • Sterilizable using gamma radiation or ethylene oxide (EtO) methods • Best fit for applications requiring good strength and sterilization
ABSi (acrylonitrile butadiene styrene - translucent)	• Translucent material

	• Good blend of mechanical and aesthetic properties • Available in translucent natural, red and amber colors
PC-ABS (polycarbonate - acrylonitrile butadiene styrene)	• Superior mechanical properties and heat resistance of PC • Excellent feature definition and surface appeal of ABS • Highest impact strength
PC (polycarbonate)	• Most widely used industrial thermoplastic • Accurate, durable, and stable for strong parts • Superior mechanical properties and heat resistant
PC-ISO (polycarbonate - ISO 10993 USP Class VI biocompatible)	• Biocompatible (ISO 10993 USP Class v1) material • Sterilizable using gamma radiation or ethylene oxide (EtO) methods • Best fit for applications requiring higher strength and sterilization
ULTEMTM 9085 (polyetherimide)	• FST (flame, smoke, toxicity) certified thermoplastic • High heat and chemical resistance; highest tensile and flexural strength • Ideal for commercial transportation applications in airplanes, buses, trains, boats, etc.
PPSF/PPSU (polyphenylsulfone)	• Highest heat and chemical resistance of all Fortus materials • Mechanically superior material, greatest strength • Ideal for applications in caustic and high heat environments

2.3.5. Composites

Composites are, in its broadest sense, a blended mix of materials that form ultimately a new, generally enhanced material. Material science works in the continuous development and improvement of existing materials, and was boosted by the plastic industry. As a consequence, many composites may be used by FDM printing technologies, since many materials make use of a thermoplastic matric. The most relevant examples are listed in the following subsections.

2.3.5.1. Composite Filament Fabrication (CFF)/Fused Filament Fabrication (FFF)

Markforge unveiled in early 2014 its new MarkOne, the first commercial carbon fiber 3D printer using continuous fiber. Markforge claims that their patent pending composite is about twenty times stiffer than regular ABS, and stronger than 6061-T6 aluminum by weight unit. Carbon Fiber CFF™ applications are fixtures, jigs, and parts that need the highest strength-to-weight ratio. Parts made with CFF™ are reinforced by continuous strands of fibers embedded in a thermoplastic matrix.

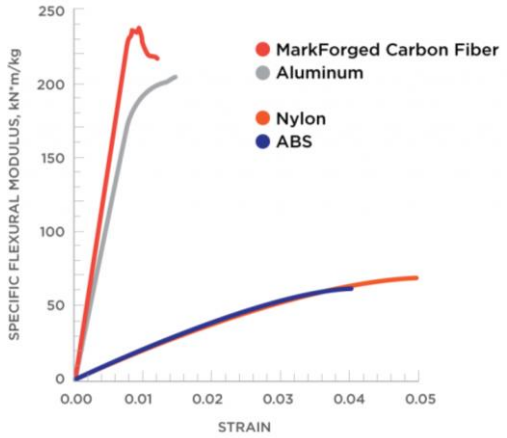

Fig. 8. Comparison of flexural modulus for Carbon Fiber, Aluminium, Nylon and ABS

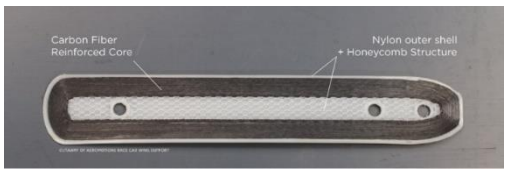

Fig. 9. Inner structure of a CFF built part

The build size of the MarkOne printer is 305mm x 160mm x 160mm, although it may be adapted to bigger sizes. As in other cases, the size is not limited by the material itself, but rather by the printer's hardware configuration. This material is already used in other applications, such as reinforcements of parts printed by regular FDM methods, such as air intake or other parts not subject to structural stress or heavy vibration conditions.

2.3.5.1.1. Carbon Fiber CFF™ (Composite Filament Fabrication)

CFF may be printed like thermoplastics, but is much stiffer than aluminum. As said above, it presents the best strength-to-weight ratio, is stiffer than 6061 Al, and is safe, easy to print, and non-toxic. Moreover, it requires no post curing, and is ready to use. Its price can reach 1.55€/cm^3 approximately.

2.3.5.1.2. Nylon FFF Filament

Nylon is a very flexible, but tough material. The nylon filament has great fatigue and impact resistance, which results in reliable parts that can last over time and withstand heavy weather conditions without a significant loss of its mechanical properties. Thus, nylon is also a great outer protective layer to keep fixtures and tooling from scratching. It is also regarded as protection for sensitive parts in machinery due to its impact and scratching resistance. Finally, it is also suitable for tabs, clips, and mechanical fasteners.

Summarizing, this material is a tough engineering plastic, with a low-friction index, flexible, and non-toxic. It may be used for tensile structures, or as reinforcement of construction materials able to withstand compression stresses, such as concrete. A cubic centimeter costs around 0.22€.

2.3.5.1.3. PLA FFF Filament

Although PLA has been sufficiently described in sections above, suffice it to say that its FFF form is low-cost, biodegradable, and has minimal shrinkage ratios. PLA is, therefore, a good material for producing quick prototypes for iterative fit and form testing. PLA is merely suitable for FFF and incompatible with CFF printing.

PLA is biodegradable, non-toxic, and relatively stiff. It is also the material with the lowest cost among the presented in the present research, with just 0.06€/cm^3.

2.3.5.1.4. Reinforced Windform polyamides

Fig. 10. Part printed with a polyamide, showing finish quality

CRP Technology is involved since 1996 in Additive Manufacturing in general, and 3D Printing in particular through the Selective Laser Sintering technology (SLS). One of the European pioneer firms in the field, CRP Technology works with its own Windform composite materials, which were born from the study-research of the R&D department of CRP Technology. Windform polyamide materials is composed of different kind of powders, patent-pending and trademarked. The following materials are the most relevant, especially for the aerospace industry. Each lists its most relevant properties, including Heat

Deflection Temperature (HDT), Ultimate Tensile Strength (UTS), and Elastic or Tensile Modulus per density unit.

- Windform SP. Polyamide-based material reinforced with carbon fibers.
    - HDT (1.82 Mpa) 186,5 °C
    - UTS per density unit 68,81 Mpa
    - Tensile modulus per density unit 5623,51 Mpa
- Windform GT. Polyamide-based material with fiber glass.
    - HDT (1.82 Mpa) 169,4 °C
    - UTS per density unit 56,21 Mpa
    - Elastic Modulus 3289,80 Mpa
- Windform XT 2.0. Polyamide-based material filled with carbon fiber. This material is known for its mechanical properties, which made it particularly applicable in demanding applications such as motorsports, aerospace, and UAV's. It retains the matte black color of its XT ancestor, and displays feature improvements in mechanical properties such as +8% in tensile strength, +22% in tensile modulus, and + 46% increase in elongation at break.

HDT (1.82 Mpa) 173,4 °C

    - UTS 83,84 Mpa
    - Elastic Modulus 8928,2 Mpa
- Windform LX 2.0. Polyamide-based material filled with glass fiber. This version is characterized by its improved Ultimate Tensile Strength, resistance to temperature, and stiffness. It stands out for functional applications and complex finished parts.
    - HDT (1.82 Mpa) 175,7 °C
    - UTS 59,9 Mpa
    - Elastic Modulus 6248 Mpa
- Windform GF 2.0. Polyamide-based material filled with added aluminum and glass. It has an improved HDT, superior stiffness, excellent surface finish, wear resistance, and first-rate detail reproduction capabilities. According to the vendor, it offers a gleaming look, which stands out in wind tunnel, design, and functional applications. It also offers a reasonable price to quality ratio. It is used for intake manifold –such as aspiration and cooling ducts, air intakes, and others-, hydraulic ducts up to 125ºC, fuel systems, and household appliances.
    - HDT (1.82 Mpa) 134,3 °C
    - UTS 50,60 Mpa
    - Elastic Modulus 4304 Mpa
- Windform PS. Polystyrene-based material suited for the production of complex casting patterns. These patterns are enough porous in order to allow the convenient wax infiltration, and therefore becoming easy to handle and to finish. As main advantages over standard polystyrene products in the market, Windform PS lists the following:
    - Better surface quality and detail reproduction
    - Less "curling" effect in the first layers
    - Very low ash content, therefore perfectly suitable for highly reactive alloys, such as Titanium alloys, besides aluminum, magnesium, steel and nickel-based alloys.

Table 4. Mechanical properties of ABS-derived materials

	ABS plus P430	ABSi	ABS-M30	ABS-M30i	ABS-ESD7
Tensile Strength	37 MPa	37 MPa	36 MPa	36 MPa	36 MPa
Elastic Modulus	53 MPa	62 MPa	61 MPa	61 MPa	61 MPa
HDT	96°C	87°C	96°C	96°C	96°C

2.3.5.1.5. Reinforced Filament Fusion (RFF) Technology

2.3.5.1.5.1. Polymer reinforced with carbon fiber and carbon nanotubes

After a long period in stealth mode, Silicon Valley's Arevo Labs came out in to unveil their proprietary technology for making high-strength 3D-printed carbon composite end products using matrix materials like ULTEM, as well as Solvay's KetaSpire PEEK, AvaSpire PAEK, PrimoSpire self-reinforced polyphenylene, and Radel polyphenylsulfone (PPSU) resins.

The 3D printing startup's technology is not a printer, but rather materials and software that can be used with several commercially available fused filament 3D printers. They also claim to be the first ones to implement software for the use of 6-axis robots, although this may arguably be subject of further discussion. Their technology is aimed at aerospace, defense, and medical OEMs.

According to the information available in their press publications, Arevo Labs' end-production 3D printing technology for carbon composites includes a high-temperature filament fusion printer head design and firmware for use with the company's new carbon fiber and nanotube reinforced high-temperature matrix polymers like PEEK. These products, plus proprietary 3D model design and analysis software, may have been fully tested with an off-the-shelf desktop printer modified by the company to print test parts on site. Arevo Labs says it is working with some printer hardware companies that are modifying their products to print end-production parts for aerospace, defense, and medical applications.

The firm claims to have had optimized matrix polymer formulations reinforced with carbon fiber and carbon nanotubes, along with extrusion technology to make the polymers suitable for additive manufacturing. To be precise, they have merely adapted a regular FDM extruder similar to those available in most 3D desktop printers in the market.

The reinforced materials are tailored to have excellent resistance to high temperatures and chemicals. For example, three grades of Solvay's KetaSpire PEEK have just been qualified by Airbus for use in aircraft interiors. One is carbon fiber filled, and another is glass fiber filled. Airbus previously qualified Solvay's Radel R-7000 PPSU, a material specifically formulated for aircraft interiors.

2.3.5.1.5.2. Bio composites

A bio composite is a material formed by a resin matrix and a reinforcement in the form of natural fibers -usually derived from plants or cellulose. Bio composites are characterized by various facts, namely: (i) petrochemical resins typically used in composites are replaced by vegetable or animal resins, and/or (ii) bolsters -fiberglass, carbon fiber, talc, or others- are substituted by natural fibers, such as wood, hemp, flax, sisal, jute, and may others. It is important to regard that each constituent of the composite must be biocompatible. Moreover, the interface between constituents should not be degraded by the environment – likely a living creature- and be able to withstand the most extreme conditions when placed in the build environment of for regular commercial purposes.

These materials have wide-ranging uses, from environment-friendly biodegradable composites to biomedical composites for drug/gene delivery, tissue engineering applications or cosmetic orthodontics.

Parts made of bio composites often mimic the structures of the living materials involved in the process. In addition to that, they improve the strengthening properties of the matrix that was used while providing biocompatibility. This is particularly important when creating scaffolds in bone tissue engineering.

The use of bio composites in the market is rising significantly, mainly due to the increase in oil price, but also for recycling and environmental obligations. The constant development of the medical and healthcare industries for advanced implant applications and bioengineering also constitutes a great basis for the growth of these materials.

There are countless projects currently being developed around plant-fiber reinforced PLA. Freedom of Creation, for instance, employs bamboo micro fibers or sawdust for their experiments in their so-called Tree-D Printer (Freedom Of Creation, 2011). As a result, the use or bio composites or bio-compatible materials opens up new unexplored possibilities in the field of recycled materials and the use of environmentally-friendly products. The use of such materials could eventually produce a cradle-to-cradle approach to fabrication, where materials may be either reused or recycled in a limitless manner, thus minimized their embedded energy and the thereby associated carbon footprint.

Fig. 11. Fiber parts by Freedom of Creation

2.3.5.1.6. Cement and glass fibers

There are countless experiments focusing on the development of material technology for the AEC industries. Although this research is still at a quite early stage of development, firms are trying to come up with materials that may be 3D printed and used for construction purposes. These technologies generally rely on the Contour Crafting technology mentioned in following chapters, although the most challenging about this particular research may be to develop a material that is able to provide the following properties:

- Mechanical properties that comply with structural regulations
- Rheology as to allow for a continuous deposition without significant interruption both during fabrication and product life cycle
- A process that allows for the correct use and deployment of such materials
- A result that implements this technology properly; this is, that lays material in such a way that it has enough overlap and between layers and continuity as to behave monolithically.

Although it is further explained in section 2.5.5.1, Winsun New Materials is arguably one of the most known examples of this sort of materials and their applications to the construction sector. The company has declared to have built 10 200-square-meter homes in 24 hours using a gigantic 3-D printer, although there is certain controversy around this fact.

2.3.5.1.7. Bio-plastics and granulate assembly

DUS Architects in Amsterdam are building the so called 3D print Canal House (DUS Architects, 2016), a fully modular house that is to host 13 rooms, with plans to print even the furniture. According to the architects, it would probably take less than three years to complete. The firm in not only the initiator and designer of the House, but also of the KamerMaker (room maker), the large portable 3D Printer which renders the project real.

Although further information on the project itself can be found in section 2.4.5.3, it is important to point out that the KamerMaker prints with a proprietary adaptation of a particular subset of bio plastics. The granulate material fed into the KamerMaker is called Macromelt, a type of industrial glue (Hotmelt) developed by Henkel. The Hotmelt is made of 80% of vegetable oil and melts only at 170 degrees Celsius,

although, technically, the KamerMaker can print with any material that melts at relatively low temperatures and then hardens again –following the FDM logic.

The aim of the project and the material development is to be able to print with a material that is (i) sustainable, (ii) of biological origin, (iii) melts at a relatively low temperature, and (iv) is sturdy and stable. DUS architects are also looking into the possibilities of using recycled materials, specifically plastics but also regarding wood pallets and natural stone waste.

As said, further information on the project itself may be found under section 2.5.5.3., where a more detailed description focusing on the architectural features of the project is offered.

2.3.6. Concrete, ceramics, and plaster

Concrete is the most widely used man-made material in construction. MIT Media Lab 3D prints concrete with variable densities using Contour Crafting techniques and similar, which are studied further in section 2.5. Please refer to this section for more information. The University of Leighsborough has also shown interest in the development of 3D printing techniques for concrete materials, developing formulae for printable concretes (*Le, et al., Hardened properties of high-performance printing concrete, 2012*) *(Le, et al., Mix Design and fresh properties for high-performance printing concrete, 2012*).

Plaster 3D printing is more expensive, accurate and brittle than the most used thermoplastics like ABS. Ceramics can be printed using simple deposition modelling (*Hinczewski, Corbel, & Chartier, 1998*), or casted to obtained tailor-made products. Plaster-like materials require no further treatment prior to or after part production, making this material especially suitable for healthcare applications for its outstanding hygienic conditions –besides relevant experiments in the realm of aesthetics and design, such as those carried out by Neri Oxman at MIT Media Lab.

Fig 12. Cast with ultra-sound to speed up healing

Fig. 13. Tailor made cast for injured

Turkish student Deniz Karasahin won the 2014 Golden A'Design Award with a new 3D-printed osteoid medical cast that uses ultrasound to speed up healing (*Martin, 2014*). The Osteoid medical cast,

tackles the problem by 3D-printing the cast to fit the shape of the patient's arm, and also providing ventilation holes.

As reported by different media, Jake Evill –a Victoria University of Wellington Architecture and Design school graduate, in close collaboration with the orthopedics department of the Victoria University of Wellington created a similar next generation cast. Named *Cortex*, it uses 3D scans and X-rays to provide tailor-made support for an injured and once printed it easily clips on to the affected area. It is lightweight, ventilated, washable and thin enough to fit under a sleeve (*Hosmer, 2013*).

2.3.7. Glass

Late 2015, Neri Oxman, Head of the Mediated Matter group at the MIT Media Lab, developed a technique for 3D printing molten glass (*Klein, et al., 2015*). This is the first time that transparent glass is 3D printed, and constitutes a complete milestone in the development of 3D printing technology. The group assembled an AM machine able to extrude molten glass in a process similar to current FDM techniques. The process, in the team's belief, could eventually be used to create architectural components or even entire façade elements for buildings in the future.

The G3DP project, as the team titled it, represents the first of its kind successfully dealing with optically transparent glass printing processes. So far, the project has printed a series of vases and bowls, although Oxman said that this brand-new printing technology could easily be adapted to an architectural scale in relatively short period of time. In Oxman's words, *"[…] we wanted to explore the possibility of creating [parts] that are at once structurally sound, environmentally informed and have the potential to contain and flow media through them*". Regarding architectural elements, they believe that glass could one day be printed to create "*a single transparent building skin*".

The G3DP printer consists of two insulated chambers, one above the other. The upper chamber serves as kiln, keeping molten glass heated to 1,000 degrees Celsius. The molten glass chamber acts as the print cartridge, moving laterally to deposit a continuous stream of liquid glass into the lower chamber via a nozzle made from alumina zirconia silica – a chemical compound that is resistant to heat. The lower chamber acts as the printer bed and anneals, or gradually cools, the glass as it builds up layer by layer. Annealing prevents the cooled glass from shattering when subjected to temperature change or impact.

Fig. 14. Vase realized by means of glass printing. Additive Manufacturing of Optically Transparent Glass (*Klein, et al., 2015*)

The versatility of 3D printing applies to this project as well. This enables the project team to generate geometrically customizable structures that are besides optically tunable by varying spatial manufacturing resolution parameters. The team also plans to study the affection of color gradients on environmental performance and the glass' solar radiation transmittance properties –unlike in traditional blowing processes.

Further thoughts on the project expect to include applications to produce aerodynamic building facades optimized for solar gain among other geometric tuning opportunities. The G3DP project was created as a collaboration between the Mediated Matter group at the MIT Media Lab, the Mechanical Engineering Department, the MIT Glass Lab and Wyss Institute. Researchers include John Klein, Michael Stern, Markus Kayser, Chikara Inamura, Giorgia Franchin, Shreya Dave, James Weaver, Peter Houk and Professor Neri Oxman (*United States Patent No. US 2015030307385, 2015*)

2.3.8. Metals

Metal 3D printing is a quite expensive methodology restricted to the fabrication of small parts. Following subsections describe each method's properties, advantages, disadvantages and limitations.

2.3.8.1. Direct metal laser sintering (DMLS)

Direct Metal Laser Sintering was developed jointly by Rapid Product Innovations (RPI) and EOS GmbH, starting in 1994, as the first commercial rapid prototyping method to produce metal parts in a single process. With DMLS, metal powder (20 micron diameter), free of binder or fluxing agent, is completely melted by the scanning of a high power laser beam to build the part with properties of the original material. Eliminating the polymer binder avoids the burn-off and infiltration steps, and produces a 95% dense steel part compared to roughly 70% density with SLS –analyzed in section 2.3.6.2.

Table 5. Direct Metal Laser Sintering properties

Abbreviation:	DMLS
Material type:	Powder (Metal)
Materials:	• Ferrous metals such as Steel alloys, Stainless steel, Tool steel; • Non-ferrous metals such as Aluminum, Bronze, Cobalt-chrome, Titanium; • Ceramics, INCONEL
Max part size:	250.4 x 250.4 x 220 mm (10.00 x 10.00 x 8.70 in.)
Min feature size:	0.127 mm (0.005 in.)
Min layer thickness:	0.0254 mm (0.0010 in.)
Tolerance:	0.254 mm (0.0100 in.)
Surface finish:	Average
Build speed:	Fast
Applications:	Form/fit testing, Functional testing, Rapid tooling, High heat applications, Medical implants, Aerospace parts

An additional benefit of the DMLS process compared to SLS is its higher detail resolution due to the use of thinner layers, enabled by a smaller powder diameter. This capability allows for more intricate and compact part shapes. Material options that are currently offered include alloy steel, stainless steel, tool steel, aluminum, bronze, cobalt-chrome, and titanium. In addition to functional prototypes, DMLS is often used to produce rapid tooling, medical implants, and aerospace parts for high heat applications.

The DMLS process can be performed by two different methods: (i) powder deposition and (ii) powder bed, which differ in the way each layer of powder is applied. In the powder deposition method, the metal powder is contained in a hopper that melts the powder and deposits a thin layer onto the build platform. In the powder bed method (shown below), the powder dispenser piston raises the powder supply and a recoater arm distributes a layer of powder onto the powder bed. A laser then sinters the layer of powder metal. In both methods, after a layer is built the build piston lowers the build platform and the next layer of powder is applied. The powder deposition method offers the advantage of using more than one

material, each in its own hopper. The powder bed method is limited to only one material but offers faster build speeds.

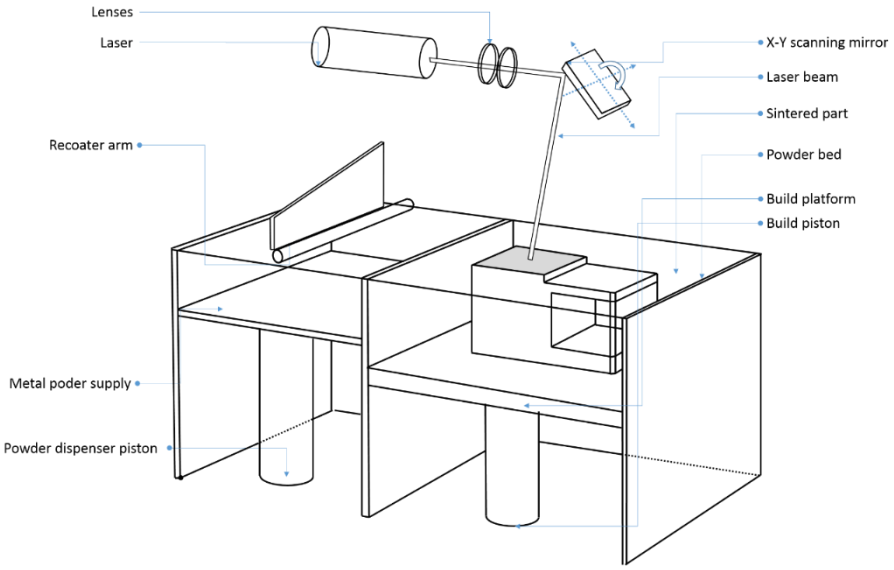

Fig. 15. Metal DMLS printing method

Arup's design for the Kurilpa Bridge knot provides a unique approach to structural detailing that seeks to supersede the traditional production of steel joints. The arguably complex geometry of the bridge has proven a starting point for this technology. Arup funded the development work and collaborated with a number of partners to realize the designs, including WithinLab (an engineering design software and consulting company), CRDM/3D Systems (the Additive Manufacturing partner) and EOS, who worked on the early development of the technology. According to Salomé Galjaard, Arup's Team Leader for this project, "*By using additive manufacturing we can create lots of complex individually designed pieces far more efficiently. This has tremendous implications for reducing costs and cutting waste. But most importantly, this approach potentially enables a very sophisticated design, without the need to simplify the design in a later stage to lower costs*" (*Niehe, 2014*).

Fig. 16. Joint Design for the Kurilpa Bridge

2.3.8.2. Selective Laser Melting (SLM)

Selective Laser Melting uses a laser to melt powdered metal in a chamber of inert gas. When a layer is finished, the powder bed moves down, and an automated roller adds a new layer of material which is melted to form the next cross section of the model. SLM is ideal for applications where high strength or high temperatures are required as it results in extremely dense and strong parts that match characteristics of the target material. SLM is a metal additive manufacturing technique similar to SLS.

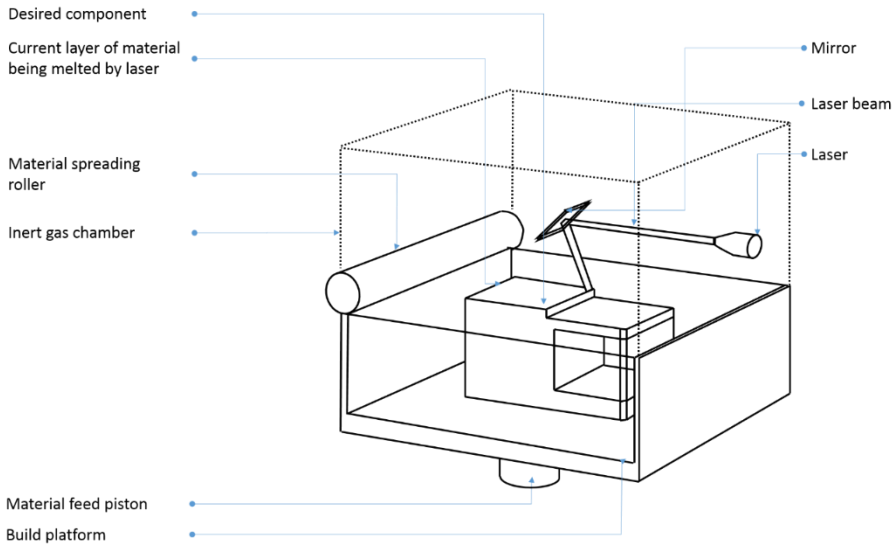

Fig. 17. Selective Laser Melting technology

The main difference between SLM and SLS is that the latter sinters the material heating to below the melting point until the particles merge with one another, while the former melts the material, creating a melt pool in which material is consolidated before cooling down to form a solid structure.

Unlike SLS, the materials used in SLM can exist in a single, atomized, component form which allows for denser, less porous builds. The types of materials available for this process include stainless steel, tool steel, cobalt chrome, titanium and aluminum. Other materials are currently under development but must exhibit certain flow characteristics in order to be process-capable.

2.3.8.3. Electro Beam Melting (EBM)

With Arcam's Electron Beam Melting (*Arcam, 2015*) method a 100% solid metallic object is produced directly from metal powder. The model is sliced into thin layers, approximately a tenth of a millimeter thick. From a magazine of powder, an equally thin layer of powder is scraped onto a vertically adjustable surface. The first layer's geometry is then created through the layer of powder melting together at those points directed from the CAD file, with a computer controlled electron beam. Thereafter, the building surface is lowered just as much as the layer of powder is thick, and the next layer of powder is placed on top of the previous one. The procedure is then repeated so that the object is shaped, layer by layer by layer, until a finished metal part is complete.

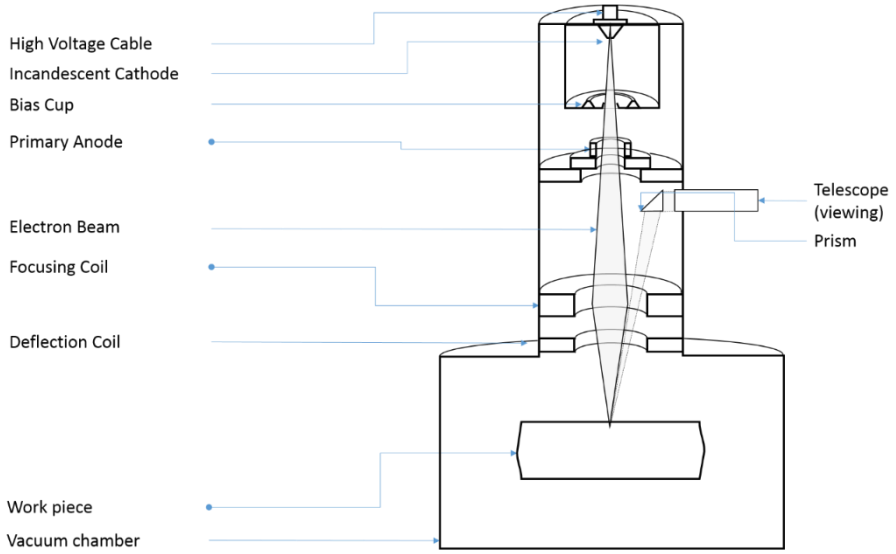

Fig. 18. EBM technology showing schematic architecture of inner machine chambers

The usage of a highly efficient computer controlled electron beam in vacuum provides high precision and quality. EBM makes possible the fabrication of homogeneous metal components such as complex tooling for spray-forming and injection molding tools and functional prototypes in a very short time. This highly efficient system produces parts from titanium powder and does so between three and five times faster than other additive fabrication methods. One other advantage is that reworking and post-processing of the part is minimized. In contrast to SLS, the electron beam fully melts the metal particles to produce a void-free part. The process occurs in a high vacuum, which ensures the part is completely solid, without imperfections caused by oxidation.

The EBM process is ideal for applications where high strength or high temperatures are required. The machine creates parts comparable to wrought titanium and better than cast titanium, with a 95 percent powder recovery yield, which results in the use of only 7 kW of average power consumption. As opposed to EBM, in laser sintering methods, 95% of the light energy is reflected by the metal powder, causing the system to be extremely inefficient.

Medical product manufacturers can benefit from the parts' high flexural strength for bone implants requiring a functional life exceeding 10 million cycles or movements. Automobile makers can build strong parts for high temperature testing, including under-the-hood applications. Aerospace engineers are more interested in the combination of a high strength yet light weight titanium part. And because the EBM process produces a homogenous solid, parts can be flight-certified.

Two variations of titanium "six four" alloy are available for the EBM S400: Ti6AL4V and Ti6AL4V ELI (Arcam, 2015). Titanium parts created on the system are accurate near-net shape and are HIP heat treatable. The system builds parts up to approximately 200 x 200 x 180 mm, with a layer thickness range of 0.05 - 0.2 mm.

EBM systems are manufactured by Arcam AB and distributed in North America by Stratasys. Outside North America, the system is available from Arcam as the EBM S12.

2.3.9. Mixed materials and processes

2.3.9.1. Laminated Object Manufacturing (LOM)

The first commercial Laminated Object Manufacturing (LOM) system was shipped in 1991. LOM™ (*United States Patent No. US 5730817 A, 1998*) was initially developed by Helisys Inc. of Torrance, California, currently Cubic Technologies. The main components of the system are a feed mechanism that advances a sheet over a build platform, a heated roller to apply pressure to bond the sheet to the layer below, and a laser to cut the outline of the part in each sheet layer.

Parts are produced by stacking, bonding, and cutting layers of adhesive-coated sheet material on top of the previous one. A laser cuts the outline of the part into each layer. After each cut is completed, the platform lowers by a depth equal to the sheet thickness (typically 0.05-0.5 mm), and another sheet is advanced on top of the previously deposited layers.

Table 6. Laminated Object Manufacturing properties

Abbreviation:	LOM
Material type:	Solid (Sheets)
Materials:	• Thermoplastics such as PVC • Paper • Composites • (Ferrous metals; Non-ferrous metals; Ceramics)
Max part size:	812.8 x 558.8 x 508 mm (32.00 x 22.00 x 20.00 in.)
Min feature size:	0.2032 mm (0.008 in.)
Min layer thickness:	0.0508 mm (0.0020 in.)

Tolerance:	0.1016 mm (0.0040 in.)
Surface finish:	Rough
Build speed:	Fast
Applications:	Form/fit testing, Less detailed parts, Rapid tooling patterns

The platform then rises slightly and the heated roller applies pressure to bond the new layer. The laser cuts the outline and the process is repeated until the part is completed. After a layer is cut, the extra material remains in place to support the part during build, which impedes the fabrication of hollow parts.

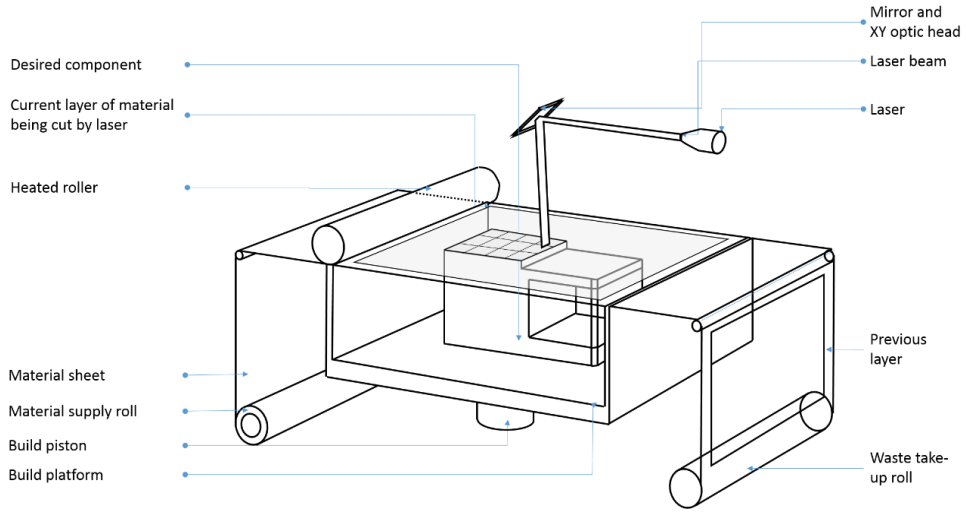

Fig. 19. Laminated Object Manufacturing technology showing material layering and rolls

2.3.9.2. Stereolitography (SLA)

SLA is the most widely used rapid prototyping technology. It can produce highly accurate and detailed polymer parts. It was the first rapid prototyping process, introduced in 1986 by 3D Systems, Inc., based on work by inventor Charles Hull (*United States Patent No. US 4575330 A, 1986)*. It uses a low-power, highly focused UV laser to trace out successive cross-sections of a three-dimensional object in a vat of liquid photosensitive polymer.

Table 7. Stereolitography properties

Abbreviation:	*SLA*
Material type:	*Liquid (Photopolymer)*
Materials:	*• Thermoplastics (Elastomers)*
Max part size:	*1498.6 x 749.3 x 500.38 mm (59.00 x 29.50 x 19.70 in.)*
Min feature size:	*0.1016 mm (0.004 in.)*
Min layer thickness:	*0.0254 mm (0.0010 in.)*
Tolerance:	*0.127 mm (0.0050 in.)*
Surface finish:	*Smooth*
Build speed:	*Average*
Applications:	*Form/fit testing, Functional testing, Rapid tooling patterns, Snap fits, Very detailed parts, Presentation models, High heat applications*

As the laser traces the layer, the polymer solidifies and the excess areas are left as liquid. When a layer is completed, a leveling blade is moved across the surface to smooth it before depositing the next layer. As in other technologies (LOM, EBM) the platform is lowered by a distance equal to the layer thickness (typically 0.05 mm), and a subsequent layer is formed on top of the previously completed layers. This process of tracing and smoothing is repeated until the build is complete. Once complete, the part is elevated above the vat and drained. Excess polymer is swabbed or rinsed away from the surfaces. In many cases, a final cure is given by placing the part in a UV oven. After the final cure, supports are cut off the part and surfaces are polished, sanded or otherwise finished.

Recently expired patents protecting SLA technology are releasing the monopolistic control over processes that have been held by the original pioneers of the 3D printing industry. This is the case of liquid-based SLA, which is becoming a major field of study for many firms, who seek to make this technology faster. Although Carbon has pioneered their own take on SLA through their Continuous Liquid Interface Production (CLIP) method, it is derived from a process patented by Chuck in 1986 before the foundation of 3D Systems Inc. to commercialize it (*Schoffer, 2016*).

2.3.9.3. Selective Laser Sintering (SLS)

SLS was developed at the University of Texas in Austin, by Carl Deckard and colleagues. The technology was patented in 1989 and was originally sold by DTM Corporation. DTM was acquired by 3D Systems in 2001.

The basic concept of SLS is similar to that of SLA. It uses a moving laser beam to trace and selectively sinter powdered polymer and/or metal composite materials into successive cross-sections of a three-dimensional part. As in all rapid prototyping processes, the parts are built upon a platform that adjusts in height equal to the thickness of the layer being built. Additional powder is deposited on top of each solidified layer and sintered. This powder is rolled onto the platform from a bin before building the layer. The powder is maintained at an elevated temperature so that it fuses easily upon exposure to the laser.

Table 8. Selective Laser Sintering properties

Abbreviation:	SLS
Material type:	Powder (Polymer)
Materials:	• Thermoplastics such as Nylon, Polyamide, and Polystyrene; • Elastomers; • Composites
Max part size:	558.8 x 558.8 x 762 mm (22.00 x 22.00 x 30.00 in.)
Min feature size:	0.127 mm (0.005 in.)
Min layer thickness:	0.1016 mm (0.0040 in.)
Tolerance:	0.254 (0.0100 in.)
Surface finish:	Average
Build speed:	Fast
Applications:	Form/fit, functional testing; Rapid tooling; undetailed parts; snap-fits; living hinges, high-heat

Unlike SLA, special support structures are not required because the excess powder in each layer acts as a support to the part being built. With the metal composite material, the SLS process solidifies a polymer binder material around steel powder (100 micron diameter) one slice at a time, forming the part. The part is then placed in a furnace, at temperatures in excess of 900 °C, where the polymer binder is burned off and the part is infiltrated with bronze to improve its density. The burn-off and infiltration procedures typically take about one day, after which secondary machining and finishing is performed. Recent improvements in accuracy and resolution, and reduction in stair-stepping, have minimized the need for secondary machining and finishing. SLS allows for a wide range of materials, including nylon, glass-filled nylon, SOMOS (rubber-like), Truform (investment casting), and the previously discussed metal composite.

Interestingly, a foundation patent related to laser technology by Fraunhofer Institute will expire in December, 2016. It is uncertain how this and other recently expired patents will affect the development of the technology, although it can be argued that, as in many other cases –such as FDM, the pricing of the technology will drop considerably *(Germany Patent No. DE 19649865 C1, 1998*). This patent affects not only SLS, but also DMLS and other metal 3D printing technologies.

2.3.9.4. Living materials and experimental printing

There exist a growing interest in the use of living materials and organic composites for printing purposes that go beyond the capabilities of the afore exposed printing methods. Efforts focus on the advancement of technologies that combine natural growth processes (such as silk formation by worms) with artificially enhanced production processes (i.e. scaffoldings). The following examples explore the boundaries between natural and artificial, and intend to become breakthrough projects that promote a seamless mix between those, thus far, differentiated realms.

Fig. 20. In Vitro Meat Habitat: Mitchel Joachim, Eric Tan, Oliver Medvedik, Maria Aiolova

The "In Vitro Meat Habitat" *(Joachim, Tan, Medvedik, & Aiolova, 2011*) architectural proposal for the fabrication of 3D printed extruded pig cells to form real organic dwellings is intended to be a "victimless shelter", as no sentient being was harmed in the laboratory growth of the skin. Mitchel Joachim's Terreform One used sodium benzoate as a preservative to kill yeasts, bacteria, and fungi. Other material in the model matrix are: collagen powder, xanthan gum, mannitol, cochineal, sodium pyrophosphate, and recycled PET for the plastic scaffold. The concept model consists of essentially very expensive fitted cured pork or articulated swine leather with an extensive shelf life.

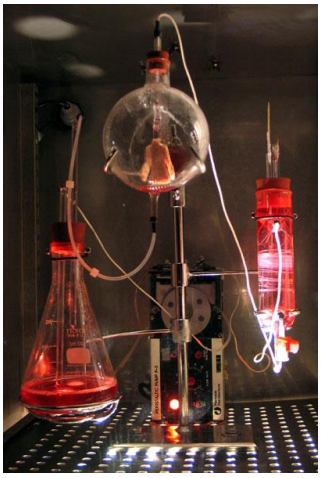

Fig. 21. Victimless leather (SymbioticA)

Another example of this technology, "*Victimless Leather - A prototype of Stitch-less Jacket grown in a Technoscientific body*" by SymbioticA (*Catts O. a., 2006; Catts & Zurr, 2002*) was displayed at MOMA in 2008 under the "Design and Elastic Mind" exhibition to prove that it was not only possible to create artificial living objects, but also that it was possible to do so without sacrificing actual animals. Again, this project uses a plastic scaffold as base for the formation of the final object of the shape. The firm expects to be able to scale up the project shortly.

The Silk Pavilion by the Mediated Matter Group at the MIT Media Lab (*Bader, et al., 2016*) explores the relationship between digital and biological fabrication on product and architectural scales. The project consists of a multi-phase installation, where a primary structure is laid out by CNC automations in order to serve as scaffolding for silkworms that utterly produce the actual finish fabric. As a result, the pavilion consists of a series of standard modular structures that are tied together. The modules' enclosure is built by worms, which segregate natural silk over the primary scaffold.

Fig. 22. Silk pavilion (Wired, 2013)

The primary structure was conceived by 26 polygonal panels made of silk threads laid down by a CNC machine. Inspired by the silkworm's ability to generate 3D cocoons out of a single multi-property silk thread, the overall geometry of the pavilion was created using an algorithm that assigns a single continuous thread across patches providing various degrees of density. The overall density variation was informed by the silkworm swarm itself deployed as a biological "printer" in the creation of the secondary structure. A swarm of 6,500 silkworms was positioned at the bottom rim of the scaffold spinning flat nonwoven silk patches as they locally reinforced the gaps across CNC-deposited silk fibers. Following their pupation stage the silkworms were removed. In the team's view, resulting moths can produce 1.5 million eggs with the enough potential as to construct up to 250 additional pavilions.

Although quite pre-defined in the beginning by means of algorithmic pre-calculations that established lighter (scarce) and darker (dense) areas, the project proved that the use of a natural environment and living creatures would leave some space for unpredicted results. Affected by spatial and environmental conditions including geometrical density as well as variation in natural light and heat, the silkworms were found to migrate to darker and denser areas. Desired light effects informed variations in material organization across the surface area of the structure.

As part of the design space definition and specific project condition, a season-specific sun path diagram dictated the location, size and density of apertures within the structure in order to lock-in rays of natural light entering the pavilion from the desired orientations.

On the other hand, parallel basic research explored the use of silkworms as entities that can "compute" material organization based on external performance criteria. The research team monitored the silkworms through tiny magnets attached to their bodies, in an attempt to understand the logic behind the formation of non-woven fiber structures generated by the silkworms. This logic can be regarded as a computational schema for determining shape and material optimization of fiber-based surface structures for further works.

The project is a collaboration between the Research and Design by the Mediated Matter Group at the MIT Media Lab in collaboration with Professor Fiorenzo Omenetto from TUFTS University and Dr. James Weaver (WYSS Institute, Harvard University). The research group also focuses on growable and 3D printable technology, as can be seen in their wearable skins project *(Bader, et al., 2016)*.

2.4. Large 3D printing technologies

The success of 3D printing technologies has reached a peak as far as industry penetration is concerned. As a result, this method is infiltrating more industries in a cascade manner, and reaching the general public for the small-scale or RP, while expanding quickly in order to create machines able to produce larger, final parts. Besides this process of industrial democratization through infiltration, it also important to point out that many of the protected Industrial Properties (IPs) are becoming open to the general public, process that is facilitated by the fact that the main related patents are currently expiring or near to expire. Furthermore, it is not rare to find cases where the development of certain technological advancements by industrial companies is due to the abuse of protected industrial products and/or patents – shown in section 2.6, which might have been arguably violated. The present section deals with the latest research fronts related to the blooming oversize 3D printing projects in the field of large-scale products in a variety of industrial sectors, mainly pointing at the construction field, the aerospace engineering industry, and the automotive sector.

2.4.1.1. General Principles

So far, large-scale 3D printing technologies follow the same principles as their rapid prototyping counterparts, explained in detail in the previous sections. Despite a certain degree of homogenization in 3D printing technologies, the market is currently undergoing a radical process of transformation, democratization, and expansion. In the architectural and construction industries for instance, 3D printing has evolved to (i) recreate impossible forms, (ii) speed up construction processes, (iii) increase accuracy and control, and (iv) lower material and human costs during the construction phase. The implementation of Building Information Modeling (BIM) by the construction companies –forced by the increasing need of management control by both the public and private sectors- and the adoption of Parametric Design for architecture cope the series of mutually benefiting processes at the design and construction stages for an industry that has traditionally fallen behind more dynamic sectors, such as the already mentioned automotive and aerospace markets. Besides these advantages, there are procedural opportunities to be explored.

Besides merely presentation or informational uses (*Ryder, Ion, Green, Harrison, & Wood, 2002*), 3D printing is involved in the fabrication process as a technique that can either be deployed on site, or used within a factory to utterly deliver the 3D printed pieces to the construction site.

In principle, large-scale 3D printing allows for:

- The enhancement of the quality of the end product through a two-fold control: on the one hand, by issuing material quality tests; on the other, by controlling part production.
- Augmented accuracy due to the lack of construction joints, or through a smarter joint design.
- Higher complexity while maintaining low costs, as any shape can be achieved without the need to develop or build costly molds.
- Structural lightness and material use optimization. The use of composite materials may allow for lighter self-bearing structures that account, in addition to the former, for other relevant building conditions -such as thermal insulation.

2.4.1.2. Deployed technologies and on-site fabrication

On site fabrication stands for any construction method where the whole building or particular pieces are built on site. This means that both the main building form and any other supplies may be produced on demand, as the construction develops in time. Depending on transportation costs, it might be feasible to build a whole factory close to the construction site, or to deploy a portable machine that might carry out all production tasks for the building units.

- **Portable factories**: this approach is currently used in traditional construction. A study of goods transportation costs is required in order to precisely define the practicability of this method as well as to determine the highest supply distance of the factory.

- **Portable machines**: as opposed to the prior method, where a whole factory is deployed, the deployment of robotic machines allows for a larger flexibility during construction. This means, a small truck can navigate the site and stop there where it is needed. The truck would carry a container where the robot is located. The robot, through a series of pre-programmed activities and routines, could then accomplish a series of complex tasks until its help is no longer required or the building has been completely finished.

This technique has been proven right by ETH PhD students, who, with the help of an ABB robot and pre-programmed routines, built a brick wall on site. Although this exercise deals with additive fabrication with prefabricated bricks, it can be easily extrapolated to 3D printing processes, as robots serve as a sheer geometrical interfaces with the construction procedure -as it has been said above, they are used to "navigate" the space through a series of well ordered, virtual workplanes.

A rail (commonly named track) attached to the floor of the transportation container completes the movement of the robotic arm, and allows to enhances the robot's performance as it increments the arm's reach distance along the length of the external axis.

Fig. 23. R.O.B., deployable robotic arm to build architectonical elements on site. (*ETH Zürich with Gramazio & Kohler, 2008*)

2.4.1.3. (De) localized pre fabrication

De-localized fabrication covers any type of fabrication that favors controlled, enclosed fabrication spaces or environments located far from the building site. Although this is generally the case in traditional architecture for most of the elements involved in the construction process -particularly in pre-fabrication-, it can also be applied to large 3D printed objects or buildings. This case would probably be of interest in highly developed countries, where labor costs are high or directly massive. As 3D printing technologies applied to architectural issues become a real option and a feasible fabrication choice, it is crucial to define whether or not a certain 3D printing technology can be successfully applied to this type of construction.

Besides the prefabrication of walls, roofs, ceilings, or other building components, 3D printing stands out for its capacity to assemble or create customized elements, especially when dealing with highly complex geometrical parts, whether they can be categorized as principal or structural building elements or not. The integration of different technologies and materials can result in finished 3D printed models that, after a series of tests and checks, can serve as high-end products.

2.4.1.4. Industrial robots as research tools

Robots can be regarded as the late-comers to large-scale fabrication methodologies in general and 3D printing methods in particular. The following institutions and research developments stand out particularly for their take on the flexibility of use of robot arms and innovative fabrication. Not only can large 3D printers help conceptualize many technical concepts that are too often addressed theoretically in many universities (*Lipson, 2007*), they are also capable of pushing the boundaries of academic research.

- The ETH can be considered a pioneer in the application of advanced industrialized methods with architectural focus, and lead the research in the field. The school owns several robots that they use as basis to explore both additive and subtractive fabrication. Among other examples, the ETH Space Frame 3D printing (*ETH Zürich with SEC Singapore, 2012-2016*) project is remarkable in its take on scaffold-less construction. This particular research emphasizes the need to control robot speed, strategy, and use in an attempt to combine material constraints and built forms (*ETH Zürich, 2015*).

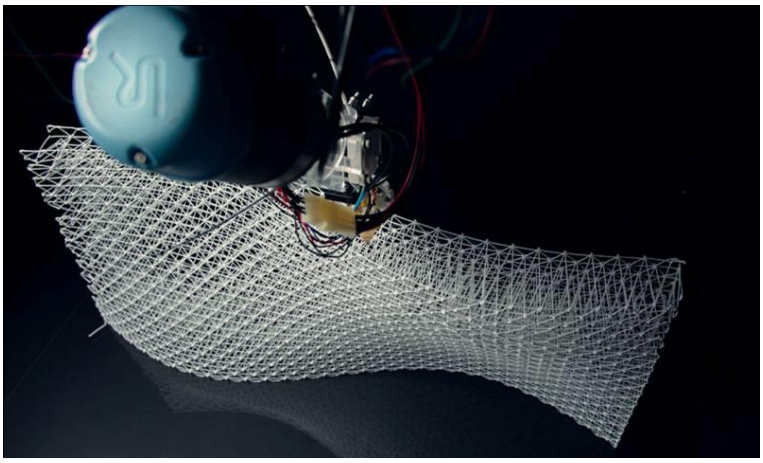

Fig. 24. ETH Space Frame 3D printing - mesh mold.

- The Bartlett School in London is also currently devoting a significant amount of efforts to the development of robot-based construction processes. Among other projects, Bartlett students developed a dome out of robot-cut foam pieces. They did so by using HAL software for Grasshopper, a platform that allows for easy robot control and programming. The Nexorade and Reciprocal Structures Robotic Workshops deals precisely with this kind of geometries and processes (*Schwartz, Gobin, & Bartlett School of Architecture, 2013*).

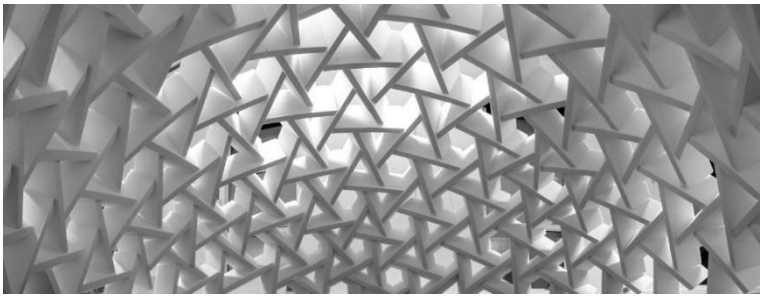

Fig. 25. The Nexorade Dome. (*Schwartz, Gobin, & Bartlett School of Architecture, 2013*)

- R&Sie is a Paris based practice focusing on alternative architectural procedures. Their work emphasizes robotic structures that mimic real biological processes with standard construction products.
- The EPSRC Centre for Innovative Manufacturing in Additive Manufacturing in UK, which concentrates a number of key Academic and Industrial Partners, including the University of Nottingham, Leighsborough University, the Boeing Company, TWI Ltd., and EOS GmbH., among others.

2.4.1.5. Full-scale 3D printing technologies applied in AEC related sectors

The main big scale 3D printing technologies typically tend to mimic -or even inherit- the processes that permit small-scale 3D printing. This means, oversize approaches to 3D printing essentially operate as scaled-up versions of their small-scale counterparts, replicating the latter's structures, functional boundaries, logics, and even materials. The most prominent oversize 3D printing technologies up to date

are Contour Crafting (CC) and D-Shape, which agglutinate and represent most of the takes and envisions on full-scale developments. While CC intents to replicate the FDM model through a nozzle-extrusion paradigm, D-Shape is a quite literal translation of the SLA printers discussed in previous sections.

2.4.1.6. Contour crafting

This technique uses a hanging nozzle or extruder that follows a predetermined path which takes material hardening times into account in order to create the design. The material, presented in a semi-fluid state, is extruded through an arm that moves in 3D space forming parallel layers. This procedure is probably the most widespread among 3D printed building applications.

In essence, the process produces a replacement for the structural concrete block wall commonly used in house construction. The process extrudes the internal and external 'skin' of the wall to form a permanent shutter that is then backfilled this with a bulk compound similar to concrete. Using thixotropic materials with rapid curing properties and low shrinkage characteristics, consecutive layers of the wall can be rapidly built up. The wall material deposition process is a two stage operation. In order to improve the finish of the visible surfaces, the shutter material is shaped by a secondary manipulator, or trowel, as it is extruded. The combination of processes results in a system that can deposit (relatively) large quantities of material while maintaining a high quality surface finish. This technology is currently leading the field in terms of a demonstrated new approach to automating the construction process.

Contour crafting was developed by Professor Behrokh Khoshnevis, and is subject of various patents -some of which have expired or will expire in a near future *(University of Southern California, 2014*). The process uses techniques from Computer Aided Manufacturing -CAM, which has been scaled-up and applied to construction, in Khoshnevis words (*Khoshnevis, Hwang, Yao, & Yeh, 2006*).

Fig. 26. Contour Crafting Nozzle extruding concrete *(University of Southern California, 2014*)

Some applications of contour crafting technology include the construction of regular homes, dwellings for developing countries, or the deployment of shelters after natural disasters. Nevertheless, one of the most critical points of these applications is that the cost reductions may target the wrong factors, as human labor is very inexpensive in developing countries or under any of the afore mentioned situations.

One of these state-of-the-art examples using this very technique is a project by WinSun materials, company that claims to have built 10 dwelling units in a single day. This company seems to have violated the patents held by USC and Professor Khoshnevis, as they use the exact same infill and extrusion technique referenced in their patents, which can be seen in section 2.6 (*United States Patent No. US 5121329, 1992*). Ma Yihe's company, as opposed to traditional contour crafting envisions, produces the elements -concrete walls, roofs, and others- in factories, and transports them to the building site. The company is said to own a 32 meter long, 10 meter wide and 6.6 meter high printer in gantry form, although it is quite difficult to find reliable information on this matter due to the company's opaque information policy. As previously said, the printer builds the structural elements in a layer by layer fashion, whereby the walls acquire extra rigidity through a reticulated reinforcement that mimics the original USC model.

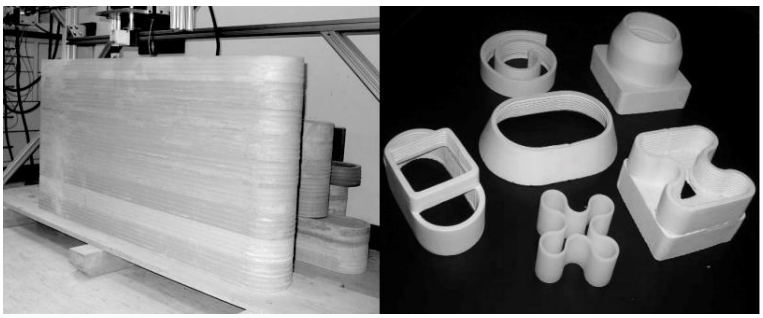

Fig. 27. Real scale contour crafted wall and scaled-down part models.

According to the company, the printer uses a composite material which combines a cement matrix and glass fibers. Pursuing China's green agenda, WinSun said in the future it plans to use scrap material left over from construction and mining sites to build its 3D constructions. However, it is crucial to at least consider structural and material regulations that might restrict this idea, as many developed countries in the world do not allow the use of waste material for building purposes in general and structural applications in particular. Despite the emergence and consolidation of Green Certifications worldwide (being LEED, BREEAM, and the Standard Passiv House the most relevant examples) that grant the use of local and recycled materials, building construction companies are still reluctant to do so. In addition to this position, the public sector is not yet flexible enough as to seriously think about the implementation of such solutions.

As explained above, ROB's 3D printer creates building blocks by layering up the cement/glass mix in triangular structural reinforcement patterns. The diagonal print pattern leaves plenty of air gaps to act as insulation in the fabricator's vision, although this might also be argued against –it is common ground that air does not work properly as thermal insulation when gaps are too wide, and that it behaves very poorly against sound and noise, having thus very weak performance as insulation "material".

These blocks are printed in a central factory, transported, and rapidly assembled on site. The parts are allegedly calculated using traditional CAD software for drawing the architectural plans, and taking care of considering insulation materials, plumbing, electrical lining and windows, which can later be outfitted once the main structure is assembled.

Fig. 28. WinSun new materials Singapore home

In the 2014 World 3D Printing Technology Industry Conference and Exhibition, Quindao Unique Technology Co. Ltd. Rolled out the largest 3D printer in the world *(Feng & Yuhong, 2014*), which suffered from the same problems attributable to the Winsun model, and arguably presenting a fabrication technology similar in principle to that of the KamerMaker (see section 2.4.5.3).

2.4.1.7. D-Shape

The other most successful big scale 3D Printing technology to date, D-Shape, has been developed by the Italian inventor Enrico Dini (*Dini, 2016; World Patent No. WO2006100556 A3 also publised as US20080148683 / EP1868793A2 / CN101146666A, 2007*). In this case, the printer is capable of printing a two story building using thin layers of sand and an inorganic binder, which Dini describes as resembling a

certain sort of marble-like material. As in regular professional 3D printers, it prints the structure objects from the bottom up, depositing the sand and binder mixture in 5-10 mm layers. Upon contact of both materials, the solidification process starts and the printer head adds a new layer. If applied to construction and architectural purposes, the vertical sections of the house requiring increased strength will be printed in a way that becomes formwork in which concrete could eventually be in-filled.

Fig. 29. Radiolaria project, a proof of concept of the D-Shape printer

Out of the many different examples that the printer has already produced, the most common D-Shape instance is the Radiolaria project, a construct that shows the possibility of building complex shapes using this technology. The Radiolaria project intends to demonstrate the virtuosity of this printing technique in terms of complex geometries and finish quality.

A real scale project using this technology is the "*Landscape House*" by Janjaap Ruijssenaars, architect at Amsterdam's Universe Architecture firm. This project intends to become the first 3D printed building when completed for the Europan contest.

Fig. 30. Janjaap Ruijssenaars' Landscape House.

2.4.1.8. The Canal House and KamerMaker Project

Canal House, a Dutch project by DUS Architects, is projected to be the first 3D printed house (*Fairs, 2013*). Printing works began with 1:20 scaled down building parts. Less than a year after the completion of the mock-up, the company moved onto the real scale realm, the actual 3D printing of the components for the “first” 3D printed house.

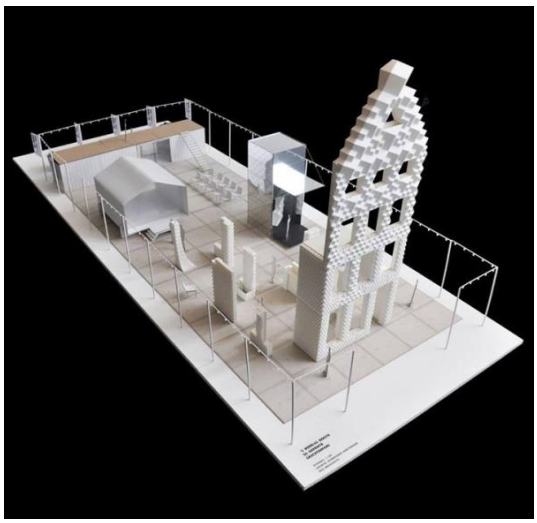

Fig. 31. Model of 3D print Canal House

The House is being printed using FDM, a common technique mentioned above with an ad-hoc printer called KamerMaker (translated as room maker). The KamerMaker XL, a 3.5 m tall printer, made its way to the Buiksloter Canal in Amsterdam, where it already printed some parts. The printer, to a certain extent similar to a large RepRap housed inside a shipping container, is using a type of plastic -an 80% bio-based Hotmelt, developed by German chemical company Henkel. The KamerMaker is the world's first movable large-scale 3D printer. It can print rooms and inhabitation spaces up to 3.0 meter long, 2.4 meter wide, and 3.0 meter high in the PLA-based, eco-concrete hotmelt material.

Each room is printed separately on site according to the scheme shown in Figure 32 before being assembled into the house unit. This way, rooms are oriented in a controlled environment and can be further carefully tested in a safe and easy accessible manner. Thus, printing errors can be prevented and minimized. All rooms are different and consist of complex, tailor-made architectural elements displaying unique design features. The rooms themselves consist of several parts, which are joined together as large Lego-like blocks. As a result, the house has a hierarchical printable structure, which eventually allows for easy part substitution.

In addition to being assembly-capable, the rooms are entirely structurally sound and complete as independent, self-bearing elements. In a second phase of the project, the separate rooms are utterly assembled into connected floors, and then stacked into the entire house. A subsidiary, yet handy, advantage is that rooms can fairly easy be disconnected in case the house needs to be relocated.

Both the outside façade and the interior are printed at once in a single element. Within the 3D printed walls are spare spaces for connecting construction, cables, pipes, communication techniques, wiring and more. The mechanical, electrical, and plumbing systems shafts inside the walls are a sheer consequence of the way the infill pattern is thought. The 6m wall has shafts of different dimensions. The larger structural shaft runs towards the locations where adjacent rooms need support. These shafts will be cast with a different material, a sort of Eco-concrete developed also by Henkel. As a consequence, the shafts will constitute the structural framework of the house. Both sides of the wall have a different set of shafts. On one side the shafts have a slight inclination from bottom-right to upper-left, while on the other side of the wall the shafts run in the opposite direction. This way the two sides together create structural crosses for structural stiffening against horizontal forces.

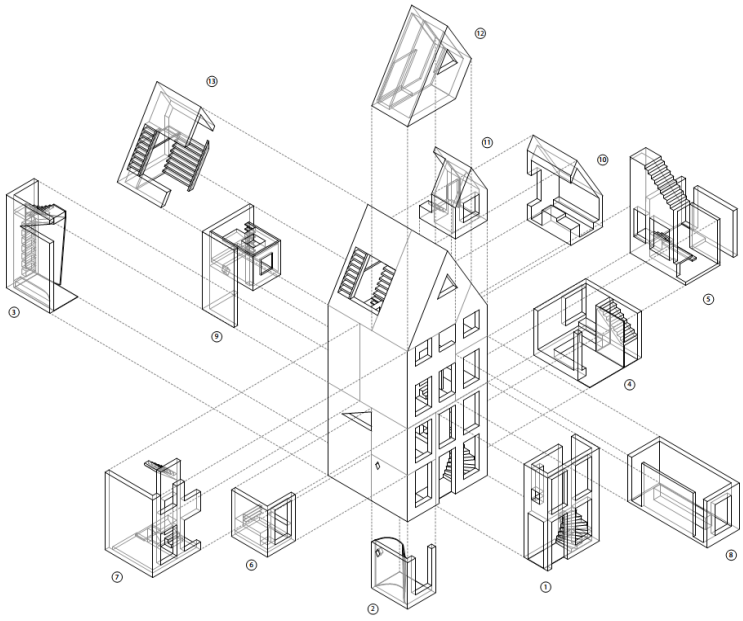

Fig. 32. Displaced axonometric view of the Canal House project showing its modules.

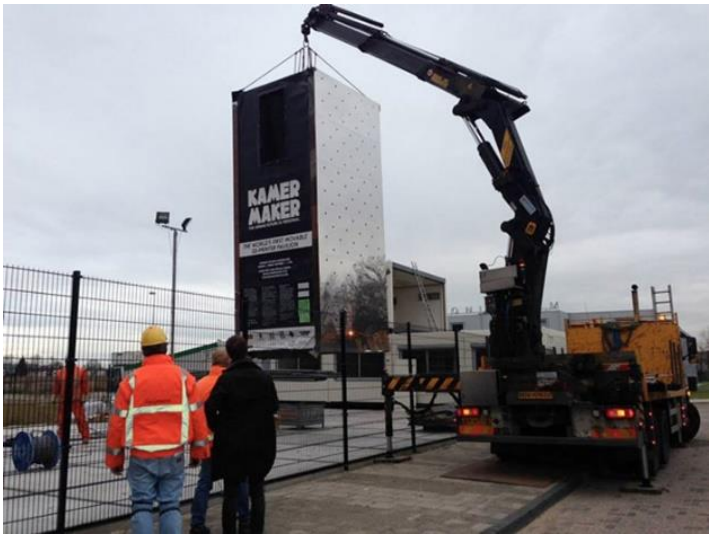

Fig. 33. KamerMaker 3D printer by DUS Architects

The design of the house makes use of the latest parametric technology available for architecture, and all the different parameters mentioned previously –shaft size, infill patterns- are scripted. The structure is also programmed, allowing the designers to control the stress and strength of the different parts while generating ornament. This allows to change the dimensions of the structural shafts during the design process to match the structural demands from the structural engineer partner Tentech, without redrawing the complex design over and over. Furthermore, it also permits the optimization of angled shading for exact solar angles, as well as other smart features commonly used in architecture. Heijmans, the project's construction partner, takes charge in building the house and developing new means of connecting the diverse modular elements together.

2.4.1.9. The Spider-Bot Project

The spider-Bot project is a large scale 3D printer designed and developed at the MIT media Lab in Boston, Massachusetts. It consists of a cable-suspended robotic gantry system that provides an easily deployable platform from which to print large structures. The main body is composed of a deposition

nozzle, a reservoir of material, and parallel winching electric motors. Cables from the robot are connected to stable points high in the environment, such as large trees or buildings.

This actuation arrangement is capable of moving large distances without the need for more conventional linear guides, much like a spider does. The system is easy to set up for mobile projects, and is thought to afford sufficient printing resolution and build volume as to be employed in real-scale production lines. Fast-curing materials like expanding polyurethane foam can be deposited to create a building-scale printed object rapidly.

Similar proposals take advantage of the ability of cable-driven hardware to cover extremely large spans and workspaces, something that becomes evident in other applications, such as the SpiderCam or SkyCam (*Saber, Abyaneh, & Zohoor, 2010*). One of the most relevant examples is the Six-Degree Freedom Cable-Suspended Parallel Mechanism for foam 3D printing developed at Laval University in Quebec (*Barnett & Gosselin, 2015*).

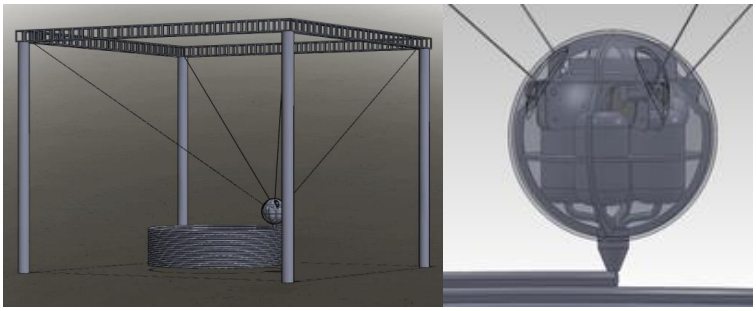

Fig. 34. SpiderBot architecture and toolkit

Another interesting feature of cable-suspended effectors is the use of tensioned elements, like ropes or cables in different forms, such as weaving. With these tensioned elements, unique structures such as bridges or webs can be wrapped, woven, or strung around environmental features or previously printed materials.

2.4.1.10. Swarm Printing

Another novel approach adopted in MIT Media Lab is based on mobile swarm printing that allows small robotic agents to construct large structures. The robotic agents extrude a fast curing material which serves both as a concrete mold for structural walls and as a thermal insulation layer.

Similarly to the KamerMaker printer project and other large-scale 3D printing methods alike, this technique is supposed to offer many benefits over traditional construction methods, such as speed, the possibility to recreate custom geometry, and lowered cost. As well, direct integration of building utilities like wiring and plumbing can be theoretically incorporated into the printing process, and it is also expected that the 3D printing process will eventually include all possible building systems.

As explained in previous sections, some architects are betting for a hybrid approach that consists of 3D printing parts of the building in a highly controlled or monitored environment (such as a factory) to utterly assemble them on site. This belief stems from the fact that it is still today more feasible than printing whole buildings given the current state of development of the technology. Printing parts is safer, easily controllable, and has a lesser cost impact on the whole building process than whole building parts or even complete installations. Furthermore, it would reduce the chances of fabricating or producing erroneous wholes, therefore minimizing construction and financial risks. The ProtoHouse (*Dezeen, 2012*), designed by the London based architecture team Softkill, follows this approach –see figure 35.

The Institute for Advanced Architecture of Catalonia has also developed a drone–like prototype that aims at automatically and autonomously building whole structures. The IAAC robotic vehicle consists of a small nozzle attached to a vacuum system provided with wheels that makes it suitable for navigating wall and steep conditions. The system is supposed to self-recognize pre-standing building parts in order to add missing building elements as it goes.

Fig. 35. ProtoHouse by Softkill Design

2.4.1.11. Local material printing: the Stone Spray project and space exploration

Based on general 3D printing principles, the IAAC Stone Spray project is a variation of the above mentioned techniques that seeks to use local materials to feed the printing nozzle. The authors argue that this research could eventually favor local production, and a smarter material use involving local resources that would eventually result in optimized energy used –both for the reduction of embedded energy and the minimization of transportation costs.

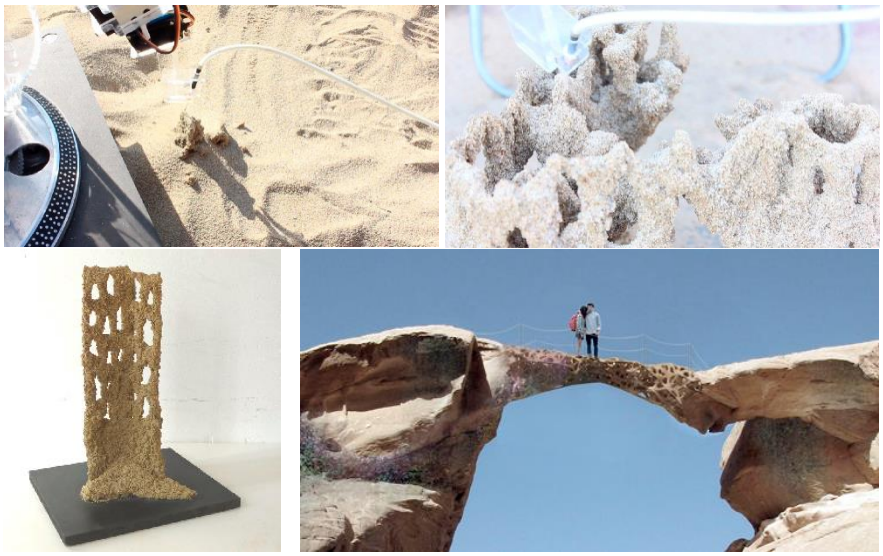

Fig. 36. Stone Spray project

The project case study uses a sand spray and an inorganic binder material to create otherwise impossible three dimensional shapes. The printer feeds itself from beach sand, although it may be capable of using other materials in the future. Although it is only suitable to create small models at the current stage, the project leaders intend to increase the scale of the models to build bridges or housing dwellings. At the current stage, the technology is only able to create relatively uncontrolled geometry, issue that need to be tackled before going into the next level of development. It is uncertain, though, whether or not the project will be interrupted.

On a different level, there is ongoing research on using 3D printing technology to build large structures in extra-terrestrial environments where human labor would be very costly and impractical by making use of local soil as primary printing material. In Europe, the architecture office Foster + Partners are collaborating with the ESA (European Space Agency) to study the feasibility of 3D printing a lunar base using lunar soil (*European Spatial Agency, 2013; Liébana & Nadal, 2016*). In the United States, Behrokh Khoshnevis, inventor of contour crafting, has partnered with NASA on a similar research project: the Contour Crafting Simulation Plan for a Lunar Settlement Infrastructure Build-Up *(Khoshnevis, Carlson,*

Leach, & Thangavelu, 2012). Besides inhabitable structures, they plan to use this technology to build roads, landing pads and aprons, shade walls, dust barriers, thermal and protection shields.

Fig. 37. 3D printed lunar base design

2.4.1.12. The aesthetics of the technology

Digital Grotesque (*Hansmeyer & Dillenburger, 2014*) is a project that uses Java-generated fractal geometry to feed big-size 3D printed parts. As these large 3D printed pieces are combined together, they form interiors that aesthetically resemble grotesque and baroque forms to a certain degree.

The leaders of the project, Michael Hansmeyer and Benjamin Dillenburger, intend to create an architecture that deals with the intricate relationship of chaos and order. This project is arguably the most eminent dissertation about the aesthetic implications of 3D printing. The idea of the project is not as much to develop a certain technology as it is to deal with the intricacies of highly complex geometrical forms while proving the spectrum of functionality that the former has to offer. Indeed, most applications of 3D printing simply intend to produce certainly regular pieces; Digital Grotesque is a project that aims at exactly the contrary: fabricating non-functional pieces impossible to obtain by traditional or industrial production standards.

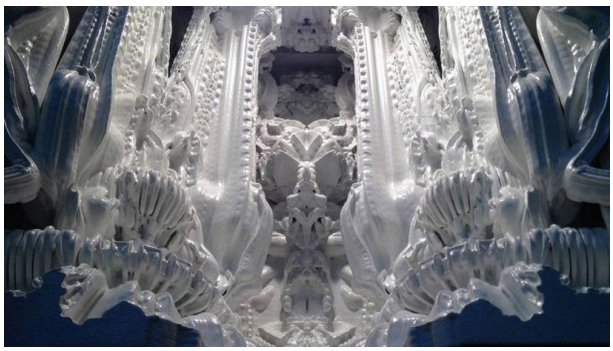

Fig. 38. Digital Grotesque

2.4.2. Metal printing

Large-scale metal printing relies on the adaptation of standard welding technologies. These technologies are already used in the automation of automotive parts, which require strict control of resolution and tolerance conditions. The MX3D project, for instance, makes use of current electro-welding and large robotic arms to develop a fully functional pedestrian bridge in Amsterdam.

Metal 3D printing is another technique related to construction that can be explored for creating full-size parts. Metal printing for small parts has already been developed through SLS techniques, although its adaptation to high-volume objects goes nowadays through the application of standard welding techniques. These unfold new opportunities to explore the fields of complex geometrical forms, intricate reinforcements, and temporary constructions. The MX3D project (*MX3D, 2015; Chowdry, 2015*), for instance, aims at building a full-scale metal bridge in Amsterdam using 3D printing with relatively standard welding techniques, following along other prior examples (Lorenc, Handlon, & Bernold, 2000). These differ slightly from the standard FDM or related printing methods in that it does not require horizontal curve-like inputs, but rather a series of points where material is fused. MX3D claims that they are going to 3D print a fully functional, intricate steel bridge over water in the center of Amsterdam to showcase their technology. In their view, this allows them to 3D print strong, complex and aesthetically intricate structures out of sustainable material at various scales. According to Tim Geurtjens, MX3D's Chief Technical Officer: "*What distinguishes our technology from traditional 3D printing methods is that we work according to the 'Printing Outside the box' principle*". In fact, they rely on the use of 6-axis industrial robots.

The bridge will be designed by Joris Laarman Lab and will, in their words, show how 3D printing finally enters the world of large-scale, functional objects. Although the team argues in favor of the use of sustainable materials in this particular project, this is not the case for metal printing. The team announced that the printed bridge will be installed across the Oudezijds Achterburgwal canal in Amsterdam, although it is still uncertain whether or not the project will be finally realized. A close look at their real development status shows that the technology is still not ready for the end-product fabrication.

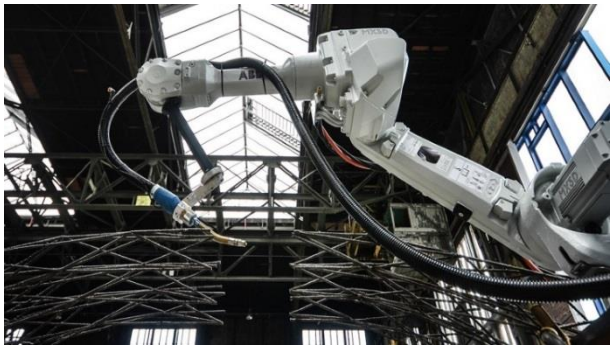

Fig 39. MX3D design for a 3D printed bridge

2.5. Procedures and software

There is a significant amount of literature about Integrated Software Systems in different industrial and research sectors. The following section intends not so much to provide the reader with a general overview of that sort of solutions, but rather to depict a comprehensive software landscape in close relationship to engineering, architectural design, and real scale fabrication.

The utilization of Integrated Systems and advanced design tooling methods within the construction industry is set to increase; architectural modelling is a growing application having many interesting sides (*Kvan & Kolarevic, 2002; Broek, et al., 2002*). Processes such as 3D printing are becoming popular in mainstream architectural modelling applications (*Burry M., 2002*) from early stages of the design process (*Simondetti, 2002*) and increasingly into construction-related phases. As named in Section 2.4.5.6., leading architects Foster and Partners (London, UK), for example, have a dedicated machine used by their Specialist Modelling Group to implement these methods using local materials from the project's environment. This is a growing tendency rapidly spreading throughout the design, architectural and construction ecosystems. Rapid Prototyping processes can be applied, conceptually at least, at any scale from desktop model to full

scale building construction. Modelling is a typical application today, while full scale construction is more speculative and is, despite the most recent contributions, beyond the latest advances in 3D printing (*Dimitrov, Schreve, & de Beer, 2006*).

The research on solutions herein focuses thus on specific hardware and software, such as proprietary and free software packages for control of robotic arms. The difficulties, advantages, and disadvantages of each solution as well as their construction applications are also discussed for a better understanding of the topic.

2.5.1. CAD software for architecture

Architectural design CAD programs are not always suitable or intended for fabrication purposes. The more specialized CAD programs become, the more difficult it turns to overcome technical difficulties inherent to the amount of information embedded in the virtual models on the one hand, and to become fluent in the software's design. In other words, the overwhelming complexity of professional Computer Aided Design software can occasionally become a serious limitation for the user.

Although it is discussed further in future sections of the thesis, architecture-oriented software can be basically divided into two main groups, aside urban design packages:

(i) software oriented towards design and/or fabrication, and

(ii) software oriented towards building design and management. It may seem possible that both groups have a common ground, but this is not really the case.

Fabrication-related design software (Computer Aided Manufacturing, commonly known as CAM) provides tooling for both architectural and product solutions, while management-oriented software goes in a different direction by offering large database capabilities that allow all building agents to control the design-to-construction workflow. This model is commonly referred to as BIM –BIM has been mentioned in section 2.4.1.

BIM models are essentially gigantic geometric-based databases, which account for cost, phasing, timing, calculations (*Chi, Wang, & Jiao, 2015*) and other management information that is normally not required for fabrication. BIM intends to incorporate all possible building information into a single building model, a sort of a comprehensive solution that starts from the design phase and spreads over to the building management phase or even beyond. These models are indeed compelling and useful, and provide incredibly valuable information to the user, but are heavy and sometimes overkill for many lighter applications. In addition to that, BIM-based projects require integration of disciplines, preparation and a high degree of specialization.

As opposed to BIM, generic 3D modelling software -such as Rhinoceros- responds better and quicker to the either simple or complex geometrical descriptions of the 3D virtual models, as it does not take further information into account. This software deals easily with non-informed models and treats them from a sheer geometrical point of view by means of either NURBs (Non-Uniform Rational Bezier Splines) or mesh topologies. These differ in their "inner" geometry conception; in fact, NURBS are parametric-driven (this is, formula-based) geometric objects, whereas meshes are, at all effects, sorted point-clouds defining either surfaces or solids. Also, NURBS are based on a strong hierarchical organization of objects, in such a way that, for instance, polysurfaces are sets of surfaces, which are driven by curves, which, in turn, depend on points. NURBS are easily translatable intro meshes, constituted by a set of generally triangular, planar faces matching a point-cloud distribution. The opposite operation, translating meshes into surfaces implies a good amount of reverse-engineering and are, thus, less prone to use in applications where a high degree of precision is required. Furthermore, spline-based software can be easily parameterized, allowing for faster and accurate results.

Parametric software has gained momentum in the last 10 years in sectors related to architecture, engineering, and construction. Its application to architecture and construction has opened and enlarged a way for architects that desire to develop complex ideas, intricate geometries, or even increase their control on ad-hoc informed models. For example, parametric software has allowed architects and builders alike to create unprecedented complex building envelopes thanks to the ability to discretize geometry through finite element models. This way, double curved surfaces can be approximated by a set of planar surfaces utterly

realized by glass or planar surfaces. This software has also found its place among the most relevant tools for design and fabrication. Please refer to chapter 3 for a more in-depth explanation of the impact of software in AEC industries.

Some of the most used modelling and design software used in architecture are described below briefly. The increasingly growing and complex software ecosystem is hardly graspable, so the focus is placed on design software packages, which share common capabilities and target the same operability aiming at the broadest spectrum possible of design interfaces. It is not intended to name every single solution, but rather to provide the reader with a list of applications and utilities that share common intentions and capabilities.

2.5.1.1. Modeling and parametric software

Modelling and parametric software: The use of McNeel© Rhinoceros (McNeel & Associates, 2016) in architecture has become increasingly popular. In part due to the similarities it has with Autodesk© AutoCAD (*Autodesk, Inc., 2016*), it is easy and quick to learn, but without many of the drawbacks from the former. One of the features the developers try to highlight and enhance continuously is its scripting capabilities, along with its parametric interface, Grasshopper. Rhinoceros is a relatively lightweight NURBS-based software that is able to produce and handle all sorts of geometry.

This makes it an ideal platform for advanced users that like to generate their own custom scripts, create generative systems (*Sass & Oxman, 2006*), or logic models. Both its scripting interface and its visual scripting interface for parametric developments are open for 3rd party developers and are easy to learn and use by any user. Due to this fact, Rhinoceros and Grasshopper are widely used in the fabrication industry, and constitute the most outstanding example of design software.

As said above, the addition of the Grasshopper visual programming interface for Rhinoceros allows users with no programming skills to easily automate tasks like contouring, nesting, labeling and many other geometric manipulations required for design and fabrication. The software, despite many limitations for advanced users (Grasshopper does not allow to use built-in recursive algorithms, for instance), is a great tool for creating intelligent and responsive systems. Rhinoceros also offers a variety of solutions for CAD-CAM integration, although these will be studied in future sections.

2.5.1.2. BIM software

The most representative BIM packages are the Autodesk© Revit (*Autodesk, Inc., 2016*), Graphisoft© Archicad (*Graphisoft SE, Nemetschek Group, 2016*), Nemetschek© Allplan *(AllPlan Systems, Nemetschek Group, 2016*), and Bentley© Microstation (*Bentley Systems, Inc., 2016*) software suites.

These allow for highly complex models both from an information and geometry point of view. Their association to internal databases makes this software highly desirable for architectural or engineering models, but constitutes a downside when it comes to pricing and rapid prototyping. As they focus on information management, they usually lack the proper tools for proficient users to produce the necessary geometric manipulations required for custom digital fabrication. On the other hand, if a digital fabrication method can become streamlined enough and not much input is required by the end user, a third party developer may write a plugin that transforms the BIM geometry data into a CNC machine tool path or robot program.

Whereas Rhinoceros is quite suitable for design and fabrication, BIM is not normally used for fabrication purposes. Nonetheless, BIM software is usually capable of exporting 3D virtual model data in one or more of the following CAD formats: International Geometry Export Standard (IGES), Stereolitography (STL), Object (OBJ), STEP, PART, or others. From those, mainly IGES and STL are considered standard file formats for 3D solid models.

Finally, there is a growing interest in free, non-proprietary software development for BIM design, which is often based on the emergent Industry Foundation Classes (IFC) standards developed and supported by the BuildingSmart platform (BuildingSmart, 2017). IFC files are used in the construction industry to enhance interoperability requirements, and allow to export geometry and built-in data fields corresponding to any international classification standard –normally UniClass for the UK market and Omniclass for the North American one (*The OCCS Development Committee, 2017*). These are means of organizing and

retrieving information specifically design for the construction industry. In addition, data may as well be further extended by user-defined fields in order to improve the flexibility of the system. Nonetheless, this interoperability is constrained to architecture and construction, where these standards emerged.

Beside the previously mentioned programs, CYPE Open BIM modeler tool is probably of the outmost interest, especially in the Spanish market. Other BIM-based software would include Trimble© Tekla, Autodesk© Civil 3D, Navisworks, and Infraworks, and Bentley© Power Rail Track, In-Roads and others.

2.5.1.3. Standard architectural and engineering software

From the whole software ecosystem, Autodesk© AutoCAD stands out for itself. It is indeed the most widely used software by architects and engineers alike. AutoCAD is mainly used for 2D drafting of plans, sections, elevations, and all sorts of architectural drawings. Its Drawing Exchange Format DXF has become an exchange standard both for two-dimensional and three-dimensional designs and even for fabrication. AutoCAD's 2D drafting capabilities and ease of use is extremely useful for simple 2D fabrication like laser cutting, water jet cutting, CNC machines, but not as much so for more complex digital fabrication methods. Over the years the software has greatly improved its 3D modelling capabilities but it is still considered less flexible that alternatives like Rhinoceros by users.

2.5.1.4. Software for fabrication and CAM. Process specific software.

CAM software is very process-specific. This means that, although a design can be produced by a number of different means or techniques -and constitute a single file, the construction technique is influenced by the actual production machine, which forces a specific bidirectional communication from the software or controller to that machine. Fabrication software, thus, depends both on the platform on which the design has been modeled, and the machine where it is to be built.

Many machine manufacturers produce their own software that convert standard 3D models into a set of instructions or program that their machine will process for fabrication. The tool path (the motion the machine needs to follow) for some methods like laser cutting, 3D printing or milling are tested so that the user rarely requires advanced programming or customization. These programs are usually written in G-Code, a programming language for fabrication, although some manufacturers develop their own.

Besides standalone CAM software, most vendors supply plugins that integrate with 3D modelling software used by engineers and designers alike, thus allowing for a complete design-to-fabrication workflow within the same environment or design suite.

The following tool classification shows the most relevant packages sorted by their host design software and fabrication methods.

- MecSoft© RhinoCam, MecSoft© FreeMILL, VisualMill, Delcam© PowerMILL. RhinoCAM is suitable for CNC processes, such as milling. This plugin integrates the CAM functionality of the standalone software VisualCAD into Rhinoceros. It allows users to create milling programs directly from 3D objects modeled in Rhinoceros and currently supports up to 5 axis milling machines.
- DeskProto offers solutions for 3D printing and RP. Contrary to other solutions available in the market, DeskProto developers claim to have created a product that focuses on design rather than fabrication, therefore opening up just a tiny window for the fine-tuning of fabrication parameters. It is therefore a suitable tool for users who are inexperienced in CAM.
- Process-specific software for fabrication and CAM also populates the universe of fabrication and design. From these, Grasshopper-specific add-ons are worth mentioning alongside other relatively unexplored software solutions that are listed here for convenience:
    - Grasshopper add-ons: As explained above, a visual programming interface like Grasshopper is useful for advanced users that choose to use digital fabrication methods that require custom manipulation of toolpaths, as it is usually the case when

programming industrial robots. From all available Grasshopper add-ins, these are the most relevant for the study:

- Silkworm is a 3D printing-specific add-on for Grasshopper. This plugin generates a G-Code program for 3D printing while allowing a complete manipulation of the code.
- HAL: Robot Programming and Control (*HAL Robotics Ltd., 2015*): According to the product's description, HAL is a Grasshopper plugin that supports programming ABB, KUKA, and Universal Robots machines. It contains a large component library that allows designers to simulate, program, control, and monitor simple or multi-robots cell in near-real time. HAL facilitates as well I/O management, error handling, and multitasking. It offers specific packages for hotwire cutting, milling and pick & place. The pay version is required in order to obtain full access to simulation and coding functionalities, as well as tooling-specific packs. Nonetheless, the HAL interface is so intricate and complex that it requires a great deal of experience programming real robotic arms.
- RoboFold Godzilla permits simple robotic simulation: this software is based on the fact that robots use simple location planes to inform their position in 3D space. This software offers:
    - I/O management, error handling, and multitasking.
    - Premade tool paths for milling, folding, and 3D printing. Timeline, robots and tools, actions, clash detection, reach, and axis limits. The pay version allows to connect the robot to a Raspberry Pi through the Mechagodzilla Code Generator.
- Robot I.O. software offers simple Grasshopper integration with a variety of robots from different vendors in a similar manner to that of RoboFold Godzilla and HAL, although their data organization and component system is simpler than those. Also, its current implementation is prone to errors.

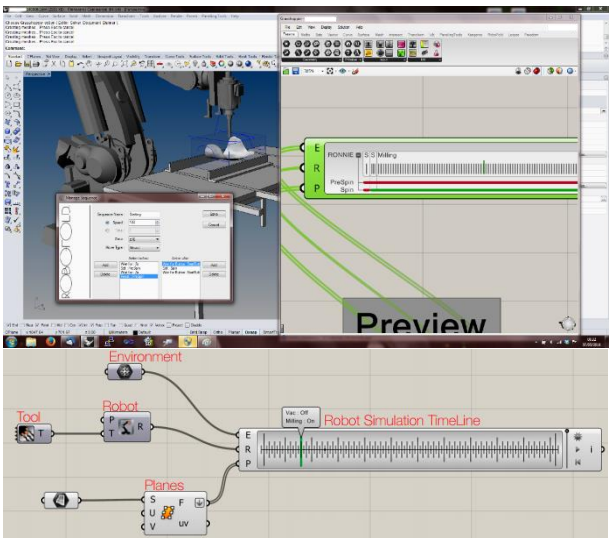

Fig 40. RoboFold and Robot.IO software packages for Grasshopper

Since robots follow a simple sequence of planes in 3D, it is necessary that the user generates this geometry prior to feed the information onto the robot. This is normally a simple procedure in the host Rhinoceros/Grasshopper application. These software packages work mainly with DAT, KRC files, and G-Code.

- CATIA and Digital Project: Used extensively in aerospace, automotive and other engineering disciplines. In architecture it is known for being used to build architect Frank Gehry's popular curved designs. A branch of Gehry's office, Gehry technologies, later developed a specific

software for architecture called Digital Project that was based on CATIA. CATIA is very rarely used by architects and Digital Project is a BIM solution that competes with software like Revit or Archicad, not making it attractive for digital fabrication.

- Other CAD software such as Inventor, Solidworks, Solidedge, or Generative Components are other CAD solutions with parametric capabilities that may be used for digital fabrication. Although solid modelers like Solidworks or Solidedge are used in many engineering disciplines, they are rarely used for architectural purposes. Generative Components, similarly as TopSolid, have been outsmarted by Grasshopper and have seen a severe decline in their use by the industry.

Finally, it is important to take into account that, although there are existing software packages available for use, it is likely that the development of new, previously nonexistent robots, will lead to the rise of new stand-alone software or plugins. Rhinoceros is a widely used and suitable platform for this scenario as well.

2.5.1.5. 3D Printing software.

3D printing software can be sorted according to a three-fold classification compelling (i) mesh-treatment software for part verification and STL mesh repair, (ii) slicing software, and (iii) integrated environments.

- **Mesh treatment software**

Mesh treatment software is dedicated to repairing meshes unsuitable for 3D printing. These programs check the original meshes for holes (naked edges) or undesired geometry (such as non-manifold geometry) and attempt to fix them automatically with easy-to-use tools generally requiring almost no input by the user. Most CAD-CAM solutions (including Rhinoceros) integrate some of the algorithms (or similar approaches) provided by these packages, where MeshRepair, ReMESH, MakePrintable, MeshLab and MeshFix are some of the most relevant examples (*All3DP, 2016*). Mesh treatment software is often free and open-source, thus sustained and supported by the users themselves.

- **Slicing software**

Slicing software (commonly known as "Slicer") performs the slicing operation on the STL meshes to obtain the toolpaths. In addition to creating the contours, slicers calculate maximum overhang angles, infill patterns and density, and shell distribution according to user input and other configurations related to the size of the extruder and the printer's size. Slicing software is quite well-known for its potential, and many times includes also G-Code generation capabilities.

Cura Engine and Slic3r are the most widely used slicing generators, and come thus integrated in most open-source printing environments. While Cura Engine is simple and suitable for unexperienced users, Slic3r requires previous 3D printing experience (*Slic3r, 2015*). In addition, Cura Engine is the standard, underlying slicer software for all Ultimaker 3D printers (*Ultimaker, 2017*), but can also be used with others, such as RepRap, Makerbot, Printrbot, Lulzbot, and Witbox. It is fully open-source and can be extended through a carefully designed plugin system.

Obviously enough, slicing software (and thus integrated environments) are one-technique only, meaning that the slicing operation can merely attack one 3D printing technique –commonly FDM. SLA and SLS printing software are normally proprietary, as they deal with ad-hoc machinery and specialty equipment dubiously tackled by any open-source program. Some of the most relevant software regarding SLA and SLS techniques comprise 3D Systems ZCorp's 3D Sprint™ and 3DXpert™ software among many others (*3D Systems, 2016*). Additionally, Formlabs offers slicers for DLP/SLA 3D Printing.

- **Integrated environments**

NetFabb is also a great tool for both mesh checking and slicing. It combines both the mesh treatment, checking, and repairing tools with the slicing capabilities of slicers. This is indeed a great integrated environment for preparing 3D printable parts for standard 3-axis desktop printers.

Repetier Host is the preferred solution within the RepRap maker community. It provides an advanced solution for proficient users who want to stay within an open source framework while being able to stay in control of each and every aspect of the 3D printing preparation. The software offers thus, an "all-in-one" solution that straddles the intermediate to advance user spectrum with a variety of tools dedicated to delivering full printing functionality, namely:

- Multi-extruder support
- Multi-slicer support via plugins (can be pre-installed with Cura Engine by default)
- Support for virtually any FDM printer in the market, especially those with 3-axis hardware configurations.

2.5.1.6. Visualization and animation software

Autodesk© 3DMax, Autodesk© Maya, or the free and open source Blender are neither fabrication nor architectural design software. In principle, they are used as artists' tools rather than as engineering's tool.

They are quite popular in industries like video game development, film making, animation and visualization. These mesh-based geometry software packages allow to create quick and simple geometrical models that can also be exported to STL as solid 3D representations of printable models. Nevertheless, the STL models produced by 3DMax are not as accurate as those produced by Rhinoceros and, in the users' experience, tend to include unreadable or unsuitable geometry for 3D printing (non-manifold geometry or open objects).

2.6. Patents

The prices of 3D printers have decreased dramatically in the last few years. One reason is believed to be the expiration of some key patents from 2009, as commented earlier this chapter. Year 2014 attended to the expiration of many patents, letting analysts believe this will cause an exponential growth of the 3D printing industry, and initiating an even deeper drop in the already significant tendency of pricing policies while driving up adoption rates of the technology by the general public.

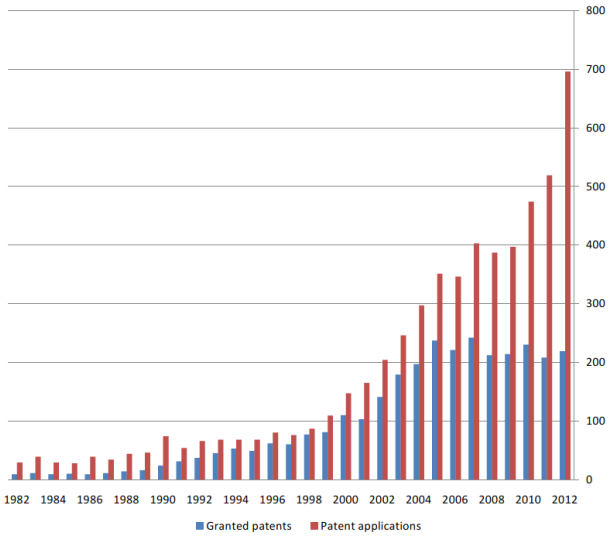

Fig 41. Granted patents and published patent applications by publication year (*UK Intellectual Property Office, 2013*)

This section shows the most relevant patents in the realm of 3D printing –particularly those related to the AEC sector and general part engineering, encompassing procedures, materials, hardware and other inventions that have marked the path to the current state of development of the technology. The amount of 3D printing related patents worldwide has increased in the last 10 to 15 years, accounting around 30.000 published patent applications since 1980. Particularly of interest is the increasing dichotomy between

applications and validations (*UK Intellectual Property Office, 2013*), which may well speak of a saturation of the 3D printing patent "marketplace". In addition, most current applications relate to apparatus to increase speed, double the filaments, and other non-quality –related issues.

Part of the thesis is subject of patent filing. Some of the following patents are result of an official search carried out by the specialized firm Barker Brettell LLP in Cambridge, UK. The search and disclosed patents refer to either of the following concepts:

(i) large-scale printing,

(ii) innovative printing methodologies,

(iii) tool path automation strategies,

(iv) software developments, and

(v) materials.

The results have been filtered to offer a selection as reliable and close as possible to the subject of the present thesis while presenting the wide range of possibilities covered and illustrated by the different applications.

2.6.1. FDM

- **U.S. Patent No. 5121329**

Held by Stratasys Inc., the Patent describes an "*Apparatus incorporating a movable dispensing head provided with a supply of material which solidifies at a predetermined temperature, and a base member, which are moved relative to each other along "X," "Y," and "Z" axes in a predetermined pattern to create three-dimensional objects by building up material discharged from the dispensing head onto the base member at a controlled rate*." (*United States Patent No. US 5121329, 1992*)

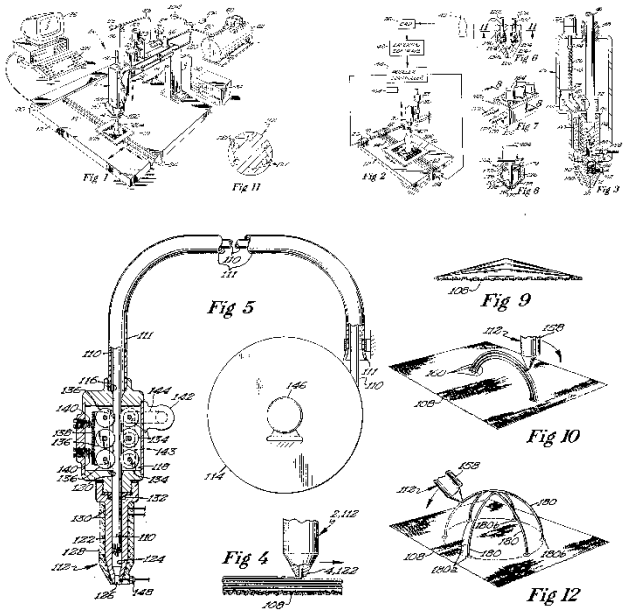

Fig. 42. US Patent 5121329

This depicts a 3-axis 3D printing system for and undefined-scale part production, commonly known as Fused Deposition Modeling –referenced throughout this document. As said before, FDM can be considered the basis of present large-scale 3D printing technology. This Patent has currently expired.

Related patents are WO 1998053974 A1, "*Method for rapid prototyping of solid models*", by John Samuel Batchelder and Steven Scott Crump and held by Stratasys Inc. since its publication on 3rd December 1998 (*World Patent No. 1998053974 A1, 1998*); EP 0666164 A2 "*A part fabrication Method*", published

in 9th August 1995 and property of the same company (*European Patent No. EP 0 666 164 A2, 1995*). The inventors are Steven R. Abrams, John Samuel Batchelder, Rida Taji Farouki, James Urey Korein, Jonathan David Korein, John Dacosta Mackay, Christopher John Ryan, Vijay Srinivasan, and Kosthantinos Athanasios Tarabanis.

- **China Patent CN 103332023 A**

This patent discloses a speed-adjustable, double-end filament yielding mechanism of a fused-deposition-like 3D printer comprising a pedestal provided with two sets of independent leading mechanisms whereby the FDM process is improved. The patent was published on 2nd October 2013, and describes a system similar to the nozzle hardware used by open-source printers *(China Patent No. CN 103332023 A, 2013*).

- **U.S. Patent No. 9168685 B2**

"*Print head assembly and print head for use in fused deposition modeling system*" depicts a print head assembly that includes a print head carriage and multiple, replaceable print heads able to be removable retained in receptacles for ease of use. It was published on 27th October 2015, by Stratasys, Inc. Its inventors are William J. Swanson, J. Samuel Batchelder, Kevin C. Johnson, Timothy A. Hjelsand, and James W. Comb (*United States Patent No. US 9168685 B2, 2015*).

- **U.S. Patent No. 2015/0037446 A1**

The Patent US 2015/0037446 A1 "*Fused filament fabrication system and method*" describes a hardware apparatus that comprises a motor for moving the system along a linear rail, a drive gear, and a set of two filaments for the selective passage of material to corresponding extruders. Brian L. Douglass, and Carl R. Douglass, both inventors and applicants, filed the application published on 5th February, 2015 *(United States Patent No. US 2015/0037446 A1, 2015*).

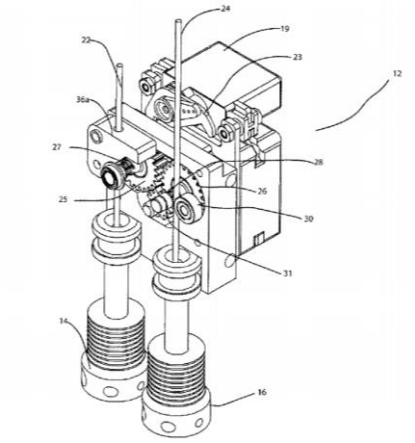

Fig. 43. US Patent 2015/0037446

2.6.2. Stereolitography

- **U.S. Patent No. 4575330 A**

The patent US 4575330 A "*Apparatus for Production of three-dimensional objects by stereolitography*" describes a "system for generating three-dimensional objects by creating cross-sectional pattern of the object to be formed at a selected surface of a fluid medium capable of altering its physical state in response to appropriate synergistic stimulation by impinging radiation, particle bombardment […]" or other means (*United States Patent No. US 4575330 A, 1986*).

2.6.3. Laminated Object Manufacturing

- **U.S. Patent No. 9216544 B2 – WO 2014100078 A1**

"*Automated additive manufacturing system for printing three-dimensional parts, printing farm thereof, and method of use thereof*" depicts, "*an additive manufacturing system comprising a platen assembly configured to restrain and release a film or substrate, a head gantry configured to retain a print head for printing a three-dimensional part on the restrained film or substrate. The additive manufacturing system may also include a removal assembly configured to draw the film having the printed three-dimensional part from the platen assembly and to cut the drawn film*". The patent was filed by William J. Swanson, Dominic F. Mannella, Joseph E. LaBossiere, Michael W. Hansen, Saurav Upadhyaya, and Ronald G. Schloesser. It is held by Stratasys, Inc., was filed on 8th March 2013 and published on 22nd December, 2015 (*Patent No. US 9216544 B2, 2015*).

2.6.4. Contour Crafting

- **U.S. Patent No. 7641461 B2**

The patent US 7641461 B2, "*Robotic systems for automated construction*", describes any solution in which a gantry robot connected to an extrusion nozzle is used for construction. The gantry system holds an extrusion device for the production of large-scale parts. The system and apparatus comprises (i) the movable gantry robot including an overhead beam, (ii) a nozzle assembly couplet to the beam, (iii) and a position controller configured to control position and movement of the former two elements *(United States Patent No. US 7641461 B2, 2010*).

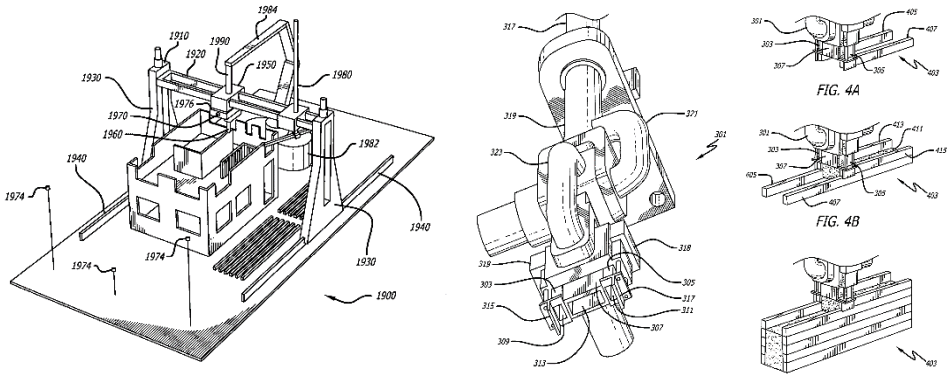

Fig. 44. US Patent 7641461

- **U.S. Patent No. 7814937 B2**

The patent US 7814937 B2, "*Deployable contour crafting*", describes the most standard vision of building 3D printing. It includes a vehicle, a gantry system and a nozzle that can extrude cementitious material. The gantry system can expand to the size of the building to be constructed and collapse into the vehicle for transportation (*United States Patent No. US 7814937 B2, 2010*).

2.6.5. Methodology

- **U.S. Patent No. 20030171841 A1**

The patent "*Method and control system for generating machine tool control data*", is oriented towards the use of numeric controlled machines. It describes a model and scheme that generate tool data from a 3D CAD file. The control program performs a feature recognition operation on data obtained form an IGES file to identify geometric features present in the solid model and yields data recognizable by the machine in order to generate computer-readable instructions for working the afore mentioned features with a fabrication machine.

The patent was PCT Filed on 31st August 2001, and published on 11th September 2003 *(United States Patent No. US 20030171841 A1, 2003*).

- **U.S. Patent No. 20150142152 A1 (on printing methods)**

Subject of this patent are "*a 3D printer system and related methods"*. Owned by Siemens, it describes both a particular hardware piece comprising (i) a processor and (ii) an accessible memory, and the thereby associated software components that make it work, including a (i) CAD kernel contained in that memory, and a (ii) product file. The combined use of these parts produces a solid physical object corresponding to the CAD solid model contained in the memory. The patent describes the printer's architecture, as well as a printer design that can include embedded CAD software and are capable of automatically interpret JT file formats –a lightweight data format that makes it possible to view and share digital 3D information in real-time, approved as an ISO International Standard. These printers support boundary representation (BREP) data, product manufacturing information (PMI), and layer information.

The patent was filed on 7th November 2014, and published 21st May 2015 *(United States Patent Patent No. US 20150142152 A1, 2015*).

- **U.S. Patent No. 20140025190 A1 (on printing standardization)**

The patent "*Single action three-dimensional model printing methods*" discusses the virtualization process of 3D objects from 2D image data. It deals with the conversion of input image data into geometric representations compatible with 3rd party printers. Furthermore, the patent presents a series of templates that encapsulate possible complex geometry representations and complicated data conversion processes of various sorts (*United States Patent No. US 2014/0025190 A1, 2014*).

- **EP 1 895 375 A1 (on a Machining step generation device)**

Filed on 20th June 2006, and Published on 5th March 2008, the patent focuses on numeric control machines. It describes a method for automating the selection of a method for NC fabrication. In fact, it focuses on selecting automatically from within a predefined set of tool path creation algorithms. That set is pre-conceived and pre-stored in the machine. It can be inferred from the patent body that it relates rather to milling and molding than to 3D printing as preferred fabrication methodologies (European Patent No. EP 1 895 375 A1 also published as WO02006137120A1, 2008).

- **U.S. Patent No. 201400336807A1 (on translating molecular models into CAD formats)**

This patent describes systems, methods, and apparatus that allow a user to convert various styles of 3D graphic representations of molecular models to CAD formats to enable printing. As other patents focusing on this kind of methods, "*Systems and methods for translating three dimensional graphic molecular models to computer aided design format*" exposes a process that results in cad data as to be used for printing purposes by vendors and fabricators alike. If focuses on the graphic representations of molecules, thus establishing hyper-specific processes that could eventually be implemented in proprietary software strictly within the field of molecular design *(United States Patent No. US 201400336807 A1, 2014*).

The patent was filed on 9th May 2014, and published on 13th November 2014.

- **U.S. Patent No. 20160075089 A1 (on manufacturing along toolpaths)**

"*Methods and apparatus for additive manufacturing along user-specified toolpaths"* describes the way an extruder moves along a deposition path, whereby objects include sometimes functionally graded material. In this instance, "*one or more input/output devices accept user-inputted path instructions that specify a set of multiple deposition paths for an extruder to travel*" (United States Patent No. US 20160075089 A1, 2016).

The patent was filed 15th September 2015 and published 17th March 2016 by MIT.

- **U.S. Patent No. 5402351 A**

The patent "*Model generation system having closed-loop extrusion nozzle positioning"* discloses methods and apparatus for fabricating three dimensional objects in accordance with a computer-generated definition of the object. The method includes the steps of evaluating the stored definition of the object, a support structure, a fabrication tool movement list, and the fabrication tool. The patent was filed 18th

January 1994 and published 28th March 1995 by International Business Machines Corporation (IBM) holding John S. Batchelder, Huntington W. Curtis, Douglas S. Goodman, Franklin Gracer, Robert R. Jackson, George M. Koppelman, and John D. Mackay as the inventors *(United States Patent No. US 5402351 A, 1995*).

2.6.6. Materials and apparatus

- **U.S. Patent No. 20080260918 A1 (on 3D printing food)**

The patent "*Manufacturing method of three-dimensional food by rapid prototyping"* focuses on SLA-like printing processes for food, although it resembles some sort of similarity to the roll-based material approach of LOM. It depicts a system that would eventually allow for producing "*three-dimensional food in a very short time without using a mold"*. Although the technology is apparently standard, its application differs from other, product-oriented methods *(United States Patent No. US 20080260918 A1, 2008*).

- **U.S. Patent No. 9215882 B2 (on chocolate)**

US Patent 9215882 B2 *"Additive manufacturing system and method for printing customized chocolate confections"* discloses an AM system for printing a chocolate confection, comprising a platen, a recirculation loop for the chocolate material, and further configured to maintain a temper of the former; and finally a print head being configured to receive at least a portion of that chocolate material, further thought and configured to extrude and deposit the chocolate onto the plate through a series of commands received by the associated software controller. This patent is assigned to Stratasys Inc. since 22nd December 2015. The inventors are Aidan Zimmerman, Daniel F. Walczyk, S. Scott Crump, and J. Samuel Batchelder (*United States Patent No. US 9215882 B2, 2015*).

- **U.S. Patent No. 20150307385**

"*Methods and apparatus for additive manufacturing of glass*" is the patent filed by the MIT on 27th April 2015 and published on 29th October 2015 to depict the invention of a glass 3D printer described in section 2.4. It comprises both the body of the printer and the printing system, as well as a compelling portrait of the material requirements for this method and its physical instantiation *(United States Patent No. US 2015030307385, 2015*).

- **U.S. Patent No. 20110079936**

The patent "*Methods and Apparatus for Variable Property Rapid Prototyping*" shows the possibility to include various materials in a single production process, as to implement different material properties in a single printed part. In a single implementation of the invention "*a plurality of materials are heated, mixed and extruded from a nozzle*", allowing for a dynamic variation of the material mixture, which allows for a gradient-like material composition. The patent was filed on 5th October 2010 and published on 7th April 2011 by Neri Oxman *(United States Patent No. US 20110079936, 2011*).

- **WO Patent No. WO 2016012486 A1 – US 20160024293**

"*Mixture for use in a fused filament fabrication process*" describes the mixture of an Inorganic Powder, a binder, and at least one polyoxymethylene (POM) for the use of a plastic material in a fused filament fabrication process. This Patent is one of the many patent files regarding plastic-like materials and their presentation method for FDM processes focusing exclusively on the material composition. This entry is a Patent Filing from 2015 which was published on 28th January 2016. The patent is held by Basf Se, accounting Nikolaus Nestle, Marie-Claire Hermant, and Kris Schmidt as inventors *(World Patent No. WO 2016/012486 A1 also filed as US 20160024293, 2016*).

- **European Patent No. EP 2514775 A1 – US 20130317164**

This filing relates to a novel support material for the FDM 3D printing process. According to the patent's body, "*The invention relates more particularly to a 3D printing process involving support materials which are easier to remove than in the prior art. The support materials according to the invention are styrene-maleic anhydride copolymers for example*". The patent was published on 24th October 2012. The patent is held by Evonik Röhm GmgH, whereas Florian Hermes, Stefan Bernhardt, Dirk Poppe, Günter

Schmitt, Markus Pridöhl, and Gerd Löhden are filed as its inventors *(European Patent No. EP 2514775 A1, 2012*).

- **European Patent No. EP 2707198 A1 – US 20140088751 – DE 102011075540 A1**

The patent "*Multicolored Fused Deposition modeling pressure*" relates to a method to obtained multi-colored three-dimensional objects by means of FDM 3D printing with a polymer strand that can be colored superficially. The patent states that "*The inventive method is based on that the polymer strand used to make the actual object, or the resulting melt is superficially colored in the nozzle or coated with additives".* As in the case of EP 2514775 A1, this patent is held by Evonik Röhm GmgH, The inventors are Kris Beks, Sonja Cremer, Ludo Dewaelheyns, Benjamin Hammann, Stephan Kohlstruk, Dirk Poppe, Günter Schmitt, Markus Pridöhl, and Gerd Löhden (*European Patent No. EP 2707198 A1 also published as DE 102011075540 A / WO02012152510A1, 2012*). The patent was published on 15th November, 2012.

- **U.S. Patent No. 9169968 B2**

This patent depicts a variety of techniques for color mixing support a user-controllable palette of colors for use when fabricating 3D objects by means of a double FDM thermoplastic extruder. The actual invention relies specifically in the mixing apparatus, which includes a cavity coupled in fluid communication with both plastic ports and the extrusion or nozzle port, whereby one or more baffles allow for a seamless mix of materials while passing in a liquid state to the extrusion port. The patent is assigned to Makerbot Industries, Llc. It was filed on 10th June 2013 and published on 27th October, 2015. The patent, titled "*Color three dimensional printing*", is authored by Nathaniel B. Pettis, Robert J. Steiner, Peter Joseph Schmehl, and Charles E. Pax (*United States Patent No. US 9169968 B2, 2015*).

US 9168699 B2, depicting an invention by Charles E. Pax, and held by Makerbot Industries, Llc. Since 27th October 2015, further expands on this subject by implementing a "*Color switching for three-dimensional printing*" method to mitigate transition artifacts and permit faster, more complete changes from one build material to another (*United States Patent No. US 9168699 B2, 2015*).

- **U.S. Patent No. 8944802 B2 – US 20140210137**

"*Fixed printhead fused filament fabrication printer and method*" describes an apparatus for a plurality of printing heads mounted to a structure over a build platform which may either rotate or move along the X and Y axes. The system comprises fixed positional print head containers, so that those can be easily affixed with respect to the platform. The patent, held by Radiant Fabrications, Inc., describes an invention by Nathan James Patterson and Kevin Lee Harris. The patent was filed on 3rd February 2015 (*United States Patent No. US 8944802 B2 | US 20140210137, 2015*).

Similar inventions are held in several patents. Some of these include (i) US 8663533 B2, "*Method of using print head assembly in fused deposition modeling system*", invented by William J. Swanson, J. Samuel Batchleder and Kevin C. Johnson, and is held by Stratasys, Inc. since 4th March 2014; (ii) US 8647102 B2, "*Print head assembly and print head for use in fused deposition modeling system*", by William J. Swanson, J. Samuel Batchleder, Kevin C. Johnson, Timothy A. Hjelsand, and James W. Comb is held by Stratasys as well since 11th February 2014 *(United States Patent Patent No. US 8647102 B2, 2014; United States Patent No. US 8663533 B2, 2014*).

2.7. Conclusions

This chapter has analyzed the current state of 3D printing technology from three different perspectives. First, it has demonstrated the high degree of development of Additive Manufacturing at small scales for rapid prototyping production purposes, which has not translated yet into its real-scale counterpart despite the research that is currently being conducted in the field. As presented in previous sections from the present chapter, 3D printing has generated a large amount of interest and advancement in small-scale object production and rapid prototyping through FDM desktop printers, leaving space for exploration in the real-scale realm. The thesis embraces this particular issue by focusing on real-scale object production, as explained in subsequent chapters. Second, it has analyzed the richness of materials available for printing. Here, it is hardly possible to find a niche for further development. Third, it has gone through printing software and methods alike in order to depict the vast landscape of solutions available in the market. Nonetheless, it is proved that research is insufficient in terms of design-to-production software integration

and standardization, another issue that the thesis tackles as a starting point for the democratization of Additive Manufacturing techniques.

As a consequence, the current thesis aims at combining the most unexplored aspects of Additive Manufacturing –scale, quality, methodology and software- through the mutually benefiting combination of large scale possibilities and the integration of those into a single and comprehensive design-to-production workflow. Furthermore, these are framed into a comprehensive analysis of the current situation of the construction market in its global context and the Spanish situation in particular.

Chapter 3

3D printing in construction: a comprehensive methodological framework.

This section analyses the considerations to take into account regarding the three main aspects of the thesis' research: theoretical applications of 3D printing technology for big scale parts and their influence on the construction industry, software integration, and hardware definition. Furthermore, guidelines for further work methodologies are defined.

3.1. 3D printing opportunities in the building industry

The present thesis seeks to explore and develop solutions for real-scale 3D printing for the building sector while maintaining a critical attitude towards their possible consequences at both theoretical and practical levels. Despite the many options and solutions for 3D printing in the market, there is still space for research and experimentation in the sectors of software, hardware, and material science. The techniques, methods, and apparatus discussed throughout the thesis offer a series of innovative approaches towards those three particular aspects.

On the other hand, it is intended to create a sustainable and reasonable theoretical framework within which it may be possible to carry out the experiments and analyze the methods and results thereby obtained. The introduction of automation, parametric and algorithmic techniques in general has opened a practice-confined discussion about the "authorship" of the construction project as a whole that affects computer-based design and methods. Beside speculative aspects of the thesis in terms of the future applications of the presented technology, the thesis intends to focus on practical and applied matters. As a result, the document disregards possible theoretical discussions related to these.

In many cases, transformative technologies are the soul of paradigmatic historical shifts. Rather than relying on holistic revolutions, it is small irruptions of technology that alter the face and course of history. The steam engine, the light bulb, atomic energy, or the microchip have definitely shaped our society in unimaginable ways at the time of their invention. On the infrastructure side, railroads, water piping, sewage systems, or the World Wide Web are examples of such transformations at global scales, some of which are still today under a process of deep transformation and keep a strong potential to reshape themselves while influencing societal establishments and non-regulated organizations.

AM in general, and 3D printing in particular, has the potential to become as much a disruptive technology as those previously mentioned. It can have profound implications on geopolitical, economic, social, demographic, environmental, and security issues the way we understand them today. The apparently

minor distinction between the operational implications of subtractive technologies and additive methods yields a number of positive issues (*Campbell, Williams, Ivanova, & Garret, 2016*):

- The ability of the technology sway assembly lines and supply chains, which may be reduced or eliminated for many products thanks to a model of de-localized production. Unlike conventional processes in which hundreds or thousands of parts are assembled, AM processes are usually packed into a single final production workflow, single machine manufacturing.
- The manufacturing industry would move from product to design, which would be transferred around the world as light digital files with the potential to be printed virtually anywhere according to certain design parameters and relatively low hardware restrictions. Just as the Internet is eliminating barriers in the digital world, 3D printing is set to eliminate them in the physical realm.
- Products and parts can be printed on demand. Although this statement may appear irrelevant or obvious, it throws significant advantages in terms of material savings both at the low and high ends. Among other implications, this fact could imply the end for the need to build-up inventories of new or spare parts.
- Manufacturing facilities could become multi-functional. As opposed to current fabrication hubs or workshops –where fabrication is planned to adopt single-object production chains, 3D printing allows for huge ranges of differentiated types of products without retooling or reconfiguring the space itself, resulting in increased flexibility and substantial savings.
- Production and distribution could undergo a process of de-globalization based upon the de-localized fabrication and shrinkage of production runs. Fabrication and assembly lines would be absorbed by a more flexible manufacturing model, whereby instead of setting up large facilities to accommodate the production of hundred thousands of parts, hundred thousands of small factories have the ability to create a single object each –a sort of "production farm".
- The influence of global economic relationships and a positive reduction of global economic imbalances as a consequence of a new import-export interaction network. Manufacturing could be in the long run pulled away from heavily focused platforms or countries, such as China, India, and others. As a general rule, the export countries' surpluses will diminish as import countries' reliance and dependence of imported products narrow down.
- The carbon footprint and negative environmental impact of industrial manufacturing-related processes would be reduced substantially as well as the overall energy of these uses. Subsequently, resource productivity or profitability could be enhanced.
- At a societal level, the foreseeable reduction of labor in manufacturing could be destabilizing in developing countries, while more developed, aging societies would benefit from an enhanced production chain with reduced labor impact. Furthermore, labor wages are higher in these countries (*World Economic Forum (WEF) with The Boston Consulting Group, 2016, May; European Federation of Building and Woodworkers (EFBWW), 2009*).
- New developments can amend the economic strength and geopolitical influence of countries willing to invest in R&D projects related to 3D printing (*Morris, 2010*).

In the past years, researchers have focused on further developing existing technologies and adapting them to new materials, as well as on pulling 3D printing away from the prototyping realm and into the end-product field. In 2009, Wohlers reported that 16% of Additive Manufacturing Process use was devoted to direct part production, 21% for functional models and demonstration mock-ups, and 23% for tooling and metal casting patterns *(Wohlers, Wohlers Report 2009: Additive Manufacturing State of The Industry, 2009*). Furthermore, recent research efforts are being directed towards the development of the so-called "programmable" materials and the improvement of printing methods for self-adaptable materials which could modify themselves without the need for human interaction *(Campbell, Tibbits, & Garret, 2014*).

Nonetheless, 3D printing still has a long road to travel in reference to product quality, since different machines display radically different or varying properties –as is the case of traditional manufacturing as well (*Wohlers, Wohlers Report: Rapid Prototyping & Tooling State of the Industry*

Annual WorldWide Progress Report, 2001). There is also a need for better materials to use in printing and greater uniformity and standardization in production quality. In fact, most developments ignore the quality of the final product in an attempt to tackle the reduction of fabrication time (*Wohlers, Wohlers Annual Worldwide Progress Report 2016: 3D Printing and Additive Manufacturing State of the Industry, 2016*).

Finally, AM still needs to face its adaptation to quick, big-scale production. In fact, many efforts are being directed in this sense despite the uncertainty surrounding the current and future pace of development, adaptation, and implementation of AM techniques. In terms of the architectural adoption of the 3D printing technology, the present thesis discusses in this and successive chapter a holistic methodological approach.

3.2. Implications of 3D printing in construction

Despite the many opportunities in terms of the technological development attributable to 3D printing methods and techniques, it can be argued that we are currently witnessing the emergence of a second generation of the technology, whereby there are still blooming development opportunities. Based upon the study of the materials, techniques, and applications of 3D printing for different purposes –found in the previous chapter-, it seems clear that, referred to the construction sector, it has the ability and potential to:

- Redefine the building techniques and evaluate the consequences of such a new methodology on the current definition of the construction sector as a whole. In this sense, the thesis discusses concepts related both to form-finding and construction. As a consequence, traditional concepts like prefabricated construction, craft-oriented workflow division, on-site fabrication, and others are put to the test.

  As presented in the previous chapter, oversize 3D printing for construction may excel at its capacity to factually bring fabrication or production closer to the actual constructions sites. The use of industrial robotic arms, which may be deployed on site, may ease in the near future the fabrication of architectural and structural elements directly during construction. The versatility and scalability of those tools are indeed advantages of the technique.

  Especially in the Spanish sector, where draftsmen and service provider staff is typically underqualified, implementing highly technological tooling on site could yield unprecedented benefits. Technology could re-qualify the sector, improve security, enhance end-product quality, and reduce construction times and costs. Furthermore, 3D printing technology could finally become a construction standard for the private and public sectors alike.

  Obviously, there is still a long and uncertain road to travel. Public administrators are not yet ready to deal with the intricacies of the implementation of such technology, and the consequences the latter may have on site organization, timing, and management. There is a need for a process standardization, affecting both the public administration and private endeavors and investors. On that side, private undertakings rely on their need to minimize production costs and times. Substituting human involvement in non-critical processes by machine-automated streams is therefore crucial for the sector. All agents –mainly designers, architects, contractors, end clients, and the public sector- involved in the construction process could eventually be interested in the enhancement and systematization of real-scale construction techniques.

- Propose the standardization for the employment of these technologies. Despite the relative youth of large 3D printing techniques, there are already many divergent efforts as far as robotics and real-scale object production are concerned (*Liébana & Nadal, 2016*). Thus, it seems desirable to point out this specific topic. Chapter 2 has shown insightfully the current attempts to make use of the 3D printing technology for architectural and construction purposes. It becomes clear that, despite the many efforts that are currently pushing in that direction, there is no clear path towards a standardized printing process whatsoever, regarding a (i) design-to-fabrication workflow and (ii) the implementation of optimized smart material infill patterning systems. The thesis offers a comprehensive approach that deals with both aspects.

3.2.1. A critical analysis of current off-the-shelf applications for oversized 3D printing. Freeform construction.

This section intends to critically analyze the existing platforms and proposals dealing with 3D printing for construction purposes and offer improvements.

The most crucial aspects to analyze the latest developments in the field described in Chapter 2 relate mainly to two fundamental aspects of the technology: (i) building scale and (ii) production time. Moreover, the possible restrictions of location and flexibility for (iii) on-site deployment may well be discussed as (iv) methodological constraints. Other, less regarded considerations, may include the interest in (v) reducing material consumption and costs, (vi) investments risks, (vii) improve the security of the workers on-site, and account for (viii) more qualified trades and crafts. Some developers involved in prefabrication methods may argue in favor of a radical redistribution of on-site work, aiming at a reduction of about a 70% of the trades involved. This means that, for a redefinition of the construction sector, fabrication and construction means need to be radically rethought and redesigned. Process automation and 3D printing may be suitable approaches for this redefinition.

The most relevant proposals in the field of AEC industries stem from Contour Crafting, D-Shape or gantry-like structured production, and the KamerMaker approach. They share the same interest and some methodological aspects worthwhile looking at while all aiming at providing solutions for real-scale printing based upon a translation of 3-axis CNC machines or even regular printing techniques such as SLA.

Contour Crafting (CC), as clearly and thoroughly exposed in the previous chapter, focuses both on a printing method for concrete and its possible commercial exploitation through gantry-like structures for the deployment of real-scale buildings. CC aims at creating a comprehensive solution that is able to respond to specific and unpredicted needs of dwelling construction with various possibilities: affordable housing, disaster remediation, or shelters. Nonetheless, this technology has a series of drawbacks worth mentioning:

- It relies on a gantry-like structure that requires of heavy industrialization on site and is costly and difficult to implement.
- The gantry or crane system is costly to deploy on site, therefore implying a prefabrication process that must take transportation requirements and costs into account.
- The 3-axis approach is inherently limited in size to that of the host structure.
- It lacks a real material development that makes it suitable for construction in developed countries.
- It relies on the substitution of non-specialized work force for qualified labor in under-developed countries, where wages are still “affordable” making it profitable to invest. This method would likely be more appropriate for developed countries where it would mean significant savings to developers and constructors alike.

D-Shape technology is radically different in its conception to Contour Crafting, although both share common setbacks. As opposed to CC, D-Shape is conceived as a scaled-up translation of SLA printers –see section 2.4.5.2, where the binding material is placed upon a bed of dehydrated or otherwise non-structural material that requires the former in order to become structurally coherent and sound for self-standing bearing conditions and operations. As in the case of CC, D-Shape relies on a gantry system that holds the printer’s “nozzle”, where the binding material is deposed. As SLA printers, D-Shape needs large amounts of material that will utterly be removed once the part is finished. The present-day state of the D-Shape technology has a fixed size material bed, which means that, even if a piece is small in footprint, the whole bed needs to be filled. Thus, reducing the height of the piece to be printed is the only possibility to minimize its impact on the amount of material use. Obviously, this goes against the logic of such an implementation, where size in general and height in particular, are design pre-requisites that play a restrictive role regarding possible “printer” conceptions and printed piece’s results. In addition to that, a significant amount of effort must be put into the post-production phase that is required to finish the pieces, due to the inaccuracy of the technique and the difficulties inherent to the rheology and nature of the material itself.

Some mayor opportunities for improvement are:

- The possibility to create systems that use just the necessary amount of material, reducing the impact on the overall costs of fabrication, as well as the embedded energy of the whole material transformation process.
- The possibility to implement more geometrically accurate models *(Dominguez, Romero, Espinosa, & Dominguez, 2012*). Whereas material constraints come indeed into play, the accuracy can be improved through a more careful study of the deposition of the binding material as well as of the method and apparatus employed for the printing process.
- The need to implement faster production systems that are able to respond in a reliable manner to unexpected demands. This means that large amounts of raw material need to be stored in advance, and that the space requirements both for storage and the printer itself would be dimensioned accordingly. This requirement is difficult to meet at all scales, whether financially, or time-wise, or even as far as physical space and soil costs are concerned. Further costs on space rental could also suppose a disadvantage of this particular approach.
- The need to implement more versatile production methodologies that can eventually produce a wide spectrum of parts without relying on extreme amounts of material supply. These are difficult to face by contractors and suppliers.
- The possibility of deploying the technology on site. Big-part production presents feasibility aspects difficult to traverse:
    - (i) on the one hand, the size of the parts requires careful planning of both infrastructure and transportation provisions;
    - (ii) on the other, working directly with concrete-based materials implies a counter-logic to that of the prefabrication, since transports are limited both by size and weight. Although this might be possible to overcome in developed countries, which normally grant reliable and dense enough transportation networks, this is again not the case for underdeveloped countries, where this technology may be a great advancement due to the minimization of transportation needs through on-site factory fabrication.
- The potential to use a versatile tool that does not have inherent size limitations, such as robotic arms or similar as opposed to mono-functional, size-fixed machines. Due to the way industrial robots are conceived, they can take on a variety of tasks and occupations, and be re-programmed within brief periods of time in order to accommodate fabrication necessities.

The KamerMaker approach is pretty much an adaptation of FDM printers to big-scale production. Both for its functional model and its physical configuration, it resembles personal desktop 3D printers. Again, this project falls into the same problems and issues as the previous two cases. As a side effect of its size and form, it presents limitations in terms of usability and transportation as the CC and D-Shape examples, which are briefly listed below.

- Size limitation due to their “box-like” printer conception.
- Hyper-specificity in terms of material, designs, and use.
- Transportation problems.

The last item in the list was tackled by the project’s design team. In fact, the KamerMaker is a printer structure that fits within a container, and that can thus be transported to the building site. The downside is, though, the highly specialized transportation equipment that it requires. Handling the printer is quite an arduous work as well, despite the apparent robustness of the machinery.

Finally, an interesting approach to 3D printing is the one represented by some experiments carried out originally at the ETH Zurich and further explored by several companies –such as MX3D- and educational institutions alike –such as the project presented in this thesis, IAAC, and others. The use of robotic arms for industrial goals is widely known for its versatility and automation process. Contrary to the automotive and aerospace sectors, where the production of serialized parts plays a key role, the AEC sector

differs enormously for various reasons: (i) the construction sector offers highly specific products, (ii) which are in addition meant to last for an undefined period of time, (iii) its products are site-specific and (iv) might take years to complete, and (v) the administrative steps required in order to successfully fulfill a construction project are extremely restrictive in terms of design, time and regulatory or legally binding terms.

- **Freeform construction**

It could be argued that the space for creativity that is allowed for in the design of cars and aircrafts due to the possibility of large serial production must, in the construction sector, be adopted in the production process instead. In other words, while aerospace products allow for chain, serialized production due to the constrained specificity of their final products, the hyper-specificity in terms of size, typology, and site of the end products in the construction sector requires a variety of tools, industrial allowances, and time flexibility of unprecedented relevance. Thus, the production line must be able to take that into account and allow for the maximum flexibility. Beyond personal taste, buildings are subject to local conditions, such as weather, materials, form-related regulations, construction types, lighting, financial possibilities, and many others. As said before, unique combinations of each parameter result in completely different instances of buildings.

This is the case, at least, of most commercial housing projects. Singular buildings, on the contrary, constitute a completely diverse scenario. Most times these have less limited budgets, more formal freedom, and other circumstances that generally contributes to their design in a positive manner when compared to commercial projects. Non-standard buildings usually present more complex geometries and details far from regular construction solutions. This case would then favor new technological advancements –such as 3D printing- for the complexity and intricacy of their building components. Parametric solid modelling tools are becoming more common in the construction arena and Rapid Manufacturing is beginning to have an impact in the design process. Digital Fabrication is enabling the production of buildings with freeform surfaces, but it is not a new process technology. The clients of the construction industry are asking leading designers to build structures that cannot be built by any known method today; new processes are a likely solution to this.

There are many well understood problems facing construction that can be engaged by new processes (*Egan, 1998*). In fact, the Strategic Research Agenda for the European Construction Sector call of 2005, has stated the requirement for new processes and new materials for construction *(European Construction Technology Platform (ECTP), 2005*). Recent calls have deepened into this very strategy and demand.

According to the advancements in methods and processes alike, it is reasonable to believe that new processes will drive down the cost of existing methods and subsequently filter down to the domestic sector (*Buswell R. , Soar, Gibb, & Thorpe, 2007*). This cascading effect is characteristic of new technological breakthroughs throughout history, being the Tunnelform system case one of its latest instances, as it shifted from Civil Engineering to the construction of dwellings *(The Concrete Centre, Mineral Products Association (MPA), 2005*). As a consequence, freeform construction is one possible response to these calls and demands at various levels.

The industry has the skills to fully engage with this reality, and Chapter 2 has shown its most relevant examples in a comprehensive manner. It becomes clear, then, that:

• Materials cost will be an important issue.

• New processes are presumably not going to be faster than traditional approaches.

• Greater performance can be achieved through a clever use of geometry.

The processes capable of delivering components large enough for a building structures is unlikely to be a scaled up version of a current process used for Rapid Manufacturing. Specialist applications will need to be developed for specific tasks. Material properties and process characteristics will be integral to the development of these new delivery processes.

3.2.1.1. Automation in construction: technological issues and systemic problems

In terms of technological development and fulfilment of customer expectations, it can be argued that the construction sector is well behind other industries such as aerospace, automotive and ship building. It is observed that construction products (mainly housing units) need lots of manual refinement due to the sequence of needlessly drafted processes prone to errors (*Del Solar, Del Río, Villoria, & Nadal, 2016*).

It is a known fact that the fundamental principles of construction have not changed for hundreds of years. Indeed concrete has been a construction material for probably over eight thousand years. The most recent "re-invention" of concrete was developed in the Egyptian and Roman time –romans realized that adding horsehair to the mix made the material less liable to crack, among other mix improvements- and is, over two to three thousand years later, still being used as a primary building material. Although figures are not entirely clear and differ from source to source, concrete is still, together with steel, arguably the largest used construction material worldwide. Not only are we building with a material developed thousands of years ago, but we are doing so additionally obeying the same ancient manual placement techniques –this is, the methods used have not evolved significantly in their conceptual presentation since their inception.

Construction technologies are innovation tools able to both foster and limit our imagination as far as design is concerned. The lack of renovating impulses leads to a situation that is stifling innovation; new methods of production and assembly often pull 'hand trades' away from the construction site rather than push profoundly new processes. As discussed above, the procurement and legal requirements that enable construction act as a disincentive to try different approaches, as regulations are normally conceived as mandatory rules of static nature that reward over-standardization in its simplest form possible. Furthermore, these same, unmodified norms apply to the variety of situations, locations, and conditions named above – being as a result unable to account for the richness of reality and becoming a quite restrictive, constraining legal apparatus. This legal framework trades consequently safety for variety or exploration.

Generally, promoters' competition for projects concentrate on first-cost; allowing scarce or no space at all for time, money or energy to be invested in innovation and R&D. The nature of the AEC industry is conservative in its means and conceptions, and follows a much defined inertia that permits only very little advancements through minor incremental changes –most of which are disputably led and controlled by leader firms and lobbyists. It basically hides away from disruptive technologies or moves that might affect the status quo of the profession or shake its basement. Where changes or improvements are made, the transient nature of the work and workforce often means those are not adopted on new projects as they might have been in a more 'static' manufacturing environment where both could be eventually controlled.

Safety is yet another essential issue; construction remains a hazardous environment –especially in emerging economies or under-developed countries where construction experiences a renovated force. According to the Report on Workplace Accidents in Spain for the year 2014 *(Unión General de Trabajadores (UGT) and Metal Construcción y Afines Federación de Industria, 2014*), the evolution of total accidents for the construction sector follows an ascending tendency, which does not, curiously enough, depend from the built volume. The total accident figure increased by a 5.53% in the period comprised between years 2013 and 2014, reaching a total amount of 42.226 incidences. Also, the report shows that accidents increased for all relevance types, including (i) "minor accidents", (ii) "accidents resulting in serious bodily injury", or (iii) "major accidents resulting in death" by 5.46%, 10.19%, and 1.06%, respectively. This means that, for the year 2014, 69 people died on a building site in Spain, and 42.157 were injured. These figures multiply disturbingly in other countries such as Qatar or China, where the volume of construction is much higher than in most developed countries and safety is not as well regarded.

In addition, the industry is likely to face even more pressures from the environmental side than it did in the past (*Guthrie, Coventry, Woolveridge, Hillier, & Collins, 1999*). In the last decade, developed countries have come up with a variety of initiatives to boost the "eco-awareness" in the built environment. The UK government, for instance, has addressed these issues through a succession of initiatives *(Latham, 1994; Egan, 1998*), and ultimately by the so-called "Constructing Excellence". The driving force pushes towards leaner, better Modern Methods of Construction (MMC) (*Lovell, 2003*), whereby some of these issues have been addressed by means of pre-assembled standardization (*Gibb & Pendlebury, 2003*). These initiatives find their counterparts in private endeavors or non-standard certificates, such as LEED,

BREEAM, PassivHaus, and others. These certificates focus both on the reduction of construction and operating costs, and intend to reduce the energy footprint of buildings through different measurement methods, although they differ in their conception. Unfortunately, it is almost impossible for these certificates to accommodate local needs, an issue that is well known in legal regulations. Again, complying with PassivHaus requirements in certain areas of the Spanish geography, for instance, could have disastrous results, as its norms are thought for the north-European climate conditions.

Despite this sensible tendency towards an improvement of quality, there is much need and space for more innovative solutions and for actual technological breakthroughs capable of rethinking the architectural and construction practice. In the years to come, construction will not only need to be able to respond to an increasing demand of affordable construction and environmentally friendly buildings -to name just a couple of examples, but also to unique challenges in aggressive environments, exceptional situations and unexplored locations. The AEC sector will be facing environmental issues requiring new materials and new solutions for buildings at the end of their life cycle, or even more creative answers such as the impressive *Fab Tree Hab*, project that deals with live materials that are inherently and naturally integrated within the environment. This proposal, provided by the Non-Profit Organization for Philanthropic Architecture, Urban, and Ecological Design Terreform One, imagines the built environment not only not consuming non-renewable resources, but as a resource generator. The Fab Tree Hab uses CNC and Rapid Manufacturing techniques to *craft* precise geometries with trees, in a unique, symbiotic, and mutually beneficial blend of the natural and digital worlds. This solution is a viable and synergetic proposal that could eventually be applied to a variety of projects, and represents a significant advancement in traditional grafting techniques to overcome outdated design solutions.

Process automation offers a large departure from conventional methods of construction. In terms of robotics, this has been investigated vastly in terms of assembly *(Gambao, Balaguer, & F., 2000; Werner, 1995*) and civil engineering *(Lorenc, Handlon, & Bernold, 2000; Kuntze, Hirsch, Jacubasch, F., & Goller, 1995)* in the past two decades. Furthermore, timid attempts have tried to bring deposition techniques closer to construction (*Williams, Albus, & Bostelman, 2004*), although there is much space for further research, as proved previously.

From the point of view of factory location and design, The Shimizu Corporation project used a large scale "on-site factory" (*Yamazakia & Maeda, 1998*), although this is demonstrated not to be the preferred model in most cases. The implementation of this sort of solutions in real projects is not a mere question of technological advancements, but rather a complex decision involving financial assets and business aspects such as the economic effect of an array of well-studied solutions. In fact, these decisions turn out to be made by any but their possible technical advantages, and normally depend on part standardization, production volume, transportation needs and costs, and many others. Large scale printing could solve problems deriving from assemblies of small-scale pieces, which is challenging both at material and software levels (*Zhang & Bernard, AM Feature and Knowledge Based Process Planning for Additive Manufacturing in Multiple Parts Production Context, 2014; Zhang, Bernard, Harik, & Kanunakaran, 2015*). Following sections elaborate further on this topic, showing the advantages of de-localized production for the construction sector or other alike.

Nevertheless, the aforementioned examples are just very early instances of practical developments involving purposes of construction automation. There are many applications that may emerge from other digital fabrication methods, discussed in the following section.

3.2.1.2. Digital Fabrication and Rapid Manufacturing trends in the construction sector

Digital Fabrication (DF) and *Rapid Manufacturing* will shift the actual construction paradigm in the years to come. Not only are architects and designers beginning to deal with parametric design techniques involving different CNC machinery; these professionals are also starting to enrich and refine their collective imagination to rise up new scenery opportunities that incorporate these technologies.

The aerospace and automotive sector revolutions took place between the 60s (with the abrupt introduction of numerical control machines), and the 90s (with the emergence of parametric modelling). These are currently blooming technologies that coincide in time in the construction industry, again lagging behind a couple of decades. The application of CAD/CAM techniques to the construction of structural

building components or facades is perhaps one of the most remarkable developments of these techniques. The Vila Olimpica, designed by Frank Gehry and considered one of the first examples of this use, was designed in CATIA, a solid modeling tool extensively used in the aerospace industry *(Schodek, Bechthold, Griggs, Ka, & Steinberg, 2005*). Some other projects have benefited from the same software-hardware partnership, from which the Guggenheim Museum in Bilbao is one of the most outstanding examples.

Nevertheless, the common applications of CNC manufacturing in construction are cutting processes used to form structural steel members and milling processes employed to create large molds from polystyrene for casting concrete or shaping glass. Gehry's Zollhoff Towers (Dusseldorf, Germany) used CNC techniques in the manufacture of major structural components.

There are many architectural and design offices exemplifying the adoption of these new technologies, and their adaptation to the construction sector. Objectile, Kokkugia, SuperManeouvre, R&Sie and many others –such as the author's initiative archi[o]logics[1]- deal with a combination of engineering, mathematics, technology, or even sociological sciences and philosophy to work on the design, rationalization, and manufacturing of complex geometries in a large range of proportions. Besides, other minor firms also worked on advanced techniques or even developed proprietary code for controlling milling tools or even robots, as seen in section 2.4., in order to develop exclusively customized functionalities. For instance, the form of structural members can be shaped to "taste", forming many different, interlocking, freeform components.

The rationalization of building geometries –such as double-curved surfaces- is becoming a familiar technique for many studios. Buro Happold, Foster and Partners, UNStudio, Zaha Hadid Architects, AEDAS, ShoP, Ove Arup and other leading engineering and design firms, have now integrated specialist geometry units within their corporate structures. The easy access to parametric design tools and visual scripting is leading towards a democratization of the design process and complex geometries with increased information. As said, it is possible nowadays to use solid modelling tools to solve freeform architectural surfaces into efficient, easy to build structures. Solid modelling is as well becoming a vehicle for design information transfer and a way to unlock creative solutions throughout the digitalization of complete building structures altogether.

In short, non-critical processes are being steadily dragged and absorbed by (non-creative) machines, allowing architects to *breathe* in a more compelling design environment. Machines are very good at repeating tasks and excel at automating simple processes, where the automation is very effective. In 1997, Pegna suggested that the larger number and the simpler the operations are, the more efficient and optimal process automations become (*Pegna, 1997*). As explained in section 2.4.5.1, Contour Crafting has recently demonstrated that the principles of Rapid Manufacturing can be applied to construction materials and proceedings (*Khoshnevis, Bukkapatnam, Kwon, & Saito, 2001; Khoshnevis, Russel, Kwon, & Bukkapatnam, 2001; Khoshnevis B. , Automated construction by Contour Crafting - Related robotics and information sciences, 2004*).

At a different level, Keynes suggests societal circumstances that may as well affect the promotion of these technologies. According to the economist, while material needs are finite for human beings, positional needs are effectively limitless. In other words, human beings are normally not happy with having high-quality products, but gradually more prone to pay additional fees for obtaining a better position with respect to others in the same society. For this reason, in a market where products are sufficiently good –a pre-requirement for their commercialization- people are willing to take or assume higher product costs in order to gain a higher status, valuing individualism, superior distinction, and exclusivity. Precisely at this point is where 3D printing attains one of its main advantages compared to other fabrication techniques: the possibility to produce different at the same or very similar price of other technologies –causing prices to further drop down in time. Furthermore, distinction is not a handicap in 3D printed pieces, as slight differences in shape, form, or size do not alter the end product's production time, quality, or means.

The access to parametric design still lacks its counterpart in digital fabrication despite the eruption of small machinery in general, and large-scale fabrication in particular. This is indeed where the present

[1] See www.archiologics.com for further information. Archiologics is a design think-tank focused on smart urbanism, algorithmic design, and complex systems.

thesis acquires its outmost importance and practical relevance, specially related to otherwise unrealizable designs or customized parts.

3.2.1.3. The specificity of the construction sector in Spain

Despite the aforementioned examples, the situation in most countries in the world, is one of a drastic stagnation regarding construction technologies. Although each country has its particular circumstances, it is worth pointing out some of the most relevant issues for the Spanish market, in an attempt to emphasize and focus on the most obscure aspects of the structure of the sector itself. This might help the reader understand the endemic situation of construction in other countries as well, since some aspects might be reflected back in other geographical or economical contexts.

First, it is crucial to underline the global context within which this brief analysis takes place. As stated in the Davos World Economic Forum, robotics has entered the modern era with the same intensity as steam machines did the second half of the 18th century. Nanotechnologies, artificial intelligence, drones, and 3D printers are all devices and concepts that are considered to modify and impact on all aspects and dimensions of society, particularly regarding workforce, work models, and labor relationships. The Davos World Economic Forum, in its Industry Agenda Document "Shaping the future of construction" *(World Economic Forum (WEF) with The Boston Consulting Group, 2016, May*) contemplates robotics as a paradigm-shifting technology driving the fourth Industrial Revolution following those of steam, electricity, and electronics. Whether the two former conveyed energy transformations for heavier mechanical operations, the last two minimize the energy used for both information transfers and the optimization of the production cycle. According to the mentioned document, it is foreseen that 3D printing will eradicate around 5 million jobs in the 15 most industrialized countries in the world.

While this can arguably be the case in the first years of the implementation of the AM technology, it is important to precisely define how this would eventually take place. Analysts and economists alike agree that hand labor, traditional crafts, and repetitive jobs will be affected first, as was the case in the first two industrial revolutions. Artificial intelligence is then thought to have an especially negative influence on the most qualified placements of the service sector, leaving space for new job placements in more technology-related sectors. The European Union (*European Commission, 2013*), estimates in 900.000 the amount of highly qualified jobs that will be required to cover that demand. Despite the initial, negative impact on the job balance attributable to the emergence and employment of robotics in many industrial markets, these technologies create new job types, generate new professions and unexplored opportunities.

High-tech advancements enter underdeveloped countries and emerging markets –such as Asia and Latin America- the last. Nonetheless, the impact on developed countries will be minor compared to that on less consolidated economies due to the reduction of cheap labor.

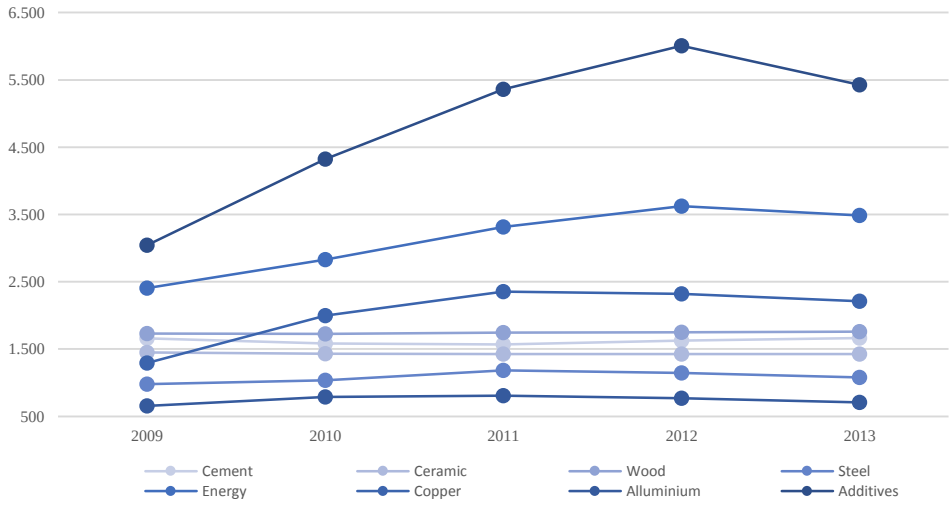

Fig.1. Commodity Prices: Spain National Index (Base January 1964, Units: index)

These questions affect the construction industry in a very particular way due to its intricate sophistications and the manner in which it has been shaped, even more so in Spain where it became the main driver of the economic growth during the last 15 to 20 years. Since the Real Estate crisis of 2007, three main aspects have been particularly stimulated, namely:

- (i) The lack of qualification of labor, clearly affected by wage fluctuations. During the expansive phase of the economic period comprised approximately between 1990 and 2005, underqualified workers lined up to obtain a placement at building sites, dragging construction's quality lower. Nonetheless, since housing product were sold easily by developers, the architectural and construction quality of the end product became almost irrelevant, and time delays where easily absorbed by inflating prices. Paradoxically, wages increased despite the absence of a real professional network of construction workers.
- (ii) The inflation of building material prices, which increased following what it "*was believed*" to be an ever-expanding market.
- (iii) A chaotic regulatory infrastructure, which is still today in constant change and very fragmented despite the efforts made to implement the Building Eurocode and other European Standards (suffice it to say that each municipality in Spain may set urban regulations, many times controversial as they contradict higher-order norms). Furthermore, European regulations hardly tackle local specificities, forcing erroneous building types and/or construction methods, which are strangely pushed through the norms.

Historically, the hourly wage of construction workers in Spain has been one of the lowest of the Eurozone, which reflected back in the quality of works and the lack of innovation of the sector *(Eurostat, 2016*). The European Federation of Builders and Wood Workers Study on Wages in Construction explains that, as in many other countries, Northern European construction workers earn about 20 to 40% more than Spanish ones *(European Federation of Building and Woodworkers (EFBWW), 2009; Eurostat, 2016*). As a consequence, qualified education is demanded double in those countries than in Spain, where not only is this an endemic innovation challenge, but an actual, every-day risk for the thus underqualified construction workers.

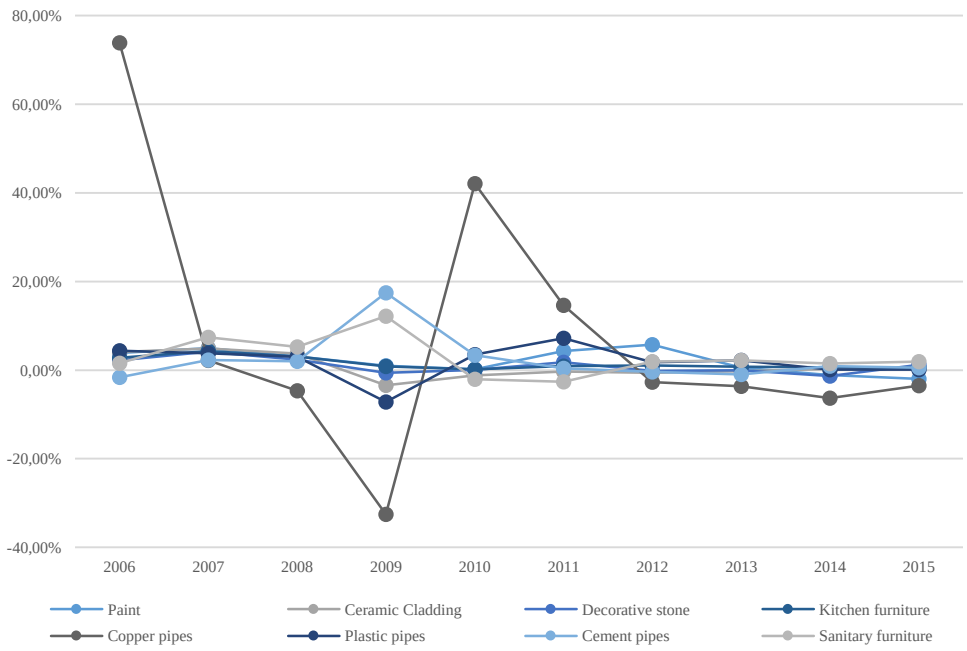

Fig.2. Spain National Index (Base 100: January 2010): Evolution of relative cost of construction Materials Prices (%)

The cost of construction in Spain has been traditionally lower than the average of all countries in the European Union. According to a study carried out by Arcadis (*Arcadis, 2016*), this was a constant that is still maintained nowadays despite the heavy fluctuation of commodity prices, such as iron ore, copper,

and oil between 2005 and 2016. This fact is certainly controversial, as it is known that the price of housing boosted drastically until, approximately, year 2007. Leaving important circumstances aside, such as the cost of soil, construction materials have increased their price in the last years according to statistical data gathered from INE and the Spanish Ministry of Industry for different periods comprised in the years between 1990 and 2013 *(Spanish National Statistics Institute (INE), 2013*). This is due partially to the improvement of traditional systems and the rise of indirect costs associated to the construction industry, thus diminishing the difference between the price of a built square meter in Spain and in the average of the European Union (*Spanish National Statistics Institute (INE), 2016*). Another two key issues are energy and transportation, which –fostered by the emergence of economies in Latin America and Asia- have also a direct impact on building costs. Furthermore, taxes on construction-related activities have increased in the past years, which will help maintain housing price despite the drop in the value of soil.

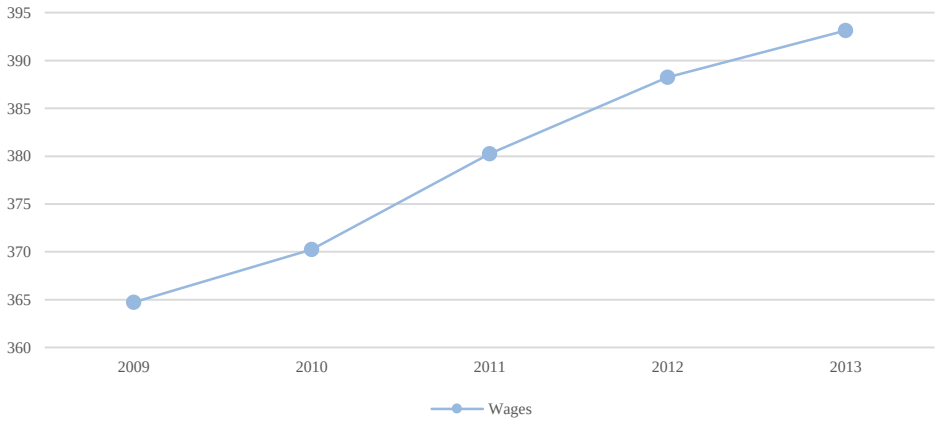

Fig.3. Spain National Index (Base January 1964, Units: index): Construction Wages

These factors have fostered an exceptional reaction of the construction industry, which is starting to overcome its historical reluctance to embrace innovative processes and initiating a trip into new, unknown construction techniques and methodologies. Recent Gross Domestic Product (GDP) data has confirmed that the engines for the EU's growth include Poland, the UK, Ireland, Spain, the Netherlands and even France. Italy and Austria, previously lagging behind, are showing some signs of recovery. Across the EU, the construction industry is expected to grow for the next three years (2016-2019) by a 2.3 percent per year, with the most buoyant markets expected to be in the UK, Czech Republic and Poland *(Arcadis, 2016*).

- **Technology as a catalyzer for innovation**

In order for construction to be a driving force of developed and emerging economies alike in the years to come, it is indeed crucial that the sector engraves technological developments into its very core. These can have diverse forms and takes, but a 180º degree turn must take place for construction to keep its strength in an economy based on digital content. New assembly methods are required to lower the impact of the building price on the overall construction costs, which must, on their end, be tackled by automation processes and directed by qualified labor, which would substitute former craftsmen by new job types or professionals such as building or construction managers, scientists, method surveyors, or construction specialists to name just some.

Adopting process automation seems to make more and more sense in sectors where specialization is certainly a new comer. Construction has an opportunity for renewal that will probably open up new ways through the implementation of R&D projects and their technological transfer into novel industrial products. The use of robotics for architectural purposes in its broadest sense is just one of the many possible ways to instrument this change, but indeed one that can stimulate the whole industry and result in an unmatched revolution with unpredictable cascading consequences.

3.3. Conclusions

This chapter has presented a study of the current state of the construction sector signifying its most relevant systemic problems. As explained in precedent sections, the construction sector suffers from an endemic scarcity of innovation due to its static nature and reluctance to adopt new technologies. Nonetheless, it is obvious that it must face systemic changes in terms of technology, manufacturing methods and the organization of work. Although BIM is pushing new means of controlling construction management, phasing and costs, a similar approach for the construction as such is mandatory. The sector needs to shift from prefabrication processes into fully deployed, integrated process automation, whereby robotics can play an important role. In addition, the enactment of this technology can potentially redefine the distribution of labor to accommodate a more qualified, viable workforce that would ultimately direct and design new manufacturing techniques and methods. The following chapter deals with the definition of a model to enable robotic 3D printing for the building industry.

Chapter 4

Towards the standardization of real-scale, robotic 3D printing. Software integration

As explained in previous chapters, 3D printing for construction is stagnated at an early stage of development, especially regarding procedural issues and material optimization. The present chapter deals with the procedural issues, democratization, and standardization opportunities for this technology.

Industrial robots are the next generation of real-scale object production. This chapter establishes an optimized workflow with these machines that integrates current construction methodologies and materials with these automation machines.

A test case that shows the integration of the design-to-fabrication process combining Integrated Robotic Systems (IRS) and Additive Layer Manufacturing (ALM) techniques is discussed. This chapter exposes as well a software integration that redefines the design-to-production process for construction purposes. A software package in form of a plugin is specifically developed for testing this approach. The add-on shows the synthesis of the powerful Rhinoceros geometry kernel together with the capabilities of robotic arms in order to become a standardization tool for Additive Manufacturing purposes.

4.1. Introduction

It can be stated that current 3D printing processes focus mostly on Rapid Prototyping (RP) *(Wright, 2001*), relying on SLA, SLS and FDM techniques rely on a layer-by-layer method, one that presents a number of limitations, among which the following are particularly worth pointing out: (i) the need for material continuity, (ii) the presence of support material in certain parts, and (iii) manual refinement needs. For instance, plastic extrusion requires in most cases support material that must be manually removed and further refined. At the other end of the spectrum, oversize approaches to 3D printing scale up desktop-oriented machines without altering their design at a conceptual level, as demonstrated throughout Chapter 2. In brief, the two main real-scale printing methods, (i) the "*scaffolding-based*" Z-printer and the gantry-like approaches -such as bridges, cranes, gantries or similar super-structures like the World's Advanced Saving Project (*WASP World's Advanced Saving Project, 2015; Lott-Lavigna, 2015*) and D-Shape printer (*Dini, 2016*); (ii) Contour Crafting techniques *(Khoshnevis B. , Automated construction by Contour Crafting - Related robotics and information sciences, 2004; United States Patent No. US 7641461 B2, 2010*). As said in sections 3.2. and 2.4, these technologies are inefficient and difficult to transport, which would require a singular risk analysis and advanced financial studies to put them into practice in real

construction projects. In addition to that, these techniques are rough, inaccurate and prone to geometrical imprecisions. (*Malaeb, et al., 2015*).

Many examples make use of these technologies for potential complex building geometries in façades or similar construction elements (*Strauss & Knaack, 2016; Strauss H. , AM Envelope: The potential of Additive Manufacturing for façade construction, 2013*). The Radiolaria Project, for instance, basically consists of a scaled-up translation of SLA printers working with a nozzle that pours adhesive binder onto a layer of raw structural material to demonstrate the geometrical capacities of the technology. On the other hand, the WinSun Singapore Home and the 3D printed canal house by DUS Architects –see Figure 1- use a method similar to Contour Crafting *(United States Patent No. US 7641461 B2, 2010; United States Patent No. US 7814937 B2, 2010*), as described in section 2.6. In these techniques, a nozzle pours concrete or a similar fused material directly in place, creating the final form or object physically. This approach seems to be more scalable and easily deployable than the former, as the building material might be brought directly onto the site where pieces are meant to be built.

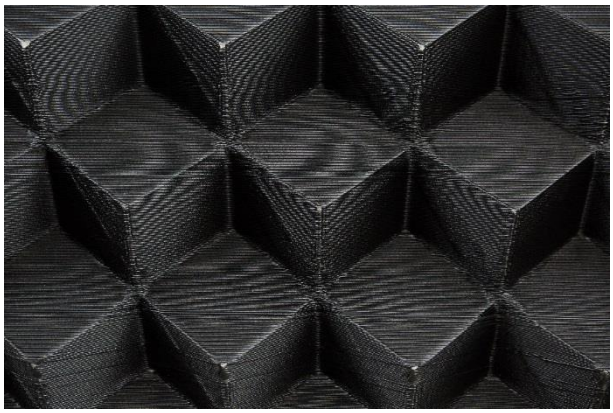

Fig. 1. Module of 3D printed Canal House, an application of FDM to full-scale 3D printing (Picture: Martin de Bouter)

Although these are interesting experiments that push the limits of construction, they present prominent issues that must be taken into account. In fact, they fail at various points:

- The most noteworthy problem is the amount of material that is required for the fabrication in D-Shape like technologies.
- The size of the involved infrastructure, which makes it unsuitable for moving production to delocalized factories.
- The need to provide more complex solutions that incorporate building systems, structural elements, and finish materials into the final products.
- The transportation of building modules to the site is a key issue which needs to be considered. This is a fundamental aspect of modular and prefabricated construction that influences the viability, feasibility and sustainability of the final product directly. The heavy weight of the pieces impacts these methodology as well, limiting its introduction and standardization.

Precisely because of the very divergent approaches, strategies, and procedures that affect large-scale 3D printing as an application of Computer Integrated Construction (*Yamazakia & Maeda, 1998*), it is possible to identify exceptional opportunities regarding the following aspects:

- **Standardized workflows** and **scalability**.
- Material **optimization** and the use of **recycled** and environment-friendly materials.
- Energy savings and use of **local and renewable energy** sources, such as household waste in both rural and non-rural communities *(Al-Khatib, Monou, Abu Zahra, Shaheen, & Kassinos, 2010; Philippe & Culot, 2009*).
- Deployment of the **fabrication machinery on site**.
- Fabrication of customized, **ad-hoc parts** with no extra-cost.

Furthermore, many of the limitations concerning 3D printing technologies for large scale objects and their applications are fundamentally due to the following reasons: (i) the highly specific knowledge that these technologies imply, (ii) the total cost of the machinery involved, and (iii) the lack of clear procedural guidelines or standardized procedures. This chapter presents a methodology that aims at overcoming these limitations through a workflow that allows for the ease of use of 6-axis robotic arms for specific 3D printing purposes.

4.2. Standardization, prefabrication, and 3D printing for construction

Prefabrication is a reality deeply embedded in construction processes in developed countries, where labor force has become a highly specialized and expensive asset as seen in the previous chapter. The industry is nowadays capable of producing all sorts of building elements in a wide range of materials and forms: sandwich panels, precast structural parts, or even whole housing units to name just some. Casting, molding, extrusion, injection and other techniques are used to create construction and industrial parts for almost all imaginable uses.

Nevertheless, there are certain limits to what industry can offer for the construction sector. Using molds only makes sense when total part production is really high, lowering the price impact on each piece or when forms are not limited to certain geometric restrictions. Construction is different to other industries by nature, which makes it impossible to compare its serialization process to that of the automotive industry, for instance.

3D printing in the building industry, can thus be oriented towards bridging the gap between construction and customized serialization, a sort of intermediate space between industrial parts and traditional construction. Although much has been said about the benefits of 3D printing and market forecasts predict its exponential growth, it seems logical to precisely determine the range of affection of 3D printing for the construction field.

Precisely where other fabrication methods cannot operate due to either geometric or size constraints, 3D printing finds its place. As a consequence, it can be applied to a number of products and methods, such as complex casting, prefabricated or monolithic structures, temporary constructions, non-structural parts, and other components that might require high degrees of customization. Besides, it can fill the need for the quick production of long series of variable parts, such as slightly differentiated façade panels (*Castañeda, Lauret, Lirola, & Ovando, 2015; Strauss H. , AM Envelope: The potential of Additive Manufacturing for façade construction, 2013*) present in singular buildings all over the world. The use of this adaptive paneling has been allowed itself by the implementation of easy, ready-to-use parametric design software for architecture and construction and RP *(Buswell R. A., Soar, Gibb, & Thorpe, 2005; Buswell R. , Soar, Gibb, & Thorpe, 2007*).

This chapter presents a comprehensive approach to deal with these issues: first, through an integrated design-to-production **methodology** for big-scale part fabrication with 6-axis robotic arms in order to provide enhanced functionality and flexibility; second, through a **material optimization tool** to be integrated in the generation of 3D-printable models by means of customized fill patterns that respond to specific material behaviors and structural conditions, which are explained in Chapter 6.

The material optimization, conceived as an enhancement of the methodology, is carried out through the stress analysis of 3D models characterized as finite element representations. This method enables form-finding based on material properties, organization, and behavior. The integration of the whole design-to-fabrication process combining IRS and ALM techniques (*Tibaut, Rebolj, & Nekrep Perc, 2014*), as well as the integrated software platform *(Panetto, 2007*) that enables this solution are shown in this chapter's sections 4 and 5.

This approach provides (i) feasible, (ii) technologically viable, and (iii) economically affordable solutions to those aspects of large-scale part production for the construction industry by introducing another level of intelligence into the four main aspects of 3D printing:

- **Workflow**: seamlessly integrating *design-to-production* processes.
- **Software**: a platform that translates design ideas into machine-readable content that makes it unnecessary for users to have high levels of expertise or otherwise understand

complex machines (see section 5). In this sense, software has a certain capability of democratization, as it is employed as bridge between design intents or ideas and their materialized counterparts.

- **Hardware**: 6-axis robots are easily transportable and deployable on site for construction processes and succeed in being able to move freely in 3D space without the limitations inherent to other oversize 3D printing methods. Furthermore, robots can be **easily transported** and **deployed on site**, resulting in a significant reduction of transportation costs. Finally, robot programs from specific vendors fit different robot sizes and models with no or little restrictions, resulting in a particularly scalable technology (see section 3) since all robot models make use of the same controller software and hardware. In other words, robotic arms follow the one-size-fits-all approach in terms of software and programming.
- **Materials**: limiting the use of materials and the associated carbon footprint attached to the fabrication through a single production process (see section 4). Material usage is reduced both by the very nature of AM and the structural optimization of parts, where only the amount of material needed is really consumed during the fabrication. Furthermore, it allows for further research in the field of material science.

Many efforts have been put into facilitating the use of desktop 3D printers in the market. Nevertheless, due to the dispersion of the printing market –consequence of its relative youth-, it seems difficult to find combined efforts that intend to unite the production process and the design workflows into a single, easy to follow procedure that targets:

- Non-specialized users.
- Feasible and technologically viable 3D designs.
- Many different software packages through small translators in the form of plugins that integrate design and their robot-readable counterparts (files).
- Automated error-checking, disclosed deeply in subsequent sections.

As figure 2 shows, current design-to-fabrication workflows require a great involvement from the user. The design-to-production workflow presented herein aims to reduce user involvement in fabrication processes, automating highly skilled tasks. It intends to create a single cycle that automatically relates virtual models with the fabrication itself, solving any design refinement needs and automating non-critical tasks.

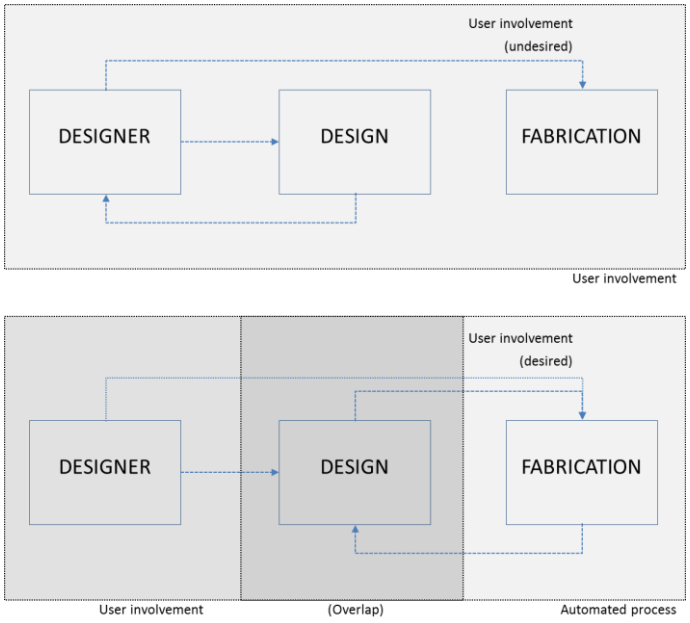

Fig. 2. Current and proposed designer-design-fabrication interactions.

This integration is achieved by including all fabrication requirements into small software packages that work as "interpreters" and "translators". 3D models are read and analyzed by the software, which solves small defects or informs the user of any modifications that need to take place in order to make a certain solid model printable. The packages integrate (i) existing **3D modeling platforms**, (ii) **machine interaction** and setup, and (iii) **fabrication** or physical interaction present in any CNC paradigm (Reintjes, 1991).

This approach differs from holistic solutions where a universal design user interface is created in an attempt to tackle the problematic of printing with robotic arms as a whole. As opposed to such a procedural take, the present thesis focuses rather on taking advantage of widely accepted CAD-CAM software, and that end-users have already incorporated into their workflows. These software packages are used as basis for completely integrated tools within the native host CAD environments hence minimizing the learning curve from the beginning. These pieces of software deal with the most obscure, abstract and intricate aspects of human-machine interactions allowing for a seamless transition between design and fabrication software in an attempt to democratize the use of industrial robotic arms for 3D printing in the construction sector.

Although the most technical aspects of the standardization of the use of robotics for construction are explained in subsequent sections, let us layout the most relevant aspects of the approach:

- The use of 3D model standards, such as IFC (Industry Foundation Classes) for BIM models or, more generally IGES and STL for mesh-based, non-informed, models.
- The calculation of the robot toolpath according to a Contour-Crafting logic –which can be expanded to obtain contour lines.
- The description of robot moves as linear movements following the toolpath.
- The definition of speeds associated to material properties.
- The integration of tool references in the file as a set of coordinates defining a plane. The addition of mass to this tool.
- The integration of these into a single package loadable by multiple software modules and AEC programs.

Consequently, any model could be easily translated into a robot-readable file making use of a simple translator integrated in the base programs. XML tags can be used to define the properties and actions named above. The use of XML based files is well suitable both for their ease of use and their readability, which makes further development easy and accessible to users and developers alike. This file can be translated in each language to the robot controller, thus minimizing the need for complex software translators, and allowing vendors to easily develop their modules.

4.3. Robotic arms as large-scale 3D printing tools.

As said above, small-part 3D printing mostly relies on stereolitography (STL) file format standards[2]. This is possible because of the way in which STL files operate: to put it simply, a STL file contains a mesh that stores the object's geometry information through its vertices and faces (normally triangular or quads) that merely hold the geometry information describing the surface of the object (this is, the STL files contain no information about color, textures, or any other attribute). This file is sliced with a special program (Slicer), which calculates a series of contours where the binding (SLS) or fused materials (FDM) are placed. The printer software translates those contours into GCode or similar, which in turn result in "piled up" layers of material.

This format has proven useful for 2+1 (this means, 2 horizontal + 1 vertical) axis FDM printers, such as 3D Systems, Stratasys, Makerbot, Prusa, and many other printers present in the desktop and

[2] The STL is a file format developed by 3D Systems that lightly describes closed solid geometry. It is considered a standard used by almost all 3D CAD applications.

professional markets. Those printers create a layer-by-layer extruded model (or similar) that replicates physically the position of the above mentioned contours.

Nonetheless, robotic arms have a radically different approach to movement control, which depends on vendor-specific hardware. Although it is explained in higher detail in subsequent chapters, suffice it to say at this point that robots are not as geometrically constraint as 3-axis machines, due to the three additional degrees of freedom. All main robot suppliers in the world *(Technavio, 2016*) provide integrated software and hardware solutions in order to design and fabricate parts for the automotive and aerospace industries, among others. However, each vendor provides unique, black-boxed packages that are incompatible with one another –actually, each vendor develops its own programming language- or any other CAD package available in the market. As a consequence, many opportunities emerge that are worth exploring, especially with applications in the AEC sector (*Rebolj, Fischer, & Endy, 2011*).

6-axis robotic arms are normally described as a series of joints and axis, which ultimately control the position of each robot part. Although it is out of the scope of the present thesis to thoroughly describe the insights of a robotic arm, suffice it to say that any robot position can be defined by specifying the angles of each joint. Figure 3 depicts a diagram of a standard robot, showing its typical movement ranges.

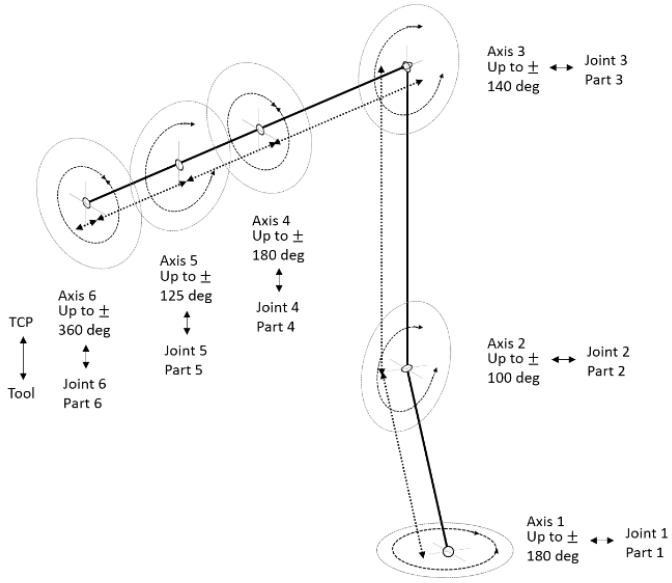

Fig. 3. Abstract description of an industrial 6-axis robotic arm –actual rotation values may differ

Robots can be thus thought as simple 3D space "tool locators" defined as a series of joints and axes (*Payne, 2011*), which ultimately replace the hand of a human worker. As opposed to other fabrication methods, 6-axis robots have **no inherent geometrical limitations aside their own size –**which can be easily scaled up by introducing tracks or external axes**.** These robots excel at their capacity to occupy any point in the 3D space confined within their operational range boundaries. The Space Frame project –shown in Chapter 2– proves that it is possible to print with no support material *(ETH Zürich with SEC Singapore, 2012-2016*), showing that robots outdo the layer-by-layer logic when they are utilized as a resource for 3D printing purposes. Thus, these machines can create spatial structures that supersede those created using other, more generic, techniques. Employing appropriate materials such as PLA, ABS-derived materials *(Sung-Hoon, Montero, Odell, Roundy, & Wright, 2002*), cement-like materials, or composites favors real-scale object production, whether for the automotive, aerospace, AECO industries, and others[3].

Most 3D printers make use of the widespread G-Code language, which enables fabricators to easily control the devices involved in 3D printers, namely stepper motors, potentiometers, hot ends, and a variety of simple sensors. Robots, due to their different hardware architecture cannot take advantage of such an approach and must be programmed, as said above, in proprietary languages –such as KUKA and RAPID

[3] According to technavio, "[…] the field of robotics technology demands continuous exploration and innovation, there are a lot of untapped opportunities [...]. This prompts many robot OEMs and new start-ups to innovate and invest in this technology." The major vendors such as ABB, iRobot, and KUKA are investing heavily in R&D to remain ahead in the market.

to name just two of the most important ones. Automating robot programming is precisely one of the most crucial aspects of the integrated design-to-production workflow.

4.4. An integrative design-to-fabrication workflow. Towards a 3D printing standard for construction.

4.4.1. Current trends in architectural modeling and fabrication

Contemporary building design methodologies implement Building Information Modeling (BIM) as building database integration platforms. As explained earlier, BIM seeks to unite all building-related information into single, comprehensive models that allow for an interaction of the different agents and stakeholders involved in the construction process, and a coordination of the different disciplines that intervene therein. Nevertheless, BIM methodologies focus mainly on building control issues, largely leaving aside the possibilities of current fabrication and construction trends.

Despite significant progress made in CAD/CAM software, the existing design-to-fabrication workflow can be still difficult to traverse for architects, designers, and builders alike. Design conception continues emerging from 2D sketches which are ultimately converted into 3D CAD models meant to depict diverse aspects of the projects in a more real and detailed way. This can be achieved either through traditional 3D CAD modeling, or by capturing an existing physical part with some sort of scanning device.

As far as 3D printing is concerned, both ways are equally valid. In fact, what matters is the virtual model from which the object will be produced and printed, as well as its post-processing. This normally means that the designer or fabricator needs to use specific proprietary software that requires qualification, such as MasterCAM with the Robot Master Plugin, or the stand-alone Robot Studio for ABB robots. Using these pieces of software is sometimes overkill for 3D printing applications, as they include unnecessary features for the 3D printing purpose, such as sophisticated algorithms for tool path creation, collision detection, and singularity analysis. In addition to that, these complex algorithms are needlessly exposed to the user, who typically has neither interest nor control over them. Either case, both designers and fabricators need to use specific proprietary software packages that require qualification which is sometimes overkill for 3D printing applications, as they present pointlessly complex features. Furthermore, these skills are normally beyond the scope of the training of architects, engineers, and designers. As a consequence, the process is burdened by a detachment between designer and final building parts during the fabrication chain –making it necessary to include CAM operator in the workflow.

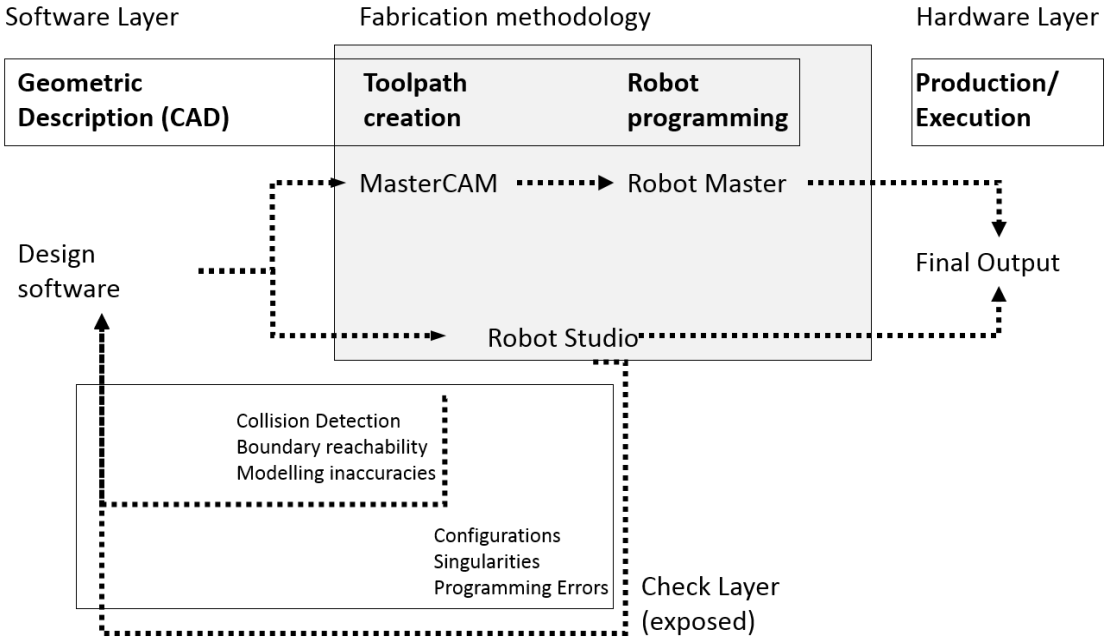

Fig. 4. Current software workflow with ABB robots and Rhinoceros.

The current tendency to use parametric software in architecture and design has led to various attempts to deal with this undesired situation. HAL (*HAL Robotics Ltd., 2015*), Firefly, Robots.IO *(Robots.IO, 2015*), and others intend to bridge the gap between design and production with robotic arms through Grasshopper[4]. Nevertheless, using a third-degree software layer adds yet another level of complexity to the equation. As explained previously, HAL and Robots.IO are merely plugins for the Grasshopper plugin for Rhinoceros. As a consequence, the user would be expected to master all three levels of software, which is highly unlikely to happen, and can eventually become discouraging for new users. Although they can be deemed disputably reliable and powerful tools, both software packages are heavily biased by their applications in architecture schools, and are unlikely to have industrial applications.

In fact, the present thesis intends to avoid this issue by simplifying the tooling and black-boxing unnecessary and undesired levels of software. While the aforementioned plugins would just replace the previously introduced CAM software with an even more complex visual programming interface for Rhinoceros, the approach taken by the thesis aims at the exact contrary situation. In fact, a natively integrated tool is developed to ease the use of the software and allow for testing by non-specialized users.

4.4.2. A modular and integrative software-based framework

The current user-CAD-CAM interaction makes necessary an integrative and easy-to-manage approach. The software integration makes it possible to benefit from the advantages of real-time model checking in order to reduce project time and costs significantly while *increasing productivity and quality*.

The integrative software-hardware interaction takes place through the automated translation of geometry into robot instructions that characterize robot axis movement via the description of a series of targets and toolpaths[5].

Geometry might be input either as NURBs or meshes. The approach presented herein achieves this by creating software components –this is, integrating software seamlessly into existing CAD platforms- that deal with the translation of different geometry types –consequence of the different software packages available- into robot instructions.

The software is eminently modular and consists hence of two kernels: (i) a geometry-calculation and a (ii) *translation* engine. The former calculates the robot tool path in the host CAD program, while the latter translates this result into machine-readable code for each robot model via an Inverse Kinematics (IK) engine (*Artifact of Code, 2016; Motta, 2005*). The IK engine is based on the "Lobster" engine description by Kangaroo's author Daniel Piker, a former member of Ove Arup's Advanced Geometry Unit *(Piker, 2014*). In addition to that, the software performs basic checks for the user to visualize whether a design can be fabricated during the conceptual phase. Finally, the software creates the necessary files and protocols required to move the robot. Figure 5 depicts the main conceptual software modules that come into play during the processing of the model's geometry and its translation process. A indicates the slicing process, whereas B is a checking process involving the built-in Inverse Kinematic engine that allows for automatic buildability checks.

[4] Grasshopper TM is a parametric tool for Rhinoceros developed by David Rutten at McNeel & Associates that implements a visual programming interface where functions are black-boxed into a series of components. These components are associated to one another in order to create algorithms.

[5] Although these concepts are explained meticulously in subsequent sections, let us describe them concisely. Targets are points or oriented locations in space, and can be represented either as a series of Cartesian coordinates on one of the multiple available workplanes, or as a series of joints' axes rotations directly. Toolpaths are simply a sequence of targets. Depending on the description of the targets, these might be either "*robtargets*" (if defined by Cartesian coordinates) or "*jointtargets*" (if defined by angle rotations).

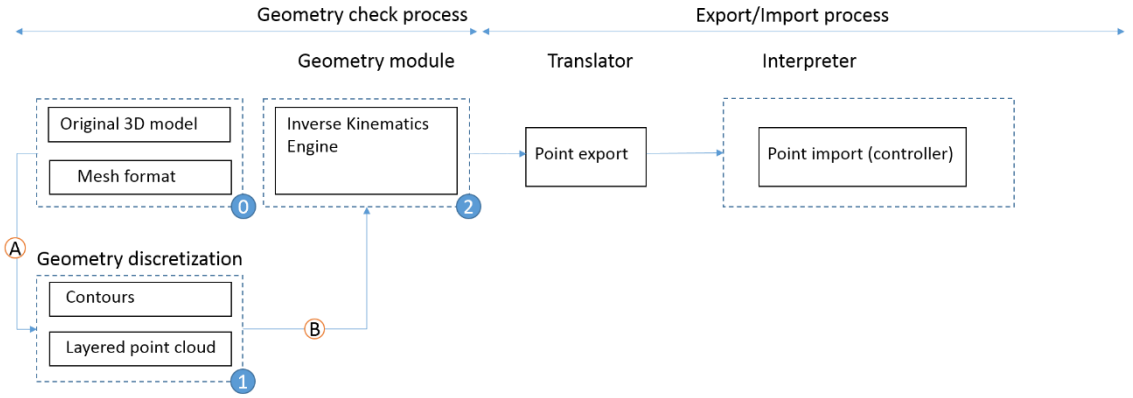

Fig. 5. Main software components and phases.

As seen in Chapter 2, **there exists no software that currently deals with this problem**. This approach stands out not only for solving this issue in a simple and effective manner, but for being the **only one available** in the market. This development is a milestone for the **democratization of robotics-oriented fabrication** (*Choi, Han, Lee, & Lee, 2005*) **and the universalization of the processes thereby implied**.

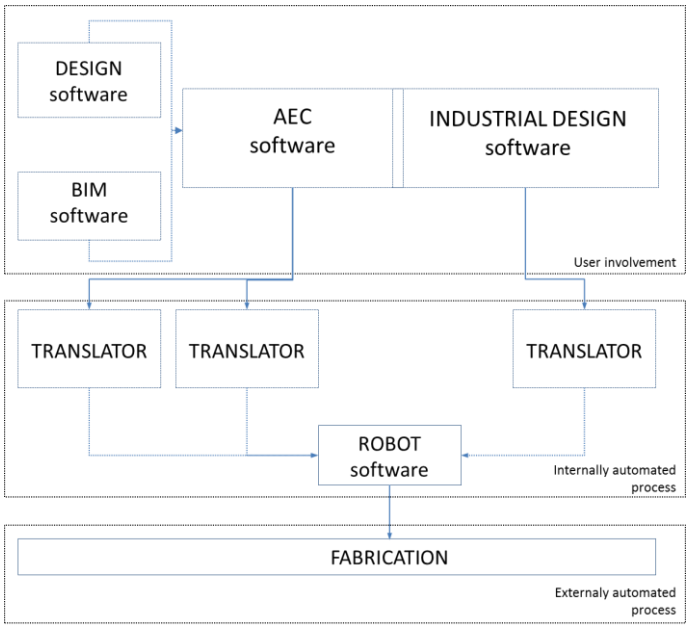

Fig. 6. Proposed workflow: automation of non-critical, fabrication-related tasks.

This modular workflow will, in addition to the above, permit users to double check their designs in real time, allowing them to minimize or even eliminate flaws during execution. User interactivity and maximized information flows are key aspects to the standardization the methodology proposes. The proposed software highlights possible flaws and their cause in design time, so that the user can correct them or decide how to continue with design. Finally, it is crucial to any digital fabrication process to include cost prediction. The real-time simulation of the fabrication process likewise includes material usage, time needs, and total manufacturing costs. These are light estimations that are consequence of the overall simulation process, which already involve costly geometrical calculations that immediately result in side predictions –accounting for the named above.

Alongside these series of methodological, the software approach implements (i) real-time design checking, minimizing or even eliminating flaws prior to execution and fabrication; (ii) advanced error prevention including collisions, singularities, and range detections; (iii) cost prediction and material usage, accounting for time needs, manufacturing costs, material needs and presets, and an easy interaction and maximized information, a key standardization aspect. All these are shown in the technological demonstrator in section 4.5.

One of the most remarkable potentials of the software, as said above, relies on its **modularity**, shown in figure 5. This mode of operation has proven very valuable and beneficial in numerous cases, as it provides parallel development capabilities and enhanced flexibility in relation to its use and adaptation to the wide range of host CAD software packages. For instance, Chaos Group´s VRay photorealistic visualization software performs in the same manner; providing a unique external kernel that runs the geometry calculation and translation operations together with translators for different pre-existing design packages. This results in a highly modular, cross-platform, and extendable software that anyone can use. The software intends to provide the same solution in order to facilitate the modularity and expandability of the whole integrated simulation process (*Law, 2014*). User involvement decreases gradually from design to production as far as software usage is concerned –see figure 6- thus allowing designers to focus on creating comprehensive designs that match their expectations without worrying about fabrication. Eventually, this solution could result in an open-source initiative for standardization, such as those led by BuildingSMART or NBS in the BIM realm.

Whereas the proof of concept has been developed for Rhinoceros and ABB, the software could be extended to any other CAD platform with solid modeling capabilities –experimentation with KUKA robots has begun at the time of printing this thesis. For instance, native CATIA, Solidworks, AutoCAD, Rhinoceros, or Revit geometry (to name just some) could be automatically translated into instructions that any robot would be able to accomplish.

4.4.3. Form-finding: material optimization through structural patterning systems

Oversized 3D printing has a great potential concerning material cost saving, as this accounts approximately for a 60%-70% of total construction costs. Although a novel method for material usage optimization through a structure-oriented infill pattern system implementing a finite-element model that responds to physical properties of materials is presented in Chapter 6, suffice it to say that the software discussed in the present chapter provides options for easy, ready-to-use **presets for diverse materials** that can be modified, classified, and extended by the user. These presets incorporate the following behaviors:

- hardening times,
- maximum robot speeds,
- robot TCP rotations,
- structural printing settings.

In addition to comprehensive material conditions and their implications on robot programming structures, it is important to point out the logic of infill patterns used in 3D printed parts. As opposed to standard, non-structural, space-packing infill patterns employed by vendors and freeware alike, the system presented in this thesis offers a compelling **material optimization approach**. Material usage minimization is not only an industrial demand and a feasibility must, but also one of the greatest contributions 3D printing technology has to offer. Furthermore, minimizing material reduces the building energy footprint at all levels, as will be discussed throughout the present document.

This strategy supports the structural analysis of parts, yielding stress-responsive patterns. As shown in Figure 11, the algorithm works in a multi-phase manner, including (i) input parsing, (ii) translation of 3D models into spring-like models, (iii) exporting to the Processing stand-alone calculation software (*Reas & Fry, 2014*), (iv) material characterization, and (v) the use of the physical logic to determine actual material thickness. The hardware technological demonstrators that prove the whole project have been built in PLA due to financial restrictions –after contacting several providers, it was concluded that concrete extruders would cost more than 10k € at least. Similar extruders used for clay materials cost around 12k € (as budgeted by ViscoTec and Händle, although WASP has recently launched a commercial clay extruder with lower load capacity for about 650 €). Various materials, including ABS and PLA with carbon fiber have been tested. Results are shown in Chapter 6 for reference.

For construction purposes, concrete is quickly gaining adepts *(Lim, Buswell, Austin, Gibb, & Thorpe, 2012*) in the field of large scale 3D printing (*Buswell R. , Soar, Gibb, & Thorpe, 2007*) and has also been considered for simulations of big-scale parts. Parts have been mainly tested against self-bearing conditions mainly, although a variety of different forces may be implemented. The algorithm is being

developed to comply with the restrictive regulations that apply to structural concrete in the region of Spain, including all in the EHE-08 (*Ministerio de Fomento (Spanish Ministry of Public Works), 2008*). It is planned to use concrete for further test parts. Please refer to Annex II for more information.

This implies an architectural reading as well. As a result of the above, the boundaries between otherwise separated building parts are blurred. In traditional construction, building elements are differentiated not only according to structural or architectural organizations, but to actual construction phasing. 3D printing optimized structural patterns could put an end to these differentiation and account for the synergetic relationship between performance and material integrity, one that can ultimately blend the physical experiments that classify form according to load applications and the digital realm where these may be simulated and studied prior to the designer's decision making. Pursuing further this strand of logic, the notion of form-finding attributed to Frei Otto (*Otto, 1995*) would acquire a more comprehensive meaning.

4.5. Software technological demonstrator: robot automation integration

As said in previous sections, a software technological demonstrator has been programmed to combine the powerful design tools from McNeel's Rhinoceros CAD software and the versatility of ABB robots and prove the advantages explained in previous sections. The demonstrator brings all above mentioned features into a single package that accounts for the whole design-to-production process.

This section shows the whole process and capabilities of the software according to the following structure: (i) justification of the software and hardware choices, (ii) plugin's interface and characteristics, (iii) translation details, (iv) geometry constraints and (v) experimentation.

4.5.1. Understanding native environments and software platforms

A careful study of the CAD software market shows that there are a series of packages that are worth looking at. From those, Rhinoceros, Revit, and AutoCAD are especially linked to the construction industry, one that seems to offer an important market gap to be exploited (*Cambashi, 2010*). For this reason, it is decided to create a technological demonstrator for these packages, starting from Rhinoceros for the case study that is presented herein. This choice is based on a number of well documented advantages, listed below for convenience:

- It is a generic platform for all main target industries:
    - construction sector, the main field of interest
    - automotive industry, a sector where advanced fabrication methods are under constant development and study
    - aerospace segment, where the potential perfection of 3D printed pieces could awake a growing interest
- It provides a very powerful geometry kernel open for third-party developers, including the most used geometry types: NURBs and meshes. Additionally, this kernel is easily accessible, expandable, and reasonably well documented.
- Rhinoceros supports several programming languages, including C#, python, and Visual Basic. Likewise, it is becoming increasingly cross-platform capable, with notable advancements in the development of Mac-based software. Furthermore, it is intended that plugins written for Windows© operating systems be fully compatible with Apple's Mac© hardware, although this is still work in progress. Most difficulties are encountered in UI programming.
- It provides an intuitive 3D interface for modeling simple and complex geometries that is gaining acceptance in the professional and academic worlds alike.

The most relevant characteristic of the above, as far as programming is concerned, is the possibility to access the host CAD program's powerful geometry kernel. Rhinoceros provides built-in programming

interfaces for scripting with the python language, while it is still possible to use professional platforms – such as Visual Studio- to develop .NET software. The OpenNURBS library grants access to the insights and intricacies of geometry within this platform, allowing any professional user to develop ad-hoc, off-the-shelf applications. OpenNURBS provides access for CAD, CAM, CAE, and computer graphics developers with tools to transfer 3D geometry, guaranteeing interoperability across different software platforms. The tools provided include (i) C++ source code libraries with Microsoft, Apple, and GNU compiler support; (ii) .NET source code to read and write 3DM formats; and (iii) quality and service. Furthermore, the commercial use of OpenNURBS is encouraged, free, and with neither copyright nor copyleft restrictions.

RhinoCommon is the cross-platform .NET plugin SDK available for Rhinoceros 5 for Windows and Mac, Rhinoceros Python scripting and Grasshopper, granting maximized access to the latest parametric design tools. The RhinoCommon SDK can be used across Rhinoceros platforms. A plugin built with RhinoCommon could potentially run on both Windows and Mac platforms with no changes, except those accountable to the User Interface, where there are still differences that must be manually solved.

The plugin accesses the geometry kernel through the RhinoCommon library provided for this particular platform and makes use of OpenNURBS for data interoperability. Other CAD packages would have different requirements, although they are usually programmable in C#.

4.5.2. A native robot interaction interface

Once the plugin accesses the geometry kernel of the software platform, it converts it into a series of targets (which will become actual 3D positions of the TCP or tool plane) which in turn constitute the toolpath. As explained in the previous section, targets are locations in space described either as a set of coordinates or joint angles, and toolpaths a sequence of targets, both of which can be programmed to control the manipulator's movement. This is a simple operation that requires little computational effort, and is explained in detail in subsequent sections. Then, an inverse kinematics (IK) engine places the robot according to the axis rotation calculation and the actual physical dimensions and possible movements of the selected robot model. This is processed automatically by the plugin's kernel.

The plugin's interface needs to be seamlessly integrated with the selected 3D platform. In order to achieve that, **native panel programming** is provided, which achieves high-quality displays. Furthermore, the display integrates the following elements:

- **Material selector**: for automatic robot presets (under development).
- **Contour definition**: material thickness.
- **Robot model selector:** from the list of implemented models or loaded by the user (under development).
- **Simulation display**: play, stop, and resume robot movement simulation. Also possibility for user to "zoom in" possible frames in detail or coarse levels.
- **Clash detection calculation**: prevent robot from colliding against physical elements.
- **Error detection:** perform out of range calculations and similar.

These options will allow the plugin kernel to calculate the necessary information to create the toolpath by evaluating targets.

4.5.3. Translating geometry into robot language and fabrication

Finally, it is necessary to translate these geometry objects (basically planes defining positions and a series of digital inputs/outputs) into movement instructions. For commercial robots this normally means curved or linear movements that must be described in robot scripting language: RAPID for ABB robots, Kuka language for KUKA robots, and so on. These files must be uploaded to the robot and executed internally within its own internal protocols. This results in actual robot operations.

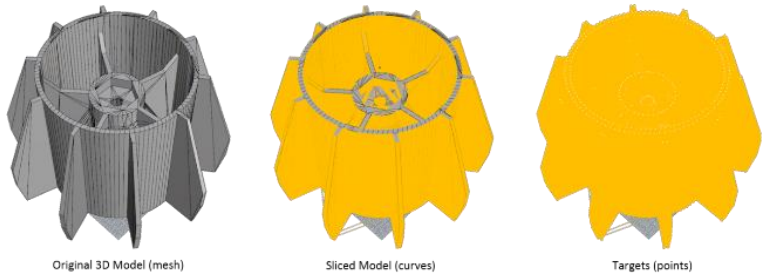

Fig. 7. Internal slicing process and conversion to points

As explained in section 4.4.2., an IK engine is used to calculate the axis position of the robot for movement visualization purposes. In actuality, two different engines are employed at different stages of the calculation. First, a Lobster-based IK engine is used for the previsualization and pre-calculation phase, where the robot's manipulator becomes visible in the 3D model as a virtual object. Second, the actual robot's controller IK engine takes responsibility for calculating the manipulator's movements in real time during procedure execution. Either case, the 6 axes' locations and/or rotations must be calculated as to obtain the final position of the manipulator. These 6 axes give the end effector (the part where the tool is attached - e.g. a gripper or drill) the full 6 degrees of freedom for location and orientation in space. Axes 4, 5 and 6, shown in figure 11, normally intersect in a common point. This very important characteristic, known as "*spherical wrist*", allows the kinematic decoupling which is essential for how the Inverse Kinematic engines works. Luckily almost all modern industrial 6 axis arms have spherical wrists. As opposed to those axes, axis 3 and axis 4 do not necessarily intersect, and are often offset by a small amount. In addition, axis 1 and 2 often do not intersect. However it is only the intersection at the wrist which is important for the IK (*Piker, 2014*).

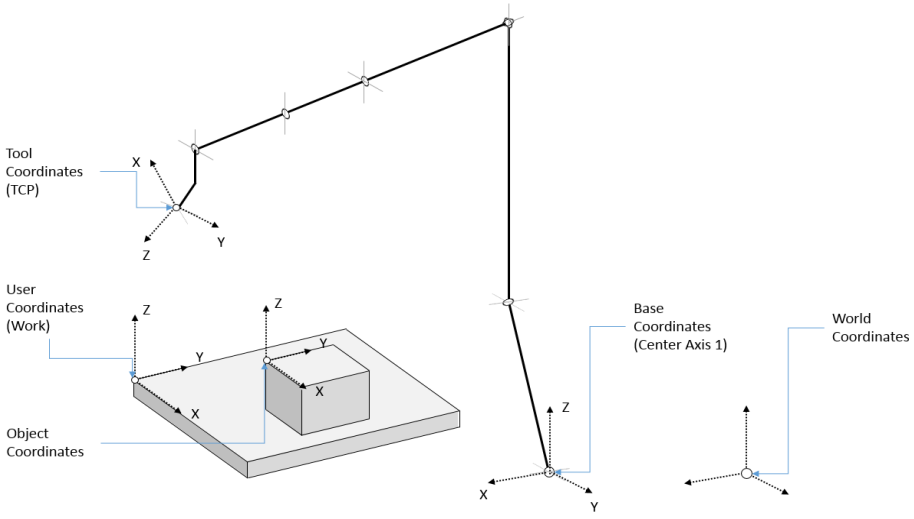

Fig. 8. Coordinate Systems: TCP, World Coordinates, Object Coordinates.

Additionally, if a point is within reach of the arm, it has generally a number of choices for how to reach it –in other words, several axes' combinations are able to yield the same location and orientation. The robot can be facing forwards towards the target, or away and reaching back overhead. Also the so-called "*elbow*" can be either up or down. These orientations, elbow modes (up, down) are built-in through a series of Boolean values in the plugin.

The robot controller figures out the joint angles for each specified position, and the corresponding interpolations when the robot moves from one point to another. These positions can be specified in base coordinates but a multitude of reference frames can be used. Usually it makes sense to specify positions in terms of tool center point (TCP) and work object (*Motta, 2005; Artifact of Code, 2016*), although the thesis' approach takes advantage of embedded programming functionality allowing for easier control based on (i) TCP, (ii) base coordinates, and the (iii) user coordinates.

The points obtained during the slicing operation are, as a result of the above, used to calculate TCP locations, which are in turn translated into a series of joint angles by the robot's controller as either *robtargets* or *jointtargets* as seen in previous sections. These differ in their internal structural definition, shown below for convenience. Jointtargets are defined through a series of axes' rotation values:

CONST jointtarget calib_pos:= [[rax_1, rax_2, rax_3, rax_4, rax_5, rax_6], [0, eax_b :=9E9, eax_c=9E9, eax_d :=9E9, eax_e :=9E9, eax_f :=9E9]];

For instance, the normal calibration position for IRB models is defined in *calib_pos* (used for the example) by the data type *jointtarget*. In addition, it is possible to directly reference external axes' rotations, as seen in the data type definition below. The normal calibration position 0 (degrees or mm) is also defined for the external logical axis a. The external axes *b* to *f* are undefined by default.

< dataobject of jointtarget >
< robax of robjoint >
< rax_1 of num >
< rax_2 of num >
< rax_3 of num >
< rax_4 of num >
< rax_5 of num >
< rax_6 of num >
< extax of extjoint >
< eax_a of num >
< eax_b of num >
< eax_c of num >
< eax_d of num >
< eax_e of num >
< eax_f of num >

On the contrary, robtargets are defined via 3D Cartesian coordinates, the orientation of the tool in the same direction as the object coordinate system, the axis configuration of the robot, and the position of the external axes, expressed either in degrees or millimeters –depending on their type. As in the previous case, axes c to f remain undefined prior to the instantiation of the variable.

CONST robtarget p15 := [[x:=600, y:=500, z:=225.3], [1, 0, 0, 0], [1, 1, 0, 0], [0, 0, 9E9, 9E9, 9E9, 9E9]];

For instance, the example above has a robot position of: x = 600, y = 500 and z = 225.3 mm in the object coordinate system, and a tool oriented in the same direction as the object coordinate system. The axis configuration of the robot for axes 1 and 4 is in position 90 to 180º, whereas axis 6 is in position 0 to 90º. The position of the external logical axes, a and b, is 0, and axes c to f have not been modified.

< dataobject of robtarget >
< trans of pos >
< x of num >
< y of num >
< z of num >
< rot of orient >
< q1 of num >
< q2 of num >
< q3 of num >
< q4 of num >
< robconf of confdata >
< cf1 of num >
< cf4 of num >
< cf6 of num >
< cfx of num >
< extax of extjoint >
< eax_a of num >
< eax_b of num >
< eax_c of num >
< eax_d of num >
< eax_e of num >

< eax_f of num >

The tool requires fine calibration by the user before printing, as the tool center point will be used to calculate the final manipulator's position and orientation. Orientations and rotations are calculated with quaternions rather than using Euclidean transformation matrices, as transformations or univocal translation of matrices to quaternions seem to throw calculation errors and precision issues. Thus, although both approaches can be used, the former is preferred due to its accuracy and simplicity. Also, quaternions can be expressed as axis-angle matrix representation, which convey Euler's theorem, which claims that any 3D, spatial rotation can be expressed as a rotation around a single vector.

Quaternions are well beyond the scope of the present work, so let us just point out both their mathematical definition and their relationship to axis-angle representations of matrix rotations. Quaternions are a R^4 four-dimensional vector space over the real numbers, which can be operated with addition, scalar multiplication, or the so-called quaternion, non-commutative multiplication. A quaternion may be defined as:

$$q_n = w1 + x\boldsymbol{i} + y\boldsymbol{j} + z\boldsymbol{k} \quad (1)$$

Where *w*, *x*, *y*, *z* are real numbers. Numbers *i*, *j*, and *k* are complex ones that obey these identities:

$$i^2 = j^2 = k^2 = ijk = -1 \quad (2)$$

To a certain extent, quaternions can be thought as a sum of a scalar and a vector. Thus, quaternions have all operator properties, except for commutative multiplication. The 3x3 orthogonal matrix corresponding to a rotation by the unit quaternion when post-multiplying with a column vector is given by:

$$R = \begin{pmatrix} w^2 + x^2 - y^2 - z^2 & 2wx - 2wz & 2xz + 2wy \\ 2yz + 2wz & w^2 - x^2 + y^2 - z^2 & 2yz - 2wx \\ 2xz - 2wy & 2yz + 2wx & w^2 - x^2 - y^2 + z^2 \end{pmatrix} \quad (3)$$

Alternatively, a quaternion can be obtained from an axis-rotation matrix. Special care must be taken, due to the so-called degeneracy effect, caused by quaternions approaching the identity quaternion or the sine of the angle approaching zero. The axis and angle are:

$$\theta = 2\arccos(w) = 2\,arcsin\sqrt{x^2 + y^2 + z^2} \quad (4)$$

$$(a_x, a_y, a_z) = \frac{1}{\sin\frac{\theta}{2}}(x, y, z) \quad (5)$$

Quaternions offer significant advantages in terms of optimization. Using quaternions it is possible to perform the same transformations as when employing 3x3 rotation axis-angle arrays, with the added advantage that quaternions require significantly less operations or instructions. Furthermore, quaternions are more reliable than matrices, since these suffer from a certain degree of inaccuracy when angles are very acute (as cosine values tend to become zero). Also, it is sometimes difficult to differentiate mirrored rotations in matrix-like calculations, since unsigned values can lead to an erroneous or faulty interpretation of the resulting vector's direction (in other words, it may be sometimes problematic to discriminate whether a vector has a direction or the opposite). Finally, quaternions find applications in the computer graphics industry, as they are quick and easy to use for programming camera interpolations, which often can be easily transformed through simple quaternion calculations –the interpolations happen when the camera moves, thus modifying its eye-end vector. The same can be applied to both robot simulation and actual movement computations, where a fast response from either the UI or the actual manipulator –through the robot's controller- is required.

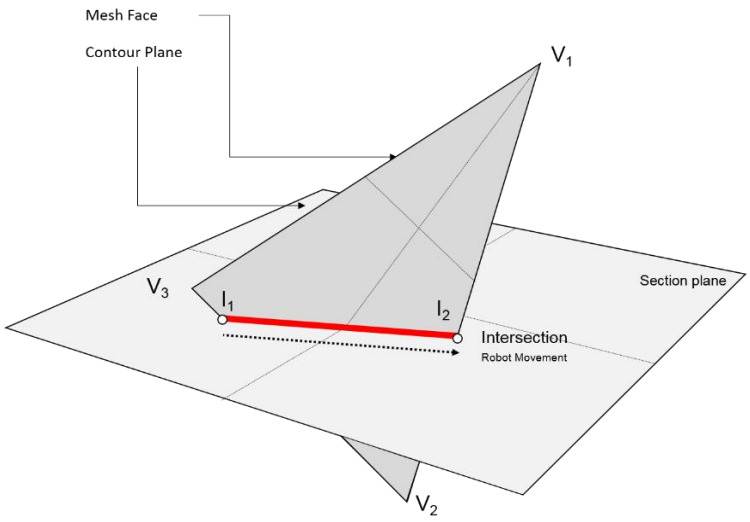

Fig. 9. Intersection of a plane with a single triangular face extracted from a mesh. I1 and I2 are the start and end point of the segment resulting, respectively.

As it has been explained above, CAD software works mostly with mesh models, which normally consist of a series of triangulated faces. Intersecting a triangular face with a horizontal plane always results in a single straight line, therefore leading to linear tool movements when translated to robot language. Figure 8 shows the intersection of a single triangular mesh face and a plane (representing the contour intersection plane). I1 and I2 mark the start and end point of the resulting segment, which depict the linear movement of the printing head. One RAPID instruction is needed for the robot to follow that particular sequence. A downside of meshes is the density needed to represent complex curved geometries or acute arcs, as these are approximations of the original curved geometry. Meshes suffer from deviations resulting from planar planes being tangent to NURBs geometry. Evidently, the less dense the mesh is, the more deviation is caused, as shown in figure 10. The software provides optimization capabilities in order to minimize the amount of vertices required to define the geometry precisely enough, without compromising computation to a great extent.

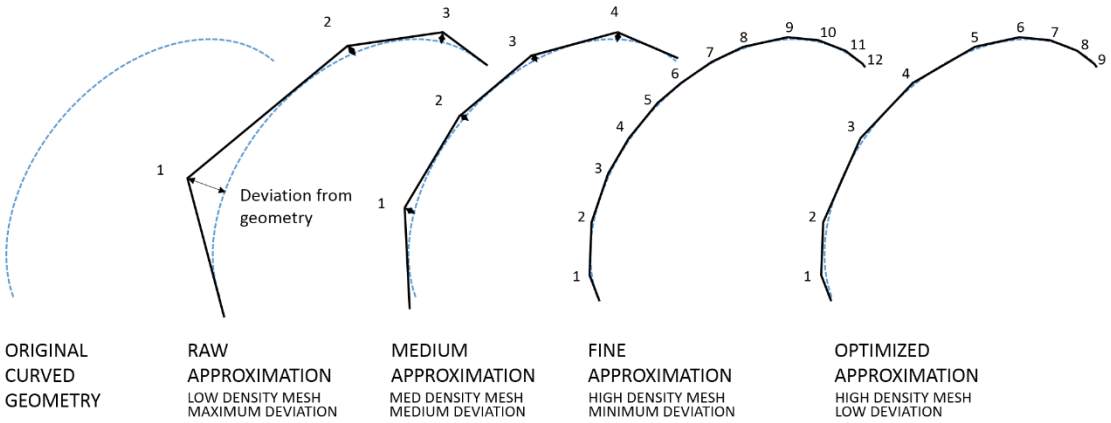

Fig. 10. Mesh approximation from a curved geometry: (a) original curved geometry, (b) raw, non-precise approximation, (c) medium approximation (denser mesh), (d) fine mesh approximation (high precision, high density polygon), (e) optimized version showing more points in zones with higher curvature ranges.

4.5.4. Experimentation

Figure 11 depicts the software organization diagram. As it can be seen, the program is structured by two main strata that constitute the program's architecture. On the one hand, the *software layer* takes care of the relationship between the host program and the plugin; on the other hand, a *controller layer* is added in order to communicate with the manipulator through its own controller. This layer depends only on the robot's hardware.

In addition to the above, the software layer takes care of the print setup. The user may enter the variables needed for a print to be calculated, namely the build parameters (see further down this section) and the robot model. Moreover, it accounts for the different optional (user) inputs in the advanced setup. The former is passed onto the program through the translator engine, while the latter is passed as a direct reference whereby the values entered by the user are employed directly without further need for complex implementations. The advanced setup variables must refer to existing references in the robot's controller, as explained in detail later in this chapter.

Finally, the controller software gathers the information and writes automatically a compelling ABB RAPID program, consisting of a Main Module –which is a vendor requirement and always needs to exist- and Part Modules –containing the movements themselves and instructions for Input and Output, so differentiated to tackle scarce memory issues from the vendor's hardware.

When exceeding 3000 points –or otherwise the number decided by the user, several part modules are created. These modules are then loaded and unloaded from the controller's memory dynamically using native RAPID functions. This ensures that the programs will always fit in the limited memory capacity of the controller, avoiding runtime errors. The number of instructions shall not exceed 32000, as the memory is limited to 40MB. This amount may be also modified by advanced users, as explained in the following paragraphs.

According to the internal architecture of a RAPID program, the user must reference tools or other global variables used in the software directly in the USER or BASE modules located in the controller, shown in figure 10 alongside the program's architecture. Since these modules are fixed in the controller's memory, this approach benefits serial production. This approach requires a basic knowledge of the controller and RAPID program structures, or otherwise of the robot's language employed. A different approach names tools and other variables directly in the header of the main module, allowing for a higher flexibility, but prone to errors. Below are typical program structures used by the translator.

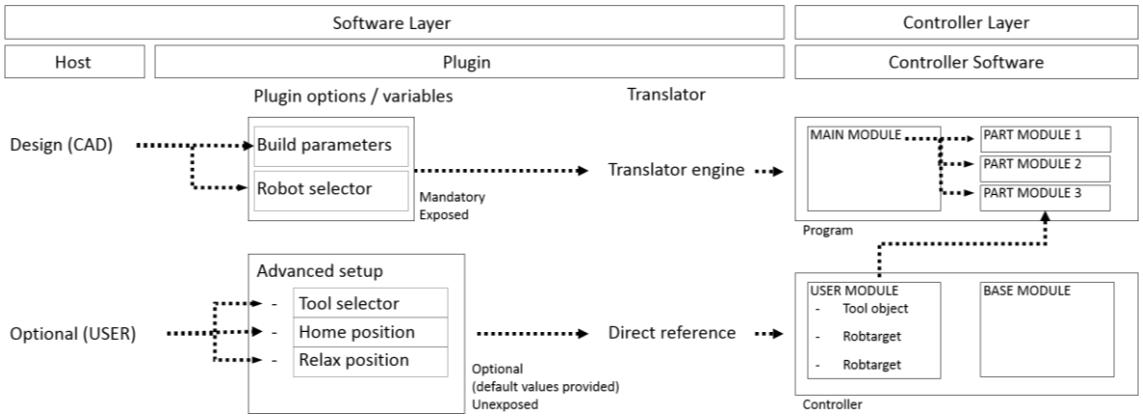

Fig. 11. Internal object references in plugin setup for ABB robot models.

The software – currently in the technological demonstrator phase- includes the following features and tools, shown in figure 14:

- **Integration** in the host program User Interface, offering a fluid operational and user-friendly experience. This integration is achieved in Rhinoceros through a Panel class, a layout element that can host different interactive tools, such as text boxes, input boxes, sliders, and other standard tools.
- **Number of instructions** per module. Default is set to 3000 –see XML description below. The associated tag for this parameter is NumOperations, as follows:

  <NumOperations>3000</NumOperations>

- **Build parameters, material constraints** and "wall" description through the following inputs:
  - (i) Wall thickness: a thickness is assigned to the part contours. This allows for structural coherence of the part, as no "space-packing" infill is defined in the

software. Furthermore, this permits that "void" objects may be printed, since the software merely considers the contours extracted from the 3D model.

- (ii) Extrusion thickness –diameter of the extruder or nozzle. This extrusion defines the layer height as well, and might be related to the material itself. The minimum extrusion thickness allowed by the software is 0.05 mm for visual optimization reasons. Further versions should account for a differentiation between extrusion thickness and layer height, although this was not necessary for the initial version shown here.
- (iii) Reinforcement density, a setting which establishes how the infill is designed and created. Initially, the software was designed to account for cement-like materials, reason why the infill is defined as a triangular reinforcement. Chapter 6 explains an algorithm for structural infill pattern design.
- Basic shipped materials include a cheap, a default, and an expensive material, although these might be easily extended by the user. Currently, the list may be expanded by adding materials manually to the list –see below for the material structure, although it is planned to add more functionality in order to allow users to add and edit materials easily.

These parameters are all included in an xml file named "DefaultParameters.xml" and stored in the plugin's folder shipped for installation. The contents of the file follow:

```
<?xml version="1.0" encoding="UTF-8" ?>
<!—DOCTYPE DefaultParameters SYSTEM "DefaultParameters.dtd"-->

<DefaultParameters>
        <HomePrint>j_Home_3dPrint_Tipo2</HomePrint>
        <HomeFig>p_Home_Fig2</HomeFig>
        <Tool>tool_Extrusor_Tipo2</Tool>
   <LoadDummyModels>FALSE</LoadDummyModels>
        <NumOperations>3000</NumOperations>
  <PathInRobot>HOME:/Programs_3d_Printing</PathInRobot>
        <BuildMaterials>
                <Material>
                        <Label>Default</Label>
                        <Cost>Example_1</Cost>
                </Material>
                <Material>
                        <Label>Cheap</Label>
                        <Cost> Example_0.5</Cost>
                </Material>
                <Material>
                        <Label>Expensive</Label>
                        <Cost> Example_2</Cost>
                </Material>
        </BuildMaterials>
</DefaultParameters>
```

- **Robot selector**: from within a limited but easily expandable robot library. The library consists of a series of pre-defined models selectable from two fields:
  - Company: ABB (KUKA, and others are expected to be included in future versions).
  - Model. Current ABB implemented models include: IRB 120, IRB 1600, IRB 2600, and many others. These robot models are defined through 2 files:
    - A file containing the geometry of the robot. This file is, for demonstration purposes with the Rhinoceros plugin, a *.3dm file containing a series of objects that follow strictly predefined naming conventions and a fixed geometrical structure. On the one hand, the file contains a series of points defining the rotation axis in the robot's relax position –this is where all axis have a rotation angle equal to zero.

- An XML file containing the actual robot definition. The tags refer to robot model information, and geometrical constraints form the vendor, mainly including maximum weight load capacity and axis rotations. Moreover, a printing "bounding box" has been included in the robot's description. Although this is conceptually wrong –as the reach of the robot depends on the tool being used-, this permits a simpler use of the software. A sample XML file containing that information follows:

```
<?xml version="1.0" encoding="UTF-8" ?>
<!--DOCTYPE RobotPhysicalLimitations SYSTEM "Robot_Limitations.dtd"--
>

<Robot_Limitations>
        <Robot_Company>ABB</Robot_Company>
        <Robot_Model>IRB 120</Robot_Model>
        <Specifics>Include your specifics here</Specifics>
  <Model3D>IRB120.3dm</Model3D>
        <Axis>
                <Pos>1</Pos>
                <AngleMax>Max angle here</AngleMax>
                <AngleMin>Min angle here</AngleMin>
                <AngleMaxSpeed>Max a here</AngleMaxSpeed>
        </Axis>
        <Axis>
                <Pos>2</Pos>
                <AngleMax>Max angle here</AngleMax>
                <AngleMin>Min angle here</AngleMin>
                <AngleMaxSpeed>Max a here</AngleMaxSpeed>
        </Axis>
        <Axis>
                <Pos>3</Pos>
                <AngleMax>Max angle here</AngleMax>
                <AngleMin>Min angle here</AngleMin>
                <AngleMaxSpeed>Max a here</AngleMaxSpeed>
        </Axis>
        <Axis>
                <Pos>4</Pos>
                <AngleMax>Max angle here</AngleMax>
                <AngleMin>Min angle here</AngleMin>
                <AngleMaxSpeed>Max a here</AngleMaxSpeed>
        </Axis>
        <Axis>
        <Pos>5</Pos>
                <AngleMax>Max angle here</AngleMax>
                <AngleMin>Min angle here</AngleMin>
                <AngleMaxSpeed>Max a here</AngleMaxSpeed>
        </Axis>
        <Axis>
                <Pos>6</Pos>
                <AngleMax>Max angle here</AngleMax>
                <AngleMin>Min angle here</AngleMin>
                <AngleMaxSpeed>Max a here</AngleMaxSpeed>
        </Axis>
        <Limits>
                <Limit>
                        <Name>A0</Name>
                        <X>...</X><Y>...</Y><Z>...</Z>
                </Limit>
                <Limit>
                        <Name>B0</Name>
                        <X>...</X><Y>...</Y><Z>...</Z>
                </Limit>
                <Limit>
                        <Name>C0</Name>
                        <X>...</X><Y>...</Y><Z>...</Z>
                </Limit>
```

```
                    <Limit>
                        <Name>D0</Name>
                        <X>...</X><Y>...</Y><Z>...</Z>
                    </Limit>
                    <Limit>
                        <Name>A1</Name>
                        <X>...</X><Y>...</Y><Z>...</Z>
                    </Limit>
                    <Limit>
                        <Name>B1</Name>
                        <X>...</X><Y>...</Y><Z>...</Z>
                    </Limit>
                    <Limit>
                        <Name>C1</Name>
                        <X>...</X><Y>...</Y><Z>...</Z>
                    </Limit>
                    <Limit>
                        <X>...</X><Y>...</Y><Z>...</Z>
                    </Limit>
                </Limits>
                <MaxWeight>Weight</MaxWeight>
            </Robot_Limitations>
```

It is expected to allow the user to include his own robot designs. The only constraint for that functionality would be (i) the mastery of the modeler himself, and (ii) that the manipulator must have 6 axis. For the most proper functioning possible, robots must attach to the spherical wrist model described in the depiction of the IK engine. Failure to do so would result in erroneous, faulty, or unexpected behavior. Besides, it is not possible to include robots which use a different programming language from those proven and pre-integrated in the software, as ad-hoc translators should then be written for that purpose.

- **Simulation preview** controls for (i) coarse and (ii) fine visualization allowing the user to understand and visualize the simulation of the building process. In the present case, geometry is programmed as mesh or polyline conduits to provide a faster preview experience. Results are shown in figures 13 and 14.
- **Advanced setup options**:
    - Tool selector: text field to define the tool to be used in the robot code. Its name must refer (point) to a *tool object* existing in either the BASE or USER modules in the robot controller.
    - Base point selector: establishes a base point for the print object, should the user desire to modify the default one. As in the case of the tool selector, the base point name must point to an existing *robtarget* object in either the BASE or USER modules. This name will be included in the program and used by the part modules (read below).
    - Relax point: is robot's relax position where all axis rotations equal 0. This is referenced in routines in the beginning and end of each program, where the robot goes. As said, the relax point is an Absolute Rotation Point defined by rotation angles.

These parameters are also included in the DefaultParameters.xml file above.

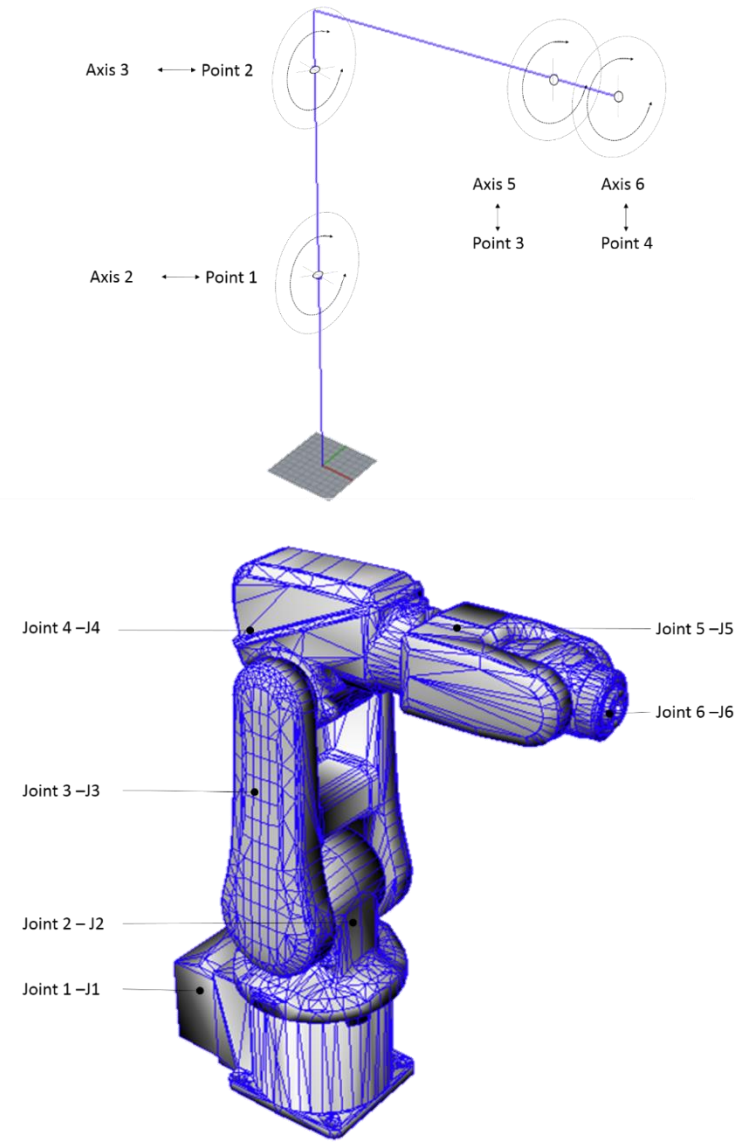

Fig. 12. Internal depiction of IRB 120 for simulation purposes

- Geometry **output** as both polylines and/or meshes for use by the designer as native Rhinoceros objects.
- Export **robot code** depending on the robot vendor. Currently, these files must be manually loaded onto the robot's controller through an USB device or using ABB's Robot Studio explorer interface. ABB export files include:
    - A pgf file containing the program. A typical program file code follows:

      <?xml version="1.0" encoding="ISO-8859-1" ?>
      <Program>
      <Module>PathTo\MainModuleFile.mod</Module>
      <Program>

    - A Main Module named according to user input containing loading/unloading operations and calls to other modules. The file containing this module is located in the user's desired path location –defined in the DefaultParameters.xml file inside the PathInRobot tag. The module is named after the user's choice. The file has a *.mod extension and has the required MAIN MODULE structure required by the vendor, including the PROC Main structure shown in the snippet below.

```
![pgf file written aside]
![pgf file contains a list of all modules in the entire program]

MODULE MainModule
        PROC main()
        ! Call to user-defined modules and procedures
                ...
        END PROC
END MODULE
```

- Movement modules, which are dynamically loaded by the controller according to the instructions in the Main Module. These movement modules are named parts and contain a maximum of 3000 instructions –or whatever the user modifies in the DefaultParameters.xml file. The amount of instructions are limited by the internal RC5 controller RAM. Movement instructions are sequenced one per line of code.

```
MODULE Part1
        PROC Part1()
! Call to movement procedures (generally MoveJ or MoveL)
! Call to IO and tool/related procedures (generally SET DO)
...
        END PROC
END MODULE
```

Figures 13 and 14 depict the current state of the technological demonstrator. It shows the interaction interface with an ABB IRB 120 and the controller panel embedded natively in the Rhinoceros UI. The software panel, although explained in detail below, it consists of the following sections: (i) build parameters, (ii) robot selector, (iii) preview and (iv) output.

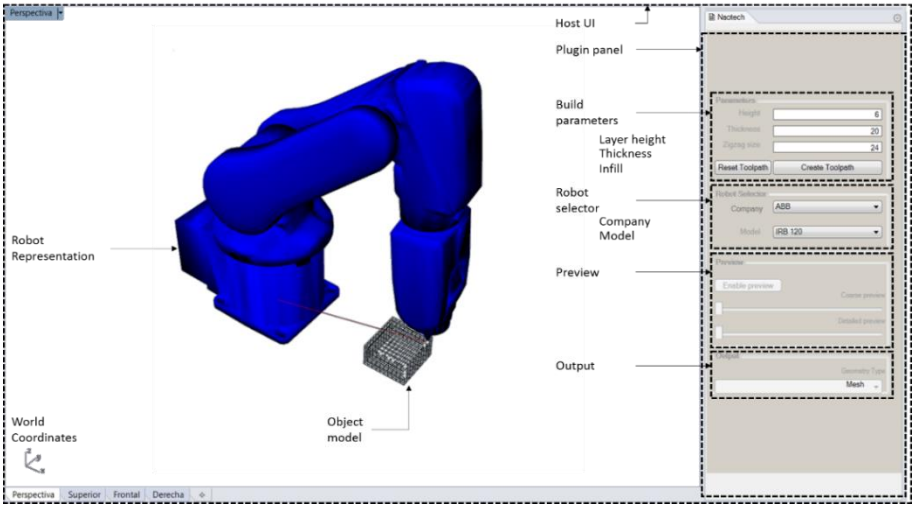

Fig. 13. Current state of the technological demonstrator.

Figure 13 shows the host UI for Rhinoceros, showing an ABB IRB 4600 in action. The geometry has been created in Grasshopper, proving that, although the plugin is meant to be used in Rhinoceros, it only does so in order to access its geometry kernel and ensure usability within the software environment. In fact, geometry can be created, acquired, or obtained through any other software or data acquisition tool alike, including, but not limited to, Parametric Design tools such as the aforementioned Grasshopper and its most known extensions Kangaroo, Weaverbird, or many others. Independently from the way the geometry was conceived, the plugin operates in the same manner without any interference or need for further treatment.

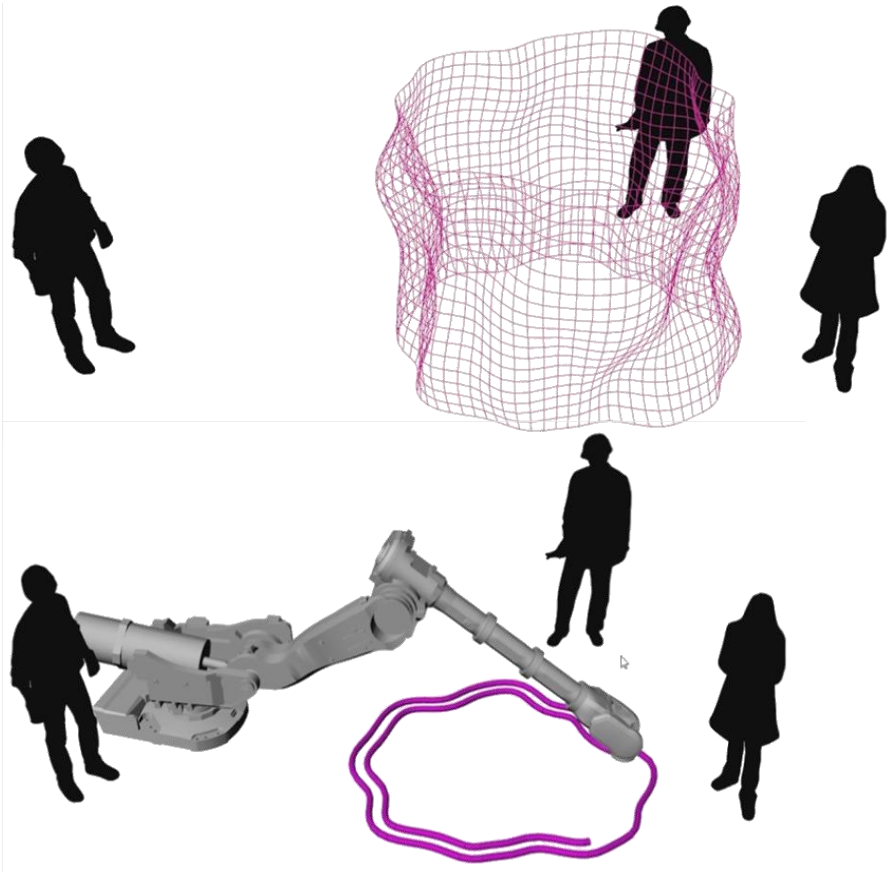

Fig. 14. Current state of the technological demonstrator showing simulation in host interface with an ABB IRB 4600: a) parametrically modelled geometry of the part displayed in wireframe mode; b) visualization of the simulated printing process with an ABB IRB 4600.

The use of Grasshopper and Parametric Design tools extends the modeling capabilities of Rhinoceros in this case, granting a richer modeling experience for the user, who could benefit from the combined potential of both tools. The conception of the plugin is, nonetheless, to provide the best and most fluid user experience with the highest possible operational value. Furthermore, the emergence of Associative Design for Building Information Modeling in construction and engineering companies, fostered by the impulse of BIM adoption levels in the UK –and slowly but steadily infiltrating the European countries-, has entered not only the development of complex, big, or convoluted projects, but the production phase through a better geometrical definition of structural parts. Dynamo©, the Revit© parametric design visual programming interface, is also considered as a possible platform upon which it would be possible to base another plugin instance. This would allow to test the modular design of the program, as Revit works with solid objects or Autodesk's© proprietary types, which differ from NURBs' or meshes' computational structure. The geometry kernel of the plugin would, as in the case for Rhinoceros, solve the geometrical calculations of contours and infill, whereas the translator kernel would literally write the movement and tool-related operations for the robot program. Nonetheless, as opposed to Rhinoceros software, Revit works poorly with mesh geometry. This would probably translate into a need to re-write part of the geometry kernel, or to simply write a whole new geometry kernel from scratch. Either way, the software benefits from its modular design, as this does not affect the translator engine, so that it can be adapted to any geometrical input.

Regardless the host CAD program, the plugin's User Interface is conceived as a single static panel, which should display the same tools and design across different platforms. This would guarantee a cross logic and homogeneous use that is deemed appropriate for the purpose of the work and its future development as a Minimum Viable Product (MVP) for actual AM industrial purposes.

4.5.5. Panel and user experience

The plugin, as explained above, includes all features into a single panel interface that is integrated in the host's UI. Figure 15 shows each of the mentioned tools for reference. On the picture's right-hand side, the combo panels are displayed to show some of the available options at the moment.

Fig. 15. Plugin's panel UI showing selectors.

The plugin's panel consists of a series of clusters that relate to the functions described in the previous paragraphs. These clusters, further specified in paragraphs below, are: (i) estimates; (ii) build parameters; (iii) advanced setup; (iv) preview controls; (v) robot selector and (vi) output. The user is asked to enter only three inputs, clearly identified in the build parameters groups: height (layer), thickness (wall), and infill (size).

- **Estimates**

The estimates cluster displays printing information relevant for the user, such as cost, printing volume, and estimated printing time. These are approximations based upon the material settings available through the material selector included within the cluster, and that relate to the material description given previously. Beside the default material settings, the user might enter new materials in the Materials.xml file released with the plugin. Default time and cost values are based on experience and test completed in the present work.

- **Build parameters**

Sufficiently explained in previous sections, build parameters describe the actual printing geometry, which will result in the final object.

- **Advanced setup**

This cluster allows the user to control hardware-related issues, such as tools and printing positions. The setup includes the definition of the initial robot position (commonly named "marks"), the print base point used as center of the object on the printing bed, and the actual printing tool used from the variety

available for the user. As said above, the tool name in the advanced setup must refer to an existing tool object in the robot's controller.

- **Preview**

The preview slider permits a real-time simulation of the printing controlled by the object. The slider starts at 0% of printing completeness, and ends at 100% of the part. It includes a button for controlling the visibility of the printing's bounding limits.

- **Robot selector**

As explained previously, the selection among the library of embedded company models. The model selector updates automatically to show those from the selected company.

- **Output**

The output cluster includes a geometry selector and two buttons: (i) the build button, to create the rhino geometry corresponding to the simulation, and (ii) the export button, to create the robot files.

The UI is conceived in a "linear", "top-bottom" manner as to allow for the easiest possible use.

4.6. Results

The proposed methodology has been tested both at a software and a hardware level. Several geometries have been successfully checked, validating solid and void 3D models from different types. Non-native geometries imported from a variety of programs were tested as well in order to Native mesh geometry was created and tested in Rhinoceros, as well as imported from other models.

A series of large-scale pieces were printed using the integrative software platform developed ad-hoc for Rhinoceros. The prints evidence that the methodology works as desired for FDM-similar techniques, and that it is ready for its adaptation to real-scale construction projects.

The platform has been tested on different machines and run under several operating systems. Diverse designs have been produced according to the above described process and tested using three different ABB robot models –IRB120, IRB1600 and IRB2600. The same printing head, electronics –see Annex I, and setup were adopted for tests running on both machines. The experiment shows that the employment of different robot controllers –the IRB120 uses an IRC5 compact, whereas the IRB1600 and IRB2600 mount an IRC5- had no impact on the workflow methodology and yielded exact results. Only the printing starting point ("*print_home*") was modified to meet the different printing beds used in both cases.

Although printing times vary slightly due to different robot controller's hardware specifications, the operational experiments prove that the technology is easily scalable and works on different robot models with little or no need for specific configurations. PLA parts were printed, although concrete-like materials can be easily adapted to the software system.

As said above, the experiment shows that the employment of different controllers had no impact on the workflow methodology and that the code produced by the plugin yielded exact results at a software level. Nonetheless, IRC5 controller turned out faster than IRC5 compact at dynamically loading/unloading part modules, which had a meaningful impact on the quality of the printed piece, which was increased. Parts produced with the IRC5 compact controller and IRB120 robot yielded small pseudo-spherical imperfections on the surface of the pieces, result of the robot stopping as a consequence of dynamic loading/unloading times.

Table 1. Part configuration.

	Nr Layers	Total Length (mm)	Base Length	Movement Instructions	Base Movement Instructions
Part 1	2001	1401880	73707	53139	2906
Part 2	4001	2732171	80208	47996	1124
Part 3	10001	7438970	317	40004	412

Annex I discusses part test development in detail. Big-scale parts sometimes displayed base fixation problems –although this is a common material problem rather than a software issue. High speeds do not allow for a proper base formation, and big-scale parts displayed printing problems due to instability when reaching heights above 40 or 50 cm. In order to tackle this problem, it was decided to set up the prints with variable printing speeds. The preferred speed for the first 100 layers –although this number may vary depending on the layer height- was 50 mm/s, while 150 mm/s or was optimal for complex geometries above that. 200 mm/s or higher can be used for bigger prints or other effects. This speed differentiation is only possible at the moment with experimental software and has not yet been implemented in the plugin itself. Tables 1 and 2 show 3 parts for comparison.

Table 2. Part print results and printer/robot configurations.

	Standard FDM printer					
	Speed Base (mm/s)	Speed Part (mm/s)	Part Modules	Time per part module (s)	Printing time (s)	Printing time (h)
Part 1	35	45	N/A	N/A	34581	9,6
Part 2	N/A	N/A				
Part 3	N/A	N/A				

	IRB 120 on IRC5 Compact					
	Speed Base (mm/s)	Speed Part (mm/s)	Part Modules	Time per part module (s)	Printing time (s)	Printing time (h)
Part 1	100	100	18	0,2	14042	3,9
Part 2	100	100	16	0,2	27364	7,6
Part 3	N/A	N/A	14			

	IRB 1600 on IRC5					
	Speed Base (mm/s)	Speed Part (mm/s)	Part Modules	Time per part module (s)	Printing time (s)	Printing time (h)
Part 1	50	100	18	0,1	14757	4,1
Part 2	50	100	16	0,1	28125	7,8
Part 3	50	150	14	0,1	49598	13,8

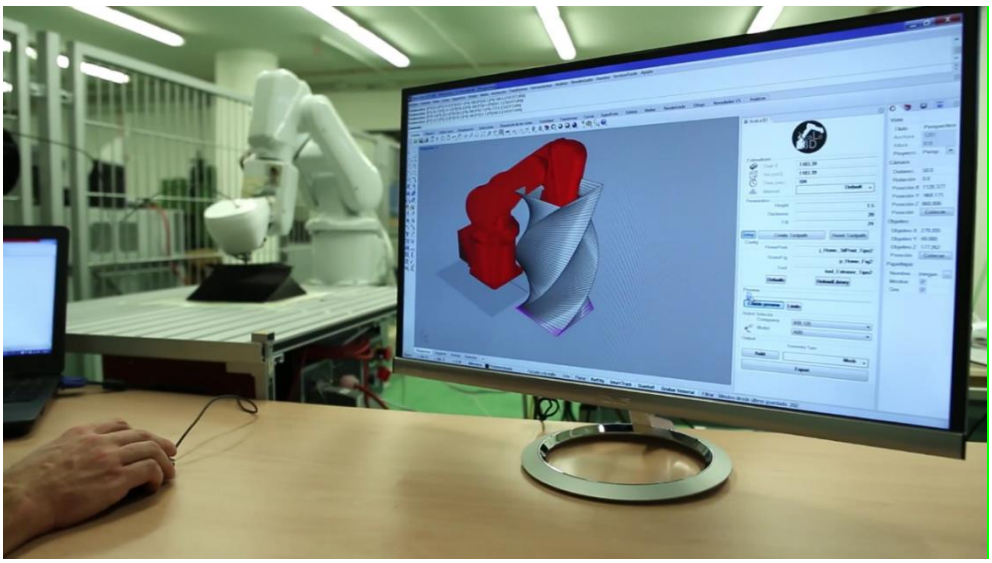

Fig. 16. Plugin software operating an IRB120 robot.

Further experiments yield printing times up to 5 times faster using robots than standard FDM techniques. Due to the controller's limitation to calculate offsets and movements between closer-than-1mm points at speeds higher than 80 mm/s, it is desirable to implement code strategies that observe this situation –for instance, reduce speed to v50 if that is the case between two any consecutive points Figures 16 to 18 show two printed parts and a close-up detail of a complex geometrical instance. Please note the finish quality of the piece, similar or better than that of the commercial printers, and able to reach a layer density up to 0.1 mm or less. The part occupies a total volume of 0.4 x 0.4 x 1.5 meters and has been printed using an IRB 1600 at a printing speed of 150 mm/s. The part is displayed here as proof of concept.

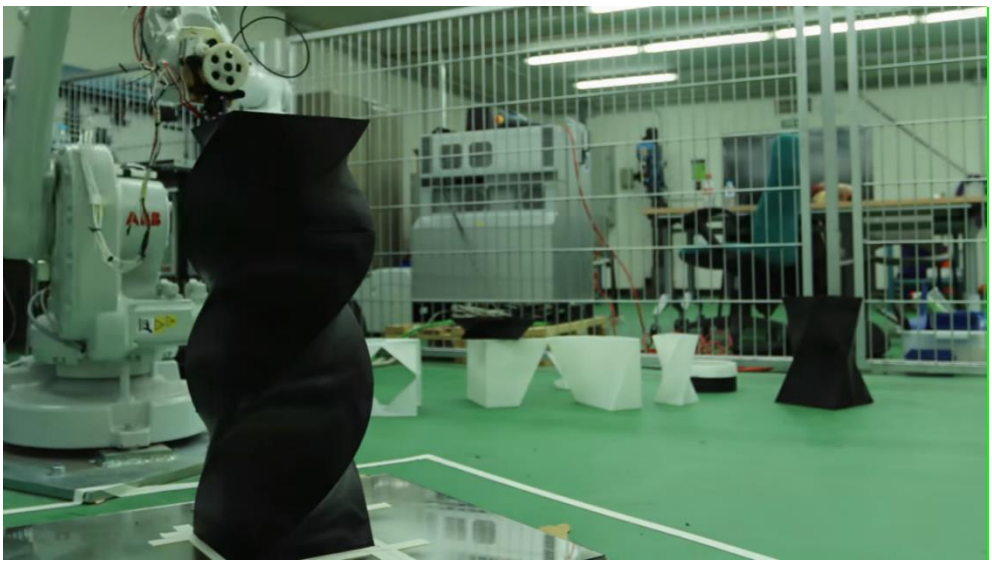

Fig. 17. Printing the part with an ABB IRB 1600 robot.

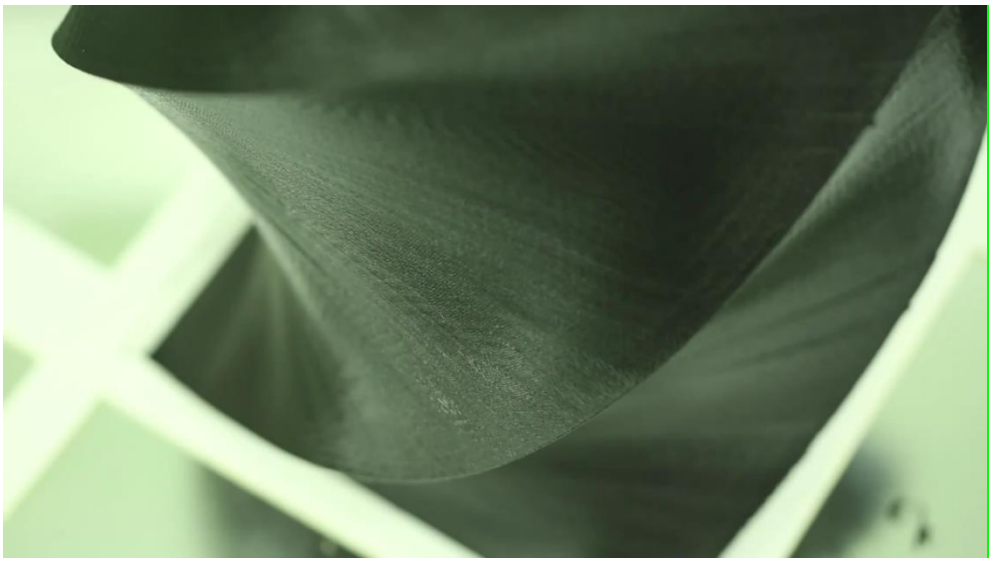

Fig 18. Close-up showing finish quality of the 0.4x0.4x1.5 m part with a 0.1 mm of layer height resolution.

4.7. Conclusions

This Chapter has presented a methodology for an integrated Design-to-Fabrication process. The integration is realized as a series of connectors or "translators" using Rhinoceros as a test case. Another piece of software is developed in order to carry out the actual translation and validate the result with a variety of ABB robots, demonstrating the interoperability between software tools supporting the design, model management, and performance evaluation prior to physical fabrication. Finally, a structure-oriented algorithm for infill patterning creation is discussed and presented. The overall performance of the combined software, hardware, and material study outmatches that of the standard 3D printers in each of the comparison fields: speed, volume, and finish quality.

Although the present research offers a compelling approach to 3D printing for the AEC related industries, a number of key issues regarding construction and sustainability can be explored thanks to the inherent advantages of the 3D printing technique, namely:

- Waste control, zero-waste production, and reduction of building footprint at construction time through a minimization of operation costs (*Castañeda, Lauret, Lirola, & Ovando, 2015*) and an increased optimization of time, and energy footprint.
- Use of organic materials, and recycled building materials for non-structural and structural parts. Organic materials, as opposed to traditional materials, can be relatively easily obtained from their raw material counterparts *(Braungart & McDonough, 2003*) and are recyclable. As an example, Waste for Life has developed an open source hot-press (compression molder) which is used to turn trash consisting of plastic bags and cardboard pulp into valuable composites (*Bailic, Matovic, Thamac, & Vaja, 2011*)
- Reduction of human errors in building sites through the automation and mechanization of the process, which account for more than 80% of total defects in housing construction *(Del Solar, Del Río, Villoria, & Nadal, 2016*). Safety would be affected positively.
- On-site deployment: using robots on-site allows for access to local and renewable energy sources. Furthermore, transportation impact is lowered or eliminated, thus its associated expenses and carbon footprint.
- Detail enhancement, finish quality through a re-qualification of tooling and labor force.

Chapter 5

Designing an off-the-shelf, affordable AM end effector

As discussed in previous chapters, 3D printing applies to a wide variety of materials. The present research intends to recreate full-scale, final parts. Despite economic restrictions, which made it impossible to employ cement-like or thereby derived materials, a fully operational, open-source nozzle development for FDM printing is provided. The section includes all calculations, components, and code considered necessary to create a robot-adaptable, feasible extruder system. The plastic extruder is shown here as proof of concept and as an orientation towards the design of a cement or concrete nozzle.

Credits: the development of this extruder would have not been possible without the financial support of Naotech Solutions S.L. and Guillermo Baraja. I would like to thank Guillermo for his patience and valuable collaboration. Two paste extruders were budgeted by the Germany-based company ViscoTec (Krassenstein, 2014) and the Italian WASP, although they were impossible to acquire due to insufficient funds. A WASP extruder is being currently installed for further research.

5.1. Introduction

This chapter presents the design of an extruder solution intended for any user, without extensive knowledge of either coding or printing, to produce and control large 3D printing based on the use of robotic arms. An important requirement also is that it has to be an affordable tool. Therefore, the design has been driven by the following design principles:

- Affordable design, which costs less than 100€ including the electronic components and printed parts
- Open source, in order to facilitate its use, adaptation, or further adoption by users and developers alike.
- Common, easy to find electronic components. The main control electronics are explained in section 5.3, and rely on Arduino MEGA boards or similar.
- Easily buildable components, to facilitate their replication.

5.2. Basic design concepts

FDM extruders consist basically of a series of devices that heat a plastic material coming in a filament form –or similar, and push it through a nozzle. The material, in a fluid state when extruded through the nozzle, cools down quickly in contact with the printing atmosphere becoming solid. This process allows for the formation of physical objects. A simple extruder architecture is shown in figure 1.

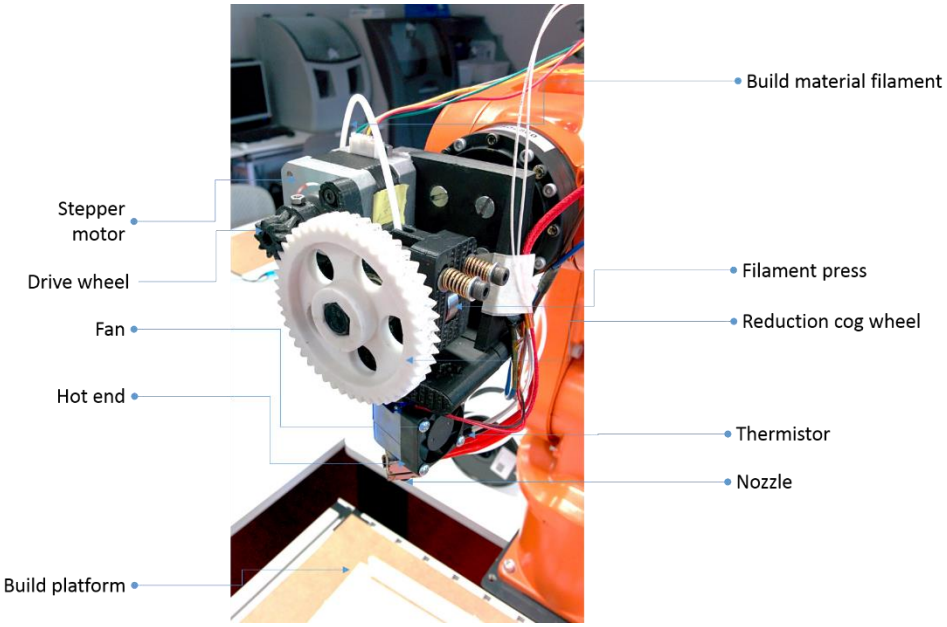

Fig. 1. FDM PLA extruder mounted on IRB120 robot's manipulator.

This architecture requires of certain controls. First, it is crucial to be able to monitor and handle the temperature of the material, both during the heating and deposition phases. This is so as different materials become fluid or liquid at different temperatures and their behavior may differ under different atmospheric conditions (height, pressure, humidity). Although these properties are subject to small variations, they considerably differ from one plastic type to another. For instance, *190-210 ºC* is considered a "standard" extrusion temperature for PLA, whereas ABS requires higher temperatures, in the range of *210 to 230 ºC*. Nevertheless, it is crucial to always consider the vendor's specifications for each material, which again may vary from the above mentioned standards. Higher temperatures may yield different results, especially when dealing or experimenting with varying printing speeds, or speeds out of the range of standard 3D printers. In the case of the present thesis, print speeds easily surpass the boundary of *200 mm/s*, which is about 4 to 5 times faster than standard FDM printers. More information about printing speeds can be found in chapter 4. The temperature can be controlled by an electronic component called thermistor – more information on this component can be found in subsequent sections.

Second, it is also important to consider the deposition speed. This can be measured in different units, although they all express the relationship between the amount of material deposed and the length of the printed part. As said, this amount can be measured in *mm/mm* (millimeters of filament per millimeter of printed part), *gr/mm* (grams of material per millimeter), and many others. The extruder proposed in this Chapter makes use of a radial impulsion system moved by a stepper motor for convenience. The speed of the deposition and the subsequent amount of material is consequently controlled by this component. As a result, the amount of material can be defined in completed cycles (rotations) per minute. The relationship between the rotations and the amount of filament needed can be calculated through the relative radiuses of the cogwheels involved in the process and the hyena screw mounted in the extruder. It becomes obvious that the relationship between printing speed and material deposition must be fixed.

Equations 1 and 2 describe the amount of material used per degree in radians for an extruder consisting of two cogwheels, where r is the radius of the wheel associated to the motor itself, and R is the radius of the main wheel pushing the material into the heater and nozzle. Equation 1 shows the relationship between the wheels, and equation 2 takes the radius r_1 of the hyena screw into account, therefore yielding the exact amount of material (measured as the total length). The length of the material per round is shown

in equation 3, result of substituting the total rotation angle (2π) in equation 2. This relationships are substantial to the printing quality and the finish of the printed part (*Kwon, 2002*).

$$angle_{material}(\alpha) = 2\pi \cdot \frac{r}{R} \cdot \alpha \cdot \frac{1}{2\pi} = \frac{r}{R} \cdot \alpha \quad (1)$$

$$len_{material}(\alpha) = 2\pi \cdot \frac{r}{R} \cdot \alpha \cdot \frac{1}{2\pi} \cdot 2\pi \cdot r_1 = \frac{r}{R} \cdot \alpha \cdot r_1 \quad (2)$$

$$len_{material}(1\ cycle) = 2\pi \cdot \frac{r}{R} \cdot r_1 \quad (3)$$

Third, the volumetric relationship between filament and extruded string is substantial to the calculation. Typical material filament diameters oscillate between 1.75mm and 3mm, and nozzle diameters are usually around 0.4mm. Further calculations must implement the relationship between both in order to define material usage precisely. Equation 4 shows the length of material used depending on those two variables: (i) $\emptyset$ is the diameter of the filament as it ships, and (ii) φ is the diameter of the nozzle, assuming that the resulting extrusion has a consistent diameter throughout the part.

$$len_{material}(\emptyset, \varphi) = 2\pi \cdot \frac{r}{R} \cdot r_1 \cdot \frac{\varphi^2}{\emptyset^2} \quad (4)$$

Finally, the ratio between this length and the tool path length (per unit) must be consistent depending on the quality desired. Different aesthetic affects can be achieved through different ratios. These are discussed in the present chapter and in Annex I. Chapter 4 shows different results.

The rotation movement of stepper motors is defined by their step angle, a variable that differs in each model. The stepping angle, on the contrary, defines the amount of steps needed in order for a full rotation to take place. For instance, a motor with a stepping angle of 2º requires 180 steps for a full rotation. Equation 4 then relates to a certain amount of steps that a motor accomplishes in a certain amount of time. It is crucial that the extrusion speed addresses the viscoelastic behavior of the molten plastic, as polymers show a certain level of elasticity. In fact, in order to avoid typical faults in the extrusion process, both the Weissenberg effect and the extrudate swell at the die exit –shown in figure 2- must be thoughtfully tackled. The extrudate swell consists of an increased extrusion diameter while the polymer solution is exiting the die, which increases with flow rate (*Vergnes, Vincent, & Haudin, 2012*). Further information can be found in the following sections.

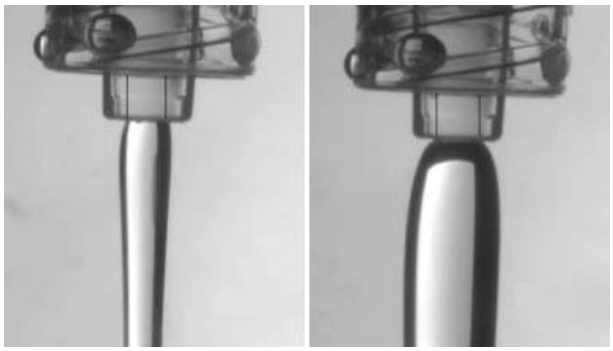

Fig. 2. Extrudate swell: the polymer solution exiting the die shows a larger diameter which increases with flow rate (Vergnes, Vincent, & Haudin, 2012).

5.3. Electronics characterization and design

The characterization of the electronics and circuitry are influenced by the fact that the main "calculation" boards are Arduino MEGA. A diagram showing the main circuitry layout and elements can be found in figure 3. As displayed in the image, a two-board design is chosen, whereby a "main controller" board takes care of the main calculations and sensor reading and an additional "motor controller" board executes the movement of the motor. This layout presents a significant advantage in terms of functionality, allowing for a separation of critical processes and the communication of the circuit with the Input/Output from the robot. This communication would be realized through the main board, while the motor board would, as said, merely control speed, direction, or even stopping operations for the extruder motor.

Following the thought explained above, the circuit presents some basic features. In fact, the logic of the layout is to achieve the simplest possible solution. A first solution was proposed, evaluated, and finally disposed of. This solution included a single Arduino board which controlled the whole execution process. The downside of this approach is that the native Stepper Motor controller library presents some issues in execution time. Not only is it designed in such a way that blocks any other functions or orders while it is running, but it also fails when reaching a high amount of turns. The latter problem could be solved easily by resetting the motor internally every nth iteration; nonetheless, it is the former which constitutes the main problem. Blocking the execution of code means inevitable to delay important readings and operations, namely temperature control and hot end connection to power source. Having a closer look at the library itself exhibits a far from optimal –or even adequate for long operation times- numerical precision.

As a consequence, a second approach is pursued that aims at solving the issues observed during the tests carried out with the first version. Although the main electronic components were maintained, it was decided to attack the main motor problem by setting up a two-kernel electronics layout that would tackle this "blocking" issue in a more comprehensive manner.

On the one hand, the main control manages the overall behavior of the tool, driving the temperature sensor (more comprehensive description on the model of the thermistor used below), the load of the hot-end, and the fan. In addition to that, it communicates one-way only with the motor board, which simply turns on the motor at the given (user-defined) temperature range.

On the other hand, the secondary board controls only the motor performance, assigning a certain rotation speed (which influences the material deposition ratio), and characterizes the motor physically. This allows also for an enhanced communication with the computer through separate buses, although it may become difficult to obtain information from both control boards simultaneously due to bus overrides, as explained later in this section.

As said, the main components constituting the circuitry are:

- (i) two Arduino boards,
- (ii) a series of relays,
- (iii) a thermistor,
- (iv) a hot end,
- (v) a motor driver,
- (vi) a stepper motor, and
- (vii) a power source.

In principle, the temperature of the thermistor must read a specific value, depending on the temperature setup of the printing material –which is provided by the vendor. For thermoplastics of different kinds, this temperature value normally oscillates between 180 and 230 ºC. If the reading is correct, then a signal is sent to the control board so that the motor can be activated. Both the motor speed and rotation direction are predetermined beforehand, as a result of a series of trial and error experiments shown in Chapter 4 and Annex I. The thermistor temperature is read every 1000 to 2000 milliseconds; this reading also defines whether or not the hot end must be activated. If the temperature reading is below the minimum printing temperature, then the hot end receives power from the energy source; otherwise, it does not. Relays act as switches for that purpose, allowing or disallowing for the energy to go through to the hot end. The motor is programmed to stop if an error occurs or in the unlikely event of a temperature drop below a certain user-defined threshold. The fan is directly connected to the power source so that it is continuously working. This setup is recommended both for PLA and ABS materials, as it enhances the behavior of the material and eases the cooling process.

Splitting the control logic into well differentiated, separate parts in order to increase the performance of the Arduino board when reading the thermistor temperature, has a series of significant advantages and disadvantages, which are mentioned here for convenience:

- It is possible to increase the performance of the overall system by avoiding interferences between the library of the motor (which uses the bus to control the amount of rotations or steps) and the rest of the code. In other words, it supports a certain degree of "multitasking".
- Parallel control: it is possible to control all elements independently, loading new code to the boards without mutual interferences.
- The code becomes easier to modify. Splitting the whole logic into two boards allows for a modular approach.
- It becomes relatively tedious to obtain information from both boards on a single computer, due to bus overrides.
- This approach raises the cost of the electronic components.

Further information about the logic of the extruder can be found in subsequent sections.

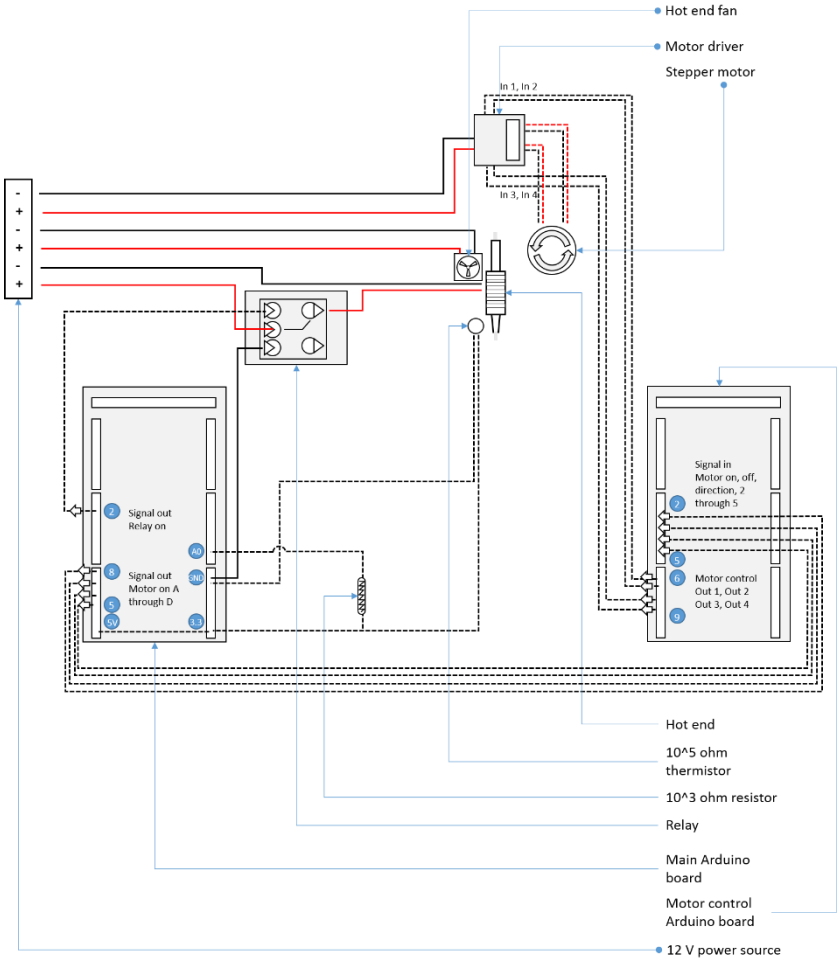

Fig. 3. Main electronics: circuitry layout.

5.3.1. Logic structure

This section describes the software used in the control boards along the electronic components used in the extruder. Software and hardware shape indeed an inseparable whole, since both depend on one another in an interrelated fashion.

The main software that controls the diverse operations involved in the process is Arduino. Arduino's latest version can be found and downloaded from the organization's website www.arduino.org. The software provides not only a stable platform for communicating and coding Arduino Boards, but also a set of libraries well suited for this purpose.

Explained further in the following section, let us just point out the main structural blocks of the Arduino controller code (see Fig. 4):

- Initialization and temperature reading: this workflow deals with the whole setup of the tool system. This initialization may differ from material to material, as quite different hardware and electronics are required.
- Looping: is the core of the control operations. The loop basically repeats the operations in fig. 2 in a sequential manner. The main board checks for the current status of the hot end, and responds accordingly:
    - If the temperature is above the minimum established temperature, then it sends a signal for the motor to rotate. If there is any interference or robot input, then the motor direction might change or it might even stop. Robot input is another layer added on top of the inner logic of the tool itself. The Arduino board also sends a signal to the relay so that it prevents the hot end from overheating.
    - If the temperature is below the minimum printing temperature, then the control board performs two operations:
        - In the first place, it sends a signal to the relay and power is let through to the hot end. A signal is sent to the motor controller to keep its current state.
        - Secondly, it checks whether the temperature has dropped below a minimum operational threshold. Should this be the case, then the board sends a "STOP" signal and printing stops for safety reasons.
- Motor Control carries out the rotation orders received from the main board. Figure 2 shows that there are basically three different motor states:
    - Forward rotation (clockwise), used for printing. As in the case of backward rotation, the speed of the motor can be set to any desired value.
    - Stopped, when willing to interrupt printing and create discontinuous printing (which can happen when dealing with multiple pieces at once or in complex parts).
    - Backward-rotation (anti-clockwise) in order to prevent from material overflow.

  Motor states are efficiently controlled by robot inputs, and depend on the geometry of the part itself. As a consequence, digital input/output functions are programmed in the robot part's routine as explained in detail in section 4.5.

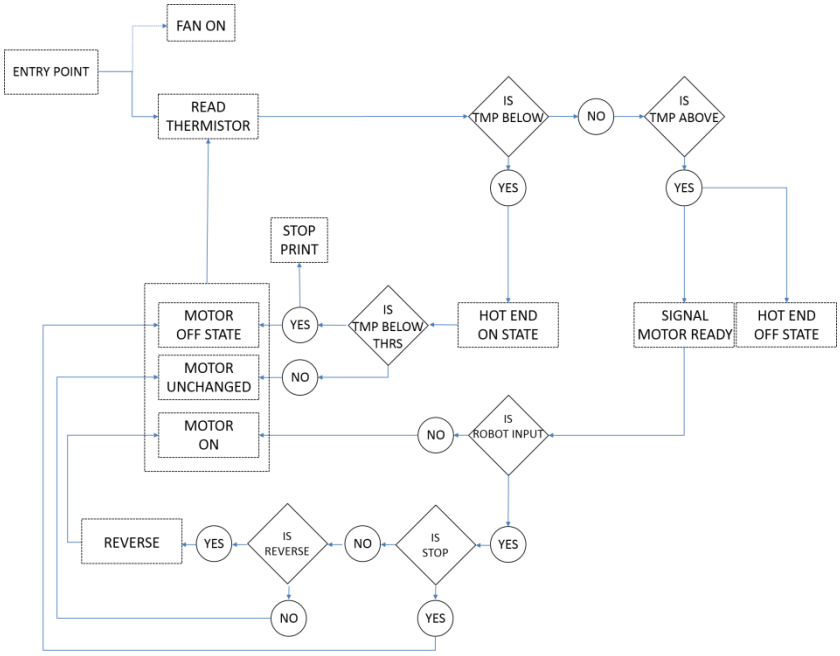

Fig. 4. Algorithmic logic

5.3.2. Arduino Code

This section explains each of the aforementioned code blocks. The logic of the code structure is sequential:

- Initialization and temperature reading: the entry level of the algorithm. The initialization consist of basically 2 operations: (i) the heating of the hot end, and (ii) cyclic temperature readings. Once the hot end reaches the desired temperature entered by the user, then the main Arduino Board sets the active variable on at the time it exists the initialization. The initialization, as it is common use, is called a single time at the beginning of the printing process, when the tool is activated. This variable –in actuality a digital output set to the ON state- communicates with the motor Arduino Board as to activate the rotation of the device. This initialization contains a single routine as can be seen in the code below. It is crucial to reference the physical electronic equipment properly, as different thermistors have different resistance values, thus affecting the calculation in the code. Wrong or mistaken resistor values might yield unstable, undesired and unpredictable behaviors or readings, which might even oscillate between physically impossible values (this is, below absolute zero, for instance).

```
void initialize()
{
  while (steinhartTemp < extrusionTemp)
  {
    calcTemp();
    digitalWrite(extruderRele, HIGH);
  }
}
```

As shown above, the *initialize* function simply contains a loop that turns on the hot end if the temperature reading is below the desired extrusion temperature. The variable *steinhartTemp* stores the temperature reading according to the Steinhart equation, explained below. The *calcTemp* function calculates the temperature according to the reading of the Semitec 104 GT-2 thermistor. This is a high heat-resistance and high-sensitive model. The high performance 104 GT-2 thermistor is used in a wide variety of FDM 3D printers and is known for its reliability. This wide use guarantees updated information and good documentation, which makes it the perfect candidate for the purposes of this development. Its reduced size makes it also suitable for a combined use with the 3DV6 hot end, which is described below.

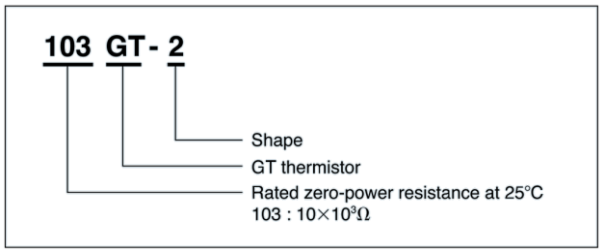

Fig. 5. Part number description.

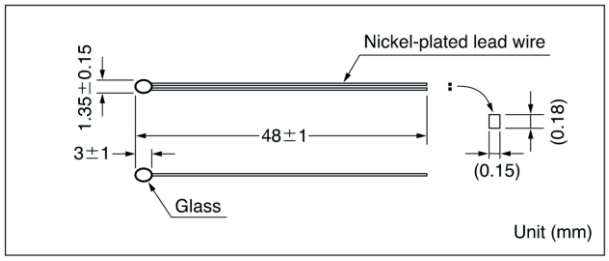

Fig. 6. Thermistor size and dimensions

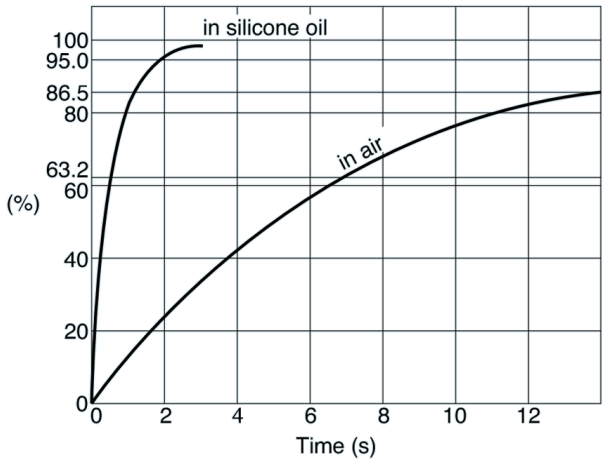

Fig. 7. Thermistor time constant

The Semitec GT Thermistor series is combined both superior feature-wise to the BT and ET thermistor as far as fast response, high reliability, wide category temperature range, high moisture proof, and high accuracy are concerned. The GT thermistor is connected by a lead wire which implements alloyed technology, reinforced by a high resistance glass coating. As indicated by its name, which follows the logic of the part number in figure 5, is a $10*10^4$ Ω thermistor. Its resistance must be addressed correctly and so included and indicated in the code.

Part No.	R_{25}*1	B value*2	Dissipation factor (mW/°C) Approx.	Thermal time constant(s)*3 Approx.	Rated maximum power dissipation (at 25°C)(mW)	Category temp. range(°C)
102GT-2	1.0kΩ±3%	3305K±2%	0.6	7	3.0	−50～+200
202GT-2	2.0kΩ±3%	3838K±2%				
502GT-2	5.0kΩ±3%	3964K±2%				
103GT-2	10.0kΩ±3%	4126K±2%				
203GT-2	20.0kΩ±3%	4282K±2%				
503GT-2	50.0kΩ±3%	4288K±2%				−50～+300
104GT-2	100.0kΩ±3%	4267K±2%				
104GTA-2	100.0kΩ±3%	4390K±2%				
204GT-2	200.0kΩ±3%	4338K±2%				
504GT-2	500.0kΩ±3%	4526K±2%				
105GT-2	1000.0kΩ±3%	4608K±2%				

Fig 8. Thermistor 104GT-2 technical specifications

According to the main_controller_v004.ino file and the *calcTemp()* function shown below, the thermistor is described according to the following variables as they must be written in the header section of the main INO file (please note that *#define* is a reserved Arduino keyword for declaring constants):

- Resistance (Ω): *#define THERMISTORNOMINAL 100000*
- B value: *#define BCOEFFICIENT 4267*. This value makes sense in the Steinhart-Hart equation, and stands as a coefficient that intends to characterize the type of thermistor.
- Nominal temperature (temperature at which zero-power resistance is measured): *#define TEMPERATURENOMINAL 25*
- The circuit resistor, which helps translate voltage into temperature according to the Steinhart-Hart model used to obtain the temperature readings in Celsius (Ω): *#define SERIESRESISTOR 10000*

The Steinhart-Hart model: The Steinhart–Hart equation is a model of the resistance of a semiconductor at different temperatures and has the following equation.

$$\frac{1}{T} = A + Bln(R) + C[\ln(R)]^3 \quad (5),$$

where:

- *T* is the absolute temperature (Kelvin).
- *R* is the resistance at the *T* temperature.
- *A*, *B*, and *C* are the so-called Steinhart-Hart coefficients, which vary depending on the type and model of thermistor, and the temperature range of interest.

The B-parametric equation form (2) yields quite reasonable and accurate values while using just one of the three parameters. The B-equation is then preferred for its simplicity and accuracy. This equation form is explained further below. Its relationship to the general form of the Steinhart-Hart equation is also disclosed for a deeper understanding.

$$\frac{1}{T} = \frac{1}{T_0} + \frac{1}{B} * \ln\left(\frac{R}{R_0}\right) \quad (6),$$

The code transforms this equation into a series of steps that allow to calculate the absolute temperature, which is ultimately converted into Celsius. The viscosity of a molten polymer is highly dependent on temperature, which becomes probably the most crucial factor for FDM printing of thermoplastics. Figure 9 shows the viscosity curves for a polystyrene (PS) at different temperatures between 160ºC and 220ºC. Thus, guaranteeing a precise control of the extrusion temperature is fundamental to the correctness of the prints, both to avoid faulty fixation problems and to optimize the specimen's printing quality. It is recommended to always print slightly beyond the temperature range specified by the vendor.

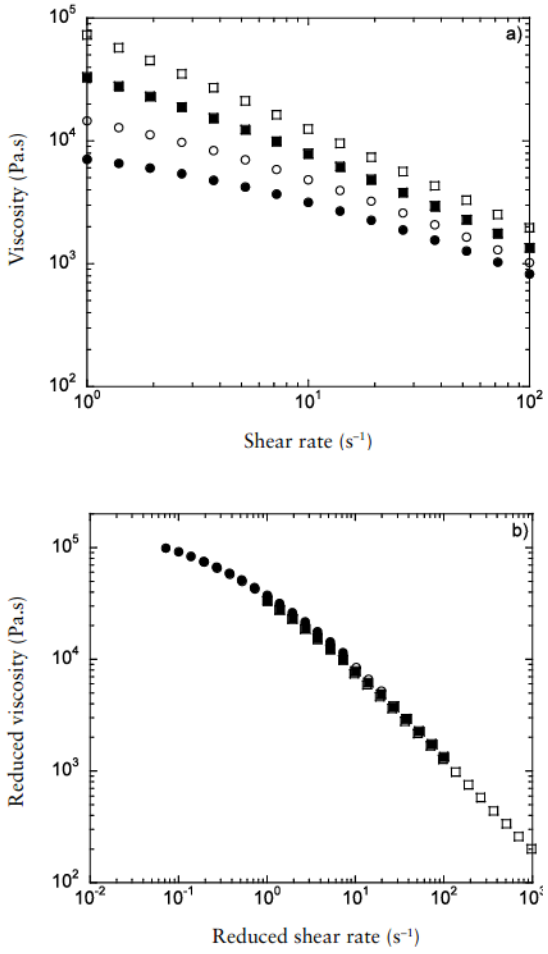

Fig. 9. a) Viscosity curves of a polystyrene at different temperatures; up to down: (blank boxes) 160 °C, (filled boxes) 180 °C, (blank circles) 200 °C, (filled circles) 220 °C; and (b) Mastercurve obtained bytime-temperature superposition of the data of Figure 2.5a at 180 °C (*Vergnes, Vincent, & Haudin, 2012*)

The actual Arduino code is contained within the *calculateTemp()* function, explained below step by step.

- Analog reading: resistance calculation. The calculation is carried out several times for each reading, allowing for an optimized and reliable result in the minimum amount of time. The average value is used as a base value for further calculations and stores the resistance of the thermistor at a given moment. This resistance must be converted to actual temperature values either by using the Steinhart-hart model equation above, or by simply using the curve from the vendor. As mentioned previously, the first option is included here for reference, although the second one would be easily coded through a key table or a similar solution.

```
void calcTemp()
{
  //------------------------THERMISTOR----------------------------
  float average;

  //------------------------ANALOG READ
  // take N samples in a row, with a slight delay
  Serial.println("Printing thermistor info");
  for (i = 0; i < NUMSAMPLES; i++){
     samples[i] = analogRead(THERM_PIN);
    Serial.print(samples[i]);
    Serial.print("/");
  }

 //Average out the readings (samples)
  average = 0;
  for (i = 0; i < NUMSAMPLES; i++){
    average += samples[i];
  }
  average /= NUMSAMPLES;

  Serial.print("Average analog reading ");
  Serial.println(average);

  //------------------------RESISTANCE
  // convert the value to resistance
  average = 1023 / average - 1;
  average = SERIESRESISTOR / average;
  Serial.print("Thermistor resistance ");
  Serial.println(average);

 //[CONTINUES IN SNIPPET BELOW]
```

- Calculate Steinhart temperature. The actual implementation of the Steinhart-Hart model through the B parametric form entitles these steps:
  - Obtain R/R_0, where R_0 is the nominal resistance of the thermistor. This calculation yields the actual relationship between the actual reading and the reading at 25ºC.
  - Calculate log, as an intermediate but necessary step.
  - Divide by B Value in order to qualify the thermistor model, as explained above. This coefficient is required to obtain proper and precise calculations.
  - Add $1/T_0$ (nominal temperature) to the result, as it is needed to regard actual atmospheric conditions in a 0 resistance state.
  - Invert
  - Substract 273 to obtain Celsius reading, since the results are given in Kelvin so far.

```
//[CONTINUES FROM SNIPPET ABOVE]
 float steinhart;
 steinhart = average / THERMISTORNOMINAL;          // (R/Ro)
 steinhart = log(steinhart);                       // ln(R/Ro)
 steinhart /= BCOEFFICIENT;                        // 1/B * ln(R/Ro)
 steinhart += 1.0 / (TEMPERATURENOMINAL + 273.15); // + (1/To)
 steinhart = 1.0 / steinhart;                      // Invert
 steinhart -= 273.15 ;                             // convert to Celsius

 Serial.print("Temperature steinhart: ");
 Serial.print(steinhart);
 Serial.println(" *C");

 steinhartTemp = steinhart;
}
```

- As explained before, the above code yields sufficiently precise readings while using the B-parameter form of the Steinhart-Hart equation (6). Nevertheless, it is also possible to obtain better and more accurate calculations by fine-tuning the so-called precision A, B, and C values of the Steinhart-Hart equation (5). Those values are obtained according to this formula:

$$\begin{bmatrix} 1 & \ln(R_1) & \ln(R_1)^3 \\ 1 & \ln(R_2) & \ln(R_2)^3 \\ 1 & \ln(R_3) & \ln(R_3)^3 \end{bmatrix} \begin{bmatrix} A \\ B \\ C \end{bmatrix} = \begin{bmatrix} 1/T_1 \\ 1/T_2 \\ 1/T_3 \end{bmatrix} \tag{7}$$

Which can be expressed as:

$$\begin{bmatrix} 1 & L_1 & L_1^3 \\ 1 & L_2 & L_2^3 \\ 1 & L_3 & L_3^3 \end{bmatrix} \begin{bmatrix} A \\ B \\ C \end{bmatrix} = \begin{bmatrix} Y_1 \\ Y_2 \\ Y_3 \end{bmatrix} \tag{8}$$

Subsequently, in parametric form:

$$\gamma_2 = \frac{Y_2 - Y_1}{L_2 - L_1}$$
$$\gamma_3 = \frac{Y_3 - Y_1}{L_3 - L_1} \tag{9}$$

Where the same calculations are applied to different temperature-resistance value pairs. Taking the above values, we obtain A, B, and C in parametric form:

$$C = ((\gamma_3 - \gamma_2)/(\mathrm{L}_3 - \mathrm{L}_2))(L_3 + L_2 + L_1)^{-1}$$
$$B = \gamma_2 - C(L_1^2 + L_1 L_2 + L_2^2)$$
$$A = Y_1 - (\mathrm{B} + L_1^2 \mathrm{C}) L_1 \tag{10}$$

The error in the Steinhart–Hart equation is generally less than 0.02 °C in the measurement of temperature over a 200 °C range (*Agilent, Inc., 2012*). As an example, typical values for a thermistor with a resistance of 3k Ω at room temperature (25 °C = 298.15 K) are:

a = 1.40 x 10-3

b = 2.37 x 10-4

c = 9.90 x 10-8

Additionally, the B or β parameter equation allows us to fetch the actual value of the B parameter found in the code shown above. NTC thermistors (such as the chosen

Semitec GT104-2 model) can be characterized with that B Coefficient. Essentially, it follows the Steinhart-Hart equation above with the following values:

$a = (1/T_0)-(1/B)* Ln(R_0)$

$b = 1/B$

$c = 0$

The B parameter equation expresses actual temperatures according to the equation below:

$$\frac{1}{T} = \frac{1}{T_0} + \frac{1}{B} * \ln\left(\frac{R}{R_0}\right) \tag{11}$$

Whereby we can obtain *T* considering that the room temperature is *25 °C* or *298.15 K = T_0*. As a consequence:

$$T = \frac{B}{\ln\left(\frac{R}{r_\infty}\right)} \tag{12}$$

Where:

$$R = r_\infty e^{B/T_0} \tag{13}$$

$$r_\infty = R_0 e^{-B/T_0} \tag{14}$$

Alternatively, the B-parameter equation can also be written as $\ln R = \frac{B}{T} + \ln r_\infty$. This equation can be used to convert the function of resistance vs. temperature of a thermistor into a linear function of $\ln R$ vs. $\frac{1}{T}$. The average slope of this function will then yield an estimate of the value of the B parameter.

- Looping is yet another fundamental piece in the control of the extruder tool as a whole. The loop code is repeated continuously in real execution time and relates, in this particular case, to the main hardware control. As required by the operations named throughout the present Chapter, the 2 main operations required involve (i) reading the thermistor temperature, and (ii) modifying the thermistor's behavior. The first one has been already introduced in the text, whereas the second one is encapsulated into the *useThermistor()* function.

```
void loop() {
  // main code here, set to run repeatedly
  if (millis() %500==0){
    calcTemp();
    useThermistor();
  }
}
```

The *useThermistor* function merely activates or deactivates the energy flow through the hot end by opening or closing the related relays. The function includes a control statement as well, as it is possible that temperature readings fall slightly below the working range stablished by the user. This can be considered a predictable behavior, thus not having to stop the whole apparatus from working.

```
void useThermistor()
{
  if (steinhartTemp >= extrusionTemp)
  {
    Serial.println("Temp is too high");
    //digitalWrite(activateMotorPin, HIGH);
    digitalWrite(extruderRele, LOW);
```

```
  digitalWrite(redLed, LOW);
  digitalWrite(greenLed, HIGH);
  Serial.println("Deactivated");
 }
 else
 {
  Serial.println("Temp is too low");
  //digitalWrite(activateMotorPin, LOW);
  digitalWrite(extruderRele, HIGH);
  digitalWrite(redLed, HIGH);
  digitalWrite(greenLed, LOW);
  Serial.println("Activated");
 }

 if (steinhartTemp >= extrusionTemp - 8) {
  digitalWrite(activateMotorPin, HIGH);
 } else {
  digitalWrite(activateMotorPin, LOW);
 }
}
```

- All previous code has a relevant impact on the printing behavior of the extruder. This influence is mechanically realized through a Stepper Motor, which performs a series of quite simple operations. As previously explained in sections 5.1 and 5.2, the motor rotates in order to push material through the hot end and the nozzle when the printing temperature is reached. Nonetheless, there are certain cases when either stopping the motor or even reversing the rotation direction can be desirable. A discontinuous material discharge requires both cases, as to avoid undesired material drops or depositions.

  Different code tryouts and electronics' layout scenarios show that, in order to achieve a reliable motor behavior, it is mandatory to avoid the exposure to the Arduino built-in Stepper library due to instability issues and repeated failures after long use. Furthermore, motors used under this library become too hot after about a single hour of non-stop use, causing the motors to fail. As exposed above, a different library is used, although it would be possible to develop a custom one that accommodates all necessities and requirements –this might be case in the near future.

  The library CustomStepper is a simple, yet handy tool to control Stepper Motors in Arduino. It is structured in a quite similar way to the natively integrated Stepper library, although it provides extended functionality in two regards:

  - First, it allows to control several motors at once.
  - Second, it does not block the execution of code. This is especially convenient when dealing with multiple parameters, inputs, and outputs at once.

```
//IMPORT LIBRARIES----------------------------------------------
#include <CustomStepper.h>
#include <avr/pgmspace.h>

//DECLARATIONS--------------------------------------------------------
//1. MOTOR
boolean rotate1 = false;
boolean rotatedeg = false;
boolean crotate = false;
boolean isMotorOn = false;

int motorOnPin = 2;
int motorVal = 0;

CustomStepper stepper(8, 9, 6, 7, (byte[]) { 8, B1000, B1100, B0100, B0110, B0010,
B0011, B0001, B1001}, 4075.7728395, 10, CW);

int ROTATE_SPEED = 40; //rpm (set according to actual rotations per minute)
```

```
//PROGRAM----------------------------------------------------------------
void setup() {
  Serial.begin(9600);//data transmission
  //stepper
  stepper.setRPM(ROTATE_SPEED);
  //sets the Steps Per Rotation
  stepper.setSPR(403.7728395);

  pinMode(motorOnPin, INPUT);
}

void loop() {
  motorVal = digitalRead(motorOnPin);
  Serial.println(motorVal);
  if (motorVal == 1) {
    digitalWrite(redLed, HIGH);
    isMotorOn = true;
  } else {
    //digitalWrite(redLed, LOW);
    isMotorOn = false;
  }

  if (stepper.isDone() &&  rotate1 == false && isMotorOn == true)
  {
    //this method sets the direction of rotation, 3 allowed values: CW, CCW, STOP
    //clockwise and counterclockwise for the first 2
    stepper.setDirection(CCW);
    //this method sets the motor to rotate a given number of times, otherwise,
    //the motor will rotate until another command is set or the direction is set to STOP
    stepper.rotate(0);
    isMotorOn = false;
  }else{
    stepper.setDirection(STOP);
    stepper.rotate(0);
    }
  stepper.run();
}
```

- Despite the efforts put on optimizing the design of the mechanized parts in order to minimize their repercussion on the plastic extrusion strand, there are some flow instability issues that must be taken into account. First, some of those are due to vibrations stemming from the motor itself, which may be solved by isolating mechanical parts from one another. Second, all molten polymers exhibit flow instabilities above critical conditions, leading to a perturbed shape of the extrudate. These defects are usually classified into two families, depending on the molecular structure and viscoelastic properties of the materials. The first one concerns linear polymers, such as a HDPE or a low density polymer, while the second one is encountered in the study of highly branched polymers which have high elasticities, such as Low Density Polyethylene (LDPE) or PS. Although the latter normally exhibit helical or gross melt fracture defects, the former is subject to more extrusion defects. Suffice it to say that these account for four different types (*Vergnes, Vincent, & Haudin, 2012*); including the two mentioned before, the defects are:
    - Sharkskinned aspect, which is exposed for high flow rates or apparent shear rates.
    - When above a critical value, the flow becomes unstable and, at a certain imposed flow rate, the extrudate presents alternate portions of smooth and sharkskinned aspect.
    - At a critical point, a jump occurs in the flow rate, leading to helical defects
    - Above that critical point, the flow conditions become stable again and the extrudate is smooth, but quickly becomes distorted when the flow rate is increased, leading to the usually called gross melt fracture defect.

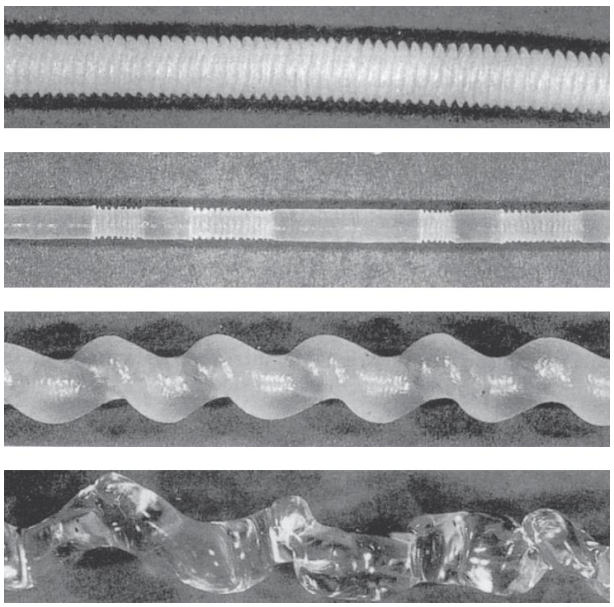

Fig. 10. Different examples of extrusion defects (up-down): a) sharkskin; b) stick-slip;c) helical defect; and d) gross melt fracture (S*ung-Hoon, Montero, Odell, Roundy, & Wright, 2002*)

These defects were encountered mainly at the first moments of extrusion, where flow is unstable due to the presence or remaining material inside the hot-end cavity. Once the cavity is emptied and filled back by new incoming filament strands, the flow becomes stable – depending on the regularity and reliability of the motor employed to push the material through. This is one of the main reasons to implement a starting routine prior to actual part printing execution routines.

5.4. Conclusions

Despite the variety of the tooling and electronics available in the market, there exists no affordable, easy-to-build and easy-to-adapt, open-source solution for a customizable FDM extruder. This chapter has shown the experiments realized throughout the development of the thesis and provided a basic layout for a fully functional, yet reliable FDM extruder apparatus that can virtually be adapted to any machine. Furthermore, the present Chapter has demonstrated the relationships between the robot code (related on its side to the part geometry itself) and the extruder.

Although several layouts were tested, the chosen version –displaying two Arduino Boards- excels at its reliability and modularity, allowing the user to modify, load or unload code independently without tampering with the electronic components. In addition to that, this layout is not significantly more expensive than others, and presents an intuitive code accessible even to unexperienced users.

Chapter 6

Material usage optimization through structure-oriented infill patterns.

Currently, no open-source nor proprietary software includes smart infill patterning calculations. Space packing infills constitute the majority or all of the available options for the final user. 3D printing for construction purposes must offer a solution to this problem, as material optimization is one of the most prominent advantages of the technology. This section offers an overview for the development of an algorithm that offers material-responsive infill patternsA simple, modular, expandable system is presented that considers the structural logic of printable parts through the voxelization of 3D virtual models into a finite element representation that is used to feed a spring model. Material properties and user customization are discussed. Several ad-hoc solutions, optimization capabilities and simulation results are tested and shown. The use of non-standard, customized nozzle designs and print materials is discussed for further optimization capabilities.

Credits: the Processing applet has been developed and written by Hugo Cifre Cardona Torró. Many thanks for his thriving ideas, enthusiasm, and great contributions.

6.1. Introduction

It is clear that material plays a fundamental role in the 3D printing technology. Material can be considered through a two-fold approach: first, as material consumption may be optimized through the usage of precisely the amount of material required for the actual final part –without further co-production or side-effects; second, as material engineering is indeed a field of study emerging in close relationship to the evolution of 3D printing techniques. Although it is out of the scope of the present thesis to actually involve the development of new materials, the use of bio-materials, composites, and cements is discussed.

As opposed to bioengineering, where tissue development is already a fact, in AECO related industries, material consumption is a crucial factor which requires further study. Large 3D printing methodologies rely on the optimization of time, material, and fabrication costs, which in turn result in an enhanced process and optimized results. Nevertheless, most of the effort is put on the study of path-optimization algorithms, or the use of robots or other digital fabrication means that fall short in the consideration of material behavior and performance

This Chapter proposes the integration of a novel tool for the generation of 3D-printable models that seeks to optimize the amount of material through customized fill patterns that respond to specific

material behaviors and structural conditions. 3D models are analyzed and treated as finite elements for stress analysis, representing a series of springs. Stress is further evaluated and traced to create an optimized representation of the object. This method enables form-finding based on material properties, organization, and behavior. A test case is presented that shows the integration of the whole design-to-calculation process resulting in a series of results that are displayed for comparison reasons and convenience.

SLA, SLS, FDM, and many other "layer-based" printing techniques present a number of limitations regarding material usage that need to be addressed when attempting to develop a compelling 3D printing solution for real-scale end products. As it has been sufficiently explained in previous chapters, the so-called oversized approaches to 3D printing intend to replicate small scale machines and parts by simply scaling them up, which, as seen in Section 2.4, results either in large amounts of material waste or a lack of qualitative process modifications.

Furthermore, those techniques focus primarily on hardware issues, whereas software control is a key piece in both the design of machinery and form. A well-designed controller program may allow for an optimization of the amount of printed material, therefore yielding a reduction of the total use of material and positive effects both at financial and environmental levels. None of the scaled-up versions of desktop-oriented printers exposed in the present thesis considers the optimization of material consumption even remotely. The proposed approach deals with the fact that material use scales up in cubic proportion as the part increases in size by offering a solution in the form of a structural-based algorithm for the calculation of infill patterns.

Normally, 3D printed parts are designed with default-patterned, non-customizable infills. Furthermore, these patterns follow space-packing logics or algorithms that ignore material properties, performance drivers, or any other material-related optimization (*Oxman & Rosenberg, 2007*). Although this might seem acceptable for small-scale parts, it is not the case when printing big-scale parts that seek to compete with their mold-produced counterparts. Furthermore, the attempts made in the design of optimized infill patterns fall short in their focus on an economically feasible model as they focus primarily on form-generation techniques *(Oxman N. , Get Real: Towards Performance Driven Computational Geometry, 2007*).

The algorithm takes the mesh geometry, material properties, a precision distance, and loads as input, and produces an optimized infill pattern as output. It works in a multi-phase manner, as shown in figure 1:

- Geometrical input through design software
- Translation of the 3D model or part into a finite-element representation
- Export to calculation software
- Material characterization and stress performance test through a spring-like model
- Creation of fill pattern following the spring deformation results

These phases are presented in the following sections. Finally, experimental results show that material can be optimized up to a 50% when compared to other techniques, such as the space-packing square-like and hexagonal infill patterns.

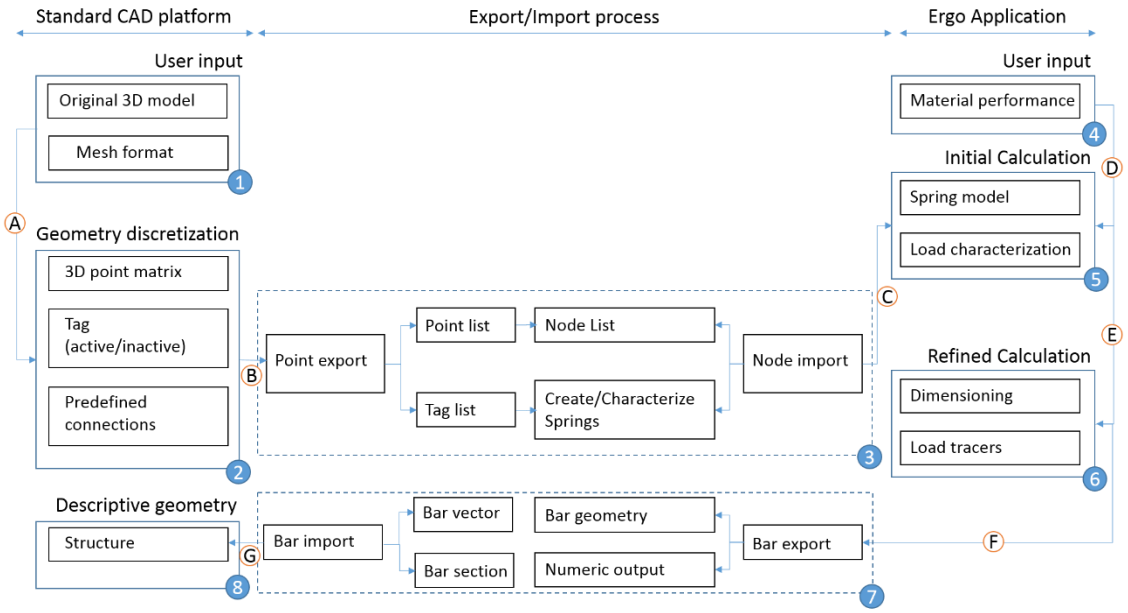

Fig 1. Main phases of the algorithm

6.2. Geometrical input through design software

The algorithm starts by analyzing a 3D model formatted as a mesh. As explained above in chapter 4, meshes are representations of volumetric shapes characterized by a series of quad or triangular faces which normally define closed solids as faceted forms in three dimensional space. In fact, triangular meshes are preferred, as these are usually easier to use for geometrical intersection calculations –triangular faces are always planar. Quad faces might also be employed, though.

The shape is read by the algorithm, which creates a series of points based on both the object's bounding box –this is, the minimum box which contains the whole geometry in the design software-, and the user input. Although it is not necessary to align the object to the world-space coordinate system, it is recommended to do so, since the bounding box will be calculated this way. Aligning the object will thus result in an optimized input.

The user is then prompted for a "division distance", which is used in turn to calculate the amount of points to be created in each direction. As a result, a 3-dimensional point cube is created. It is important to point out the impact of this input in the overall performance of the algorithm, as smaller subdivision amounts quickly result in large point matrices. These points are used to characterize the form object, and will utterly become points of structural analysis.

Table 1. Calculation of pre-defined points.

	OBJECT ALIGNED			OBJECT ROTATED 45 degrees around Z (vertical) axis		
	Xdim (mm)	Ydim (mm)	Zdim (mm)	Xdim (mm)	Ydim (mm)	Zdim (mm)
Size object	100	200	5	100	200	5
Size bbox	100	200	5	144	288	5
Div dist (mm)	1			1		
Point nr/dim	100	200	5	144	288	5
Point nr (total)	100000			207360		
Div dist (mm)	0,5			0,5		

Point nr/dim	200	400	10	288	576	10
Point nr (total)	800000			1658880		
Div dist (mm)	0,25			0,25		
Point nr/dim	400	800	20	576	1152	20
Point nr (total)	6400000			13271040		

Table 1 shows the amount of points obtained during the discretization process of a sample 3D model. As it can be seen, the number of points increases easily, so the algorithm needs to optimize the amount of points (data) in order to minimize its execution time. Currently, the algorithm merely compares nearby points using a pre-defined behavioral pattern, thus allowing for an n-factor execution time. In other words, the execution time of the algorithm is linearly proportional to the amount of points describing the discrete representation of the original 3D object. This is possible thanks to a characterization of the points according to their location, and following the logic hereby described:

- Points located on the faces of the bounding box (F1 through F6): 6 cases
- Points located on the edges of the bounding box (E1 through E12): 12 cases
- Points located on the vertices of the bounding box (V1 through V8): 8 cases
- Points located in the interior of the bounding box (I): 1 case

The total bounding box dimension is calculated during the point discretization. This pre-calculation permits to obtain the maximum and minimum point locations in each dimension, yielding the lower and upper bounds within which the discrete elements are placed.

Table 2. Amount of points per location case –relative to maximum and minimum bounding box size

	General formula			Example		
Size	Xdim (mm)	Ydim (mm)	Zdim (mm)	Xdim (mm)	Ydim (mm)	Zdim (mm)
Object	100	200	5	100	200	5
Bbox	Xb	Yb	Zb	144	288	5
Divdist (mm)	DivDist			1		
Point nr/dim	Xb/DivDist	Yb/DivDist	Zb/DivDist	144	288	5
Point nr(total)	Xb/DivDist*Yb/DivDist*Zb/DivDist			207360		
V1-V6	6			6		
E1/E3/E5/E7	Yb/DivDist*4			1152		
E2/E4/E6/E8	Xb/DivDist*4			576		
E9/E10/E11/E12	Zb/DivDist*4			20		
F1/F3	(Yb/DivDist)*(Zb/DivDist)*2			2880		
F2/F4	(Xb/DivDist)*(Yb/DivDist)*2			82944		
F5/F6	(Xb/DivDist)*(Zb/DivDist)*2			1440		
I	(Xb*Yb*Zb)/(DivDist^3)-sum(V+E+F)			118342		
Total points	(Xb*Yb*Zb)/(DivDist^3)			207360		

In actuality, this results in a scenario with 27 possible different cases, where most of the points will be classified as I, that is, contained within the interior of the bounding box of the object. To be more precise, cases V1 through V8 will be represented with a single point each; cases E2 through E12 will depend directly on the number of subdivisions which are themselves a result of the division distance shown in

Table 1; and cases F1 through F6 will contain also a number of points that will depend on the subdivisions of the thereby implied X, Y, or Z dimensions. Although it is not necessary for the proper execution of the algorithm, it is possible to calculate and determine the exact number of instances belonging to each scenario or case. Table 2 shows both the calculation and the results for the example displayed in Table 1.

6.3. Voxelization: Translation of the solid model into a 3D finite-element representation

6.3.1. Verification of the discretization: obtaining points inside or on the object.

Once the points have been calculated and stored in a list, the algorithm creates a special tag for each one describing whether or not they are contained within the actual solid object. This binary tag will allow for a significant reduction of computational time, since only those points that comply with the above mentioned conditions will be considered for the actual spring calculations. The points, although existing in the program, are therefore qualified as active and non-active. Every single point in the matrix is tested, and only the active points are used as spring vertices.

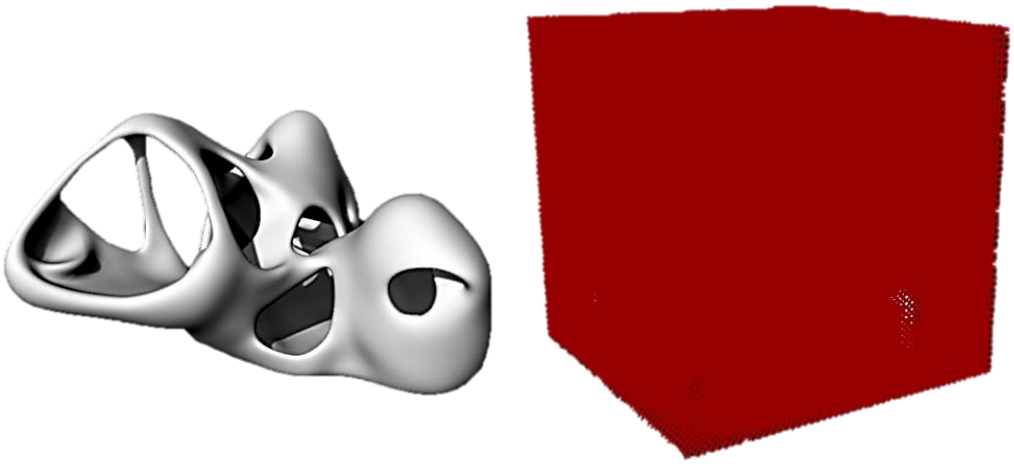

Fig 2. Initial test model – complex geometry showing point boundary box discretization

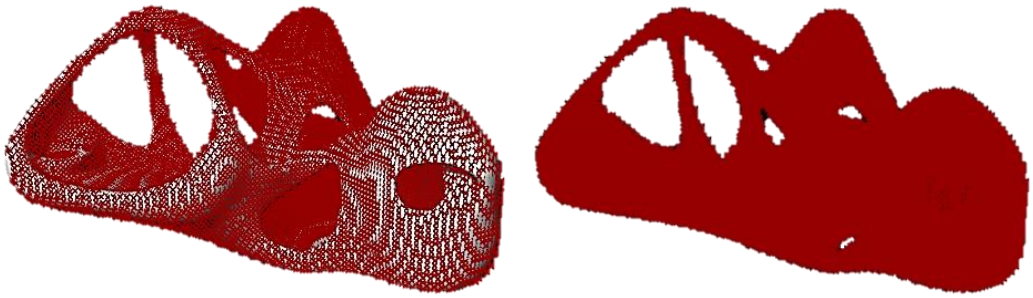

Fig 3. Model showing filtered points on surface and points –nodes- to be exported

6.3.2. Pre-calculation of connections to springs.

Points are named according to the graphic shown in Figure 4, following a top to bottom, anticlockwise logic. A coordinate system is established to calculate the case type, as each one is defined through the relative distance of the point of study to both the origin and the farthest point within the range of the bounding box. V5, for instance, has a 0 distance to the origin point of the bounding box and a

maximum distance in each direction to the outmost point, where V3 is placed. V3, therefore, has a maximum distance to the relative origin, whereas 0 when compared to the outmost point. Any other point can be characterized following the same logic, this is, obtaining its relative distance to both points in each direction. All points with 0 Z-distance belong to the same plane, defined as F6. If the points laying on that plane have also a maximum or minimum distance to the origin X or Y axes, they will become edge points –E5, E6, E7, and E8. Furthermore, if this is the case for both X and Y axes, then the points are vertices – V5, V6, V7, and V8. This logic can easily be used to populate the whole three-dimensional point matrix.

Table 3. Deterministic point connection distribution

Case	Start pt	Connect pts		Start pt	Connect pts		Start pt	Connect pts
1	V1	E1 E4 F5 F1 F4	10	E2	V3 E11	19	E11	V3
2	V2	E2 F2	11	E3	V3 E2 E11 F2	20	E12	V4 E3 E7 F3 I
3	V3	-	12	E4	V4 E1 E3 E12 F5 I	21	F1	V2 V6 E1 E10 F2 F5 I
4	V4	E3 F5 F3	13	E5	V6 E6 E10 F1 F6 I	22	F2	V3 V7 E2 E11
5	V5	E9 E5 E8 F1 F4 F6	14	E6	V7 E10 E11 F2	23	F3	V3 V7 E3 E11 F2
6	V6	E10 E6 F2	15	E7	V7 E11 F3 I	24	F4	V4 V8 E4 E12 F1 F5 F6 F3 I
7	V7	E11 F2	16	E8	V8 E5 E7 E9 E12 F4 F6 I	25	F5	V2 V3 E2 E3 F2 F3
8	V8	E12 E7 F6 F3	17	E9	V1 E1 E4 E5 E8 F1 F4 I	26	F6	V6 V7 E6 E7 F1 F2 F3 I
9	E1	V2 E1 E2 E10 F5 I	18	E10	V2 E2 E6 F2	27	I	E6 E10 E2 E11 E3 F2 F5 F3

Once the points are characterized, according to their relative position within the bounding box of the object, and tagged as active or non-active for the calculations, it is possible to further proceed to create the springs that will ultimately define the final shape or pattern of the object's infill.

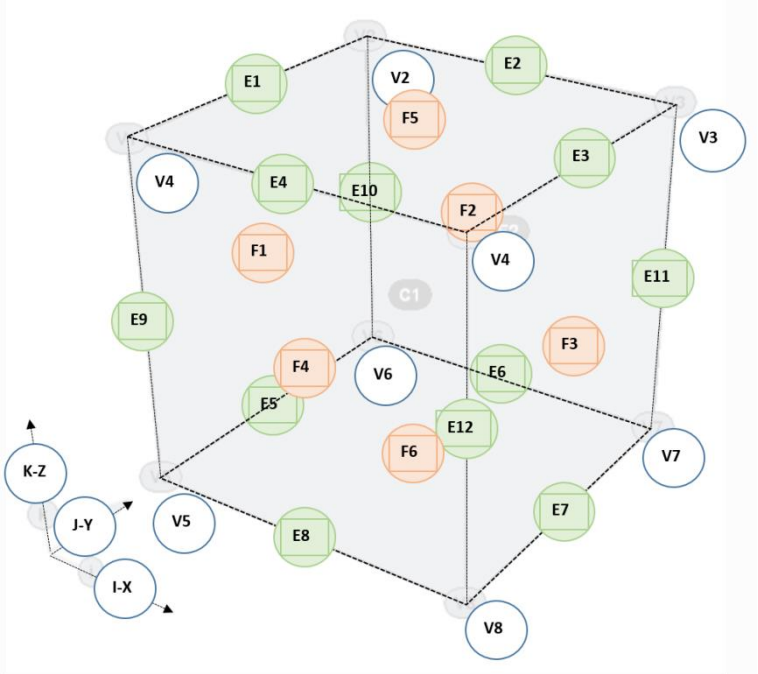

Fig 4. Point naming convention

The points have predefined connections that build springs. These springs respond to both compression and tensile stresses and are further characterized by the material properties that the user or designer intends to replicate or study. As explained above, a deterministic approach is taken in order to determine the connections emerging from each point. These connections are displayed in Table 3, and shown in Figures 5 through 7.

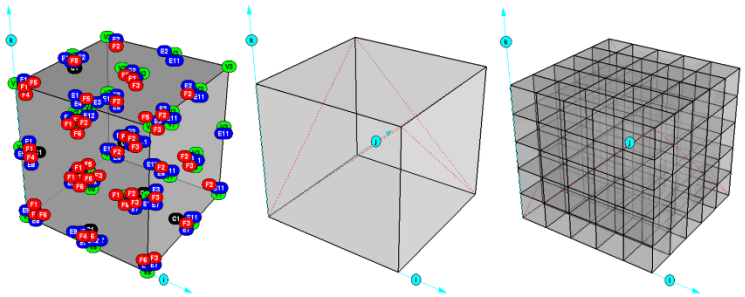

Fig. 5-7. Point connections for each type case, main connections per box, bounding box subdivision

6.4. Export to calculation software

The next step in the algorithm is the export the point matrix to the calculation software, which is a stand-alone application written in processing, a widely used software development interface for data visualization real-time data analysis (*Reas & Fry, 2014*) coded in JAVA. Since the above described process is driven entirely in CAD software –specifically in Rhinoceros and Grasshopper, it becomes necessary to "translate" the geometry data into language readable by the processing application. This is achieved by exporting 2 files simultaneously, the first containing the geometrical information of the points –a simple list of X, Y, Z coordinates, and the second the active/inactive tags for each point as well. This is a relatively easy task, and accomplished by a simple Python script embedded in the Grasshopper definition that carries out the initial part of the model depiction as a finite element model. Cross-referencing both files results in a simple way to again characterize each of the elements in the calculation software.

The algorithm is clearly divided into logical parts. To be more specific, the separation between the geometry core –where the discrete representation of the model is created- and the stress calculation itself –performed by the stand-alone application- makes the algorithm particularly modular. This feature will be used in the future to release a comprehensive product that might be able to adapt itself to a variety of CAD software packages, through a bridge or "translator" for each CAD platform. Once the translation is complete, the stand-alone stress simulator will easily perform on any model and return the required pattern data.

As a result, the algorithm is capable of taking any pair of files –containing the correct information in both size and format-, and automatically create a stress simulation from which it is possible to obtain not only the deformed shape of the object, but the trajectories of both compression and tensile stresses. Beside the purely geometrical information, these stresses are given as numerical data and treated as such for calculating the final pattern size or section. The workflow of this method is explained in subsequent chapters with more detail.

6.5. Material characterization and stress performance test through a spring model

As explained in previous chapters, the interactive model runs a structural performance calculation to optimize material usage in the original virtual representation. This model characterizes the object through a series of springs, which work either as compression or tensile bars depending on the forces applied onto them. The main force that influences the model is gravity, although horizontal forces might as well be applied. As explained further in following chapters, forces define the stresses under which the bars work according to Hooke's Law. All diagonal bars –connections V5-V4, V4-V7, V7-V2, V2-V5, V5-V7, V4-

V2- are placed on the surfaces defining the faces of each sub-cube. All edges –E1 throughout E12- are subject to either compression or tensile forces, and assumed to have pure stresses. In other words, all bars are subject to either force type, but not both.

Most printable materials nowadays (such as thermoplastics, ceramics, clay, or concrete to name just some) have all very well defined and marked structural behaviors against either force type, but it is rare to find composites that perform well under both types of forces or stresses. Despite some significant advances in 3DP-related material sciences (*Klein, et al., 2015*) it is still too costly to use composites or bio composites as reliable 3D printable materials. This fact is taken as a starting point for the material characterization and the discrimination between bars of one type or another, since they will portray the response or reaction of the material to its specific loads.

Table 4 shows compressive and tensile strengths of some common 3D printable materials, besides concrete and steel, which are displayed for reference. As explained in section 4.4.3. concrete, although not widely adopted, is becoming a relevant material for 3D printing *(Lim, Buswell, Austin, Gibb, & Thorpe, 2012; Buswell R. , Soar, Gibb, & Thorpe, 2007*). In table 4, the fields PLA and ABS marked as Makerbot display values obtained for printed pieces under different conditions, and similar mechanical properties to compressive, tensile, and flexural stresses to those of standard PLA or ABS test parts *(Makerbot Industries, Ltd., 2014*). These values can be used as reference for dimensioning the infill patterns result of the calculation.

Table 4. Mechanical properties of some printable materials

	STANDARD		MAXIMUM	
	YIELD STRENGTH (N/mm2)			
Material	Compression	Tensile	Compression	Tensile
PLA (Makerbot)	17,91	46,73	93,70	65,67
ABS (Makerbot)	7,58	34,01	48,92	38,12
PLA (Standard)	N/A	50	65	70
ABS (Standard)	46,54		120	
Concrete H25	24,52	0,29		
Clay	Variable	N/A	Variable	N/A
Ceramics	Variable	N/A	Variable	N/A
Steel S275 (reference)	275	275		

It is also crucial to point out another relevant consideration in the development of the algorithm: the internal and external loads applied during the stress calculation. Since the application calculates the optimized infill pattern and the parts are usually self-standing, non-bearing elements, the springs respond only to gravity and the own weight of the object itself. No other forces –except those from horizontal agents- are taken into account, although a variety of different forces may well be implemented, including –but not limited to- punctual forces or field-like forces. Furthermore, the software subject of the present chapter starts from the premise that no printable concrete has been developed yet that complies with the highly restrictive regulations that apply to structural concrete in the region of Spain, where this algorithm is being initially tested [EHE-08 *(Ministerio de Fomento (Spanish Ministry of Public Works), 2008*) and the thereby implied UNE, UNE-EN, UNE-ISO].

Commercial structural calculation software packages work in the same manner, this is, describing the building geometry as a finite element model which discretizes bars according to a certain structural behavior of both constructive elements –such as beams or columns-, and materials –concrete, steel-. Since relevant work is currently being carried out in this direction, it is planned to improve and expand the user control on the force definitions that might apply to the models, following the logic of some above mentioned standard CAD packages and others alike.

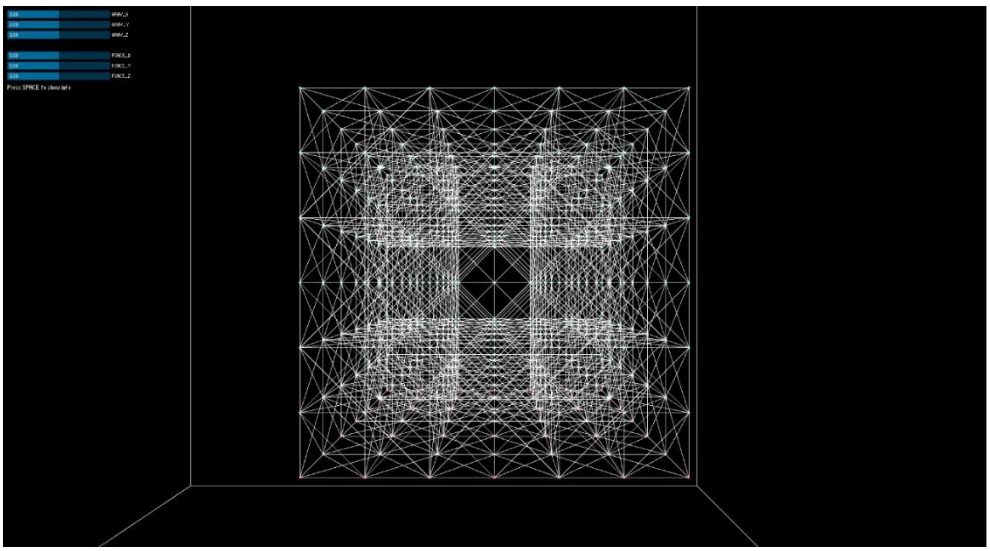

Fig 8. Simple cube-like geometry imported in calculation software. No stress displayed as no forces are present.

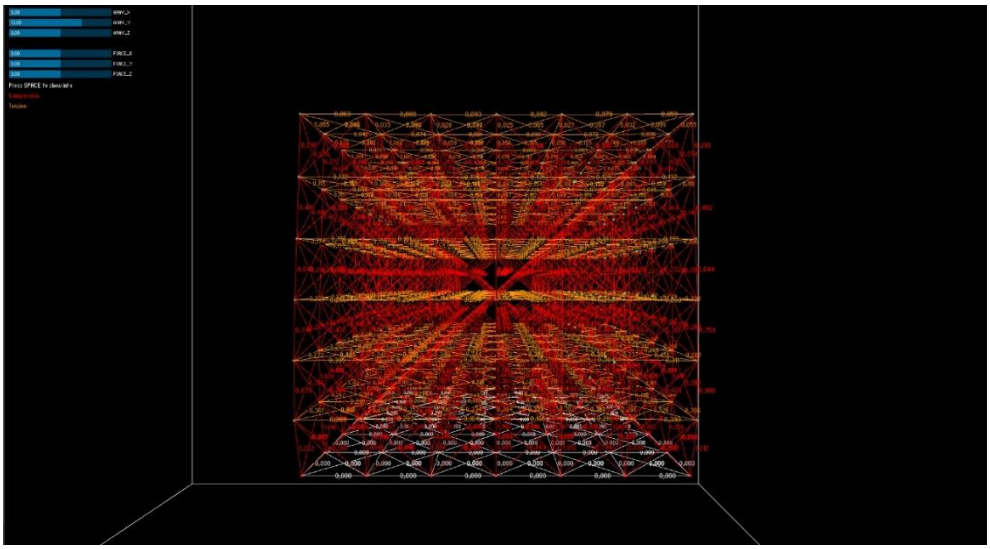

Fig 9. Simple cube-like geometry imported in calculation software displaying elongations and force types accordingly.

These bars can be further processed in order for them to be properly sized and dimensioned according to the mechanical properties of the materials shown in Table 4 –the most commonly used 3D printable materials, or simply defined by the user while characterizing the material during the process. In our case, the software needs to deal not only with a certain load pre-condition, but also with material deformations which result in changes or modifications to the original geometry. The algorithm, thus, shows not only the original geometry and the deformed geometry, but also the optimized material state to be used for the infill patterning.

Indeed, the present study seeks to blur the boundaries between traditionally separated building parts: walls, foundations, columns, beams, slabs, and other constructive elements were differentiated not only because of their structural or architectural function, but also because of the way traditional construction is planned. In fact, 3D printing optimized structural patterns could put an end to these questions and produce a refined account with regards to the synergetic relationship between performance and material integrity, one that can ultimately blend the physical experiments that classify form according to load applications and the digital realm where these may be simulated and studied prior to the designer's decision making.

Figures 8 through 11 show the import process and elongations in two different pieces. Red lines depict compressed bars while yellow ones represent elongated elements. Figure 9 displays a cube-like model subject to a slight left-to-right horizontal force as seen in the controls located in the upper-left corner. Figure 11 shows the stress state for a self-bearing structural condition of a complex part. The stresses displayed correspond to a material performance in a default tensile and compressive behavior.

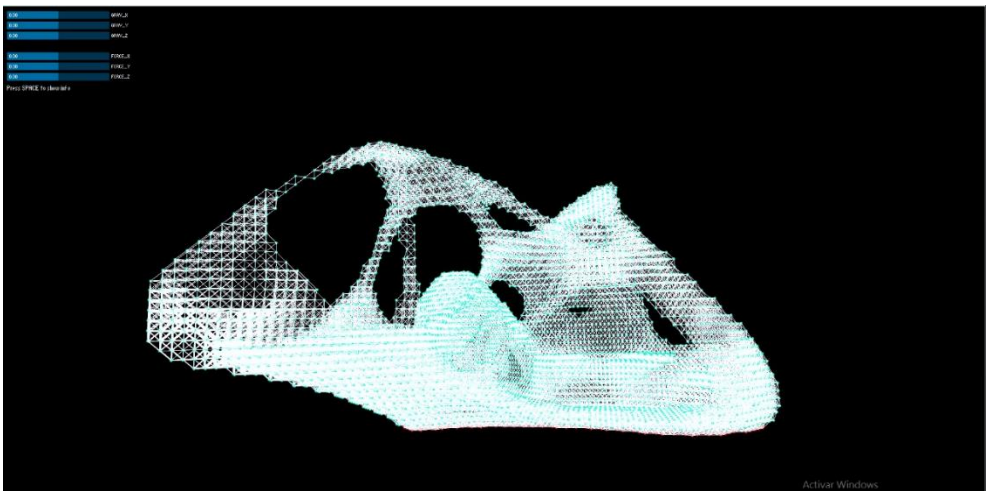

Fig 10. Complex test geometry imported in calculation software. No stress displayed as no forces are present.

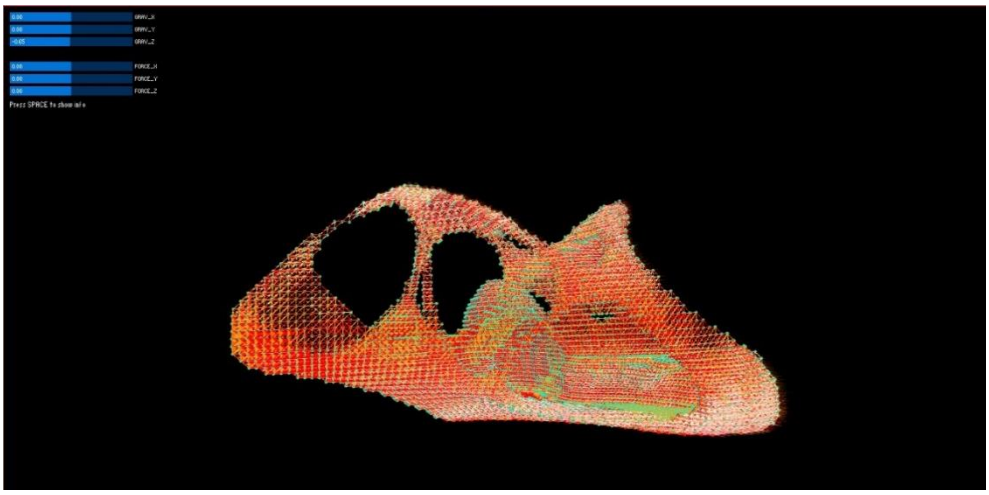

Fig 11. Complex test geometry imported in calculation software.

6.6. Creation of the fill pattern following the spring deformation results. Dimensioning.

Finally, the software comes to an equilibrium state where all springs have all a well determined stress. This stress responds to a certain spring elongation, as well as to the relationship between the different interconnected nodes. The equation used to calculate the force load under which one bar element works responds to Hooke's Law, as mentioned in previous section. This physical equation brings together material deformation and a corresponding force according to the following equation:

$$F_{axis} = -k \cdot \delta_{axis} = -k \cdot \delta_x \quad (1)$$

Where δ_{axis} is the axial elongation of the material, and F the normal component of the force applied onto a section perpendicular to the bar. k is a constant that describes the behavior of each material.

Once the axial force is known, a simple formula can be used to calculate actual material thickness, which is in turn employed to calculate the final geometry. Each bar responds to the formulas displayed below, largely applied for the sizing or dimensioning of reinforced concrete or simple concrete structures. As it has been explained above, bars are characterized in a previous state of the algorithm as either compressive or tensile. The dimensioning of the different elements makes use of the following equations:

$$\sigma_{axis} = \sigma_x = \frac{F}{A} = \frac{N}{A} = k \quad \tau_{xy} = 0 \tag{2}$$

$$\sigma_y = 0 \qquad \tau_{yz} = 0 \tag{3}$$

$$\sigma_z = 0 \qquad \tau_{zx} = 0 \tag{4}$$

Where N or F is the stress in N, and A the area of the section of the bar perpendicular to its longitudinal axis (see Figure 12) measured in mm2. As shown in Table 4, materials have different behaviors to tensile and compressive stresses, thus yielding different section areas or dimensions under diverse force types. Bars are assumed and designed in the software to be cylindrical, therefore having the same Modulus of Inertia in every single direction. Figure 13 shows the components of the stress state in a cylindrical bar both on a perpendicular and on an inclined plane.

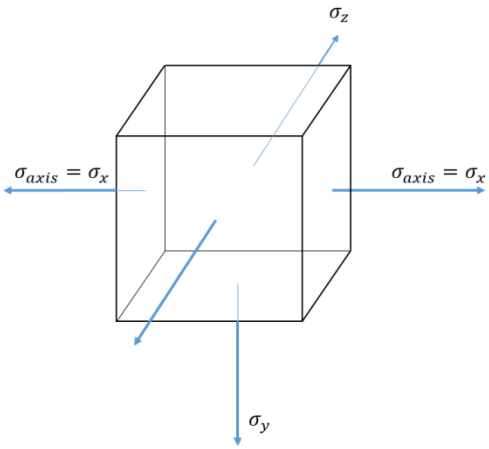

Fig 12. Components of the stress state in a bar subject to pure tension or compression stress

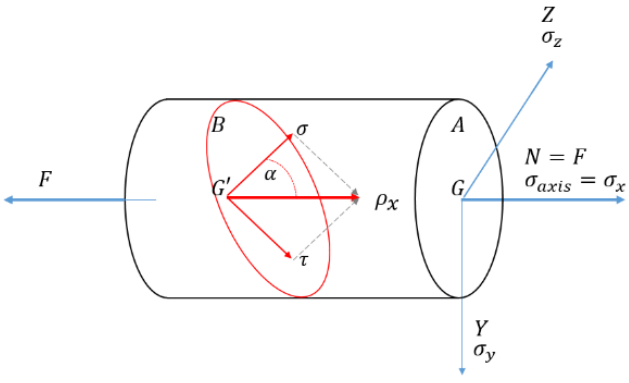

Fig 13. Components of the stress state in a bar subject to mixed tension and compression stress.

This formula is safe both for concrete and steel computations, and might be valid as well for composite materials, as long as they are sufficiently proven to work homogeneously. The stress in the inclined bars is calculated according to:

$$\begin{bmatrix}\rho_x\\ \rho_y\\ \rho_z\end{bmatrix} = \begin{bmatrix}\sigma_x & 0 & 0\\ 0 & 0 & 0\\ 0 & 0 & 0\end{bmatrix} \cdot \begin{bmatrix}\cos\alpha\\ \sin\alpha\\ 0\end{bmatrix} \xrightarrow{yields} \begin{matrix}\rho_x = \sigma_x \cdot \cos\alpha\\ \rho_y = 0\\ \rho_z = 0\end{matrix} \quad (5)$$

Whereby normal and transversal stresses are defined by:

$$\sigma = \vec{\rho} \cdot \vec{\mu} = \sigma_x \cdot (\cos\alpha)^2 \quad (6)$$

$$\tau = \sqrt{\rho^2 - \sigma^2} = \sigma_x \cdot \cos\alpha \cdot \sin\alpha \quad (7)$$

6.7. Further work: stress-following agents and load visualization.

As a final feature the software includes the option to display a visualization of the paths the forces follow in order for the part to reach its optimized state of equilibrium. Although this particular feature offers relevant structural information, it is a key informative tool when redesigning or understanding the topological behavior of the forces applied to the part and how these forces "travel" through the part.

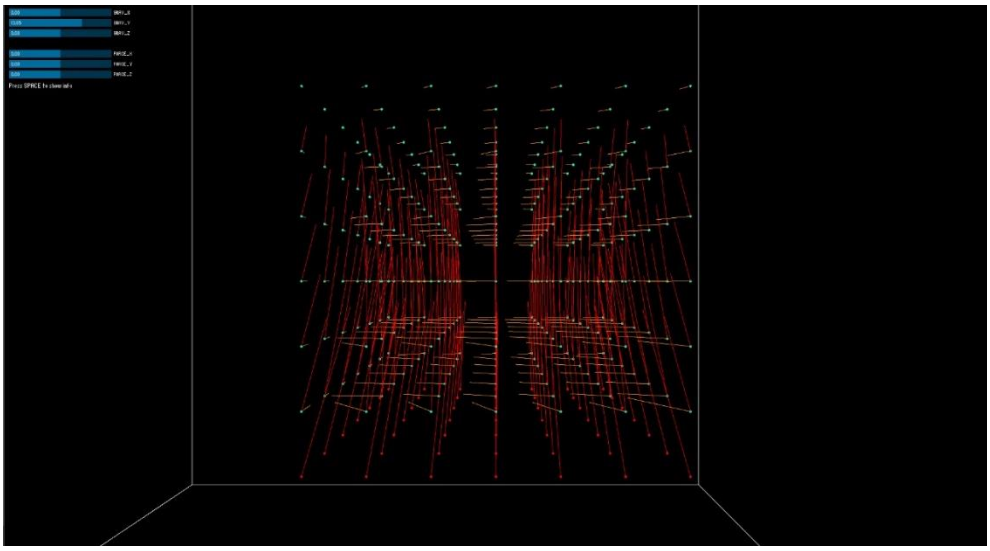

Fig 14. Resulting forces at nodes for a simple geometry

This is achieved by a load-sensitive agent system, whereby agents are created that re able to read and respond to either compression or tensile stresses. In order to optimize the calculation time, the virtual space occupied by the part is divided into a series of voxels –one per particle. The agents, called tracers, read the resulting force in each voxel and use it to define their velocity vector at each frame of the simulation. Furthermore, the agents create trails that depict their subsequent locations throughout the simulation. This way, it is possible to clearly visualize the behavior of the whole part.

Figure 14 shows the resulting forces at each node in a simple geometrical example, while figure 15 displays the current state of development of the agent system. Yellow lines in figure 15 depict the paths of the forces in a cube-like point distribution that responds to the force and conditions described for figure 9. Further work is being performed on this particular subject to incorporate more complex geometries.

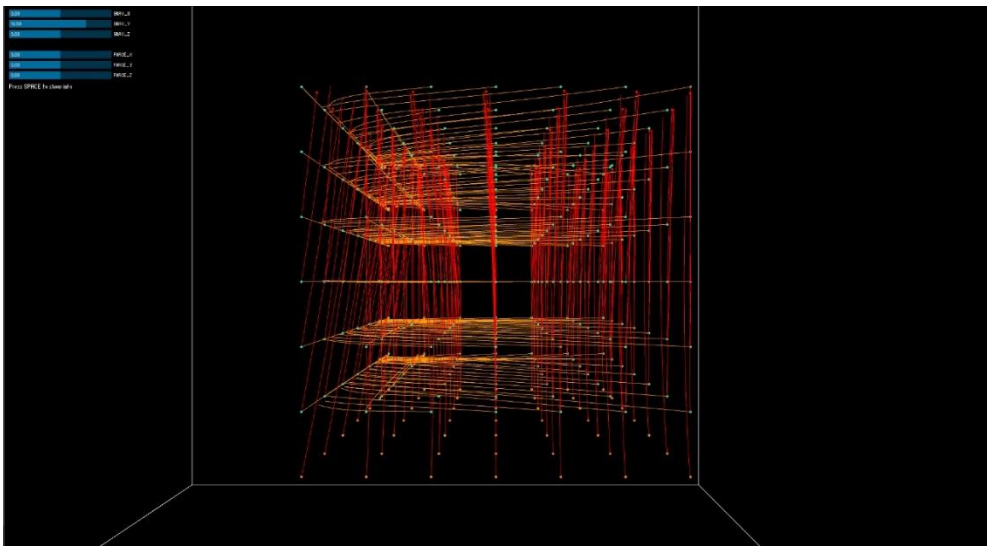

Fig 15. Traveling agents showing compression and tensile stresses

6.8. Results

The present work tackles the combination of two increasingly important issues related to techniques and materials: (i) minimal material usage and the (ii) optimization of the structural behavior of printed parts.

The algorithm hereby presented creates an infill patterning system that aims at saving time and reducing expenses when printing large-scale objects, a crucial factor for serial production. Aside the multiple advantages of such an approach, the algorithm offers significant information in design time, allowing designers and fabricators to make informed decisions while outlining their parts or prototypes. Furthermore, the algorithmic logic hereby explained seeks to provide a structural approach to infill patterning, an issue that has not yet been properly dealt with. This functionality could eventually bring 3DP one step further by implementing structural regulations or particular industrial conditions into the fabrication workflow, allowing for a seamless integration of 3D technology within the regular operation apparatus.

Table 5 shows the initial results of the affection on material consumption of different patterning systems (hexagonal, square, spiral, and algorithm) sorted according to the following parameters: (i) specimen types, (ii) extruder diameter, and (iii) infill density.

Table 5. Initial test results of patterning system according to specimen types and showing material use.

SPECIMEN 1: Cube 3x3x3 cm							
Extruder Ø (mm)		0,4			0,3		
Infill density		25	75	100	25	75	100
Pat. type		Hexagonal pattern					
Mat. use	length (m)	111	333	445	197	593	791
	Volume (10^{-3} m^3)	55	167	223	55	167	223
Pat. Type		Square pattern					
Mat. use	length (m)	227	682	909	404	1212	1617
	Volume (10^{-3} m^3)	114	342	457	114	342	457
Pat. Type		Spiral pattern					
Mat. use	length (m)	107	322	432	190	572	769
	Volume (10^{-3} m^3)	54	162	217	54	162	217

Pat. Type		Algorithm test					
Infill density		4	1	0,5	4	1	0,5
Mat. Use	length (m)	21	337	1348	1	337	1348
	Volume (10^{-3} m³)	10	169	677	5	95	381
SPECIMEN 2: Cylinder radius 1.5 x 3 height							
Extruder Ø (mm)		0,4			0,3		
Infill density		25	75	100	25	75	100
Pat. Type		Hexagonal pattern					
Mat. Use	length (m)	84	254	339	150	452	603
	Volume (10^{-3} m³)	42	128	170	42	128	170
Pat. Type		Square pattern					
Mat. Use	length (m)	176	529	705	313	940	1254
	Volume (10^{-3} m³)	88	266	354	88	266	354
Pat. Type		Spiral pattern					
Mat. Use	length (m)	127	254	339	156	467	622
	Volume (10^{-3} m³)	64	128	171	44	132	176
Pat. Type		Algorithm test					
Infill density		4	1	0,5	4	1	0,5
Mat. Use	length (m)	16	259	1038	16	259	1038
	Volume (10^{-3} m³)	81	130	522	4	73	293
SPECIMEN 3: Double-curved surface							
Extruder Ø (mm)		0,4			0,3		
Infill density		25	75	100	25	75	100
Pat. type		Hexagonal pattern					
Mat. use	length (m)	88	264	352	156	470	626
	Volume (10^{-3} m³)	44	132	177	44	132	177
Pat. type		Square pattern					
Mat. use	length (m)	177	533	711	316	948	1264
	Volume (10^{-3} m³)	89	268	357	89	268	357
Pat. type		Spiral pattern					
Mat. use	length (m)	86	257	346	152	458	615
	Volume (10^{-3} m³)	43	129	174	43	129	174
Pat. type		Algorithm test					
Infill density		4	1	0,5	4	1	0,5
Mat. Use	length (m)	68	273	1092	68	273	1092
	Volume (10^{-3} m³)	34	137	548	19	77	308

All results displayed in the thesis are software-based, and require further empirical studies involving specific electronics and hardware parts, which are out of the scope of the present study. Despite this fact, initial tests –see Table 5- show that material can be optimized up to a 50% when compared to the afore mentioned space-packing algorithms for infill generation. It is also important to note that the latter provide no structural logic to the system, and are a mere "scaffolding" onto which the parts are printed. This material optimization does not depend on hardware design or end effectors, but rather on a software

level. Table 5 shows results of material usage according to different patterning systems, test parts, and nominal extruder radii. Undesired cases are highlighted.

As shown in Table 5, from all space-packing logics, the spiral patterning surpasses both the square and the hexagonal ones, as the former has a lower form factor than the latter two. In other words, the spiral is closest to a circle shape than squares or hexagons.

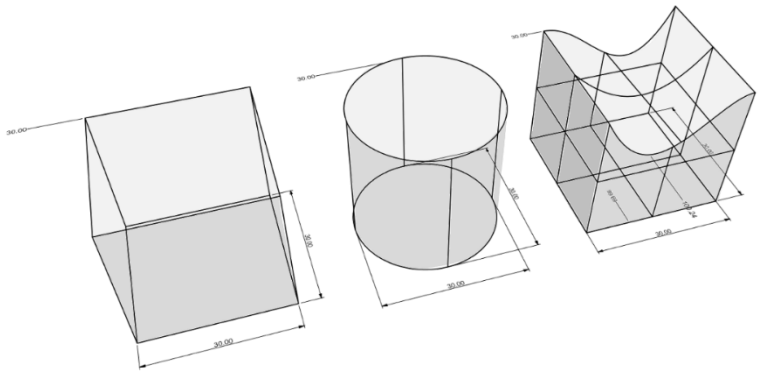

Fig 16. Design and definition of initial test specimens

All pieces have been simulated with a layer height of 0.15mm, and a single shell reinforcement, which is ignored in the infill calculation for all cases. Material is measured in length and volume, as the first is relevant for printing time, whereas the second indicates the actual amount of material required for building the part. Please note that material volume depends both on the infill density and the nominal extruder radius, and is independent from the actual length of the printer's path. As shown above, 3 parts or specimens are tested: (i) a 30mm x 30mm x 30 mm cube; (ii) a 15mm radius and 30 mm high cylinder; (iii) and a double-curved surface.

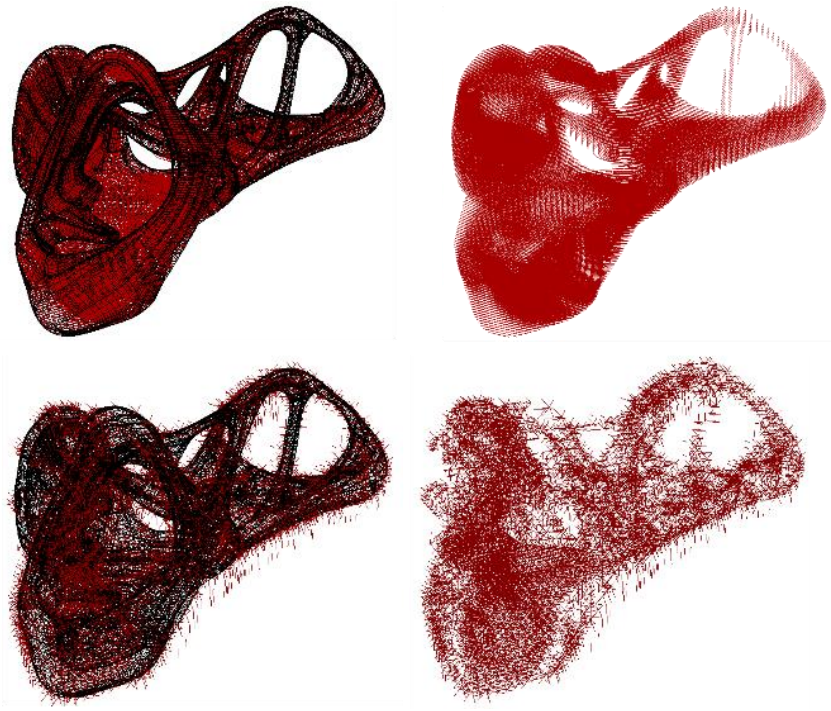

Fig 17. 3D view of complex part design result: spiral pattern (above) and optimized infill pattern (below)

The algorithm is tested against 3 different infill patterns: squared, hexagonal, and spiral-like, the last being the most challenging because of its efficiency. All parts yield similar results: the algorithm can save up to 72% of both material and printing time for similar infill densities when examining 2mm-sided

square units to their algorithm-generated counterparts considering the same extruder radius for all bars – see total material length. Material savings can potentially become higher with accurate printer nozzles or the possibility to implement variable-flux printing technologies which might take variable bar radii into account. Most prominent results are obtained in specimen 1, which requires 21 meters of extruded material when using an algorithm-design pattern, whereas the minimum hexagonal distribution yields 111 meters – savings of approximately 82%. Specimen 2 requires only 16 meters of material using the algorithm, and 84 using standard hexagonal patterns, which mean savings of –savings of circa 80%. Finally, specimen 3 shows a 68 to 88 ratio, or savings up to 22%. As can be seen, these significant material and time savings vary much between specimens, so further research in needed.

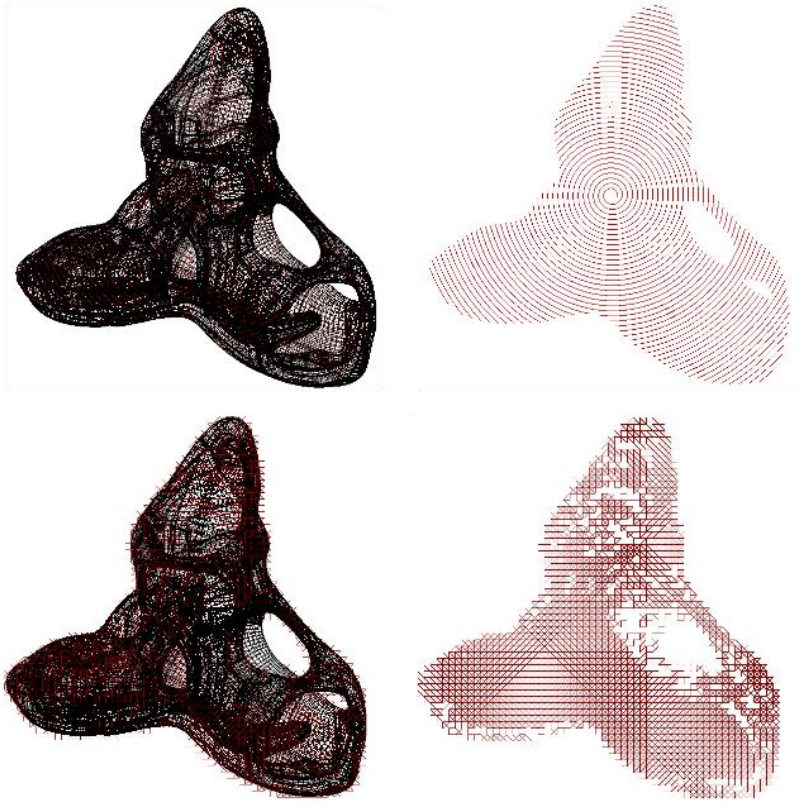

Fig 18. Plan view of complex part design result: spiral pattern (above) and optimized infill pattern (below)

Initial results of complex part design analysis are promising as well. Figures 17 and 18 display a comparison between the spiral pattern and the optimized one for the complex part shown in figures 10 and 11, although more parts should be tested for more comprehensive data analysis. These figures depict the different infill densities obtained by traditional and optimized means. For this particular piece, 24109 mm of printing material is needed for the non-optimized, spiral-like pattern, while 12784 mm are needed for the algorithm-generated one.

In addition to this new functionality, parts could be calculated not only to be self-bearing, but to become structural elements within a larger system, whether for the automotive, aero spatial, or construction industries. Finally, the study intends to depict a modular system that might eventually be implemented in a variety of software packages, thus allowing for a patterning standard that could replace the most currently used infill patterns, which are shown for comparison reasons.

Chapter 7

Conclusions and future work

This chapter summarizes and validates the thesis as a whole, while responding to the issues and opportunities found in the research on the state-of-the-art 3D printing technologies. Moreover, it proves the methodological focus while attending to the need for a critical discussion of the importance of such technologies for the AEC sector.

7.1. Conclusions

Chapter 2 depicts intensively a technological frame within which digitalization acquires importance as a general and transversal concept, whereby 3D printing is considered a disruptive tool that comes to distress the digital fabrication market as such.

Although much has been done in the field, additive fabrication for construction remains a technology yet to be explored. Its capacity to influence current methodological workflows offers a wide range of possibilities, both from a procedural point of view as well as from its potential to redefine the practice from within. Its positive effect on the environmental impact of the construction sector is able to reshape material sustainability at all levels. From the different options available at the market, it is additive manufacturing with robotics the most versatile and scalabe by far, which is methodically explained in Chapter 2. Furthermore, robotics applied to architecture is also an unmapped field of research with a bright future ahead.

The thesis has presented an integrative framework for a unified design-to-production process based on the study of their mutual relationships within the context of an economically and materially feasible business model to be applied to actual industrial needs and requirements. Chapter 4 explains the automation of the fabrication process through a ground-breaking integration seeking to unite all diferent processes and fabrication processes into a single, user-driven workflow. Defects in the current process workflow is analyzed in chapters 2 and 4, whereby an integrated solution is proposed. This integration is realized both theoretically and through a Rhinoceros-based add-on consisting of a series of translators and modules. The software package, used as technological demonstrator, exceeds current solutions in different aspects: first, it is more easily adapted within the host's program UI; second, it is easier to use; third, it is more informative than existing software; fourth, it is extremely user-friendly even for the most unexperienced users.

Furthermore, the process presented in the workflow has been validated with a variety of ABB manipulators and controllers, as well as with a single KUKA. These successful instantiations attest the interoperability between the design-oriented software tools, their management as 3D virtual models, and their suitability to fit and stand out at physical construction processes. The interoperability is enhanced

through a system similar to that of IFC in the construction industry. In other words, an xml-based file standard is proposed as to homogenize the 3D printing process with different robot firms. Finally, an algorithm is presented in Chapter 6 that outsmarts current space-packing infill algorithms by implementing the structural logic and a load analysis of the parts. Annex I deals specifically with this issue showing that, despite the relevance of providing improved materials, specific printing setups have a major impact on the structural behavior of printed parts, which is far from being isotropic and homogeneous. As a result, the combined performance of software, hardware, and materials outdoes that of both standard and professional 3D printers, especially in what concerns to printing speed, printable volume, finish quality, and versatility. These results are shown in Chapters 4, 6, and Annex I.

Moreover, a series of advantages and key aspects are exposed in relation to construction and sustainability. These advantages, although not the main focus of the thesis, stay a side-effect of the potential inherent to the proposed 3D printed method and apparatus within the building or construction sector. These advantages account for an improved waste management and control, "wasteless" production, and the thereby related minimization of carbon footprint during operation. Furthermore, the technology proves beneficial at an economic level, thanks to the reduction of operation costs, time optimization, and decreased energy footprint. At a social level, implementing these methods would arguably have a valuable impact on the construction agents and crafts themselves, representing an opportunity for the further requalification of construction labor and workforce.

In summary, the thesis has demonstrated that an innovative approach towards real scale 3D printing processes as fabrication methods is not only possible, but desirable. As stated in Chapter 3, there are significant implications of these innovative, integrative approaches for real-scale objects and industrial applications, such as:

- Propose critical thoughts and definitions of a new architectural and construction paradigm, as well as their implications for the construction sector, as explained in chapter 3. This paradigm benefits from the ability to use robots on-site as prefabrication tools.
- The development of a system that responds to the lessons learnt from the case studies and includes the critical aspects of the construction sector while combining both into a single, compelling methodology:
    - The definition of an integrated AM method for construction towards the standardization of 3D printing construction processes combining both on-site prefabrication and assembly.
    - The development of a technological demonstrator that implements a software-hardware integration showcasing the mentioned examples of integration. This is achieved through:
        - The outline of a file format standard for interoperability purposes.
        - The software integration, accomplished by a Rhinceros add-on and proved in several robot systems and hardware.
- The smart use of geometry and the optimization of material together with the subsequent positive impact on systemic environmental issues through the automated design of structural infill patterns. This system enables parts to be, for the first time, calculated according to actual stresses and loads.
    - The proposed patterning calculation system increases the functionality of current space-packing patterns, both at qualitative and quantitative levels through an optimization algorithm:
        - Qualitatively, since it offers a first-time conceptual development.
        - Quantitatively, as it proves to reduce material consumption in a range between 22% and 80%, depending on the complexity of the geometry and loads.
- Opportunities for material sustainability that implies a significant reduction of the environmental impact of large-scale fabrication procedures:

- The use of local materials and derived energy savings
- The development of new materials, composites, and bio-materials
- The use of local, renewable energy sources.

7.2. Future work

Despite the contributions of the work, 3D printing for large scale objects remains an interesting subject for further exploration. The employment of organic and recycled materials for non-structural building elements acquires an unprecedented magnitude as a result of their ease of use. Although this tendency first materialized about two decades ago, the static regulatory framework impeded its real application on buildings relevant to the market, remaining of minor or marginal use. 3D printing for construction opens up a new set of possibilities and constitutes a disruptive technology highly regarded by all agents involved in the construction development process. Organic materials, as opposed to their traditional counterparts, can be easily obtained from their raw state, and are easily reusable and recyclable. This unveils a great potential regarding the energetic exploitation of non-recyclable materials and the reuse of materials following a "Cradle to Cradle" approach.

Following this strand of logic, chapter 6 deals with the use of composite materials, widely used for printing purposes at all scales and present in a variety of forms and technologies, especially FDM. As it is shown throughout the chapter, material performance has only a limited impact on the structural behavior of parts, which is far more dependent on the printing setup and quality itself. In this sense, the printing method is more relevant to the matter as a whole.

The use of recycled or simple non-standard materials in real-scaled 3D printed objects is still being cut off by the restrictive regulatory norms that apply to both construction and structural elements in the AEC sectors in most developed countries –where these technologies are currently being developed and tested. Regardless of the potential of 3D printing in this specific sectors, its development will continue to be slowed down by the impossibility of a real industrial implementation in many markets worldwide. As a consequence, the collaboration with official quality and certification agencies is a must, thus allowing for the emergence of new public and private collaboration paradigms. Moreover, it will become necessary to design new, more appropriate tests in order to correctly prove the structural behavior of parts, since printing operations have a relevant affection as shown in Chapter 6.

The re-qualification of labor force could account for a significant reduction of human errors in the course of on-site building operations. Due to process automation and the mechanization of non-critical, though hazardous or unsafe processes, more than 80% of defects in housing construction, for instance, could be prevented. As a consequence, risk management and safety on site would be positively affected.

The use of robots on site eases the access to local, renewable energy sources. Two main possibilities for fabrication with robotic arms are discussed –see Chapter 4: on-site and delocalized fabrication. Although delocalized fabrication in specialized warehouses is normally preferred for quality control issues, it is shown that on-site fabrication has a number of advantages worthwhile mentioning. On the one hand, it allows for a quick and easy response to every-day problems, since robotic arms are flexible and versatile enough as to be able to be programmed to accommodate any need. On the other hand, pre-fabricating parts on-site eliminates any need for the transportation of machinery, heavy parts, or any other gear that these would imply when fabricated in a different location. As a consequence, the use of on-site prefabrication reduces or eradicates transportation costs and their derived environmental impacts. 3D printing for construction, as proven in the thesis, has the ability to reclaim the use of essentially natural materials, which require minimum transformation and transportation, as they come from nearby locations.

As a consequence of the above, the construction of on-site prefabricated parts with large-scale 3D printing technologies constitutes, despite the numerous challenges still to be faced, an unique and unmatched technological revolution within the digitalization of the architectural practice and the construction related-sectors altogether. Probably, the most relevant factor for 3D printing to become democratized is the inclusion of the fabrication procedures in the design cycle, thanks to the development of tools that allow for the integration of both processes into a single, continuous, iterative workflow. In addition to that, 3D printing's intrinsic ability to shift the current material sustainability model will benefit

the AEC market at a wide variety of levels. The above mentioned reduction in material usage, transportation costs, or the use of local and renewable materials will indeed reduce the energy and carbon footprint both during construction and over the lifecycle of buildings.

Real scale 3D printing is an unprecedented opportunity. The exponential growth of this technology points at a radical change in the architectural and construction sectors, although it is impossible to project a reliable scenario as to how fast this change will be, especially due to the more than predictable massive use of robotics and artificial intelligence in the near future.

Future work will focus on varios aspects related to the thesis' subject. In summary, there is development to be be done in the realm of software, hardware, and materials. It is the intention of the author to increase the TRL of the technology as much as possible (current readiness level is estimated to be 5, as it has proved to work properly under controlled conditions in the laboratory), in order to enter the industry through H2020 calls or similar potential funding possibilities. The forthcoming work is thus organized under the three categories (software, hardware, and materials) mentioned above, which are listed according to timelining priorities:

- Improving software to achieve higher control:
    - Extend current robot library and contact robot vendors for better interaction.
    - Enhance automatic module creation engine for higher optimization of small or simple parts.
    - Program automatic material support creation for complex parts and visualization in CAD software for enhanced control prior to fabrication.
    - Implement up to 36 axes to be atomatically operated by the software, since this amount is the maximum that can be controlled by the IRC5 robot controller.
    - Allow users to either create or upload non-standard or customized tools in visualization.
    - Improve exchange file standard format and standardization.
    - Upload to a github platform or similar the standardization procedures in order to comply with the OSAT philosophy.
- Increasing hardware control:
    - Testing, besides ABB and KUKA robots, Fanuc and Universal Robots in order to expand the functionality of the whole system. ABB and KUKA robots have been successfully tested.
    - Improving printing bed to achieve a planarity of ± 0.1 mm on a 2000 x 2000 mm surface. Contacts with specialty equipment companies has begun.
    - Including the smart sensorization and centralized control of robot and tool status.
- Enhancing sustainability-related issues through opportunities emerging from material usage and development:
    - The improvement and further testing of the material optimization algorithm in order to systematically study and parameterize its benefits and to better measure its results.
    - The formulation of an orderly, systematic methodology to analyze material test follow-ups of printed specimens and parts.
    - The better integration of the material optimization algorithm within the printing software or host CAD platform.
    - The development of 100% structurally sound, reliable, regulation-compliant, printable concrete.
    - The inclusion of a fiber-mixing technology in a special printing nozzle.

- The development of a quantification and measurement device and system to control actual savings.
- The use of local materials in-situ.
- The development of renewable, recyclable, reusable materials suitable for printing in order to minimize material waste.
- The development of printing methods and apparatus for bio-materials and composites for the healthcare industry as a side activity.

At an industrial level, it is crucial to enhance the technology readiness level to a TRL 6-8 in an attempt to enter the automotive and construction markets through H2020 or similar calls. This work has begun through the co-foundation of XcaLe3D, an UK-based company aiming at providing real-scale printing solutions. The company has begun collaboration with The Welding Institute for H2020 and Innovate UK proposals.

Annex I

Test development. Process and improvements

Annex I summarizes the efforts and steps taken in the development of the method and apparatus essential to the thesis and thoroughly presented throughout. Advancements in printed parts are explained by means of a series of tests and attempts that physically display the otherwise considerably abstract state of development of both hardware and software layers of the thesis demonstration project. As introduced previously, the material environment and technology chosen for these mock-ups is plastic. Both PLA and ABS are employed for the most fundamental demonstrations purposes.

This annex shows a series of parts explaining their flaws, imprecisions and other issues result of the faulty fabrication process in a summarized yet streamlined manner. These parts, organized in chronological order, intend to illustrate defects in the scope and maturity of the project itself as to critically improve its value. Each part is analyzed to demonstrate further improvement needs and to highlight qualities and the progress made during the elaboration of the technological demonstrator.

The current scenario is considered to be equivalent to a pre-industrial minimum viable product (MVP) at all levels.

8.1. Process

The process obeys a stage-like structure outlined according to a series of deliverables and goals defined following a pre-defined, yet flexible structure. The chapter covers only the main stages of the process.

8.1.1. Stage 1: definition of part requisites and first printing attempts.

This first stage relates to tests executed in order to establish material needs and to calibrate the robot as to adapt its speed to the material needs. Print programs are created directly in RAPID using either RobotStudio or the FlexPendant. An ABB IRB120 was used for the calibration. The instructions used for the movement are not automated and follow all the same code pattern:

MoveL Offs(robotTarget, x,y,z),vV,zZ,tool;

As seen in the code above, the variables needed to define a movement operation are:

- The robot target (variable "*robotTarget*"), used as origin for the calculations. This target is normally a point on the object or its centroid. x, y, and z are the actual point coordinates.
- Travel speed (vV). Measured in mm/s, robot TCP speed normally oscillates between 50 to 70 mm/s for standard desktop prints and 100 up to 300 mm/s in robotic printing. Nevertheless, models printed at this stage were fabricated at 100 mm/s to try to shrink the amount of variables to be studied and focus on geometry. No material flow control or stream estimate was calculated, as the focus was essentially put on the combination between layer height and zone precision.
- Layer height defines the finish quality and material continuity throughout the part. First attempts ranged from 0.1 to 0.2 mm. Figure 1 depicts a part made with a single shell using 0.15mm high layers.
- Zone precision (zZ) is essential to the actual part outline and its correct geometrical definition. Zones in robots are defined as spheres around the toolpath points. These zones, without further explanation, define substantial parameters affecting part properties and the actual volume within which the robot begins to move towards the next point in the program. In other words, each point is assigned a precision zone, which in turn defines a sphere of a certain radius, a sort of bounding volume around the toolpath point. When the robot tool plane enters the zone, it begins moving towards the following location or robot target in the code. This means that, if the zones are not correctly defined, the points will never be reached and the geometry will fail. Furthermore, the toolpath interpolation within the sphere's volume is completely and absolutely defined by internal algorithms in the robot's controller, making it a challenging task for the user or programmer to control this movement.

  As a general rule, defining the smallest possible value for zones is recommended for 3D printing linear toolpaths. Nonetheless, over-constraining precision might have negative effects on the prints, since trying to force the robot to exactly reach the defined toolpath robot targets causes the robot to stop exactly at the point's position, which can result in material overload. It was found appropriate to use "*zone 0*" instead of "*fine*" for every point in the toolpath except for the last ones –where the toolpath increases its height to commence another layer.
- Tool. The extruder defined according to the robot variables: size, weight, and inertia.

First tests were 50mm x 50mm x 50mm in size. These controlled volume allows to calibrate the above mentioned variables alongside the extrusion speed. As said earlier, it was decided to fix the extrusion speed by setting the motor to 60 rotations per minute. This allows to better control the variables related to movement and geometry. The part revealed the following issues:

- Incorrect layer height. These attempts accounted for a height of 0.2mm, which turned out a clearly too high value for the amount of material extruded and the TCP speed. Thus, the diameter of the resulting filament was too less as to ensure the expected material continuity - parts suffer from layer detachment.
- Inapt printing bed issues. The first trials were completed directly on the IRB120 bed or on a flexible extruded polystyrene foam (XPS) bed. Both displayed improper conditions as printing beds due to either their inaccurate planarity –in both cases-, or their rugous finish –in the case of the XPS bed. The foam bed allowed for a more compelling and thoughtful study of the height required for the first layer without calibration or extruder collision problems. Nonetheless, XPS –as many other foam-like materials, does not withstand high temperatures –such as those reached by the hot end-, causing uneven surfacing conditions during the test as the hot end approximated the bed surface. The effects of this particular issue are clearly visible and can easily be identified as wavy traces at the beginning or bottom of the finished part – see Figures 1 and 2. Further try outs intended to amend this issue, as a proper base fixing condition is essential to the correct finish of the part.

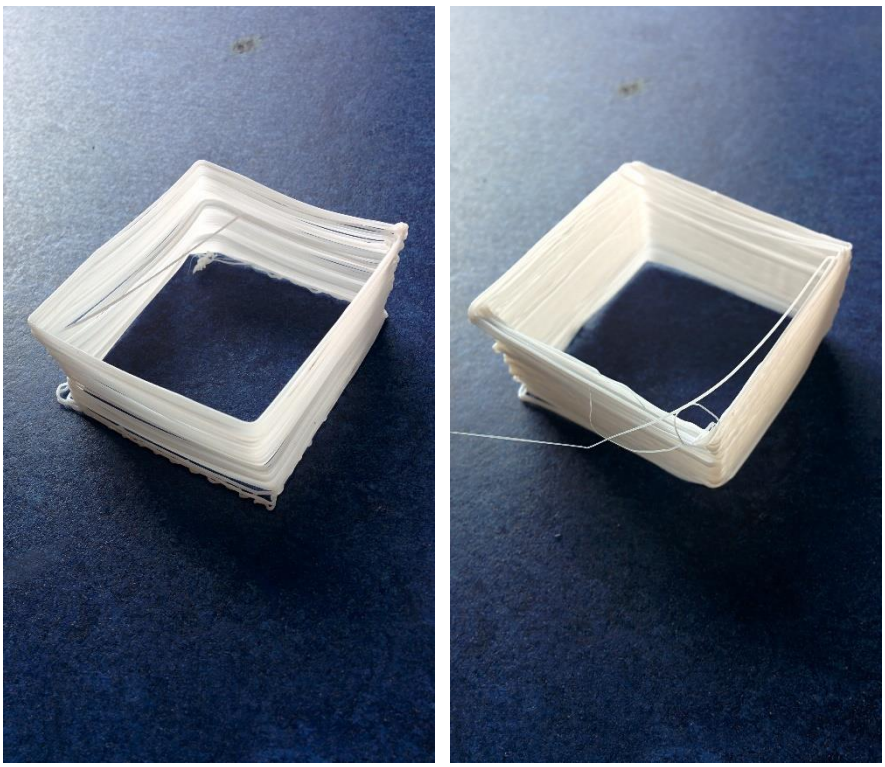

Fig. 1 and 2. First and second extruded pieces showing their numerous flaws: corner design, excessive layer height, faulty base placement, and incorrect finish.

- Lack of control over the inputs in the code controlling the extruder and hot end. Motor, extruder, fan, and thermistor sensor were controlled by external software through an Arduino and RAMPS board through the external open-source printing software Repetier-Host. The impossibility of coordinating robot movement and extruder during the actual extrusion process made it clear that a different approach was needed. Extrusion was continuous at this point and robot programs and routines did not yet implement any sort of digital input and output control (such as the initialization of the extruder).
- Defective tool design and fabrication. Version 1 of the extruder was burdened by a number of relatively prominent problems. Its numerous flaws included:
    - An undesired TPC's Z axis orientation which practically impedes the movement of the 5th robot axis.
    - An improper size caused by the necessity of mounting and dismounting the tool in an accessible way. This fact causes the tool to span excessively and become literally a flexible part. This lack of rigidity triggered undesired tool movements in each change of direction and concave parts, causing again a wavy effect in each position. This undesirable condition can distinctly be appreciated in the test pieces, where all sides had 90º angles, yielding thus abrupt axis movements and variation of directions. In addition to that, the span reduces notably the reach of the robot close to its base.
    - Lack of rigidity in the extruder adaptor. For prototyping reasons, tool parts were 3D printed using standard 3D printers. Although this approach is quite handy for research and favors ease of response to design shifts, these plastic parts were not conceived with the adequate mechanical properties. In addition to that, the adaptor lacked even the most basic support for avoiding bending in the joint. Mechanized parts would solve this problem in an effective way, although they would need further design refinement due to certain fabrication constraints. Figure 1 in chapter 5 shows the first working version of the extruder and its adaptor to the robot.

- Defects caused by the routine. Besides the above stated issues, the materiality of the finished piece is remarkably influenced by the routine set up. As mentioned previously, the initial routines subject of this section explored layer height affections, zone definition control and material-related matters. In this concern, it was detected that the vertex at which the extruder incremented its height caused the parts to fail, as the continuous extrusion of material resulted in the deposition of excessive material. This circumstance, despite not being a relevant problem in the first layers, becomes an especially relevant aspect as the height increments. The excess of material set off a nozzle collision with the printed part initially moving the latter from it place causing inaccuracies and ultimately its total printing failure.

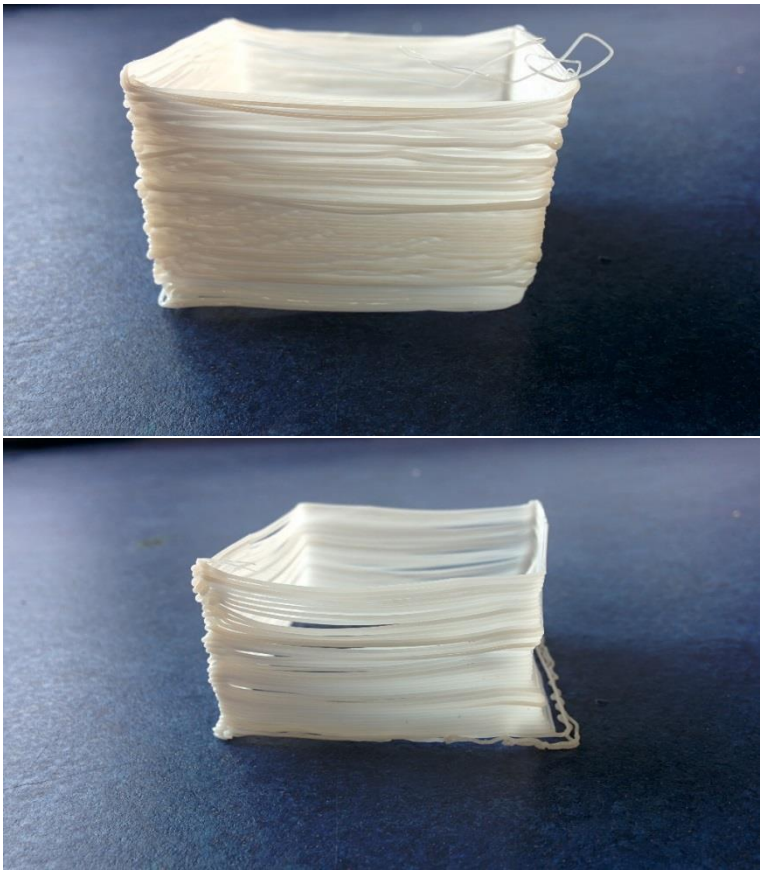

Figs. 3 and 4. First and second extruded pieces showing their numerous flaws: corner design, excessive layer height, faulty base placement, and incorrect finish (focus on layering and uneven height due to excessive increment in layer height)

- Material arrangements. First parts were printed using a 0.4mm diameter plastic extruder. The plastic extruders was then substituted by a more accurate and reliable 3DV6 all-metal extruder. The nozzle diameter was preserved as to keep material flow unmodified for simplicity reasons. Following tests attempted to amend these issues and increased the test size up to 100mm x 100mm x 50mm, although both the shape and printing technique were preserved. These parts shared some of the flaws of previous attempts, especially those caused by the faulty extruder design explained earlier in this section. The extruder related issues convey especially faulty corner conditions caused by the vibration of the hot end at each change of direction.

Nonetheless, a second version of the extruder was committed to solve the most relevant of the above mentioned issues, and that are exposed here for clarity purposes. The extruder had a TCP-X axis orientation, granting more flexibility in the 5th axis. Furthermore, the connector distance to the extruder was reduced to minimize the actual span between the robot and the tool itself, which had a positive effect in terms of stability. This provided more stiffness and reliability at printing time. Figures 6 and 7 show a great improvement in relationship to the accurate geometrical characterization of the finished printed part.

Further progress was made in the design of the printing apparatus and its hardware. This progress had a two-fold evolution:

- A more compelling hardware preparation, involving an enhanced printing bed as well as an improved extruder design. The hardaware preparation comprise:
    - An appropriate bed that maintains the part in place. A wood board was used as base. Tape was placed on its top along lacquer, which served as gluing material in order to enhance the adhesion of the part.
    - The wood base was planar enough and sufficiently calibrated for parts up to 200mm x 200mm in size.
    - The optimal distance for the first printing layer was found to be not higher thatn 0.1 mm. A completely planar base is thus required. Calibration becomes thus a complex issue, as it is to be performed manually.
- An ameliorated software and coding structure which focuses on the precise definition of speed, zones, and layer height.
    - Zone z0 was found to be optimal for all vertices.
    - Speed was optimal at 100mm/s to 150mm/s
    - Layer height was best between 0.1 and 0.15mm.
- Furthermore, the increase in the size of the parts unveiled otherwise unforeseen flaws apparently caused by the movement of the robot itself. As a result of this enlargement, it became visible that those edges of the pieces printed in the world's X direction were executed with a lesser level of accuracy than those along the Y axis. This means that a single piece could expose different levels of finish qualities, which was an undesirable situation that needed further exploration and a careful study.

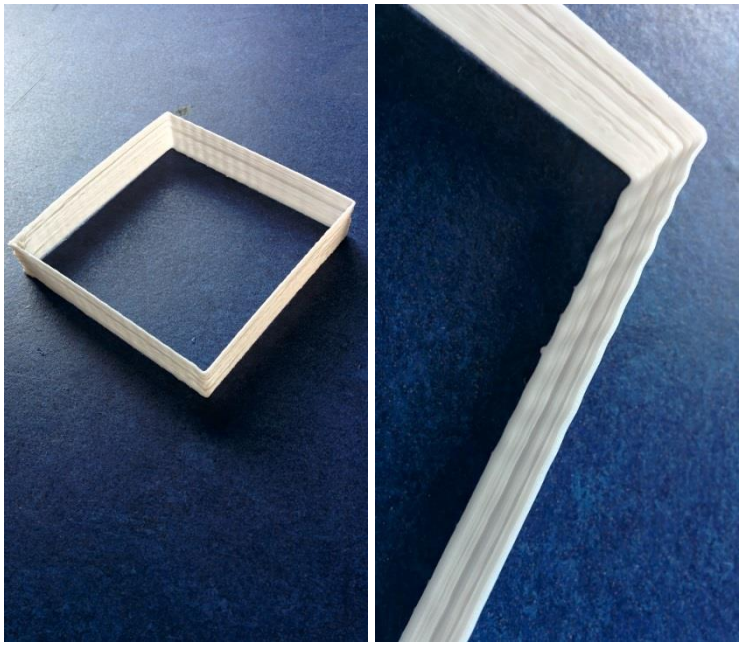

Figs. 5 and 6. Third instance printed with extruder version 0 showing faulty edge and undesirable wavy appearance (due to excessive vibration of the hot end)

8.1.2. Stage 2: routine improvements and printing enhancements.

Stage 1 tested several routines programmed manually directly through Robot Studio or the IRB120 Flex Pendant. Basic square-like shapes were thus far preferred for their simplicity, as they were easy to control and modify with those interfaces.

Nevertheless, once the setup of zones and height was determined, it was necessary to intensify the efforts on the software side. The process of obtaining more complex shapes and comprehensive routines needed to take place, although it was yet unclear whether it was possible to obtain satisfying results without the finished development of the rhino plugin –explained in chapters 4 and 5. Programming directly through the robot interface was a tedious task when dealing with large amount of points representing complex or bigger shapes.

As a result, a two-way simultaneous software development took place. On the one hand, simple routines were develop in order to accommodate immediate designs or to quickly test printing conditions; on the other hand, the improvements achieved through the python –first approach- code were steadily accommodated in the plugin's core.

Initial routines were based upon simple geometrical forms with single-line boundaries –this is, a single shell was applied with no infill patterning system. This approach had a significant visual advantage: it offers consistent visual information as to how precise the robot movement is. Also, if the tool is not precise enough or it vibrates, this will have an important affection on the part. Both issues are easily identifiable matching different flaw printing aspects, many of which have been thoroughly explained above and shown in figures 1 through 6.

Further elaborations of the code rely on offset-dependent point calculation, which is code-convenient, but computationally demaning. This means that each robot position along the toolpath is calculated with respect to a single base point as relative displacements or vector translations. In other words, points are not defined merely as a set of x, y, z coordinates in absolute space, but relative to a fixed point in space. Associating the geometry in this terms allows for a higher code flexibility and improves the ease of use by the end user, who does not need to worry about complex setting. During the test process, it also allows for an enhanced process and a quicker response to design changes.

Additionally, the routine could be easily modified and reworked to produce more equally-shaped parts at only through slight variations in speed, zone, and layer height settings. These could vary by part, allowing to study and calibrate the printing process with various materials, finish qualities and materials.

Further refinement accounted for the variables herein discussed:

- Speed, zone, and layer height
- Maximum number of layers or largest possible height in order to control when the routine needs to stop or continue to the part.
- Cube sizeX and sizeY, should parts have different size lengths.
- Extruder type and tool data.

The simplicity of the code at this stage did not devise any additional problem with the parts and permitted to establish and fix printing parameters. Supplementary developments took place in order to address the need for higher geometrical complexity. Not only were RAPID routines written in Robot Studio or the Flex Pendant; python routines were created as ad-hoc geometry translators. These python routines worked as simple plugins that took advantage of the lessons learnt in previous stages, and accounted for the variables named above. Moreover, these routines included a series of presets that facilitate the use and creation of parts directly from the Rhinoceros host interface. These series of tools served as tests for the methodology presented in Chapter 4, whereby the robotic movement was directly automated from the geometrical design in the host program.

7 and 10 sided polygonal 3D parts were programmed directly from the first python "translators" that automated the associated RAPID routines. Objects were truncated cones which base could be inscribed within a 10cm radius circle. Although the final size of the product could not be deemed as a full-scale product, it already exceeded most of the size limitations of commercial and professional 3D printers alike. Results are shown and analyzed below.

These parts were programmed with an enhanced shell system that boosted quality as well as the geometrical capacity of the prints. Figures 8 through 11 show the printing process of a regular 10-sided truncated cone. The thick wall design alongside an interior reinforcement geometry is visible as well.

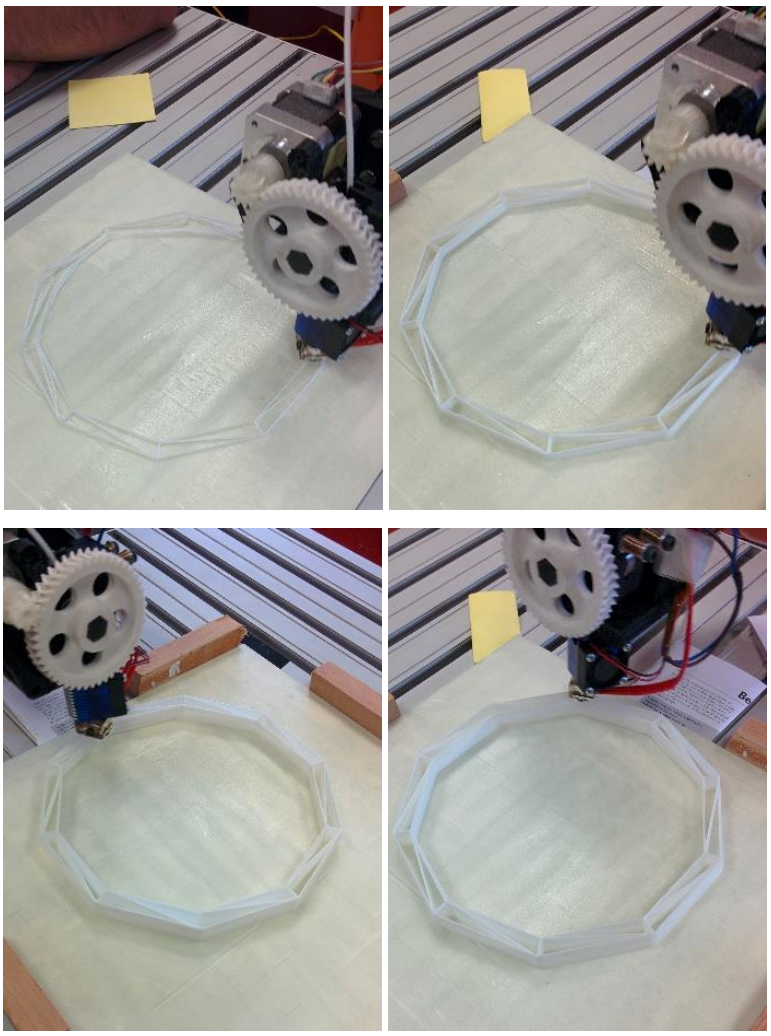

Figs. 7 -10. Robot printing the 10-sided polygonal structure with reinforcement infill

As in previous cases, the piece was printed at a "v100" speed (100 mm/s) and 0.15 mm in layer height. It is crucial to verify the zones (currently using z0) as to define perfect vertices and edges, but the speed of the robot and the amount of deposed material must match.

Future instances of the software increasingly tackled printing speed from a more complex and compelling perspective. Figures 11 and 12 depict graphically the speed diagram and acceleration behavior of a generic robot model –actual values differ amongst models. As shown in the diagrams, the speed value is not linear, causing points close to the actual part vertices to be less accurate. This is a result of the robot attempt to reach the defined printing speed in the shortest time possible following its own speed curve. Therefore, not only were wave-like depositions detected in previous try-outs caused by the vibration of the extruder itself, but also due to turbulences in the motors as the robot speeds up (leaving a point) or down (reaching a point). This aspect can be dealt with through a careful setup of the brake parameters through RAPID code and a meticulous arrangement of a comprehensive robot library in order to account for the slight differences between the behaviors of the diverse robot models. While this is a common feature throughout all robots in the world, each company and model have different hardware conditions, which translates into an immense effort in terms of comprehension, testing, and setup when dealing with global tools.

As a consequence, incrementing printing speeds with robotic arms becomes a much more arduous task than with certain CNC machines, where speed can more easily be controlled through more abrupt and steep speed curves.

As ABB states (ABB, 2016), "*in order not to get false alarms from the brake ramp supervision when using ABB robots and tracks, the parameters have a default conservative setting. Conservative means*

that the ramp should represent the worst case brake performance achieved by the track in combination with robot motion". In other words, brake ramp limits are conceived to not be activated unless motors or speeds well exceed predefined speed curve values, allowing for extra fine tuning by the user or the programmer. Precisely this space between each model's curve and the brake ramp limit might be explored as to improve the robot's performance during the printing task.

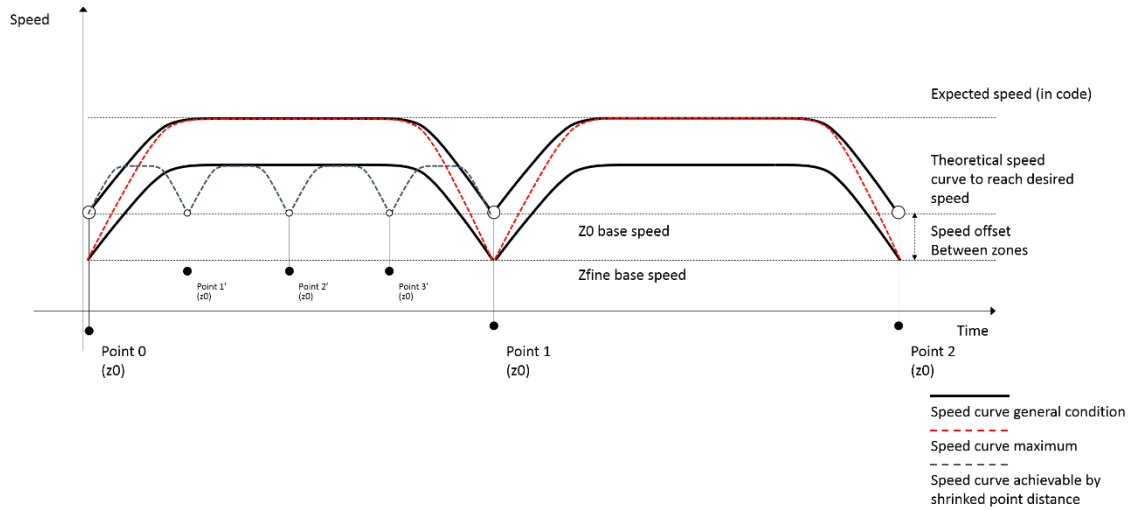

Fig. 11. Generic robot speed diagram (behavior at a macro scale).

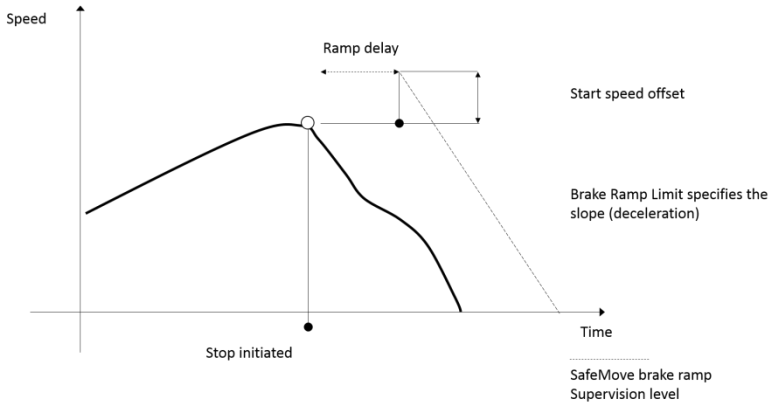

Fig. 12. Generic ABB robot speed diagram (behavior at micro scale).

Although defining the influence of the motor torque control on the speed behavior of the robot is out of the scope of the thesis, let us just introduce some basic concepts. Traditional means of motor control depended on current voltage like AC drives and DC drives. As early as 1995, ABB developed an innovative technology to enable unprecedented performance in their electric motors so as to deliver dramatic energy savings by matching motor speed and torque to the driven load requirements. Direct Torque Control (DTC), implemented in ABB's premium variable-speed drives (VSDs), directly controls motor torque instead of trying to control the currents analogously to DC drives trhough PWM (pulse-width modulation). This excludes modulators from the whole electronic component design, thus avoiding the inherent time delay in processing control signals (ABB, 2015) while achieving control dynamics that are close to the theoretical maximums thanks to an enhanced development process since their invention. On top of these advantages, DTC dispenses accurate torque and speed control down to low speeds, as well as full startup torque down to zero speed. As a consequence, a more direct motor speed transmission is provided to the manipulator, therefore delivering a better printing experience with higher part qualities the end user.

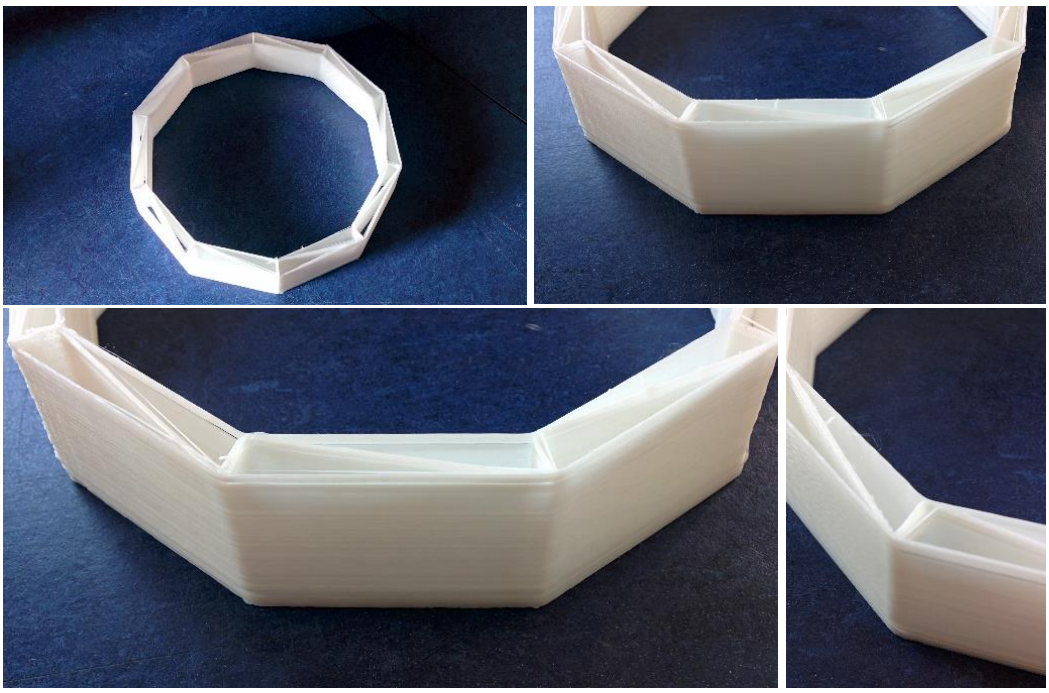

Figs. 13 -16. The 10-sided polygonal structure with reinforcements. Close-ups showing the end product's final quality. Particular attention is paid to vertices and reinforcement.

Close-ups in figures 15 and 16 demonstrate that the z0-like corners display some degree of curvature, allowing the robot to not stop at vertices. As discussed above, this fact increases the system's printing speed "*de facto*", especially when compared to "traditional", CNC-like 3D printers. Nonetheless, it is crucial to account for certain geometrical imprecisions at this scale when dealing with robotic printing –see figures 11 and 12.

Another relevant topic regarding printing speed is the need for parts to be securely glued at their base in order to avoid undesirable part movements, vibrations, or collisions by reason of excessive material deposit or uneven layering. At a software level, RAPID code allows for an exceptionally flexible speed control, which can be stated and set per movement –this is, speed is a variable of each movement function and expressed either in degrees or mm/s depending on what component the speed is affecting (for joints or wrists, speed is expressed in deg/s, while for linear speeds m/s are used). KUKA code, on the contrary, relies on a global variable approach for this specific matter, originating a quite intricate and unreadable code if willing to tweak speed to a high degree. To be more precise, ABB provides a more object-oriented programming experience whereby speed is an object which can vary easily withing the movement commands, whereas KUKA requires a specific method call or variable overwrite (such as $VEL.CP = val) to vary movement speed. As a consequence, ABB's RAPID code was preferred for both its lightness and ease of use.

In order to physically account for these fixation issues –tackled at a software level, it was ensured that a proper fixation base was provided. Experiments showed that once the first 10 to 15 layers (this is, the first 10 to 22.5 mm) have been posed, the part is set to be built correctly. Figures 13 to 16 exhibit some details showing the quality of the finished print. The part exhibited sufficient structural stability and rigidity, as most errors detected in previous instances of the development were effectively addressed at this stage. Figures 16 and 17 emphasize the finish layer quality achieved as a results of the numerous accomplishments and analysis performed on previous parts –see figure 17 for reference. These figures portray higher vertex control, a relatively smooth and planar surface finish, and the infill structure. A closer look at the vertices reveals the lack of precision of the geometry to a certain extent, as a consequence of an imprecise zone definition -a curved toolpath is created. Figure 18 shows various erroneous attempts that suffered from a faulty base fixation or issues related to speed that impeded a suitable layer-to-layer binding.

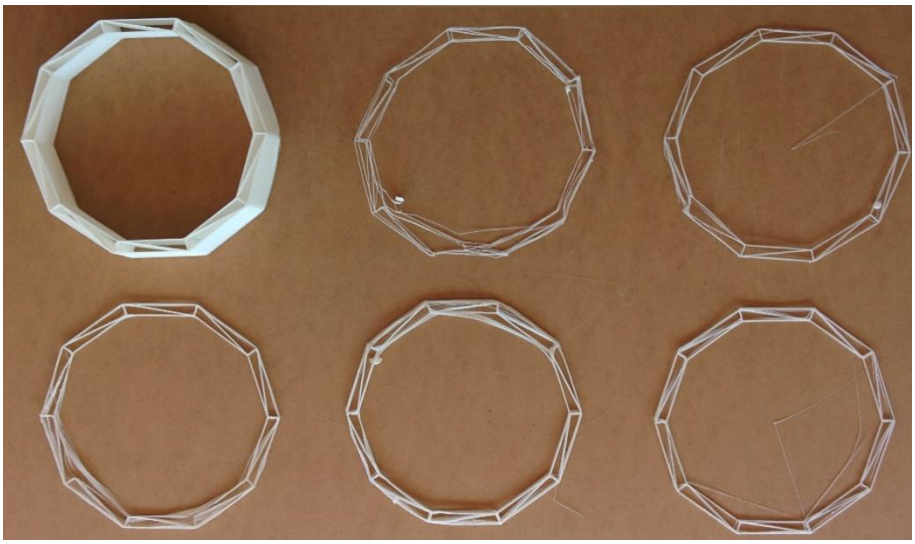

Fig. 17. 10-sided polygonal structure: all attempts displaying deficient base preparation and irregular shaping consequence of the piece moving during the printing process. Part 2 (middle, up) displays a particularly poor geometry, part 4 (bottom left) has an irregular interior shape due to a disconnected edge. Part 1 displays a correct formation.

The lessons learnt from the 10-gonal part were applied on a heptagonal truncated cone which base could be inscribed in a diameter of 22 cm. This part shared some of the features of the previous case:

- It followed the same form principle.
- Again, although the final part could not essentially be considered big scale, its size exceeded the bed size limits of most commercial desktop 3D printers.

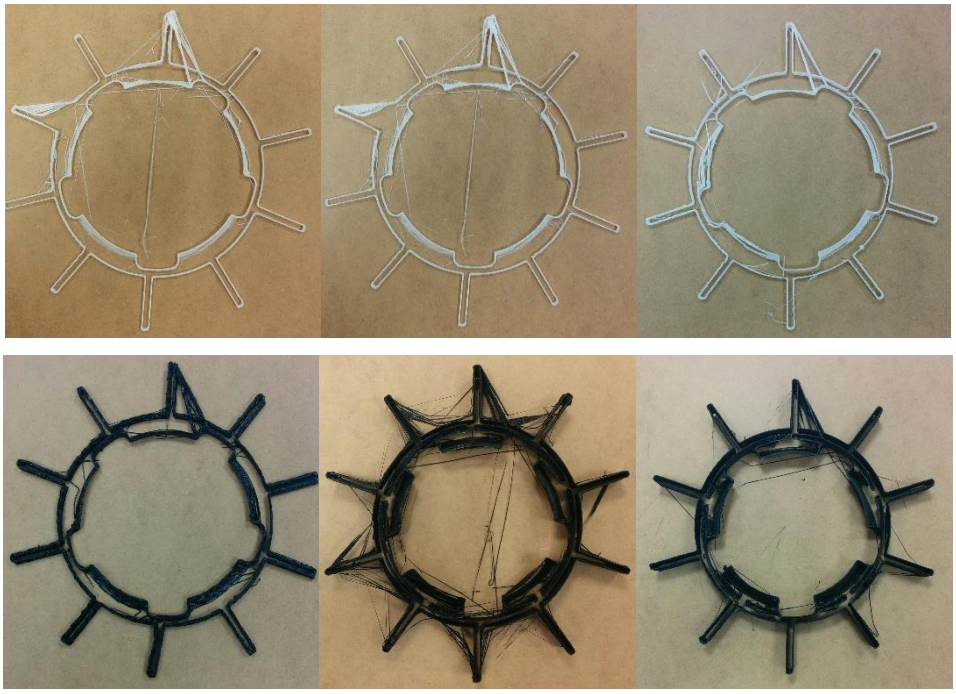

Fig. 18a through 18f (top left to bottom right): outcomes of an enhanced robot routine, showing defects present in n-gonal parts.

Furthermore, the part exceeded 20 cm in height, a size limit present in almost all desktop 3D printers and professional printers alike. The object was printed in black PLA following the same process and settings as in the previous example. Basically, the print had the same quality and problems, which mostly derived from the movement of the robotic arm. Figures 19 through 22 show different steps of the printing process, from the first layers (up left) to the almost finished part (bottom right).

As seen in the pictures, prints started from their base centroid. The software was improved to better adjust questions related to user demands in terms of software usability within the host design interface. All print tool paths were calculated relative to the centroid of the part, which had its physical representation counterpart predefined in the printing bed. Parts were printed in a reliable manner at this stage and would only display minor issues of surface quality or geometric imprecisions at very small scales.

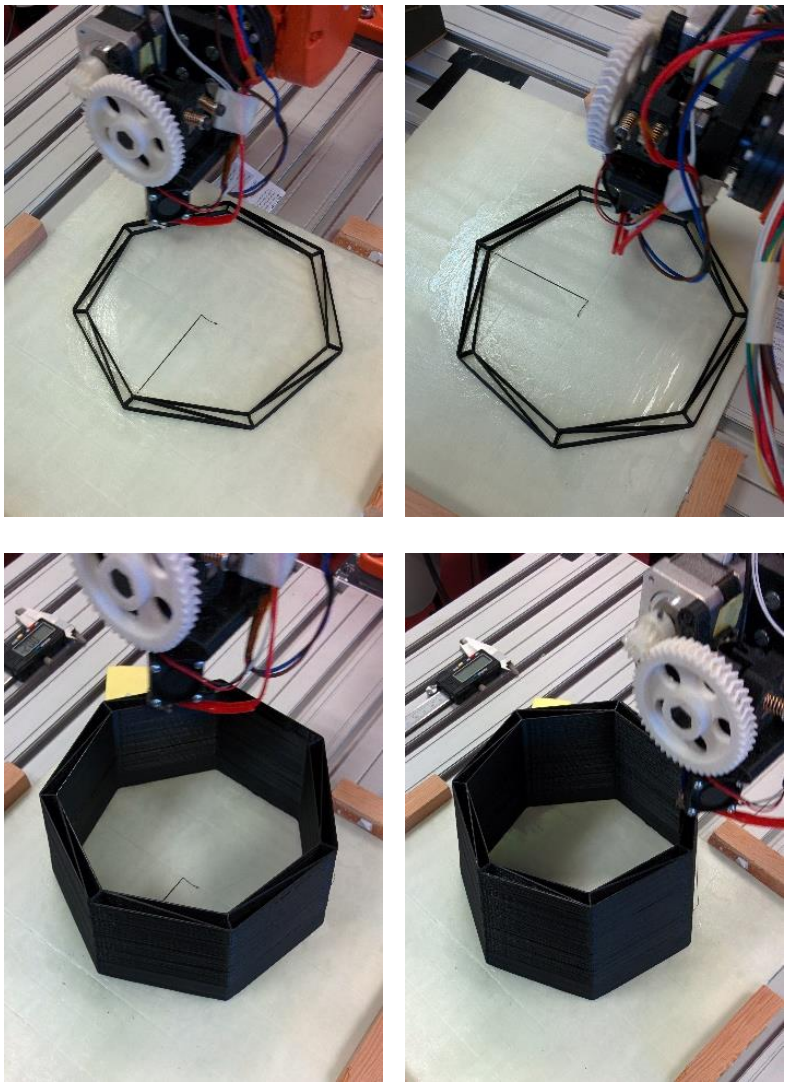

Fig. 18-21. Robot printing the 7-sided polygonal structure with reinforcements. Note the total height of the piece

The extruder tool was still controlled by external means, using Repetier Host in manual mode. Figure 24 shows a plastic “blister” consequence of the extruder deposing material at a static point. The detachment between robot control and material deposition triggered this sort of errors, whereby all fabrication sub-processes were asynchronous. As a result, it was necessary to turn of the motor and the whole extruding apparatus in order to finish the part properly. Synchronizing both operations through the hardware control of both extruder and robot turned out to become crucial at this stage. Figure 25 shows a “weak” line consequence of the motor stopping during the fabrication process. Since the motor was activated manually, it was necessary to keep on sending extruding functions to the motor during the preparation of the part, causing undesirable side effects, such as: (i) forcing a technician to constantly supervise the printing process, and (ii) yielding erroneous or faulty results as a consequence of distractions.

Besides this series of disadvantages, the fabrication process had improved as a whole, performing correctly in a controlled manner.

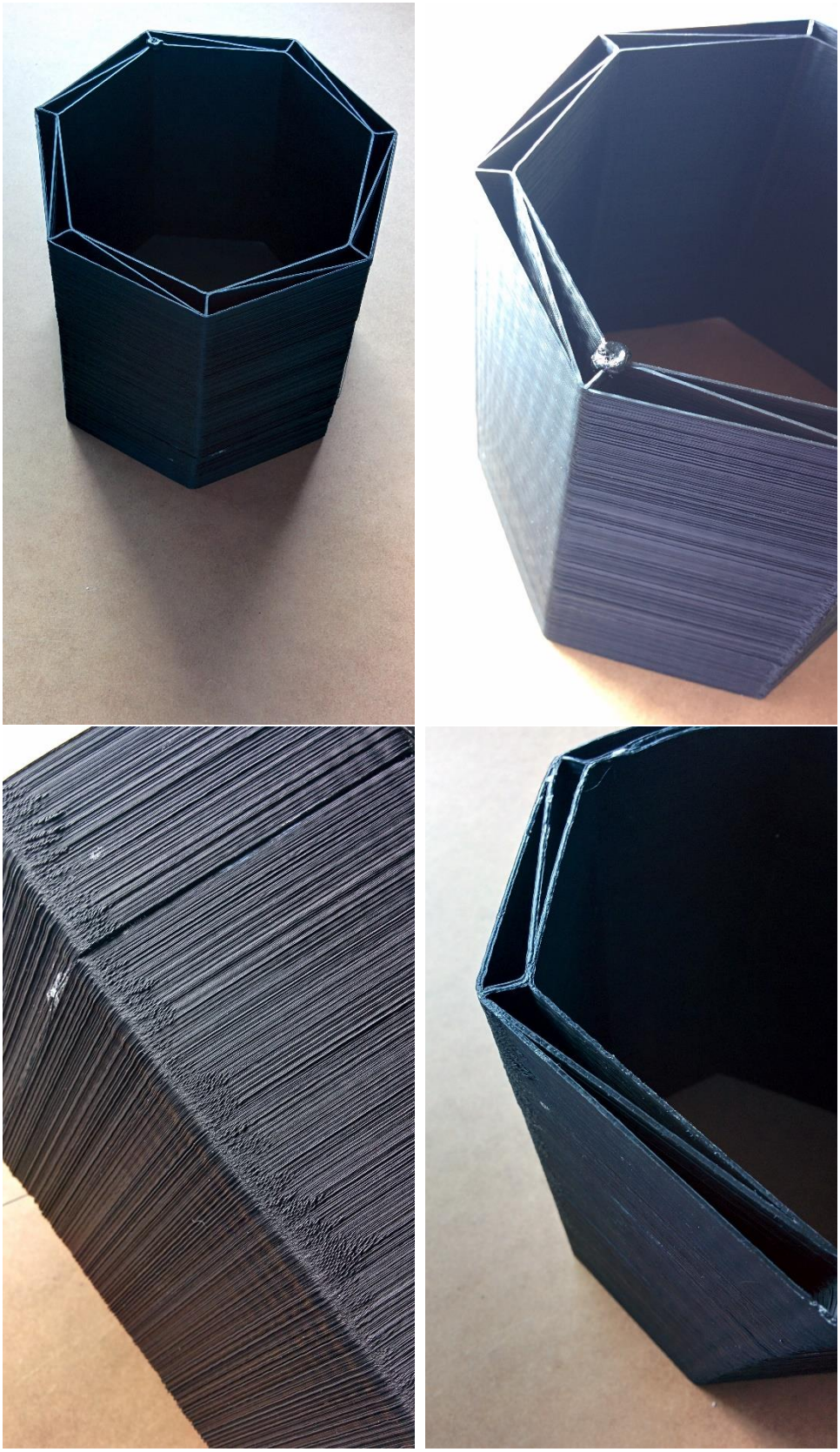

Fig. 23-26. Details of the 7-sided polygonal piece, displaying: overall shape (upper left), final point of the print with continued material extrusion (upper right), layer deposition quality (lower left), and detail of the top-most layer (lower right).

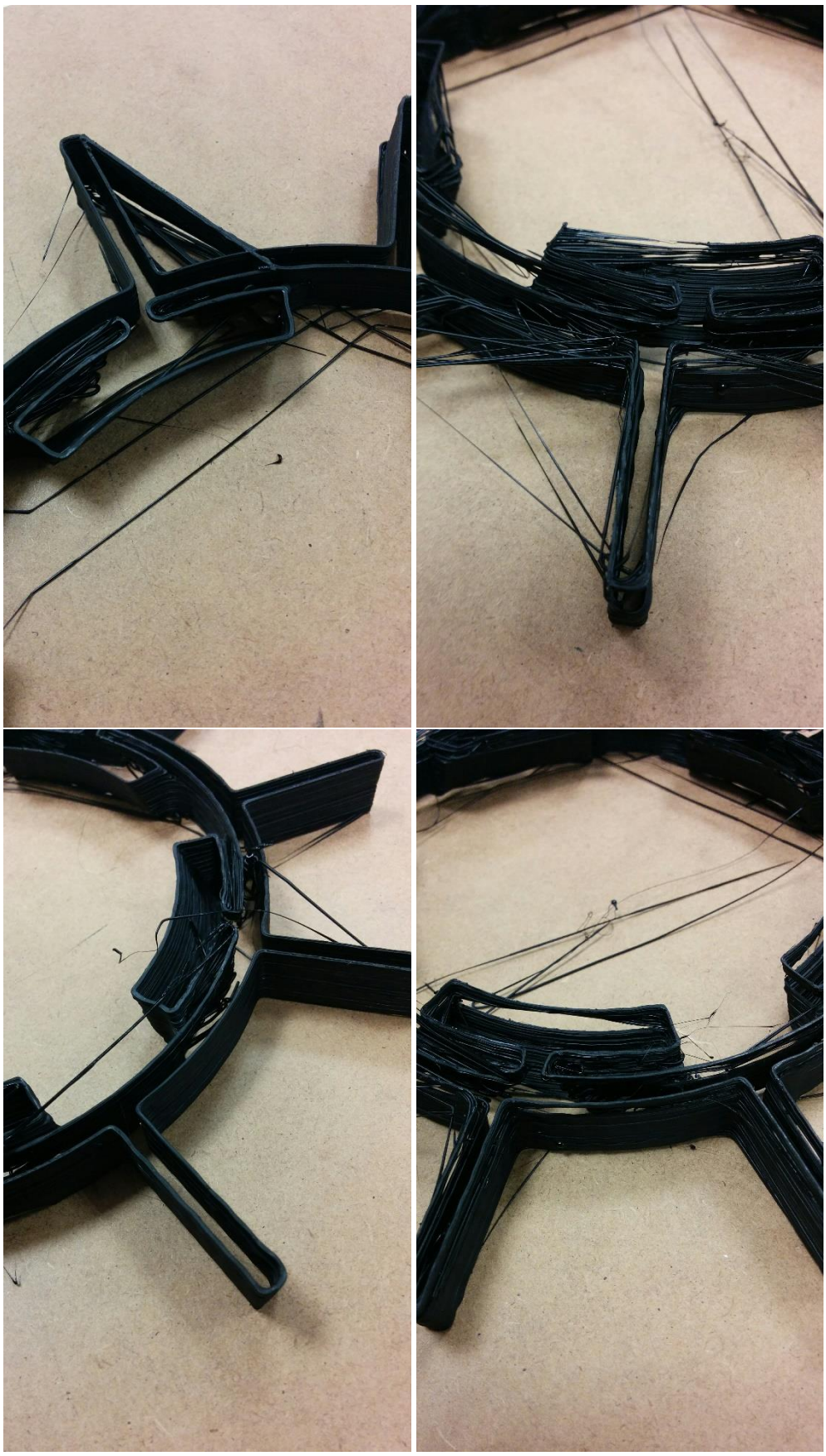

Fig. 27. Most common flaws in a complex part: continuous printing, poor extrusion, bad attachment to bed, undesired curvy look at vertices and vibration.

8.1.3. Stage 3: complex parts. Overcoming the limitations of the robot controller.

Once the main printing errors were overcome, it was decided to focus on more complex parts and the flexibility to produce any kind of shape from within the CAD software. The main development required further software capabilities in order to host complex shapes. As explained in Chapter 4, parts were sliced in order to obtain contours from which actual tool-paths would be created based on the curves' vertices.

Complex or big shape 3D mesh models can reach virtually millions of points. Particularly intricate geometrical forms or highly curved surfaces require large amounts of faces as to avoid displacements and deviations from their original NURBs surface representations. Dealing with such an amount of data is unusual in robotics, where robot controllers have a very limited RAM memory capacity. For instance, the IRC5 Compact Controller's RAM memory is 40MB only; this is normally fine for most robotic applications, but indeed a relevant limitation when dealing with complex mesh data.

Thus, reducing the number of points per layer (that is, reducing the amount of sides), permitted the object to grow in height. It was crucial at this stage to continue the development in order to include dynamic loading and unloading of modules for high resolution 3D objects where 500k points or more are encountered on a regular basis. Conversations with ABB technical staff and custom tests revealed that the maximum amount of movement instructions per loaded module in the RAM memory turned out to reach about 30 to 40 thousand points. Optimizing programs became thus a priority task, since most parts would exceed this number by far. Reducing the amount of decimal positions in routines proved effective, but not sufficient to solve the problem.

Figure 28 depicts the enhanced program structure showing the typical module loading/unloading system implemented in the software. The software creates, on the basis of the contours obtained from slicing the 3D virtual model, a single main module and a series of modules containing the actual movement instructions, as explained in Chapter 4. These modules are then loaded, called, and unloaded by the main module in order for the program to be capable of producing shapes of any amount of points (robot targets).

While the Controller's RAM memory is constrained, ABB RAPID's code (as it does KUKA language as well) allows for dynamic memory module loading. This is, the main module can load and unload function modules. The solution was, therefore, splitting the code into loadable modules that could be dynamically used by the program. As explained in Chapter 4, it was originally decided to split the programs in modules with 3000 instructions or less. While the total amount of points was an issue before including this functionality, the development turn its focus into optimizing loading and unloading times. As explained in section 4.6, different controller models had different response times –but the challenge remained. IRB 120 with IRC5 Compact errors were more obvious than those from IRB1600 or IRB 2600, which had an IRC5 controller. Loading time resulted in excessive material deposition, which could be solved by either modifying the amount of points per module –resulting in smaller module file sizes-, or stopping the motor during the loading operation, which required the finalization of the DI/DOs setup.

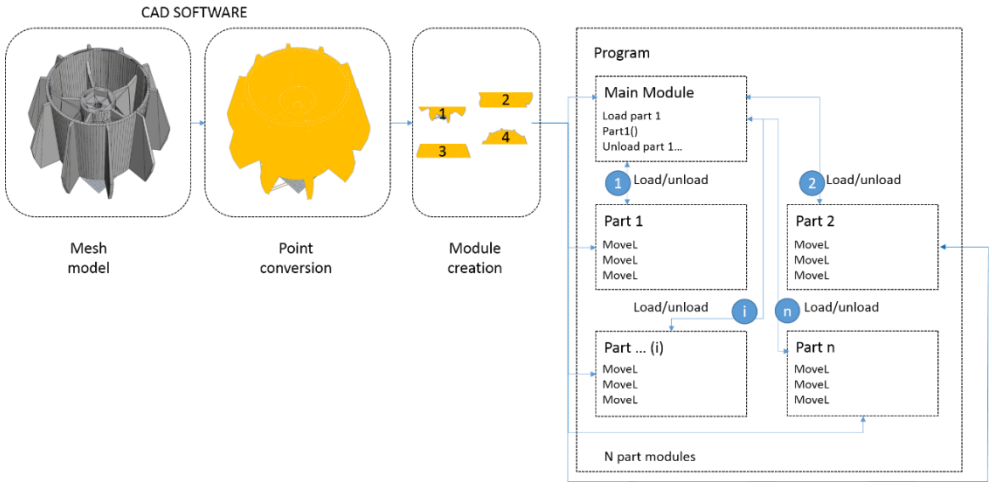

Fig. 28. Program structure and operation with dynamic module loading/unloading.

On top of improving the internal program structure, supplementary geometrical conditions were tested. Not only were regular parts designed, also single-curved and double-curved parts were pursued. The enhanced translator engine allowed for better control and more complex parts. These are exhibited in figure 29. Objects exceeded by far the size of their earlier counterparts, and had virtually no limitations in terms of size or geometry.

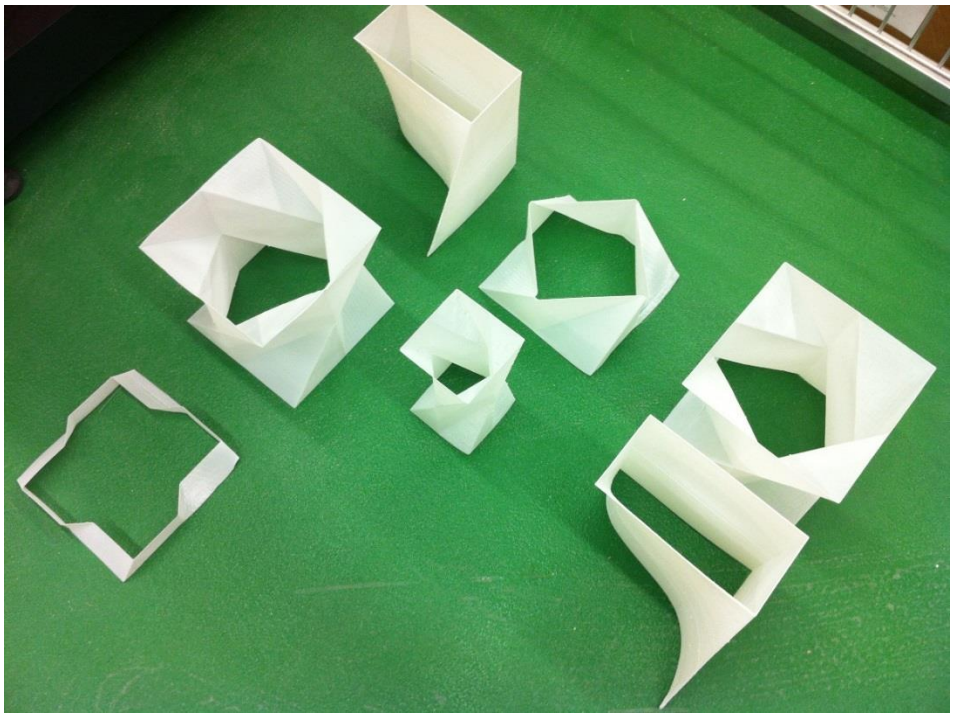

Fig. 29. Initial large-scale part testing showing 7 parts testing various conditions and sizes.

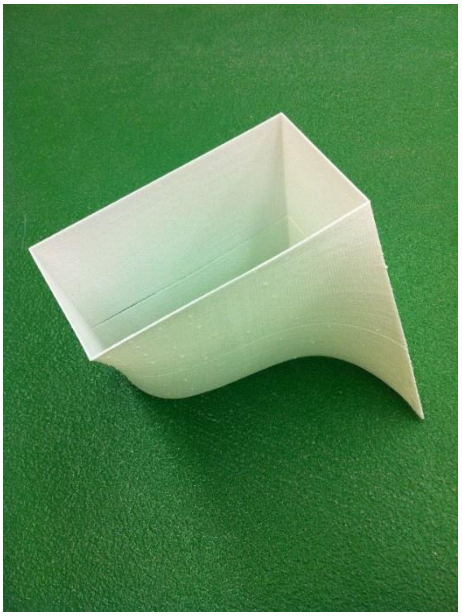

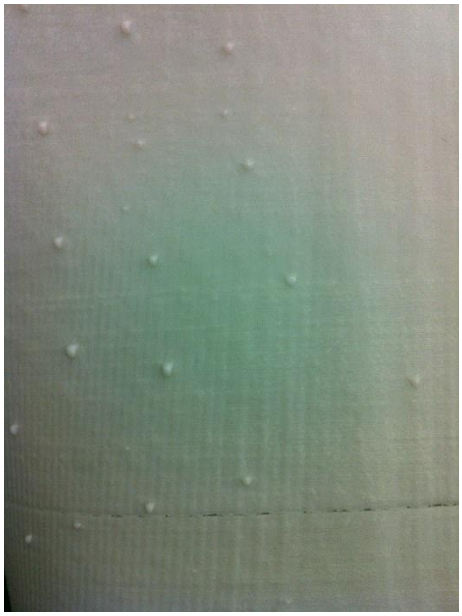

Figs. 30, 31. Double curved surface, contained within a 0.4 m x 0.4 m x 0.4 m volume with a 0.15 mm of layer height resolution and v = 50 mm/s

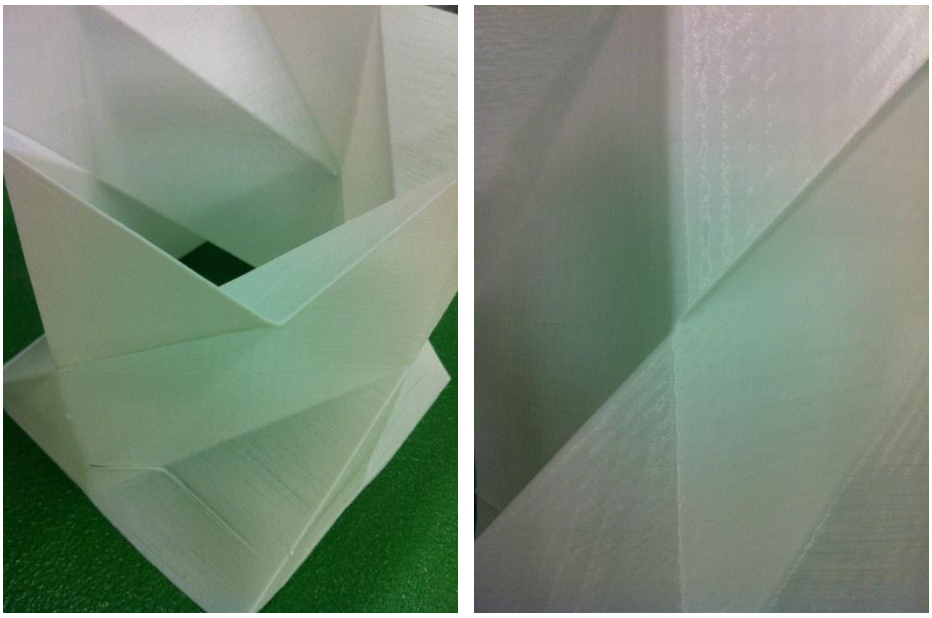

Fig. 32, 33. Planar complex geometry form, confined within a 0.4 m x 0.4 m x 0.4 m volume with a 0.15 mm of layer height resolution and v = 50 mm/s

Subsequent pictures show some results of the prints, taking special care in portraying finish qualities of the parts at this stage. Figures 30 and 31 show a double-curved part printed by use of a dense 3D virtual mesh model. As explained above, the mesh density increases as to represent the curved geometry in the most reliable way possible. Dots on the surface –close-up in figure 30- are actual plastic bubbles formed during module loading as a result of the robot stopping at "random" locations –established by the point split amount set in the code generator.

Figures 32 and 33 show a planar geometry displaying points of singularity. By means of a simple 90-degree rotation, complex geometry can be obtained. This case presents a lesser number of points due to a relatively lightweight use of the 3D mesh geometry needed to represent the solid model. As a results, less dots appear on the surface, as less modules need to be loaded by the controller. Figure 33 focuses on the quality of the singularity point, as well as on the fact that 45º tilted parts have been successfully printed. The part fits within a 0.4 m x 0.4 m x 0.4 m volume and has been printed at 50mm/s on an IRB 1600 with an IRC5 controller.

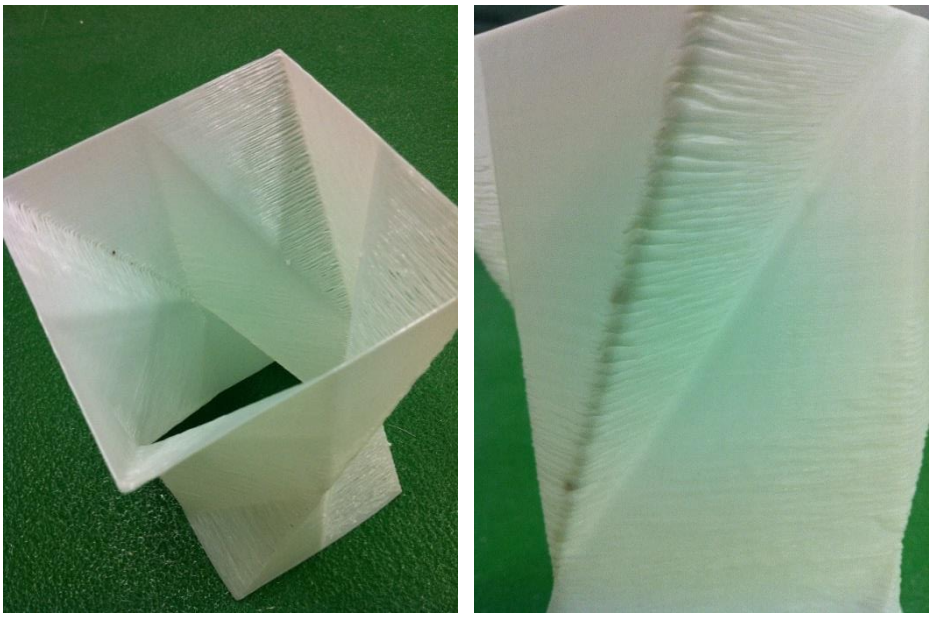

Fig. 34, 35. Planar complex geometry form: 0.05 m x 0.05 m x 0.4 m volume, 0.15 mm of layer height resolution and v = 50 mm/s

Material properties vary drastically with hardening times. Whereas figures 30 and 31 depict a successfully printed part showing a correct layer finish and deposition technique, this part might not be easily replicated at a smaller scale using the same printing speed. Adjusting speed then is crucial to the proper finish of parts, as layers require some hardening time prior to the deposition of another layer. Figures 35 and 36 exhibit the same object scaled down on the XY plane while maintaining its height. This experiment allowed to verify the varying material conditions and the need for adaptability in printing speeds when having short layer loops recurrently. The geometry shows lack of planarity at the edges, and an irregular, wavy distribution of filament across the different horizontal sections of the part. Since the part has the same amount of points as the previous object, the faulty variation in the surface finish can only be due to the material itself. Figure 35 displays the quality of the edges where the angle is minimum in the part. As it can be seen, errors are more visible when the surface is tilted. This part fits within a 0.05 m x 0.05 m x 0.4 m volume and has been printed at the same speed and on the same conditions and hardware as the previous one.

Final tests were conducted to reproduce these and other geometries at different speeds on the IRB120. Figure 36 exhibits a 0.2m x 0.2m x 0.4m part printed at 150mm/s, three times faster than previous ones. Motor speed remained unchanged, resulting in less material deposition per length unit. In other words, if motor speed is constant, then the shells become thinner at a faster scale. The quality of the print was not affected.

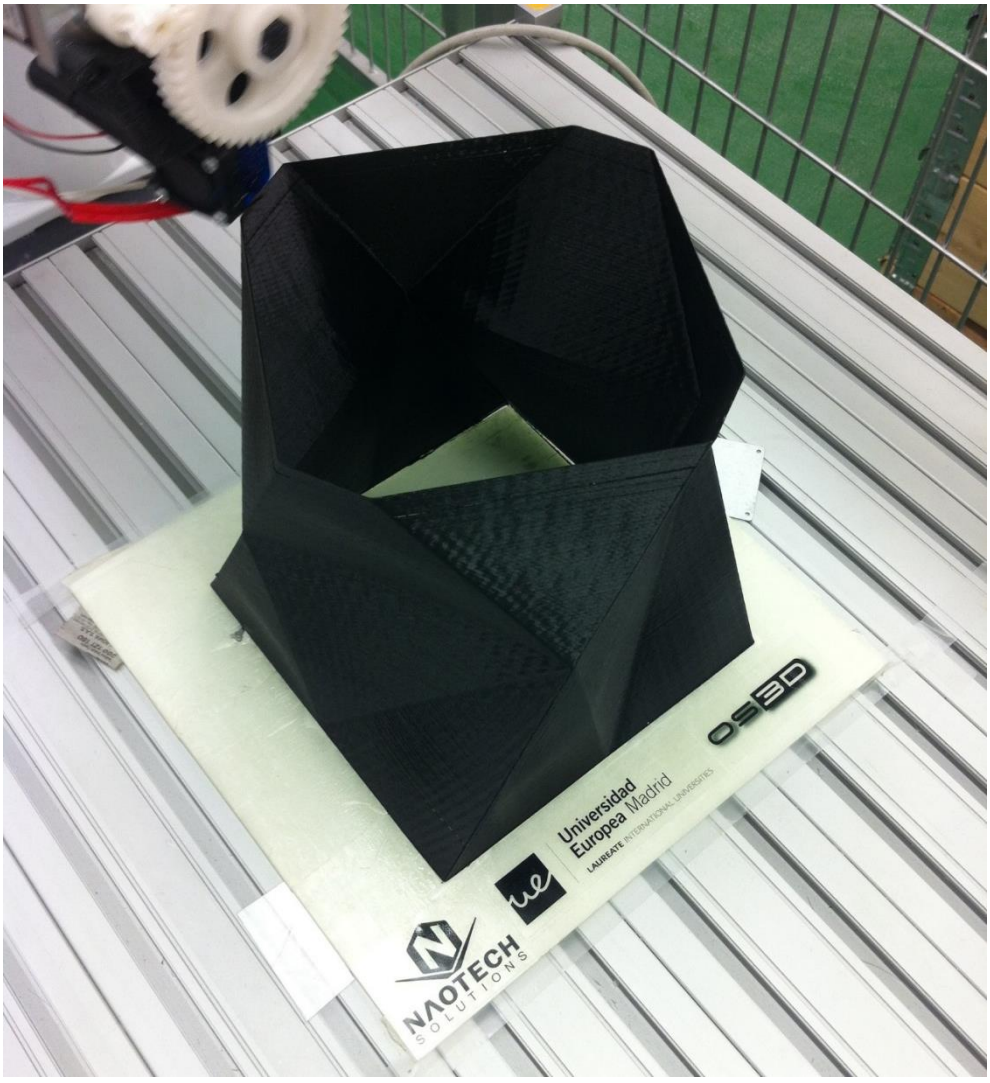

Fig. 36. Planar complex geometry form, confined within a 0.2 m x 0.2 m x 0.4 m volume with a 0.15 mm of layer height resolution and v = 150 mm/s

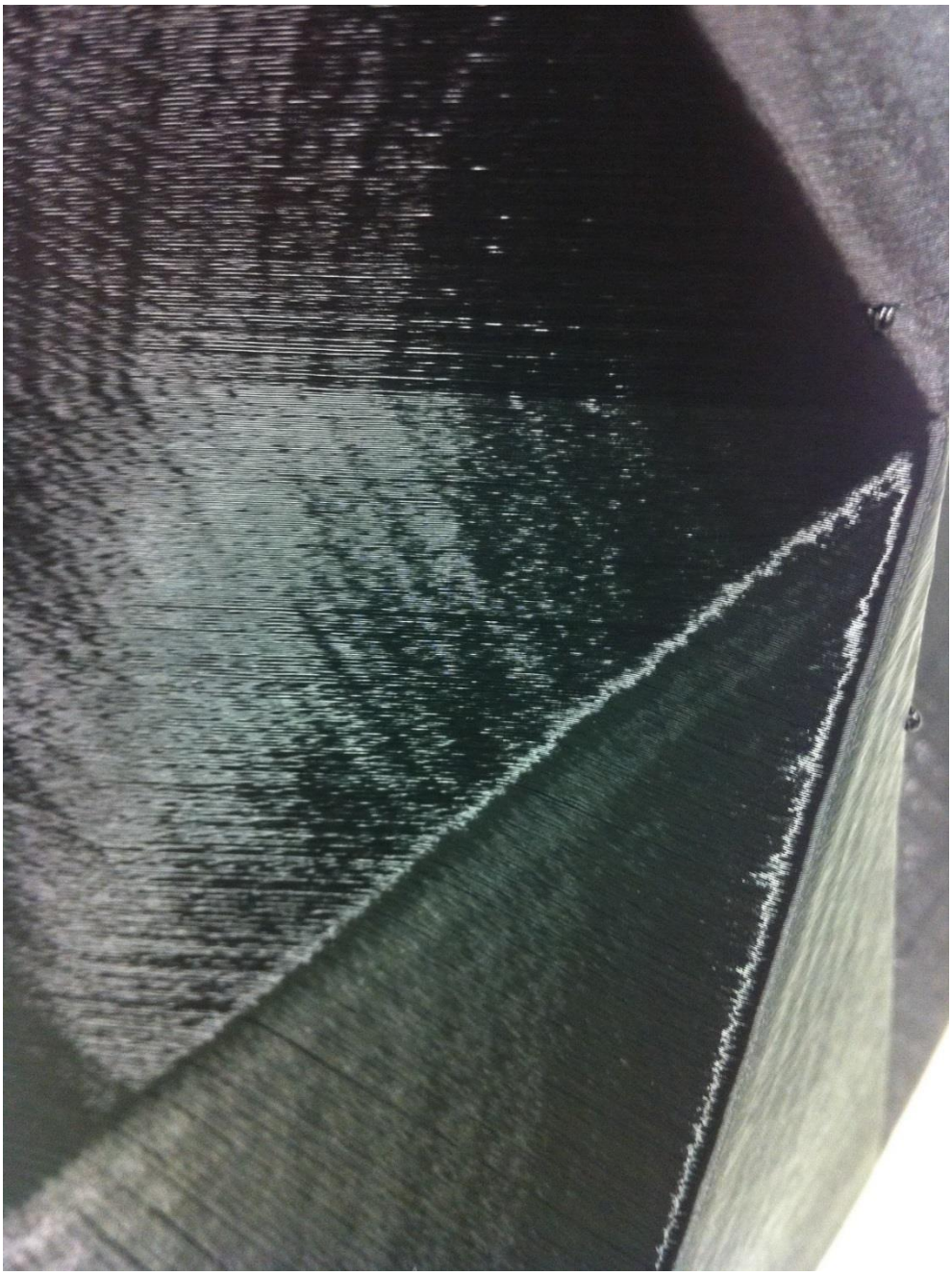

Fig. 37. Close-up of the part shown in figure 35. Note the finish quality and the glossy finish, the “curvy” edges, and the plastic bubbles result of excessive, uncontrolled hot-end time during the dynamic module loading operation performed by the IRC5 Compact controller.

Final tests were conducted to reproduce these and other geometries at different speeds on the IRB120. Figure 37 exhibits a 0.2m x 0.2m x 0.4m part printed at 150mm/s, three times faster than previous ones. Motor speed remained unchanged, resulting in less material deposition per length unit. In other words, if motor speed is constant, then the shells become thinner at a faster scale. The quality of the print was not affected.

8.2. Conclusions

These series of experiments served as try-outs, set-ups, and fine-tuning tests for the development of the methodology and apparatus constituting the main core of the thesis. PLA and ABS material presets –which are by default used in the plugin- were obtained from this cycle of tests.

The experiments led to a series of conclusions:

- It is crucial to define the printing speed and the material deposition rate in combination with one another. The relationship between both can be found in Chapter 5, whereby an optimal ratio was found to be 60 rotations per minute and a printing speed of 150mm/s. Obviously, this correlation may vary depending on a variety of hardware variables, such as wheel radius, for instance.
- Prints can host tilted surfaces up to 45º without failing. This must be taken as an absolute value, only applicable to FDM with thermoplastics. Other materials may behave differently and have larger restrictions. A recommended value that would allow a piece to be printed without supports was found to be 32º. This must be taken into account as a limitation given the current state of the software, where no fill is needed. Also, the software does not currently calculate supports.
- It was proven that the method worked as desired. Parts were printed on different hardware and software platforms seamlessly.

Finally, these results fostered the execution of structural analysis and stress tests –shown in Annex II. These tests were carried out in order to check the structural performance of the final physical objects and the material properties involved. As a consequence of the results obtained and after a careful analysis of the fabrication process, future works were established to include the following issues, which were addressed consequently in subsequent stages:

- Fix further stability issues.
- Fix calibration issues.
- Develop IO communication between robot and tool including the lessons learnt from the experiments.

Annex II

Material tests

Annex II exposes material tests carried out to prove material properties of printed parts. Material properties in 3D printed parts depend on two main factors: on the one hand, their printing setup; on the other, how the test itself is prepared regarding the layer printing direction. Printed parts behave in a different manner to molded or injected parts, as these are continuous and homogeneous throughout all sections. 3D printing technology, on the contrary, presents structural weakness lines at fixed intervals matching the layer height. Furthermore, the orientation of those has a relevant impact on the structural behavior and reliability of the printed parts, as load is distributed unevenly through the different layers. Moreover different load types and stresses perform in different manners according to the fiber direction.

The present annex exposes a series of structural tests that were performed for parts printed with different configurations, speed, infill patterns, and materials. PLA and PLA composites (with diverse carbon fiber proportions) are tested and shown.

9.1. Test methodology

The test has been designed to check and obtain results that yield the atual mechanical properties of printed parts. These results depend not only on the material itself, but also on a series of geometry related variables. On the test part, these conditions include:

- Infill pattern and proportion of solid versus void area in each section
- Filament direction
- Layer height
- Printing temperature
- Printing speed
- Part size

The demonstration tests specimens against three main stress entitling tensile, compression, and flexural loads. Three different shapes or type parts have been used accordingly in order to conform to the machinery geometry and press directions. The compression part is a simple cube, whereas the tensile part is a Z-shaped piece that resembles regular test parts. Flexural parts are prismatic parts with one dimension significantly greater than the other 2. Further information on the geometry and its properties can be found in section 6.3, as each force type has different requirements.

All parts displayed in this chapter have been printed with the same shape and infill pattern geometry –depending on the load type- for comparison reasons. Nonetheless, they all present slight changes due to fabrication inaccuracies, which are displayed in each data table for clarity. Test parts were designed for, set up, and printed using a Prusa iSteel 3, following the conditions hereby disclosed:

- All parts must have the same amount of infill material
- All parts must have the same outer shape
- As a result, all parts must have the same structural section per printed layer
- All parts have been printed with the same extrusion temperature
- All parts must be printed in two main directions. Generally speaking, parts may be oriented towards an innumerable set of directions and orientations when being laid on the printing bed. Nonetheless, only two have been selected for demonstration purposes and structural logic reasons. In order to prevent geometrical inaccuracies, the parts have been designed and laid flat on the bed –thus avoiding the need for support material- along either the X or Y axis of the 3D printer, as shown in the figure below.

Any modification to any of the settings described above –and disclosed for each part- affects the final results. The following sections explain each test set up thoroughly along with the part requirements for each specific case. The two main part types have two subtypes according to the filament direction (X or Y axis as explained below).

The fiber direction influences the mechanical behavior of the part, which displays different results under similar load conditions for both tested directions. This divergence demonstrates the weakness of the layering technique in 3D printing and how inappropriate settings might critically affect the feasibility of a printed part in terms of structural stability and mechanical "tightness". Case 1 shows the principal printing direction along the Y axis –perpendicular to stress whereas case 2 shows the fibers laid out along the X axis –this is, following the X axis direction.

The test material is a blend of PLA and carbon fibers in a 75% matrix to 25% addition mix balance. The experiments seek to obtain a relationship between the following variables:

- Material resistance to tensile stress
- Fiber direction in printed parts

In an attempt to attain the most reliable possible values, all tests are further characterized by the most influential variables, namely: (i) material, (ii) fiber direction, (iii) effective load area, and (iv) effective structural area. The effective load area is the area where the load is applied, whereas the effective structural area relates to the amount of material that is actually subject to stress on a layer basis.

- **Norms and standards:**

Tests have been realized in an authorized destructive laboratory complying with the norms and regulations thereby applicable or the closest adaptation possible. In fact, the following norms have consulted, referenced, adapted and followed for either determining the test set-ups themselves, or taken into account as far as the determination of the geometry and form of specimens is concerned.

- UNE-EN 6038:2015. Aerospace series - Fibre reinforced plastics - Test method - Determination of the compression strength after impact (Endorsed by AENOR in January of 2016.)
- UNE-EN 6037:2015. Aerospace series - Fibre reinforced plastics - Test method - Determination of bearing strength (Endorsed by AENOR in January of 2016.)
- UNE-EN 196-1:2005. Methods of testing cement - Part 1: Determination of strength.
- UNE–EN ISO 180:2001. Plastics – Determination of Izod impact strength (ISO 180:2000)
- UNE-EN ISO 14130:1999. Fibre-Reinforced plastic composites. Determination of apparent interlaminar shear strength by short-beam method. (ISO 14130:1997)

- ISO 291: 1998 (Withdrawn). Plastics. Standard atmospheres for conditioning and testing (ISO 291:1997)
- ISO 294-1:1996. Plastics - Injection moulding of test specimens of thermoplastic materials - Part 1: General principles, and moulding of multipurpose and bar test specimens. (ISO 294-1:1996/Amd. 1:2001)
- ISO 295:1999. Plastics - Compression moulding of test specimens of thermosetting materials (ISO 295:1991)
- ISO 2818:1997. Plastics - Preparation of test specimens by machining (ISO 2818:1994)
- ISO 3167:2003. Plastics - Multipurpose test specimens (ISO 3167:2002)
- ISO 10724-1: 2002. Plastics - Injection moulding of test specimens of thermosetting powder moulding compounds (PMCs) - Part 1: General principles and moulding of multipurpose test specimens. (ISO 10724-1:1998)
- ISO 1268-10:2005. Fibre-reinforced plastics — Methods of producing test plates ISO (1268-10:2003). Parts 5 *Filament Winding* and 6 *Pultrusion moulding* were particularly regarded.
- ISO 13802:2006. Plastics - Verification of pendulum impact-testing machines - Charpy, Izod and tensile impact-testing (ISO 13802:1999, including Corrigendum 1:2000)
- ISO 2602:1980 (E). Statistical interpretation of test results – Estimation of the mean - Confidence interval.
- EN ISO 1302:2002. Geometrical Product Specification (GPS).
- UNE-EN ISO 25178-70:2014. Geometrical product specification (GPS) - Surface texture: Areal - Part 70: Material measures (ISO 25178-70:2014) (Endorsed by AENOR in January of 2015.)
- ISO 1101:2003. Geometrical Product Specification (GPS) - Geometrical tolerancing - Tolerances of form, orientation, location and run-out (ISO 1101:2012, including Cor 1:2013) (Endorsed by AENOR in April of 2013.)
- UNE-EN ISO 17450-1:2015. Geometrical product specifications (GPS) - General concepts - Part 1: Model for geometrical specification and verification (ISO 17450-1:2011)
- UNE-EN ISO 14638:2015. Geometrical product specifications (GPS) - Matrix model (ISO 14638:2015) (Endorsed by AENOR in March of 2015.)
- UNE-EN ISO 3040:2015. Geometrical product specifications (GPS) - Dimensioning and tolerancing - Cones (ISO 3040:2009)

9.2. Tests description and results

9.2.1. Compression tests

Compression stress tests are inherently crucial to the definition of part geometry and its behavior as mechanical entities. As in the case of the tensile stress tests, this test series has been executed to attest the mechanical properties of PLA-enhanced materials and their relationship to printing setup and techniques.

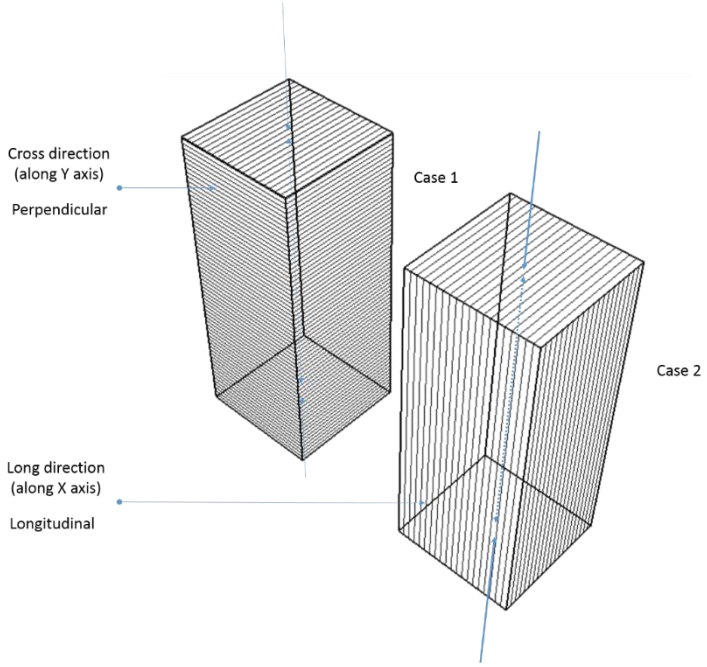

Fig. 1. Possible filament layouts –along X and Y directions- and physical PLA specimen

Figure 1 shows the two part sub-types used for the destructive compression analysis. Although the upper layer is undifferentiated at all effects, the vertical ones have normal directions to one another. Case 1 displays a geometry with filament layers oriented perpendicular to the load direction -vertical; case 2 filament orientation is parallel to the load -horizontal. Although both sub-types have theoretically the same amount of material, geometry, infill proportion, and weight. Consequently, it is possible to study the different load paths that traverse the part when using different filament configurations from the analysis of the crack geometry and other structural fatigue signs.

The test specimen was modeled with a dimension of 20mm x 20mm x 50mm, but its actual size may differ due to slight printing inaccuracies. Although specimens were produced to comply with standardized tolerances, the experiments yield different results depending on the accuracy of the parts, which is displayed on the tables following each test. These threw hints as to how the printing quality influenced the final part in terms of structural capacity.

- **Test 1:**

  The part and material set-up follow:

  - Material settings: PLA Carbon 25%;
  - Geometry settings: 20% fill; fiber parallel; S =20.3 x 20.8mm, mass 11.49g;

  Test results:

  - L= 59.6 mm g;
  - V= 180 N/sg;
  - F= 679 Kp; T= 15.8 N/ mm^2.

Table 1. Part print set up and results

	Part setup		Geometry setup					Test		
Stress type	Fill density	Fiber direction	Effective load area, (cm)	Effective load area (cm^2)	Effective structural area (cm^2)	Mass (g)	L (mmg)	V (N/sg)	Load Force (kp)	T Stress (N/mm^2)
Compression	20%	Parallel	20.3 x 20.8	99.195	19.839	11.49	59.6	180	679	15.8

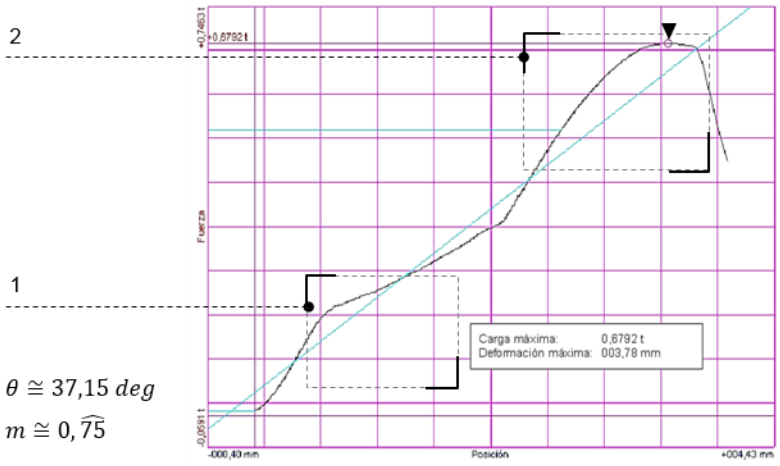

Fig. 2. Part 1, results of compression stress test

- **Test 2:**

  The part and material set-up follow:

  - Material settings: PLA Carbon 25%;
  - Geometry settings: 20% fill; fiber parallel; S =20.3 x 20.8mm, mass 11.49g;

  Test results:

  - L= 59.6 mm g;
  - V= 180 N/sg;
  - F= 731 Kp; T= 17.0 N/ mm^2.

Table 2. Part print set up and results

	Part setup		Geometry setup					Test		
Stress type	Fill density	Fiber direction	Effective load area, (cm)	Effective load area (cm^2)	Effective structural area (cm^2)	Mass (g)	L (mmg)	V (N/sg)	Load Force (kp)	T Stress (N/mm^2)
Compression	20%	Parallel	20.3 x 20.8			11.49	59.6	180	731	17.0

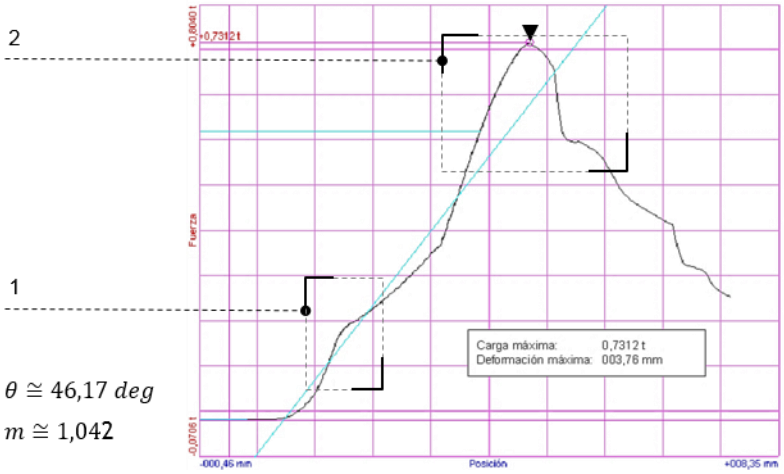

Fig. 3. Part 2, results of compression stress test

- **Test 3:**

  The part and material set-up follow:

  - Material settings: PLA Carbon 25%;
  - Geometry settings: 20% fill; fiber perpendicular; S =20.3 x 20.8mm, mass 12.27g;

  Test results:

  - L= 59.6 mm g;
  - V= 180 N/sg;
  - F= 813 Kp; T= 18.9 N/ mm^2.

Table 3. Part print set up and results

	Part setup		Geometry setup					Test		
Stress type	Fill density	Fiber direction	Effective load area, (cm)	Effective load area (cm^2)	Effective structural area (cm^2)	Mass (g)	L (mmg)	V (N/sg)	Load Force (kp)	T Stress (N/mm^2)
Compression	20%	Perp	20.3 x 20.8			12.27	59.6	180	813	18.9

$\theta \cong 64{,}36\ deg$

$m \cong 2{,}083$

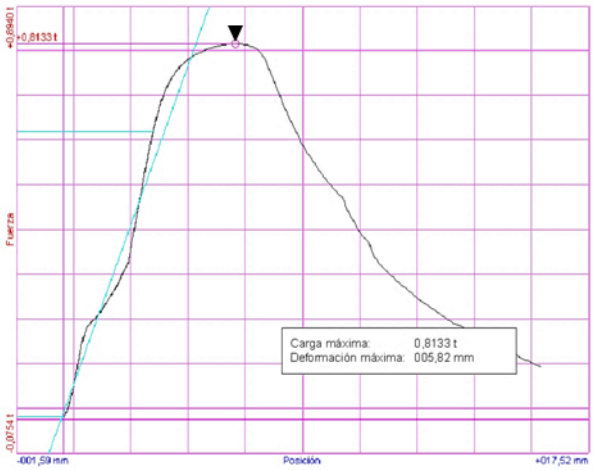

Fig. 4. Part 3, results of compression stress test

- **Test 4:**

  The part and material set-up follow:

  - Material settings: PLA Carbon 25%;
  - Geometry settings: 20% fill; fiber perpendicular; S =20.3 x 20.8mm, mass 12.27g;

  Test results:

  - L= 59.6 mm g;
  - V= 180 N/sg;
  - F= 786 Kp; T= 18.2 N/ mm^2.

Table 4. Part print set up and results

	Part setup		Geometry setup					Test		
Stress type	Fill density	Fiber direction	Effective load area, (cm)	Effective load area (cm^2)	Effective structural area (cm^2)	Mass (g)	L (mmg)	V (N/sg)	Load Force (kp)	T Stress (N/mm^2)
Compression	20%	Perp	20.3 x 20.8			12.27	59.6	180	786	18.2

$\theta \cong 65{,}72\ deg$

$m \cong 2{,}212$

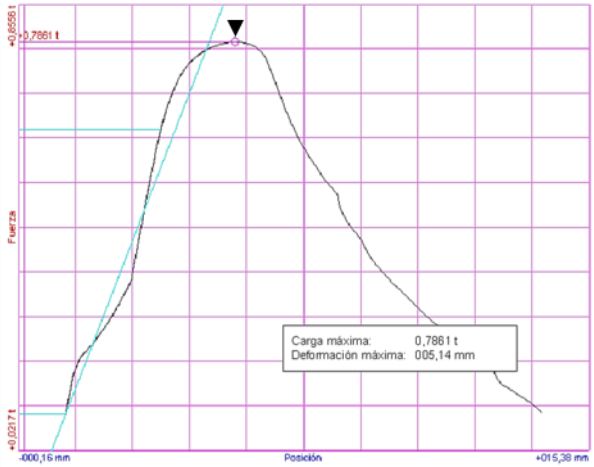

Fig. 5. Part 4, results of compression stress test

9.2.2. Tensile stress

3D printed parts are normally subject to no external loads, especially if considering rapid prototyping features and applications. While compression stress analysis is typically conducted for testing specimens and evaluating material behavior, tensile stress is less likely to be found in the scrutiny of printed parts. In other words, printing parts are, if at all, habitually subject to compression forces. As the present thesis deals with 3D printing for construction purposes, it is necessary to do a comprehensive research on this particular matter. Tensile stress tests are, thus, a complimentary check for both material and mechanical properties, and must be considered as such. Layer orientation is even more crucial in tensile models than in compression models, as the effective area is reduced creating weak lines or planes. Figure 2 depicts a typical layer situation showing the weak line caused by layer deposition. Actual proportions are arduous to calculate due to the dimensions of the printed filament.

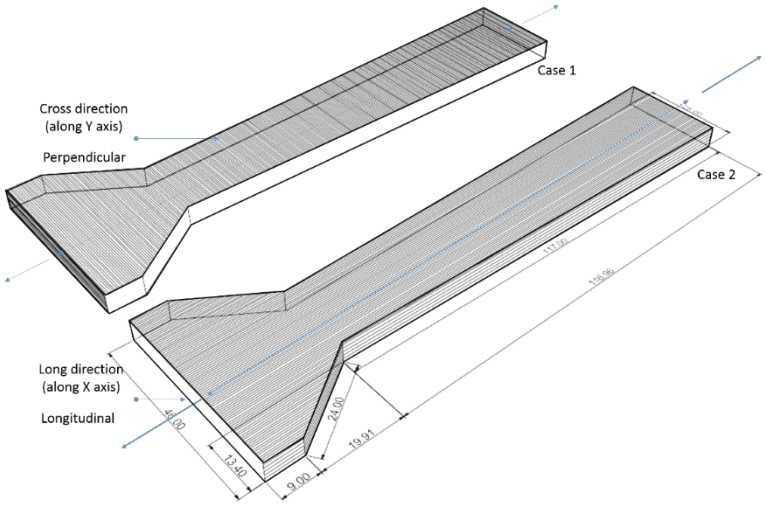

Fig. 6. Possible filament layouts and actual test parts –along X and Y directions.

Figure 6 shows the two part sub-types used for the destructive tensile analysis. As it can be seen, their shape differs considerably from that of the part used for compression analysis. The shape intends to allow for a good grip in the machine while allowing to exactly define a minimum structural section exactly in the middle of the part. The direction of the upper and vertical layers changes radically the behavior of the part, as the load travels either along the fiber or across different fibers. Case 1 illustrates a geometry with a filament perpendicular to the stress direction; case 2 filament is oriented in a direction parallel to its force, thus allowing for a maximized use of the fiber section. As in the case of compression tests, parts have been designed with the same amount of material, geometry, infill proportion, and weight. Hence, it is possible to study the different load paths that traverse the part when using different filament configurations.

The part has a bounding dimension of 146mm x 46mm x 5.5mm. Its actual geometry is described above in figure 6.

- **Test 1:**

  The part and material set-up follow:

  - Material settings: PLA Carbon 25%;
  - Geometry settings: 20% fill; fiber perpendicular to applied force; perpendicular fiber direction; S =19.45 x 5.10, mass 14.12 g;

  Test results:

  - V= 30 N/sg;
  - F= 147.5 Kp;
  - T= 14.6 N/ mm^2.

Table 5. Part print set up and results

	Part setup		Geometry setup				Test		
Stress type	Fill density	Fiber direction	Effective load area, (cm)	Effective load area (cm^2)	Effective structural area (cm^2)	Mass (g)	V (N/sg)	Load Force (kp)	T Stress (N/mm^2)
Tensile	20%	Perp	19.45x 5.10	99.195	19.839	14.12	30	147.5	14.6

$\theta \cong 51{,}91\ deg$

$m \cong 1{,}275$

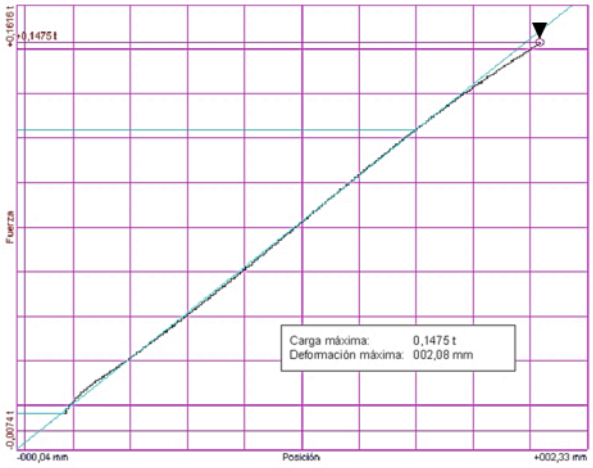

Fig. 7. Part 1, results of tensile stress test

- **Test 2:**

  The part and material set-up follow:

  - Material settings: PLA Carbon 25%;
  - Geometry settings: 20% fill; fiber perpendicular; S =17.7 x 5.13, mass= 14.12 g;

  Test results:

  - V= 30 N/sg;
  - F= 141.2 Kp;
  - T= 15.2 N/ mm^2.

Table 6. Part print set up and results

	Part setup		Geometry setup				Test		
Stress type	Fill density	Fiber direction	Effective load area, (cm)	Effective load area (cm^2)	Effective structural area (cm^2)	Mass (g)	V (N/sg)	Load Force (kp)	T Stress (N/mm^2)
Tensile	20%	Perp	17.7x 5.13	90.801	18.160	14.12	30	141.2	15.2

$\theta \cong 50,78deg$

$m \cong 1,225$

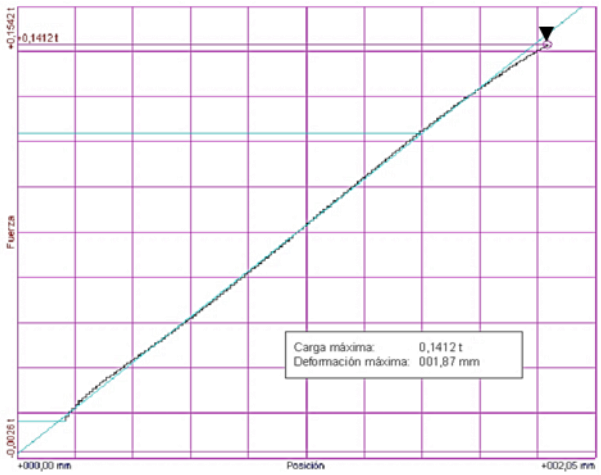

Fig. 8. Part 2, results of tensile stress test

- **Test 3:**

  The part and material set-up follow:

  - Material settings: PLA Carbon 25%;
  - Geometry settings: 20% fill; fiber perpendicular; S= 17.75 x 5.10; mass= 14.12 g;

  Test results:

  - V= 30 N/sg;
  - F= 146.7 Kp;
  - T= 15.9 N/ mm^2.

Table 7. Part print set up and results

	Part setup		Geometry setup				Test		
Stress type	Fill density	Fiber direction	Effective load area, (cm)	Effective load area (cm^2)	Effective structural area (cm^2)	Mass (g)	V (N/sg)	Load Force (kp)	T Stress (N/mm^2)
Tensile	20%	Perp	17.75x 5.1	90.525	18.105	14.12	30	146.7	15.9

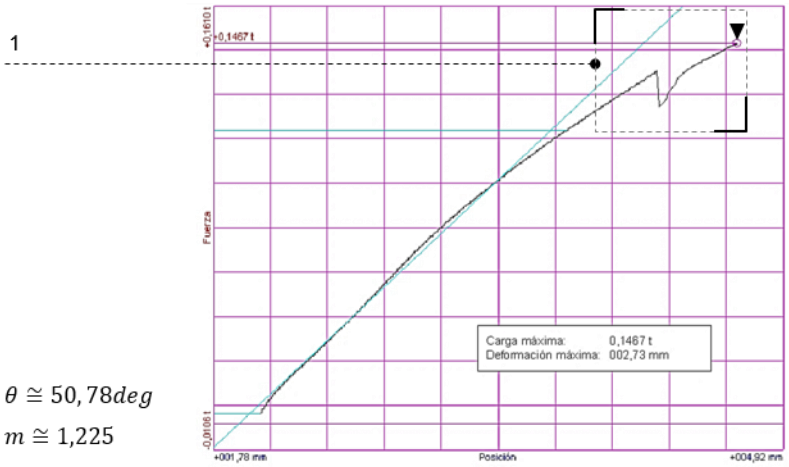

Fig. 9. Part 3, results of tensile stress test

- **Test 4:**

  The part and material set-up follow:

  - Material settings: PLA Carbon 25%;
  - Geometry settings: 20% fill; fiber perpendicular; S= 18.15 x 5.15; mass= 11.19 g;

  Test results:

  - V= 60 N/sg;
  - F= 196.2 Kp;
  - T= 20.6 N/mm^2.

Table 8. Part print set up and results

	Part setup		Geometry setup				Test		
Stress type	Fill density	Fiber direction	Effective load area, (cm)	Effective load area (cm^2)	Effective structural area (cm^2)	Mass (g)	V (N/sg)	Load Force (kp)	T Stress (N/mm^2)
Tensile	20%	Perp	18.15x 5.15	93.4725	18.6945	11.19	60	196.2	20.6

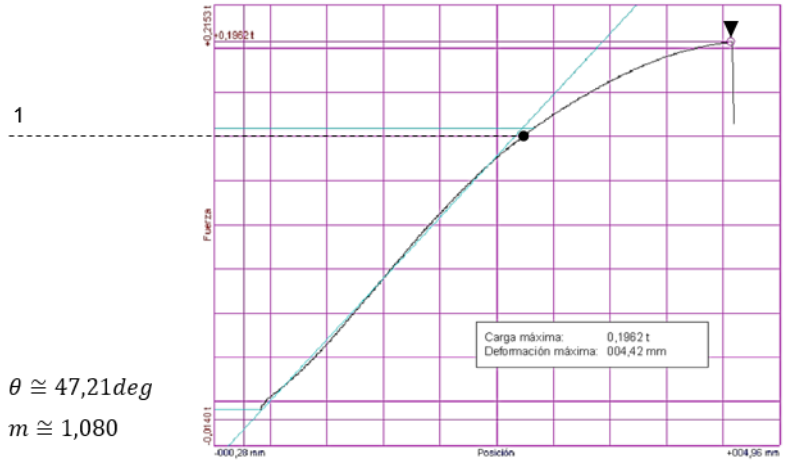

Fig. 10. Part 4, results of tensile stress test

- **Test 5:**

  The part and material set-up follow:

  - Material settings: PLA Carbon 25%;
  - Geometry settings: 20% fill; fiber perpendicular; S= 18.13 x 5.20; mass= 11.19 g;

  Test results:

  - V= 60 N/sg;
  - F= 178.8 Kp;
  - T= 18.6 N/ mm^2.

Table 9. Part print set up and results

	Part setup		Geometry setup				Test		
Stress type	Fill density	Fiber direction	Effective load area, (cm)	Effective load area (cm^2)	Effective structural area (cm^2)	Mass (g)	V (N/sg)	Load Force (kp)	T Stress (N/mm^2)
Tensile	20%	Perp	18.13x 5.20	94.276	18.8552	11.19	60	178.8	18.6

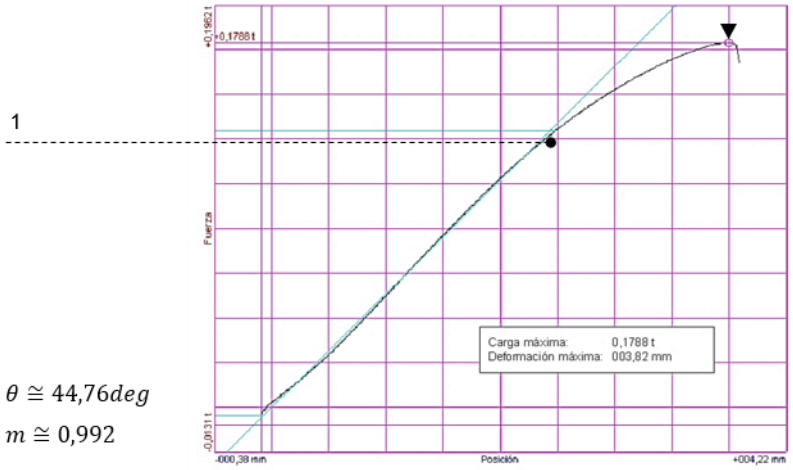

Fig. 11. Part 5, results of tensile stress test

- **Test 6:**

  The part and material set-up follow:

  - Material settings: PLA Carbon 25%;
  - Geometry settings: 20% fill; fiber perpendicular; S =18.12 x 5.26; mass 11.19 g;

  Test results:

  - V= 60 N/sg;
  - F= 195.8 Kp;
  - T= 20.1 N/mm^2.

Table 10. Part print set up and results

	Part setup		Geometry setup				Test		
Stress type	Fill density	Fiber direction	Effective load area, (cm)	Effective load area (cm^2)	Effective structural area (cm^2)	Mass (g)	V (N/sg)	Load Force (kp)	T Stress (N/mm^2)
Tensile	20%	Perp	18.12x 5.26	95.3112	19.0622	11.19	60	195.8	20.1

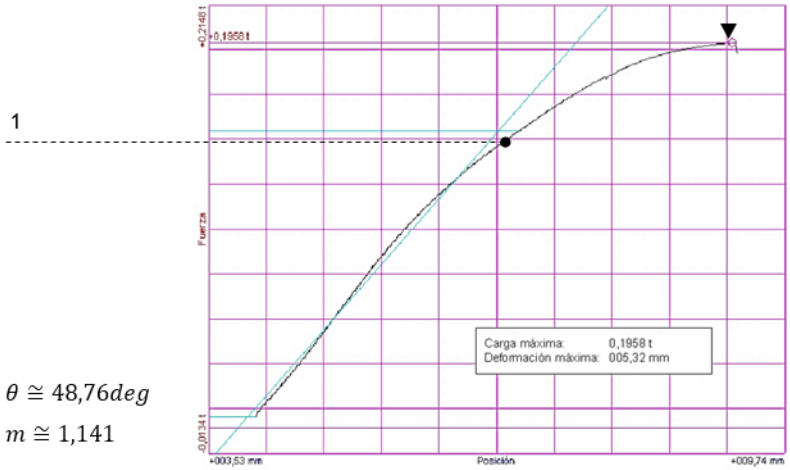

Fig. 12. Part 6, results of tensile stress test

- **Test 7 – Section B:**

  The part and material set-up follow:

  - Material settings: PLA Carbon 25%;
  - Geometry settings: 20% fill; fiber perpendicular; S =3.5 x 18.8; mass 10.07 g;

  Test results:

  - V= 20 N/sg;
  - F= 315.6 Kp;
  - T= 47.0 N/mm^2.

Table 11. Part print set up and results

	Part setup		Geometry setup				Test		
Stress type	Fill density	Fiber direction	Effective load area, (cm)	Effective load area (cm^2)	Effective structural area (cm^2)	Mass (g)	V (N/sg)	Load Force (kp)	T Stress (N/mm^2)
Tensile	20%	Perp	3.5x18.8			10.07	20	315.6	47.0

$\theta \cong 47{,}55deg$

$m \cong 1{,}093$

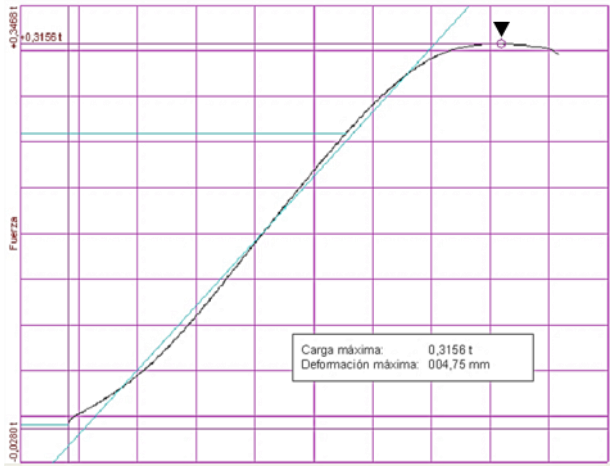

Fig. 13. Part 7, results of tensile stress test

- **Test 8 – Section B:**

  The part and material set-up follow:

  - Material settings: PLA Carbon 25%;
  - Geometry settings: 20% fill; fiber perpendicular; S =3.5 x 17.26; mass 10.23 g;

  Test results:

  - V= 20 N/sg;
  - F= 311.8 Kp;
  - T= 50.6 N/mm^2.

Table 12. Part print set up and results

	Part setup		Geometry setup				Test		
Stress type	Fill density	Fiber direction	Effective load area, (cm)	Effective load area (cm^2)	Effective structural area (cm^2)	Mass (g)	V (N/sg)	Load Force (kp)	T Stress (N/mm^2)
Tensile	20%	Perp	3.5x17.26			10.23	20	311.8	50.6

$\theta \cong 42{,}54deg$

$m \cong 0{,}917$

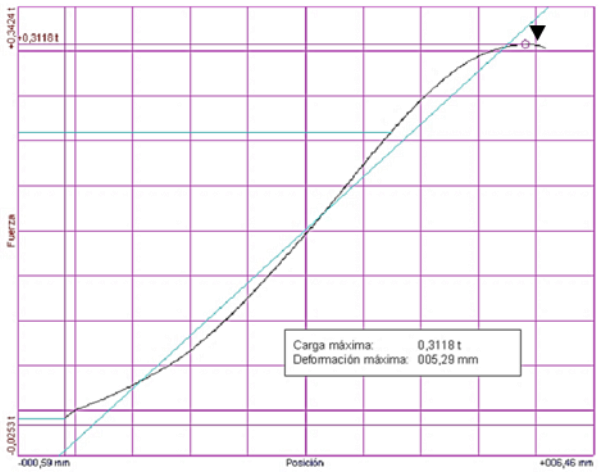

Fig. 14. Part 8, results of tensile stress test

- **Test 9 – Section B:**

  The part and material set-up follow:

  - Material settings: PLA Carbon 25%;
  - Geometry settings: 20% fill; fiber perpendicular; S =3.42 x 20.14; mass 6.67 g;

  Test results:

  - V= 20 N/sg;
  - F= 59.0 Kp;
  - T= 8.4 N/mm^2.

Table 13. Part print set up and results

	Part setup		Geometry setup				Test		
Stress type	Fill density	Fiber direction	Effective load area, (cm)	Effective load area (cm^2)	Effective structural area (cm^2)	Mass (g)	V (N/sg)	Load Force (kp)	T Stress (N/mm^2)
Tensile	20%	Perp	3.42x20.14			6.67	20	59.0	8.4

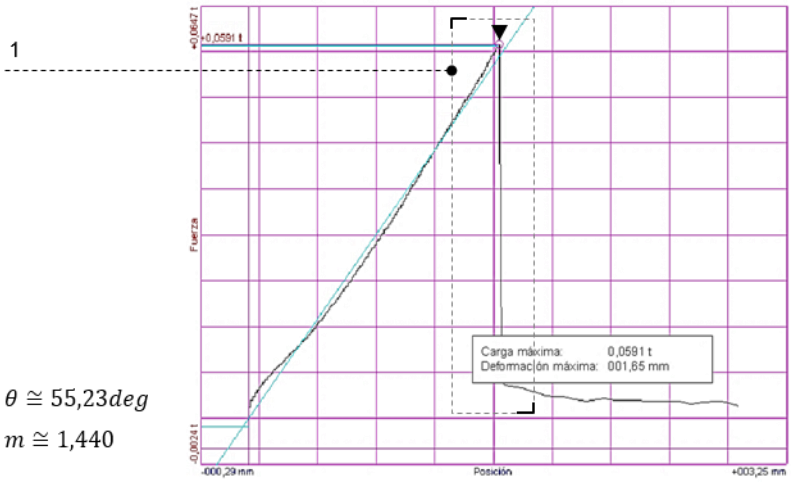

Fig. 15. Part 9, results of tensile stress test

- **Test 10 – Section B:**

  The part and material set-up follow:

  - Material settings: PLA Carbon 25%;
  - Geometry settings: 20% fill; fiber perpendicular; S = 3.6 x 19.04; mass 6.60 g;

  Test results:

  - V= 20 N/sg;
  - F= 70.9 Kp;
  - T= 10.1 N/mm^2.

Table 14. Part print set up and results

	Part setup		Geometry setup				Test		
Stress type	Fill density	Fiber direction	Effective load area, (cm)	Effective load area (cm^2)	Effective structural area (cm^2)	Mass (g)	V (N/sg)	Load Force (kp)	T Stress (N/mm^2)
Tensile	20%	Perp	3.6x19.04			6.60	20	70.9	10.1

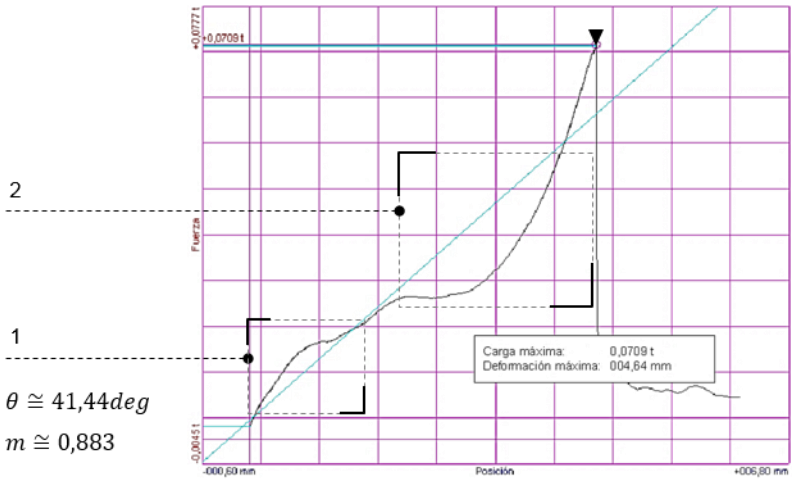

Fig. 16. Part 10, results of tensile stress test

9.2.3. Bending stress

Bending or combined compression-tensile stress is typical in building formations and structures. Although this is normally not the aim of general 3D printed parts, the present thesis aims at eventually creating a method and apparatus to print large objects for the construction industry, among others. Looking at bending stress and analyzing the material and geometrical behavior of parts is thus a key issue in the analysis of the structural performance of printed parts. As in previous cases, the filament layout plays an important role in the part's behavior, as well as printing settings such as printing speed, temperature, or layer height.

Test parts are conceived following the same rules applying to previous cases, and respecting the exact same geometrical constraints. Figure 17 illustrates a typical part situation with different filament layouts.

Parts are 20mm x 20mm x 100mm in size, allowing for enough "beam" length as to be able to evaluate the influence of bending under different situations. Generally, length between supports is 100 mm. Actual dimensions and test conditions are disclosed for each case scenario.

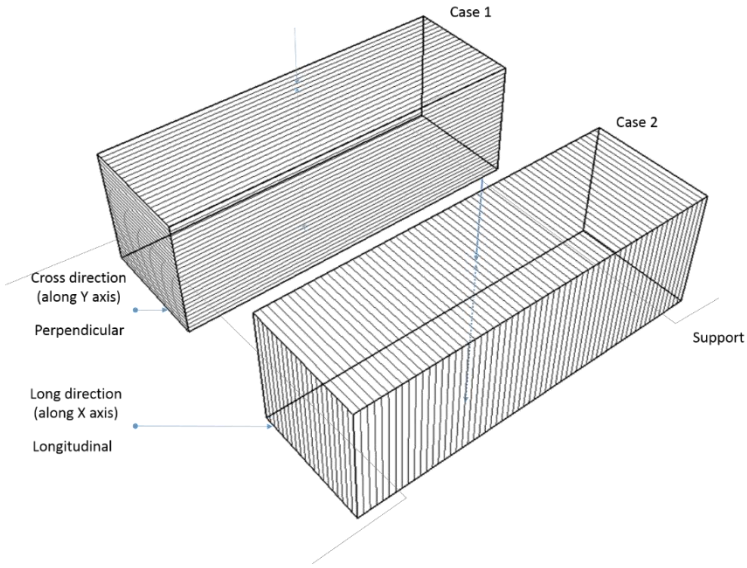

Fig. 17. Possible filament layouts –along X and Y directions

- **Test 1 – Section B:**

  The part and material set-up follow:

  - Material settings: PLA Carbon 25%;
  - Geometry settings: 20% fill; fiber parallel; S = 51.77 x 3.86; mass 26.27 g;

  Test settings:

  - L = 134.2mm (part);
  - D = 100mm (supports);
  - V= 5 N/sg;

  Test results:

  - Deflection = 31.96mm;
  - F=53.7 Kp;
  - Tf = F*dist/(A*B2) = 68.35 N/mm^2

Table 15. Part print set up and results

	Part setup		Geometry setup					Test				
Stress type	Fill density	Fiber dir	Effective load area, (A xB, cm)	Effective load area (cm²)	Effective structural area (cm²)	Mass (g)	L (mm)	D (mm)	V (N/sg)	Defl (mm)	Load Force (kp)	Tf (N/mm²)
Bending	20%	Para	51.77 x 3.86			26.27	134.2	100	20	31.96	53.7	68.35

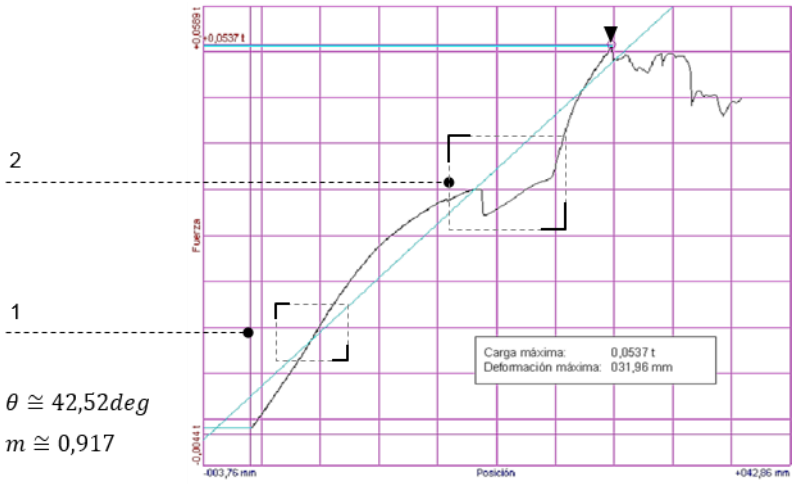

Fig. 19. Part 1, results of bending stress test

- **Test 2 – Section B:**

  The part and material set-up follow:

  - Material settings: PLA Carbon 25%;
  - Geometry settings: 20% fill; fiber perpendicular; S = 19.94 x 20.24; mass 25.32 g;

  Test setting:

  - L = 150mm (part);
  - D = 100mm (supports);
  - V= 20 N/sg;

  Test results:

  - Deflection = 5.84mm;
  - F=136.5 Kp;
  - Tf = F*dist/(A*B2) = 16.4 N/mm^2

Table 16. Part print set up and results

	Part setup		Geometry setup					Test				
Stress type	Fill density	Fiber dir	Effective load area, (A xB, cm)	Effective load area (cm²)	Effective structural area (cm²)	Mass (g)	L (mm)	D (mm)	V (N/sg)	Defl (mm)	Load Force (kp)	Tf (N/mm²)
Bending	20%	Perp	19.94 x 20.24			25.32	150	100	20	5.84	136.5	16.4

$\theta \cong 42{,}52deg$

$m \cong 0{,}917$

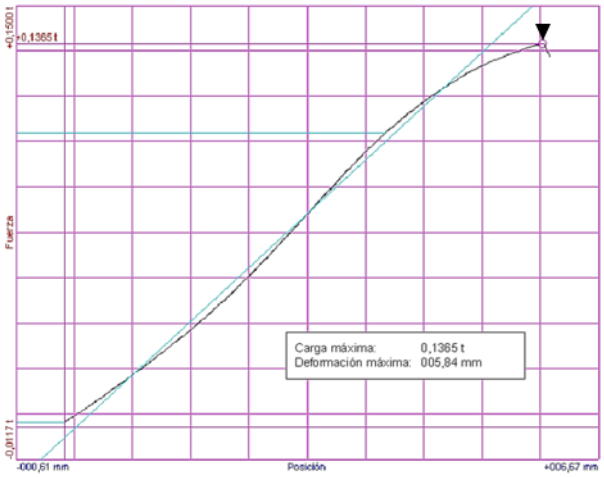

Fig. 20. Part 2, results of bending stress test

- **Test 3 – Section B:**

  The part and material set-up follow:

  - Material settings: PLA Carbon 25%;
  - Geometry settings: 20% fill; fiber perpendicular; S = 19.94x20.24; mass 25.32 g;

  Test setting:

  - L = 150mm (part);
  - D = 100mm (supports);
  - V= 20 N/sg;

  Test results:

  - Deflection = 5.9mm;
  - F=137.4 Kp;
  - Tf = F*dist/(A*B2) = 16.5 N/mm^2

Table 17. Part print set up and results

	Part setup		Geometry setup					Test				
Stress type	Fill density	Fiber dir	Effective load area, (A x B, cm)	Effective load area (cm^2)	Effective structural area (cm^2)	Mass (g)	L (mm)	D (mm)	V (N/sg)	Defl (mm)	Load Force (kp)	Tf (N/mm^2)
Bending	20%	Perp	19.94 x 20.24			25.32	150	100	20	5	137.4	16.5

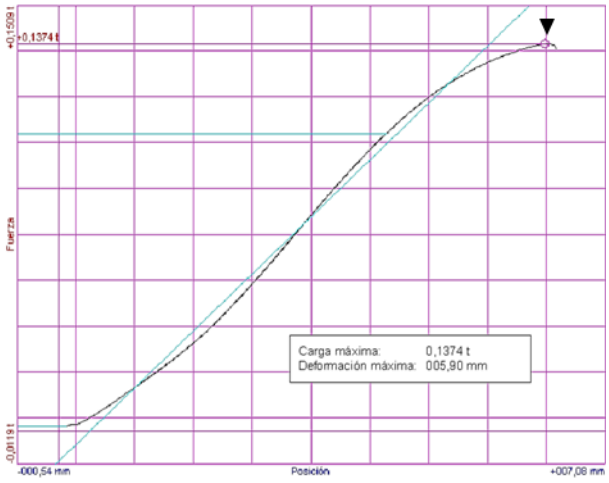

$\theta \cong 43{,}96\ deg$

$m \cong 0{,}964$

Fig. 21. Part 3, results of bending stress test

- **Test 4 – Section B:**

  The part and material set-up follow:

  - Material settings: PLA Carbon 25%;
  - Geometry settings: 20% fill; fiber perpendicular; S = 19.94 x 20.24; mass 25.32 g;

  Test setting:

  - L = 150mm (part);
  - D = 100mm (supports);
  - V= 20 N/sg;

  Test results:

  - Deflection = 3.5mm;
  - F=93.8 Kp;
  - Tf = F*dist/(A*B2) = 11.3 N/mm^2

Table 18. Part print set up and results

	Part setup		Geometry setup					Test				
Stress type	Fill density	Fiber dir	Effective load area, (A xB, cm)	Effective load area (cm²)	Effective structural area (cm²)	Mass (g)	L (mm)	D (mm)	V (N/sg)	Defl (mm)	Load Force (kp)	Tf (N/mm²)
Bending	20%	Perp	19.94 x 20.24			25.32	150	100	20	3.5	93.8	11.3

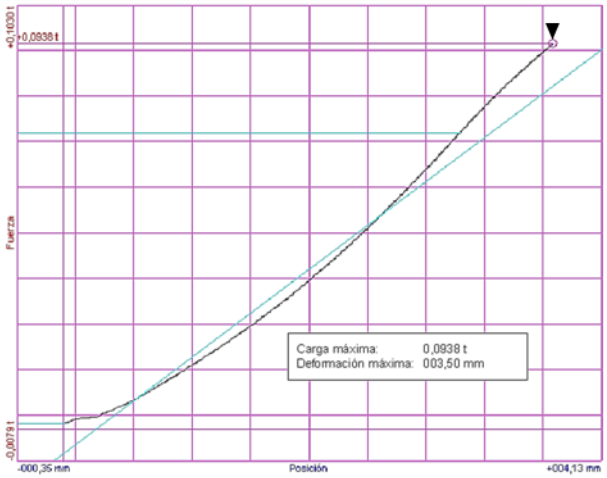

$\theta \cong 34{,}61 deg$

$m \cong 0{,}690$

Fig. 22. Part 4, results of bending stress test

- **Test 5 – Section B:**

  The part and material set-up follow:

  - Material settings: PLA Carbon 25%;
  - Geometry settings: 20% fill; fiber perpendicular; S = 19.94 x 20.24; mass 26.27 g;

  Test setting:

  - L = 150mm (part);
  - D = 100mm (supports);
  - V= 20 N/sg;

  Test results:

  - Deflection = 2.95mm;
  - F= 74.3 Kp;
  - Tf = F*dist/(A*B2) = 8.9 N/mm^2

Table 19. Part print set up and results

	Part setup		Geometry setup					Test				
Stress type	Fill density	Fiber dir	Effective load area, (A xB, cm)	Effective load area (cm²)	Effective structural area (cm²)	Mass (g)	L (mm)	D (mm)	V (N/sg)	Defl (mm)	Load Force (kp)	Tf (N/mm²)
Bending	20%	Perp	19.94 x 20.24			26.27	150	100	20	2.95	74.3	8.9

$\theta \cong 34{,}61deg$

$m \cong 0{,}690$

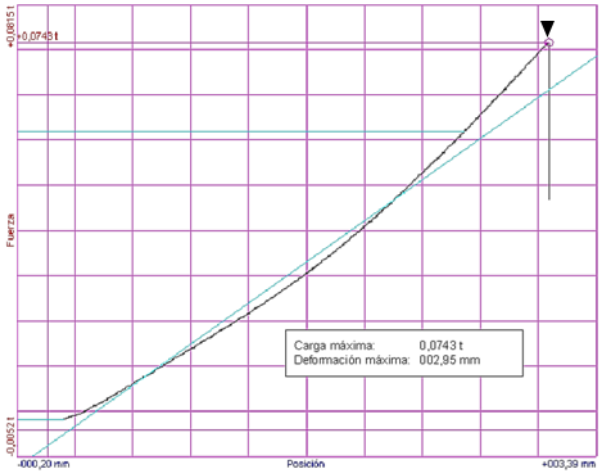

Fig. 23. Part 5, results of bending stress test

9.3. Fracture type analysis

PLA parts display typical fracture types and geometries as a general rule. Despite this fact, there are several specific issues that must be taken into account, showing particularities in respect to how the piece was built. As said above, the printing setup affected the behavior of the part, which can clearly be read in the fractures themselves.

This section shows different fractures and the resulting part geometry of several specimens after the stress test, performing a visual analysis in order to evaluate the results obtained in section 8.2. A more comprehensive analysis is out of the scope of the thesis, but sufficient data is gathered and provided for further research.

The main differences between parts displaying different filament orientations are related to layers slipping on others or the infill behavior. The orientation of the strains influences the tests depending on the force direction as well.

9.3.1. Compression fractures

Compression tests display a characteristic behavior. The outcome of the several experiments that were put into practice throughout the structural studies turned out consistent. Regardless the fiber direction, all parts displayed a certain degree of movement or slipperiness between material layers. In those parts where layer where perpendicular to the applied force, this yielded a fracture pattern that evidenced the diagonal path of the force traveling through the piece (this is, the force travelled the part in a non-vertical way, gaining a horizontal factor in each layer. This misalignment of the vector's base and end points generated, as said, a horizontal component that the part is unable to withstand at certain weak points of the geometry, namely between 2 consecutive layers of material. Thus, the part breaks on side at the bottom and on the opposite side at the top. Each fracture shows the same visual appearance, therefore sharing their properties and behavior. At each fracture, a bending-like failure is observed.

In addition to that, it is noticeable that fractures display a certain degree of elasticity before the final structural failure of the part. The compressed face segments exhibit a large inward-oriented movement that seems to be absorbed by the flexible infill pattern used in each piece. Once these segments are unable to take in more load, then the outer corresponding face segments –located in the opposite sides- are subject to the horizontal stress, causing them to fail and break as a consequence of a too large tensile stress.

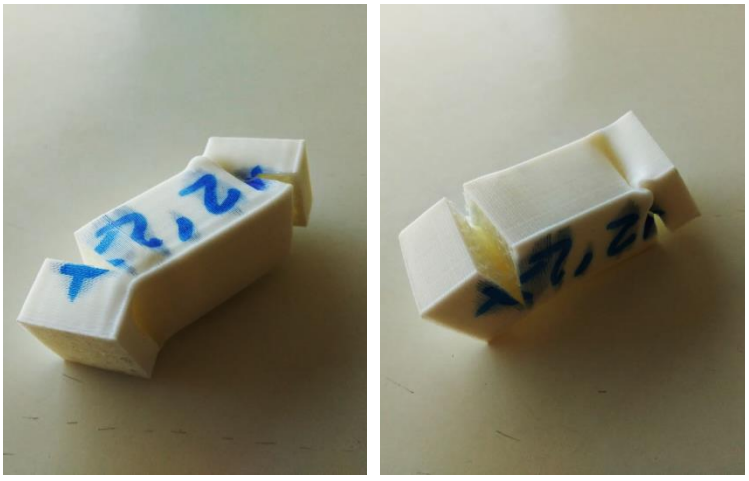

Fig. 24. Part displaying fracture after compression stress test –strains perpendicular to force.

As seen in figure 24, the failure pattern under sheer compression stress differs greatly from archetypical compression patterns where the fracture is produced approximately at the middle of the part following a double inverted cone-like form. As said above, this is due to the way the load "travels" through the discontinuous infill.

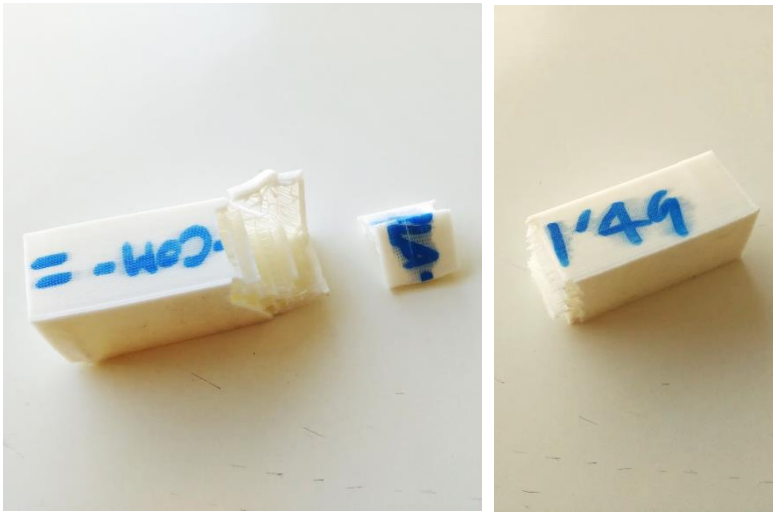

Fig. 25. Part displaying fracture after compression stress test – strains parallel to force.

Parts with fibers parallel to the applied force have a slight different performance. Although tests are prepared and conducted following exactly the same steps, the distinct morphology of the specimens plays and important role. In this case, parts break merely at one end of the part, and in a more abrupt way. Although the force travels the same way, it seems that the fiber continuity along the force's vector allows the part to withstand horizontal components better to some extent. As a consequence, the parts fail in a more abrupt way, showing a fracture 45º angled fracture. This is a common type among compression tests where the part's structural soundness is insufficient to withstand high loads or pressures. This pattern may also be due to improper test preparation in some cases, although this does not seem to be the case as this pattern is repeated recurrently throughout the test performed on these part types. Figure 26 depicts two different parts with a similar fracture type.

9.3.2. Tensile fractures

Fractures to tensile stresses are also meaningfully characterized by the part's printing setup. In the first case, the parts with a fiber direction parallel to the test force (from now case 1) break clean at the piece's weakest spot –that prepared for the test as such. On the contrary, specimens with a perpendicular fiber orientation display more irregular fracture patterns (case 2). Despite some failed parts, most tests displayed a consistent tendency to break at the same segment (see figures 26 and 27). Approximately 10% of the parts broke at a different segment, which may be caused either to faulty printing conditions or defective specimen preparation, despite the efforts done to avoid those.

Figure 27 shows the typical fracture pattern of a case 2 piece. As it can be seen, the fracture is not clean, and the first layer of material (shell) slithered on the second, demonstrating a high degree of material inconsistency. As a consequence, it is possible to improve the mechanical behavior of the part by "gluing" the different layers together. Shells are used to improve the finish quality of parts and can be defined in many 3D printing software packages, although shell layers are less usually structurally coherent as it would be desirable. Although this is the case for the parts printed with this particular setup and strain orientation, the fracture continues to be archetypical in both its location and geometry.

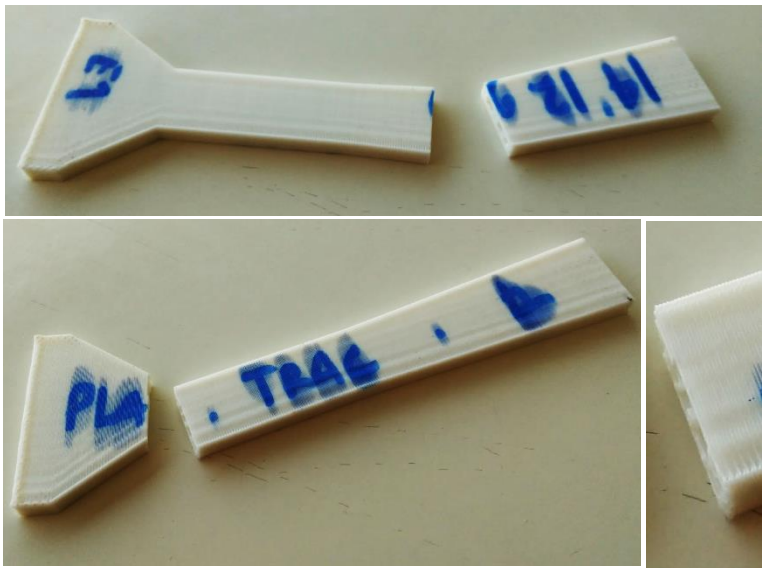

Fig. 26. Part displaying fracture after compression stress test – strains parallel to force: a (up) an atypical situation, b (bottom left) typical fracture location and morphology; c (bottom right) close-up.

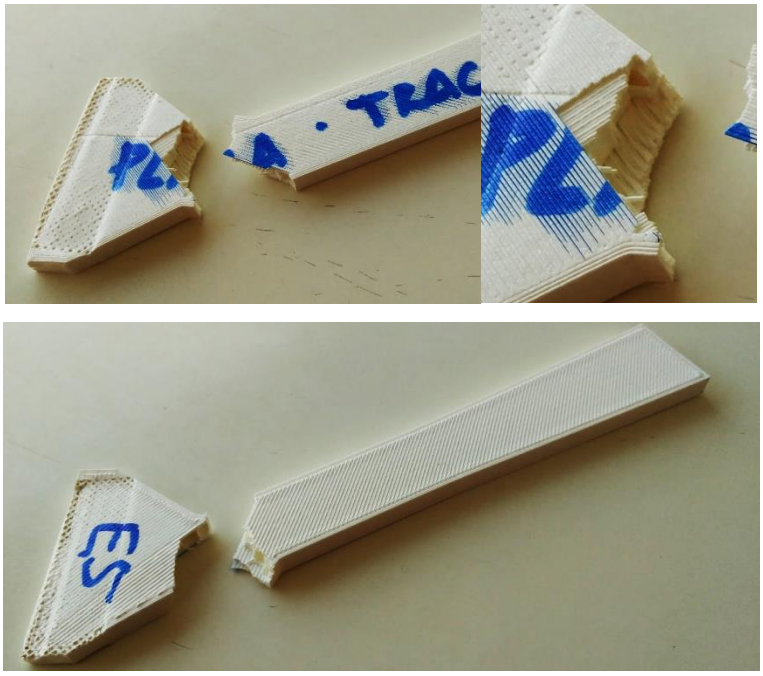

Fig. 27. Part displaying fracture after compression stress test – strains perpendicular to force: a (upper left) a typical fracture with "slippery" layers, b (upper right) close-up of fracture showing shell layers and infill; c (bottom right) typical fracture location and morphology.

Figure 26 depicts two different situations, both belonging to case 1. Although responding to the exact same conditions, figure 27 a. shows a fracture in an unexpected location of the part. The cause of this unexpected behavior is difficult to trace back, since it might be result of either an erroneous print –whereby the two consecutive layers of materials have not become coherent- or faulty testing. The first option is more likely to have triggered this particular affect, as tests were carefully planned and carried out. On the other hand, it is well known that FDM 3D printing still lacks the desirable reliability in terms of successful part repeatability –in other words, no two parts printed by using the same 3D printer and setup are exactly the same. Figure 27 b (above) is the typical and expected fracture, seen in approximately 90% of the test cases.

In comparison to compression tests, the fiber orientation seems to affect less the fracture typology in tensile studies.

9.3.3. Bending or flexural stress-related fractures

Flexural stress fracture geometrical patterns are seemingly the most similar among the different strain alignment option studies tested throughout. In both cases the fracture obeys the expected shape and logic, where the upper fibers are subject to compression (clean break) and the lower fibers to traction (as in the tensile stress, showing an irregular geometry). All in-between layers are characterized the same way according to their relative location to the neutral strain. In the specimens, this strain does not exist as such, and is substituted by a set of infill cells, which structural behavior is hardly predictable.

Figures 28 a) and b) show a typical case of a part with upper and lower fibers perpendicular to the force direction and the main part's axis. Figure 29 shows a part with fibers parallel to the part's main axis instead, which bears a relative importance as to justify its slightly better structural capacity of pieces to flexural stress. The fracture geometry is also affected, as long strains located in the lower face withstand more load due to the material's ability to elongate. Case 1 parts break due to material discontinuity issues, thoroughly discussed in previous cases.

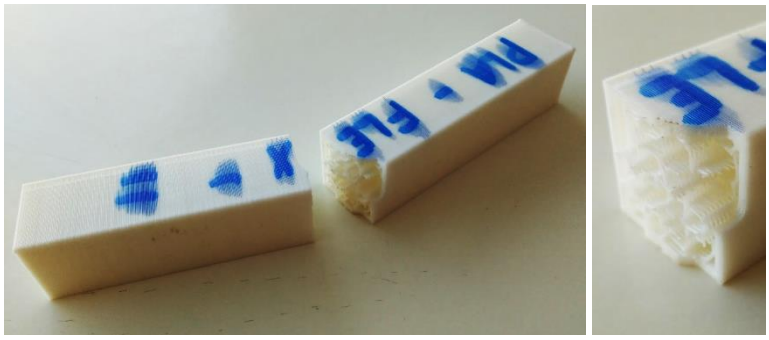

Fig. 28. Part displaying fracture after flexural stress test – strains parallel to force: a (left) a typical fracture, b (right) close-up showing infill deformation.

Fig. 29. Part displaying fracture after flexural stress test – strains perpendicular to force: a (left) a typical fracture, b (right) close-up showing infill deformation.

9.4. Use of concrete for 3D printing

Although there are only very few data sources for specific developments of concrete and concrete-like materials for 3D printing purposes, it is worthwhile mentioning some of the most relevant results obtained in the different studies. Although the major emphasis of the present chapter is put on printing setup differences, depicting concrete's features is also central to the thesis as a whole, all the more so when referring to architectural and building solutions *(Le, et al., Mix Design and fresh properties for high-performance printing concrete, 2012*).

The rheology of concrete is always a complex matter in construction, and is not only project-specific, but depends also on environmental conditions, humidity, temperature, and air quality among others. Different concrete types may be developed for obtaining different structural properties and behaviors. In "Hardened properties of high-performance printing concrete", Le, T. T. et al, present the "*effects of the layering process on density, compressive strength, flexural strength, tensile bond strength and drying shrinkage […] together with the implication for mix proportions*" (*Le, et al., Hardened properties of high-performance printing concrete, 2012*). The extrusion process was in this work shown to

retain the intrinsic high performance of concrete, despite some minor differences in terms of flexural and compression strength for a 9 mm diameter nozzle. Furthermore, this technology presented 75% less voids than mold-cast control, as illustrated in Figure 30. Concrete for 3D printing may be intuitively developed by taking advantage of the properties of self-compacting concrete and sprayed concrete.

Another work worth looking at in terms of the determination and characterization of a feasible concrete formula for 3D printing purposes, "Design of Concrete for 3D printing", (*Torres, 2016*), emphasizes on three main aspects:

- The elaboration of several high-resistance mortar tests
- The study of hardening times
- The incorporation of glass fibers in the concrete mix

The same work highlights the following premises for the elaboration of tests: (i) the use of relatively low water-to-cement ratios (ranging between 0.3 and 0.35); (ii) maintain sand to cement ratios as close to 1 to 1 as possible, and not lower than 0.67; and (iii) the incorporation of superplasticizer additives (*Erdogdu, 2005*) in order to achieve high resistance and good mechanical properties from the beginning and to better control the viscosity and density of the material. Superplasticizers have been studied for other concrete applications, such as projection or molding (*Morin, Tenoudjia, Feylessoufib, & Richard, 2001*) and is also regulated. Refer to The American Concrete Institue (*American Concrete Institute, ACI, 1998*) or UK Technical Sheets, (*UK Cement Admixtures Association (CAA), 2016*) for further information. Besides, the concrete material for printing must comply with a series of conditions, including, but not limited to: (i) a minimum fluidity as to guarantee that it can be pumped through the extruding device's piping system, and to avoid stuck gravel or undesired obstructions that would impeded the cored deposition of material; (ii) the "printability" of the material, understood as its capability to maintain the geometry once layered; (iii) the resistance of the material as it is being deposed and subject to bear loads; and (iv) the minimization of the time necessary to obtain the mentioned properties.

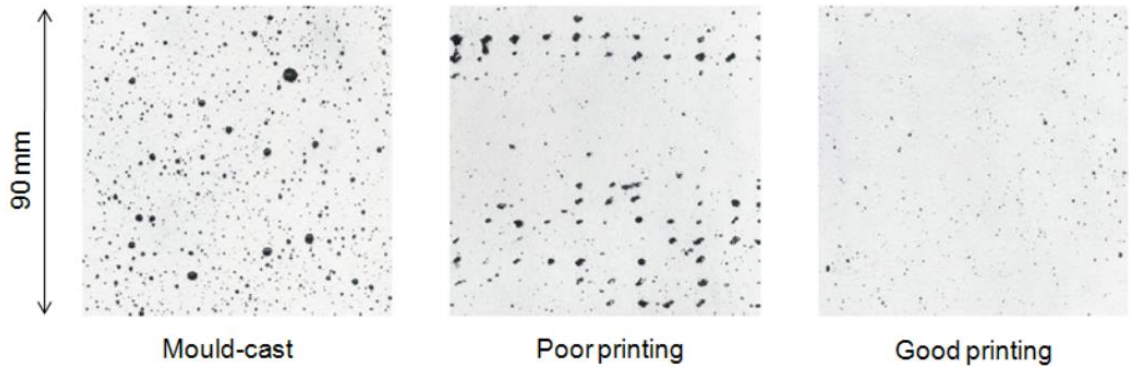

Fig. 30. Printed versus mould-casted concrete (Le, et al., Mix Design and fresh properties for high-performance printing concrete, 2012).

In the mentioned work, it is stated that it was possible to achieve hardening times lower than 50 seconds, which can be deemed optimal for 3D printing purposes at slow speed in large parts. The embedment of fibers of various types, sizes, and materials increased the initial and final flexural and compression yield stress capacity of the parts. These fibers accounted for a total of a 2% of the total printed material's weight, being especially meaningful those accounting for glass fiber materials.

Finally, the modification of some of these variables proved to have no relevant effect on the final material performance. For instance, the reduction of the mixing time did not affect the yield stress of tests, and can be surprisingly considered a quasi-irrelevant variable in structural terms.

9.5. Conclusions

Results show that PLA blended with carbon fibers in a 75% to 25% mix proportion does not significantly increase or enhance the original material's structural resistance. It was expected to obtain

substantially different results in terms of rigidity and stress in comparison with regular PLA. As a result, it can be stated that printing setup is more crucial to the behavior of the part than otherwise anticipated.

PLA material blends were expected to become crucial in the application of 3D printing to the building industry. Nevertheless, result speak otherwise. PLA with carbon fiber is far from matching the mechanical properties of concrete, steel, or wood. Despite the major advantages of printing plastic or composite materials in terms of flexibility or geometrical possibilities, PLA cannot compete for structural reasons. In fact, the PLA with carbon fibers blend used during the test, withstood merely a 0.005% of the maximum load capacity of B 500 SD steel (which elasticity module is E=250000 N/mm2), 0.05% of H 30 concrete (E = 26000 N/mm2), or 0.1% of wood (ranging between E=9000 N/mm2 and E=20000N/mm2). As a result, it is difficult to think of any PLA enhanced blend suitable for either construction or engineering purposes beyond those of non-structural parts.

On a more 3D related side, it becomes clear that the layer orientation has a quite reasonable impact on the behavior of the part as a whole. Beyond the materials properties themselves, fiber direction is a crucial set-up for the prints. As opposed to mold-produced parts, where material is distributed evenly and homogeneously, 3D printing relies on layers, which undoubtedly creates weak planes every layer. It is difficult to define and asses the exact influence of such a constraint on the performance of the part, since it itself depends on a series of settings, namely: (i) layer height; (ii) printing temperature; (iii) elapsed time from layer to layer.

For instance, smaller layer heights contribute positively to the tightness of the part, resulting in more solid and compact parts. A layer height of 0.1 mm will leave less space for weak lines than 0.2 mm, especially if parts are printed at the same pace. Printing temperature is also critical. Higher temperatures cause the material to fuse and reach a more fluid state, which again favors material continuity and layer coherence. For instance, printing large pieces above the vendor's recommended temperature might be a good idea for experienced users. Furthermore, higher temperatures require longer hardening times, which relates to the third issue. Although accurate measurements would be needed, printing on top of semi-fluid layers benefits the part, whereas printing on cold material creates weak spots or planes. Adjusting these three parameters is essential to determine and improve the quality of the final part.

The analysis of the load-to-deformation curves throws information worthwhile discussing:

- Compression tests show that PLA enhanced material displays a certainly regular curve. The curve shows a quasi-constant steepness in the elastic deformation phase. Beyond the maximum deformation or load point, the part deforms plastically without offering further stress capacity. Although parts are printed in the same manner and with identical methods, no piece is exactly the same. Small variations in shape and form affect their behavior.
- Tensile tests show more similar results across the different experiments. All parts have quite perfect curves resembling an ascendant linear gradient, although certain experiments stand out for having steeper curves. Again, this is due to the geometric conditions mentioned above and can be caused by either improper part geometry or the direction of the fibers. Only one part displays an irregular curve, probably due to erroneous printing.
- Bending stress tests are similar to tensile stress tests in that they display very similar results and share characteristics among themselves.

List of figures

Chapter 2

Chapter 3

Chapter 4

Chapter 5

Chapter 6

Annex I

Annex II

List of tables

Chapter 2

Chapter 4

Chapter 6

Chapter 8

Related publications and patent applications

Patent applications:

European Patent Application GB1515360.4 filed on 28 August 2015. Patent Reference NGK78451P.GBP. *Methods, Systems, and Apparatus for Construction of Three-Dimensional Objects*. Inventors: Baraja, G. & Nadal, A. Patent Holder: XcaLe3D (Formerly Naotech S.L.).

Published articles:

Nadal, A., Cifre, H., Pavón, J. & Liébana, O. (2017). Material use optimization in 3D printing through a physical simulation algorithm. *Automation in Construction*. Doi: 10.1016/j.autcon.2017.01.017. Journal Impact Factor (2015): 2.422 (8/61 in CONSTRUCTION & BUILDING TECHNOLOGY, Q1)

Del Solar, P., Del Río, M., Villoria, P., & Nadal, A. (2016, April). Analysis of Recurrent Defects in the Execution of Ceramic Coatings Cladding in Building Construction. *Journal of Construction Engineering and Management, 142*(4). Doi: 10:1061/(ASCE)CO.1943-7862.0001075. Journal Impact Factor (2015): 1.152 (26/61 in CONSTRUCTION & BUILDING TECHNOLOGY, Q2)

Nadal, A. & Pavón, J. (2014). The Self-Organizing City: An Agent-Based Approach to the Algorithmic Simulation of City-Growth Processes. Practical Applications of Intelligent Systems, pp. 397-407. *The 8th International Conference on Intelligent Systems and Knowledge Engineering, Nov. 20-23, 2013, ShenZhen, China*, doi: 10.1007/978-3-642-54927-4_38. Best Student Paper Award, ISKE, 2014.

Liébana, O., & Nadal, A. (2016). Digital Crafts, 3D Printing In Architecture. Arquitectura Viva. *Arquitectura Viva: Soluciones Españolas* (187.9), pp. 71-75.

Mayoral, E. & Nadal, A. (2011). Emergencias: Patrones de organización e inteligencia colectiva. *Fabworks: Diseño y Fabricación Digital para la arquitectura, Docencia, Investigación y Transferencia*. pp. 26-35. Universidad de Sevilla, Sevilla. ISBN: 978-84-939604-2-1

Articles being processed for publication:

Nadal, A., Pavón, J. & Liébana, O. (2016). Perspectivas para la impresión 3D en la construcción. *Revista Europea de Investigación en Arquitectura*. Accepted, pending publication, January 2017.

Pending articles:

Nadal, A., Pavón, J. & Liébana, O. (2016). Impresión 3D para la construcción: un enfoque basado en el procedimiento y los materiales (3D printing for construction: a procedural and material-based approach). *Informes de la Construcción, Centro Superior de Investigaciones Científicas CSIC*. Pending final review, first review passed with minor comments. Journal Impact Factor (2015): 0.227.

Glossary of terms

3D	Three-Dimensional
3dm	Three-Dimensional Model (Rhinoceros File Format)
ABS	Acrylonitrile Butadiene Styrene
AEC	Architecture, Engineering and Construction
ALM	Additive Layer Manufacturing
AM	Additive Manufacturing
AT	Appropriate Technology
BIM	Building Information Modeling
BREEAM	Building Research Establishment Assessment Method
BREP	Boundari REPresenattion
CAD	Computer Aided Design
CAM	Computer Aided Manufacturing
CC	Contour Crafting
CFF	Composite Filament Fabrication
CNC	Computer Numeric Control
DI	Digital Input
DO	Digital Output
DDM	Direct Digital Manufacturing
DMLS	Direct Metal Laser Sintering
DTC	Direct Torque Control
DXF	Drawing Exchange Format (CAD file format)
EBM	Electron Beam Melting
ESA	European Space Agency
FDM	Fused Deposition Modeling
FFF	Fused Filament Fabrication
GDP	Gross Domestic Product
GIS	Geographic Information System
HDPE	High-Density Polyethylene

HDT	Heat Deflection Temperature
IFC	Industry Foundation Classes
IGES	International Geometry Export Standard (CAD file format)
INO	Arduino Code File Type
IP	Industrial Protection
ISO	International Organization for Standardization
JT	DirectModel files (Siemens' CAD file format)
LDPE	Low Density Polyethylene
LEED	Leadership in Energy and Environmental Design
LOM	Laminated Object Manufacturing
MEP	Mechanical Electrical, and Plumbing
MVP	Minimum Viable Product
NBS	National BIM Standard
NURBS	Non-Uniform Rational Bezier Splines (geometrical topology)
OBJ	Object (Wavefront's CAD format)
OSAT	Open-Source Appropriate Technology
PC	Polycarbonate
PE	Polyethylene
PEI	Polyetherimide
PLA	Polylactic Acid
PMI	Product Manufacturing Information
PP	Poly Propylene
PPSF	Polyphenylsulfone
PPSU	Polyphenylsulfone
PS	Polystyrene
PVA	Polyvinyl Alcohol
PWM	Pulse-Width Modulation
RM	Rapid Manufacturing
RP	Rapid Prototyping
RFF	Reinforced Filament Fusion

SBR	Styrene Butadiene Rubber
SLA	Stereolitography (3D printing method)
SLM	Selective Laser Melting
SLS	Selective Laser Sintering
SM	Substractive Manufacturing
STEP	(CAD file format, see ISO 10303-21:2016)
STL	Stereolitography (CAD file format)
TCP	Tool Center Point
TRL	Technology Readiness Level
UAV	Unmanned Aerial Vehicle
UI	User Interface
UTS	Ultimate Tensile Strength
VSD	Variable-Speed Driver
WASP	World’s Advanced Saving Project
XPS	Extruded Polystyrene foam

References

3D Systems. (2014, May 21). *3D Systems - Project-460 plus 3D printer*. Retrieved from http://www.3dsystems.com/3d-printers/professional/projet-460plus

ABB. (2015, April 14). *White Paper: DTC, A motor control technique for all seasons*. Retrieved from https://library.e.abb.com/public/0e07ab6a2de30809c1257e2d0042db5e/ABB_WhitePaper_DTC_A4_20150414.pdf

ABB. (2016, June 15). *SafeMove App Manual*. Retrieved from http://developercenter.robotstudio.com/BlobProxy/manuals/SafeMoveAppManual/doc72.html

Abrams, S. R., Batchleder, J. S., Farouki, R. T., Korein, J., Korein, J., Mackay, J., . . . Tarabanis, K. (1995, August 9). *European Patent No. EP 0 666 164 A2*.

Agilent, Inc. (2012, January 16). *Practical Temperature Measurements: Application Note 290*. Retrieved from http://cp.literature.agilent.com/litweb/pdf/5965-7822E.pdf

Al-Khatib, I. A., Monou, M., Abu Zahra, A. S., Shaheen, H. Q., & Kassinos, D. (2010). Solid waste characterization, quantification and management practices in developing countries. A case study: Nablus district– Palestine. *Journal of Environmental Management*, 91(5), 1131-1138. doi:10.1016/j.jenvman.2010.01.003

All3DP. (2016, September 22). All3DP. Retrieved from 12 Best STL repair (online) software tools (some are free): all3dp.com/best-stl-file-repair-mesh/

AllPlan Systems, Nemetschek Group. (2016, 11 10). AllPlan 2017. Retrieved from https://www.allplan.com/es.html

American Concrete Institute, ACI. (1998). ACI 212.4R-93 (Reapproved 1998). Guide for the Use of High-Range Water-Reducing Admixtures (Superplasticizers) in *Concrete*, p. 10. United States.

Arcadis. (2016, August 17). International Construction Costs 2016. Retrieved from https://www.arcadis.com/media/0/1/8/%7B01859B81-2914-4914-BBFC-4C9B8A8B616F%7DInternational%20Construction%20Costs%202016.pdf

Arcam. (2015, November 16). EBM® Electron Beam Melting – in the forefront of Additive Manufacturing. Retrieved from http://www.arcam.com/technology/electron-beam-melting/

Ardiny, H., Witwicky, S., & Mondada, F. (2015, June). Autonomous Construction of Separated Artifacts by Mobile Robots Using SLAM and Stigmergy. *Proceedings of the 2015 Conference on Autonomous and Robotic Construction of Infrastructure*, pp. 34-46.

Artifact of Code. (2016, February 10). Robot TCP Description. Retrieved from http://www.artifactofcode.com/blog/tag/technical

Augugliaro, F., Lupashin, S., Hamer, M., Male, C., Hehn, M., Mueller, M., . . . D'Andrea, R. (2014, July 11). The Flight Assembled Architecture installation: Cooperative construction with flying machines. (IEEE, Ed.) *IEEE Control Systems*, 34(4), 46 - 64. doi:10.1109/MCS.2014.2320359

Autodesk, Inc. (2016, 16 10). *Revit. Retrieved from Revit families product home page*: http://www.autodesk.es/products/revit-family/overview

Bader, C., Patrick, W., Kolb, D., Hays, S., Keating, S., Sharma, S., . . . Oxman, N. (2016). Grown, Printed, and Biologically Augmented: An Additively Manufactured Microfluidic Wearable, Functionally Templated for Synthetic Microbes. *3D Printing and Additive Manufacturing*, 3(2), pp.79-89. doi:10.1089/3dp.2016.0027

Bailic, C., Matovic, D., Thamac, T., & Vaja, S. (2011, September). Waste-based composites – Poverty reducing solutions to environmental problems. *Resources, Conservation and Recycling*, 55(11), pp. 973-978.

Barnett, E., & Gosselin, C. (2015, June). Large-Scale 3D Foam Printing With A Cable-Suspended Robot. *Journal of Additive Manufacturing*. doi:10.1016/j.addma.2015.05.001

Batchelder, J., Curtis, H., Goodman, D., Gracer, F., Jackson, R., Koppelman, G. M., & Mackay, J. (1995, March 28). United States Patent No. US 5402351 A.

Batchelder, S., & Crump, S. (1998). *World Patent No. 1998053974 A1*.

Beks, K., Cremer, S., Dewaelheyns, L., Hammann, B., Kohlstrik, S., Poppe, D., . . . Löhden, G. (2012, November 15). *European Patent No. EP 2707198 A1 also published as DE 102011075540 A / WO02012152510A1*.

Bentley Systems, Inc. (2016, 9 23). Design Modeling Software. Retrieved from Product overview: https://www.bentley.com/en/products/product-line/modeling-and-visualization-software/microstation

Bogue, R. (2013). 3D Printing: The dawn of a new era of manufacturing? *Assembly Automation*, 33(4), pp. 307-311. doi:10.1108/AA-06-2013-055

Braungart, M., & McDonough, W. (2003). *Cradle to Cradle: Remaking the way we make things*. New York: North Point Press.

Broek, J., I., H., B., S., A.F., L., Z., R., & J.S.M., V. (2002, April). Free-form thick layer object manufacturing technology for large-sized physical models. *Automation in Construction*, 11(3), pp. 335-347. doi:10.1016/S0926-5805(00)00108-4

BuildingSmart. (2017, 01 26). International home of Open BIM. Retrieved from buildingsmart.org

Burry M. (2002, April). Rapid Prototyping, CAD/CAM and human factors. *Automation in Construction*, 11(3), pp. 313-333.

Buswell, R. A., Soar, R., Gibb, A. G., & Thorpe, T. (2005). The potential of Freeform Construction processes. *Proceedings of Solid Freeform Fabrication symposium*, (pp. 505-512). Austin, Texas, US.

Buswell, R., Soar, R., Gibb, A., & T., T. (2007, March). Freeform construction: mega-scale rapid manufacturing for construction. *Automation in Construction*, 16(2), pp. 224-231. doi:10.1016/j.autcon.2006.05.002

Cambashi. (2010, July 23). Specialist AEC Suppliers Lead the Way in Europe. Retrieved July 28, 2012, from *European software suppliers lead the way for Europe's architecture and construction sector designers*: http://www.cambashi.com/specialist-aec-suppliers-in-europe-lead-the-way

Campbell, T., Tibbits, S., & Garret, B. (2014, May). *Atlantic Council. The Next Wave: 4D Printing, Programming the material world*. Retrieved from http://www.atlanticcouncil.org/images/publications/The_Next_Wave_4D_Printing_Programming_the_Material_World.pdf

Campbell, T., Williams, C., Ivanova, O., & Garret, B. (2016, October). *Atlantic Council, strategic foresight report: Could 3D Printing Change the World? Technologies, Potential, and Implications of Additive Manufacturing*. Retrieved from http://www.atlanticcouncil.org/images/files/publication_pdfs/403/101711_ACUS_3DPrinting.PDF

Castañeda, E., Lauret, B., Lirola, J., & Ovando, G. (2015). Free-form architectural envelopes: Digital processes opportunities of industrial production at a reasonable price. *Journal of Façade Design and Engineering*, 3(1), pp. 1-13. doi:10.3233/FDE-150031

Catts, O. a. (2006). Towards a New Class Of Being: The Extended Body (Extract from ISEA06/Zero1 Symposium). Intelligent Agent, 06(02), pp. 01-07.

Catts, O., & Zurr, I. (2002, Augus). Growing Semi-Living Sculptures: The Tissue Culture & Art Project. *Leonardo Magazine*, 35(4), pp. 365-370.

Ceresana. (2011, December). *Market Study: Bioplastics* (3rd ed.). Constance, Germany: Ceresana.

Chi, H., Wang, X., & Jiao, Y. (2015). BIM-Enabled Structural Design: Impacts and Future Developments in Structural Modelling, Analysis and Optimisation Processes. *Archives of Computational Methods in Engineering*, 22(1), pp. 135-151. doi:doi: 10.1007/s11831-014-9127-7

Chiarugi, M., Dini, E., & Nannini, R. (2007, January 11). *World Patent No. WO2006100556 A3 also publised as US20080148683 / EP1868793A2 / CN101146666A*.

Choi, H. S., Han, C. S., Lee, Y., & Lee, S. H. (2005). Development of hybrid robot for construction works with pneumatic actuator. *Automation in Construction*, 14(4), 452-459. doi:10.1016/S0926580504001219

Chowdry, A. (2015, June 17). *These 3-D Printers are going to autonomously build a bridge in Amsterdam*. Retrieved from Forbes (online version): http://www.forbes.com/sites/amitchowdhry/2015/06/17/3d-printer-bridge/#4333b47921f9

Crump, S. (1992, June 9). *United States Patent No. US 5121329*.

Del Solar, P., & Del Río Merino, M. (2015, April-June). Metodología para seleccionar oportunidades de mejora continua en promociones de viviendas. *Informes de la Construcción*, 67,538,e073, pp. 1-9. doi:10.3989/ic.13.142

Del Solar, P., Del Río, M., Villoria, P., & Nadal, A. (2016, April). Analysis of Recurrent Defects in the Execution of Ceramic Coatings Cladding in Building Construction. *Journal of Construction Engineering and Management*, 142(4). doi:10:1061/(ASCE)CO.1943-7862.0001075

Dezeen. (2012, October 23). Protohouse by Softkill Design. Retrieved May 26, 2014, from http://www.dezeen.com/2012/10/23/protohouse-by-softkill-design/

Dimitrov, D., Schreve, N., & de Beer, N. (2006). Advances in three dimensional printing – state of the art and future perspectives. *Rapid Prototyping Journal*, 12(3), 136-147. doi:10.1108/13552540610670717

Dini, E. (2016, January 24). *D-Shape*. Retrieved from http://d-shape.com/

Dominguez, I. A., Romero, L., Espinosa, M. M., & Dominguez, M. (2012, November). Impresión 3D de maquetas y prototipos en arquitectura y construcción. *Revista de la construcción*, 12(2), pp. 39-53. doi:10.4067/S0718-915X2013000200004

Douglass, B. L., & Douglass, C. R. (2015, February 5). *United States Patent No. US 2015/0037446A1*.

Duro Royo, J., Mogas, L., & Oxman, N. (2016, March 17). *United States Patent No. US 20160075089A1*.

DUS Architects. (2016, January 26). *3D Print Canal House: Worlds' first 3D Printed Canal House built at an expo-site in Amsterdam*. Retrieved from http://www.dusarchitects.com/projects.php?categorieid=housing

Egan, J. (1998, November 01). *Rethinking construction - The Egan Report*. Retrieved from Constructing excellence: constructingexcellence.org.uk/rethinking-construction-the-egan-report/

Erdogdu, S. (2005). Effect of retempering with superplasticizer admixtures on slump loss and compressive strength of concrete subjected to prolonged mixing. *Cement and Concrete Research*, 35, pp. 907-912.

ETH Zürich. (2014, May 22). *Flight Assembled Architecture*. Retrieved from http://www.idsc.ethz.ch/research-dandrea/research-projects/archive/flying-machine-enabled-construction.html

ETH Zürich. (2015). *Gramazio Kohler Research: Extruder Structures*. Retrieved March 30, 2016, from http://gramaziokohler.arch.ethz.ch/web/e/lehre/284.html

ETH Zürich with Gramazio & Kohler. (2008). *R.O.B*. Zurich, Switzerland.

ETH Zürich with SEC Singapore. (2012-2016). *Space Frame 3D printing*. Mesh Mold. Zürich, Switzerland.

European Commission. (2013, July 4). *La Comisión Europea lanza una gran coalición para la creación de empleos en la economía digital*. Retrieved July 8, 2015, from http://europa.eu/rapid/press-release_IP-13-182_es.htm

European Construction Technology Platform (ECTP). (2005, December 23). *Strategic Research Sgenda for the European Construction Sector: Achieving a sustainable and competitive construction sector by 2030*. (E. C. (ECTP), Ed.) Retrieved from www.ectp.org

European Federation of Building and Woodworkers (EFBWW). (2009, July). *EFBWW Study: Wages in Construction*. Retrieved December 23, 2005, from www.efbww.org

European Spatial Agency. (2013, January 31). *Building a Lunar Base with 3D Printing*. Retrieved April 23, 2014, from http://m.esa.int/Our_Activities/Space_Engineering_Technology/Building_a_lunar_base_with_3D_printing

Eurostat. (2016, April). *Wages and Labor Costs*. Retrieved May 30, 2016, from http://ec.europa.eu/eurostat/statistics-explained/index.php/Wages_and_labour_costs_-_Further_Eurostat_information

Eurostat. (2016, April). *Wages and Labor Costs: Estimated Hourly Labor Costs*, 2015. Retrieved May 2, 2016, from http://ec.europa.eu/eurostat/statistics-explained/index.php/Wages_and_labour_costs

Fairs, M. (2013, March 27). *Des Hi-Res: The Race begins to print the first 3D printed House*. pp. 28-35. London: Dezeen.

Feng, L., & Yuhong, L. (2014). Study on the Status Quo and Problems of 3D Printed Buildings in China. *Global Journal of Human-Social Science*, 15(5).

Feygin, M., Schkolnik, A., Diamond, M. N., & Dvorskly, E. (1998, March 24). *United States Patent No. US 5730817 A.*

Freedom Of Creation. (2011, March 31). *Freedom Of Creation Develops Tree-D printing in Wood.* Retrieved April 1, 2011, from http://www.3dsystems.com/blog/foc/freedom-of-creation-develops-tree-d-printing

Gambao, E., Balaguer, C., & F., G. (2000, September). Robot assembly system for computer integrated construction. *Automation in Construction*, 9(5-6), pp. 479-487. doi:10.1016/S0926-5805(00)00059-5

Gibb, A., & Pendlebury, M. (2003). *Standardisation and pre-assembly: project tool kit* (2nd ed.). London: Construction Industry Research & Information Association (CIRIA).

Goldman Sachs. (2013). 2*013 Annual Report. 25 Ways We Saw the World Change in 2013: Emerging Trends, Transformative Impacts, and how we are helping our clients around the world drive and leverage them*. Retrieved November 10, 2015, from http://www.goldmansachs.com/investor-relations/financials/archived/annual-reports/2013-annual-report-files/annual-report-2013.pdf

Graphisoft SE, Nemetschek Group. (2016, 9 14). *Archicad*. Retrieved from http://www.graphisoft.com/archicad/

Guerrero, A., & Espinosa, M. M. (2014). Avances en RepRap: Impresión 3D de código abierto. *DYNA*, 89(1), pp. 34-38. doi:10.6036/5659

Guthrie, P., Coventry, S., Woolveridge, C., Hillier, S., & Collins, R. (1999). *The reclaimed and recycled construction materials handbook*. London: Construction Industry Research & Information Association (CIRIA).

HAL Robotics Ltd. (2015). Hal Robotics. Retrieved January 24, 2016, from http://www.hal-robotics.com/

Hansmeyer, M., & Dillenburger, B. (2014, August 13). *Digital Grothesque*. Retrieved from http://www.digital-grotesque.com/fabrication_images.html?screenSize=1&color=1#2

Helm, V., Selen, E., Gramazio, F., & Kohler, M. (2012). Mobile robotic fabrication on construction sites: DimRob. *2012 IEEE/RSJ International Conference on Intelligent Robots and Systems*. Deajeon, Korea: IEEE. doi:10.1109/IROS.2012.6385617

Hermes, F., Bernhardt, S., Poppe, D., Schmidt, G., Pridöhl, M., & Löhden, G. (2012, October 24). E*uropean Patent No. EP 2514775 A1*.

Hinczewski, C., Corbel, S., & Chartier, T. (1998). Stereolithography for the fabrication of ceramic three-dimensional parts. *Rapid Prototyping Journal*, 4(3), pp. 104-111. doi:10.1108/13552549810222867

Hongzhi, Z., & Quan, W. (2013, October 2). *China Patent No. CN 103332023 A*. Retrieved from google.com/patents/CN103332023A?cl=en

Hosmer, K. (2013, July 2). *3D-Printing Technology Produces Modern Exoskeletal Cast*. Retrieved July 5, 2013, from http://www.mymodernmet.com/profiles/blogs/jake-evill-exoskeletal-cortex-cast

Hull A., C. W. (1986, March 11). *United States Patent No. US 4575330 A.*

Joachim, M., Tan, E., Medvedik, O., & Aiolova, M. (2011). *Terreform1: In Vitro Meat Habitat*. Retrieved September 23, 2012, from http://www.terreform.org/projects_habitat_meat.html

Khoshnevis, B. (2004, January). Automated construction by Contour Crafting - Related robotics and information sciences. *Automation in Construction Special Issue: The Best of ISARC 2002*, 13(1), pp. 5-19. doi:10.1016/j.autcon.2003.08.012

Khoshnevis, B. (2010, January 5). *United States Patent No. US 7641461 B2*.

Khoshnevis, B. (2010, October 19). *United States Patent No. US 7814937 B2*.

Khoshnevis, B., Bukkapatnam, S., Kwon, H., & Saito, J. (2001). Experimental investigation of contour crafting using ceramics materials. *Journal of Rapid Prototyping*, 7(1), pp. 22-41. doi:10.1109/100.956812

Khoshnevis, B., Carlson, A., Leach, N., & Thangavelu, M. (2012, October). *Contour Crafting Simulation Plan for Lunar Settlement Infrastructure Build-Up. NIAC Phase I Final Project Report*. Retrieved from http://www.nasa.gov/pdf/716069main_Khoshnevis_2011_PhI_Contour_Crafting.pdf

Khoshnevis, B., Hwang, B., Yao, K. T., & Yeh, Z. (2006). Mega-scale fabrication by Contour Crafting. I*nternational Journal of Industrial and Systems Engineering*, 1, pp. 301-320.

Khoshnevis, B., Russel, R., Kwon, H., & Bukkapatnam, S. (2001, September). Crafting Large Prototypes: Contour crafting utilizes computer-aided ancient sculpting techniques for fabrication of large components. I*EEE Robotics & Automation Magazin*e, 8(3), pp. 33-42.

Klein, J., Franchin, G., Stern, M., Kayser, M., Inamura, C., Dave, S., . . . Houk, P. (2015, October 29). *United States Patent No. US 2015030307385*.

Klein, J., M., S., Kayser, M., Inamura, C., G., F., Dave, S., . . . Oxman, N. (2015). Additive Manufacturing of Optically Transparent Glass. *3D Printing and Additive Manufacturing*, 2(3), pp. 92-105. doi:10.1089/3dp.2015.0021

Krassenstein, B. (2014, December 12). *3dprint.com*. Retrieved from https://3dprint.com/29913/viscotec-dosage-paste-extruder/

Kuntze, H., Hirsch, U., Jacubasch, A., F., E., & Goller, B. (1995, March). On the dynamic control of a hydraulic large range robot for construction applications. *Automation in Construction*, 4(1), pp. 61-73. doi:10.1016/0926-5805(94)00036-M

Kvan, T., & Kolarevic, B. (2002, April). Rapid Prototyping and its application in architectural design. *Automation in Construction*, 11(3), pp. 277-278. doi:10.1016/S0926-5805(00)00110-2

Kwon, H. (2002, August). Experimentation and Analysis of Contour Crafting Process Using Uncured Ceramic Materials. *Dissertation Presented to the Faculty of the graduate School University of Southern California in Partial Fulfillment of the requirements for the Degree of Doctor of Philosophy*.

Latham, M. (1994). Constructing the Team: Joint Review of Procurement and Contractual Arrangements. UK, *Department of the Environment*. London: HMSO.

Law, A. (2014). *Simulation modeling and analysis* (5 ed.). Boston: Mac Graw Hill.

Le, T. T., Austin, S. A., Lim, S., Buswell, R. A., Gibb, A. G., & Thorpe, T. (2012, January 19). Mix Design and fresh properties for high-performance printing concrete. *Materials and Structures*, 45, pp. 1221-1232. doi:10.1617/s11527-012-9828-z

Le, T. T., Austin, S. A., Lim, S., Buswell, R. A., Law, R., Gibb, A. G., & Thorpe, T. (2012). Hardened properties of high-performance printing concrete. *Cement and concrete research*, 42(3), pp. 558-566. doi:10.1016/j.cemconres.2011.12.003

LeManager, S., Hiltner, K., & Shewry, T. (2012). *Environmental Criticism for the Twenty First Century*. (S. LeManager, T. Shewry, & K. Hiltner, Eds.) London: Routledge Publishers.

Liébana, O., & Nadal, A. (2016). Digital Crafts, 3D Printing In Architecture. Arquitectura Viva. *Arquitectura Viva: Soluciones Españolas*(187.9), pp. 71-75.

Lim, S., Buswell, R., Austin, S., Gibb, A., & Thorpe, T. (2012, January). Developments in Construction-Scale additive manufacturing processes. *Automation in Construction*, 21, 262-268. doi:10.1016-S0926580511001221

Lipson, H. (2007). Printable 3D Models for Customized Hands-on Education. *Mass Customization and Personalization* (MCPC) 2007. Cambridge, Massachusetts, USA.

Lorenc, S., Handlon, B., & Bernold, L. (2000, May). Development of a robotic bridge maintenance system. *Automation in Construction*, 9(3), pp. 251-258.

Lott-Lavigna, R. (2015, September 21). *Cities: Watch this giant 3D printer build a house*. Retrieved September 23, 2015, from http://www.wired.co.uk/article/giant-3d-printer-builds-houses

Lovell, H. (2003). *Modern methods of house building*. Postnote, UK Parliament, Parliamentary Office of Science and Technology, London. Retrieved December 2009, from http://www.parliament.uk/documents/post/postpn209.pdf

Luebkman, C. (2015). 2050: *Designing Our Tomorrow*. 111 River Street, New Jersey, New York, US: Wiley.

Makerbot Industries, Ltd. (2014). *PLA and ABS Strength Data (ASTM D256, D695, D638, D790)*. Retrieved September 27, 2015, from https://eu.makerbot.com/fileadmin/Inhalte/Support/Datenblatt/MakerBot_R__PLA_and_ABS_Strength_Data.pdf

Malaeb, Z., Hachem, H., Tourbah, A., Maalouf, T., El Zarwi, N., & Hamzeh, F. (2015, June). 3D Concrete Printing: Machine and Mix Design. *International Journal of Civil Engineering and Technology*, 6(6), pp. 14-22.

Martin, D. (2014, April 23). *Top43DPrinting*. Retrieved May 3, 2014, from Highly innovative, ultra durable 3D printed cast bags A'Design Award: http://top43dprinting.com/highly-innovative-ultra-durable-3d-printed-cast-bags-adesign-award/

McNeel & Associates. (2016, 10 18). Rhinoceros. Retrieved from Home page: http://www.rhino3d.com/en/

Meiners, W., Wissenbach, K. D., & Gasser, A. D. (1998, February 12). *Germany Patent No. DE 19649865 C1*.

Ministerio de Fomento. (2008, July 18). Real Decreto 1247/2008, de 18 de Julio, por el que se aprueba la instrucción de hormigón estructural (EHE-08), Anexo 2, Relación de normas UNE recogidas en la EHE-08. Gobierno de España. *Boletin Oficial del Estado*. Madrid, Madrid, España: Gobierno de España.

Morin, V., Tenoudjia, F. C., Feylessoufib, A., & Richard, P. (2001). Superplasticizer effects on setting and structuration mechanisms of ultrahigh-performance concrete. *Cement and Concrete* Research, 31, pp. 63 -71.

Morris, I. (2010). *Why the West rules – For now: The Patterns of History, and What They Reveal About the Future* (1 ed.). Farrar, Strauss, and Giroux. Retrieved October 12, 2010

Motta, J. (2005). An Investigation of singularities in robot kinematic chains aiming at building calibration models for off-line programming. *Journal of the Brazilian Society of Mechanical Sciences and Engineering*, On-line version, 27(2), pp. 1-5. doi:10.1590-S1678-58782005000200013

MX3D. (2015, October 16). *Mx3D Bridge*. Retrieved November 24, 2015, from http://mx3d.com/projects/bridge

Nestle, N., Hermant, M.-C., & Schmidt, K. (2016). *World Patent No. WO 2016/012486 A1 also filed as US 20160024293*.

Niehe, P. (2014, June 05). *ARUP*. Retrieved July 06, 2014, from Construction steelwork makes its 3D printing premiere: Arup engineers are pushing the boundaries of 3D printing to take the technology firmly into the realm of real-world, hard hat construction: http://www.arup.com/news/2014_06_june/05_june_construction_steelwork_makes_3d_printing_premiere

Otto, F. (1995). *Finding Form: Towards an Architecture of The Minimal* (English ed.). (I. Meissner, Trans.) Stuttgart, Fellbach, Germany: Axel Menges GmbH.

Oxman, N. (2007). Get Real: Towards Performance Driven Computational Geometry. *International Journal of Architectural Computing* (IJAC), 4(5), pp. 663-684. doi:10.1260/147807707783600771

Oxman, N. (2011, April 7). *United States Patent No. US 20110079936*.

Oxman, N., & Rosenberg, J. L. (2007). Material-based Design Computation: An Inquiry into Digital Simulation of Physical Material Properties as Design Generators. *International Journal of Architectural Computing* (IJAC), 5(1), pp. 26-44.

Panetto, H. (2007). Towards a classification framework for interoperability of enterprise applications. *International Journal of Computer Integrated Manufacturing*, 20(8), pp. 727-740. doi:10.1080-0951192060099641

Parvin, M., & Williams, J. (1975, November). The effect of temperature on the fracture of polycarbonate. *Journal of Material Science*, 10(11), pp. 1883-1888. doi:10.1007/BF00754478

Patterson, N., & Harris, K. (2015, February 3). *United States Patent No. US 8944802 B2 | US 20140210137*.

Pax, C. .. (2015, October 27). *United States Patent No. US 9168699 B2*.

Payne, A. (2011). A Five-Axis Robotic Motion Controller for Designers. *ACADIA 2011 Annual Conference: Integration Through Computation* (13th-16th October), (pp. pp. 1-9). Calgary/Banff.

Pearce, J. M., & Mushtaq, U. (2009). Overcoming Technical Constraints for Obtaining Sustainable Development with Open Source Appropriate Technology. *Science and Technology for Humanity* (TIC-STH), IEEE, pp. 814-820.

Pearce, J., Morris Blair, C., Laciak, K., Andrews, R., Nosrat, A., & Zelenika-Zovko, I. (2010). 3-D Printing of Open Source Appropriate Technologies for Self-Directed Sustainable Development. *Journal of Sustainable Development*, 5(4), pp. 17-29.

Pegna, J. (1997, February). Exploratory investigation of solid freeform construction,. *Automation in construction*, 5(5), pp. 427-437.

Pettis, N., Steiner, R., Schmehl, P., & Pax, C. (2015, October 27). *United States Patent No. US 9169968 B2*.

Philippe, F., & Culot, M. (2009). Household solid waste generation and characteristics in Cape Haitian city, Republic of Haiti. *Resources, Conservation and Recycling*, 54(2), pp. 73-78. doi:10.1016/j.resconrec.2009.06.009

Piker, D. (2014). *Lobster: Inverse Kinematics for Robotic Arms*. Retrieved October 10, 2014, from http://api.ning.com/files/KRgE1yt2kgG2IF9H8sre4CWfIDL9ytv5WvVn54zdOx6HE84gDordaHzo0jqwP-Qhry7MyRQ4IQxY1p3cIkqEDj1FAVVR2Xg0/Lobster_IK.pdf

Porter, S., Christopher, W., Lloyd, R., Williams, I., & Banks, S. (2003, September 11). *United States Patent No. US 20030171841 A1*.

Pwder. (2012, August 07). *Pwder 3D Printer*. Retrieved October 20, 2012, from http://pwdr.github.io/

Reas, C., & Fry, B. (2014). *Processing: A Programming Handbook for Visual Designers and Artists* (Second ed.). Boston, Massachussets, US: The MIT Press.

Rebolj, D., Fischer, M., & Endy, D. (2011). Can we grow buildings? Concepts and requirements for automated nano- to meter-scale building. *Advanced Engineering Informatics*, 25(2), pp. 390-398. doi:10.1016/j.aei.2010.08.006

Reintjes, J. (1991). Numerical Control: Making a New Technology, *Oxford Series on Advanced Manufacturing*, Book 9. Oxford: Oxford University Press.

Rezeyat, M. (2015, May 21). *United States Patent Patent No. US 20150142152 A1*.

Robotic Business Review (RBR). (2016). *Companies*. (I. EH Publishing, Editor) Retrieved March 11, 2016, from http://www.roboticsbusinessreview.com/companies/category/top_50/list

Robots.IO. (2015, September 2). *Robots IO*. Retrieved January 24, 2016, from https://robots.io/wp/

Ryder, G., Ion, B., Green, G., Harrison, D., & Wood, B. (2002). Rapid Design and Manufacture Tools in architecture. A*utomation in Construction*, 11(3), pp. 279-290. doi:10.1016/S0926-5805(00)00111-4

Saber, O., Abyaneh, S., & Zohoor, H. (2010). A cable-suspended robot with a novel cable based end effector. *ASME 2010 10th Biennial Conference on Engineering Systems Design and Analysis*. 3, pp. pp. 799-808. Istambul, Turkey: ASME. doi:10.1115/ESDA2010-25312

Sass, L., & Oxman, R. (2006). Materializing Design: The Implications of Rapid Prototyping in Digital Design. *Design Studies*, 27, pp. 325-335. doi:10.1016/j.destud.2005.11.009

Schodek, D., Bechthold, M., Griggs, K., Ka, K., & Steinberg, M. (2005). *Digital design and manufacturing: CAD/CAM applications in architecture and design* (Fist ed.). Hoboken, New Jersey: Wiley and Sons.

Schoffer, F. (2016, May 15). *Tech Crunch: How expiring patents are ushering in the next generation of 3D printing*. Retrieved July 17, 2016, from https://techcrunch.com/2016/05/15/how-expiring-patents-are-ushering-in-the-next-generation-of-3d-printing/

Schwartz, T., Gobin, T., & Bartlett School of Architecture. (2013, March 4-6). *The Bartlett Nexorade and Reciprocal Structures*. Retrieved May 23, 2014, from http://thibaultschwartz.com/?g1_work=the-bartlett-nexorade-and-reciprocal-structures

Simondetti, A. (2002). Computer-generated physical modelling in the early stages of the design process. *Automation in Construction*, 11(3), pp. 303-311. doi:10.1016/S0926-5805(00)00105-9

Slic3r. (2015, June 20). *Slic3r, G-Code Generator for 3D Printers*. Retrieved from slic3r.org

Smith, R. Y., Smellie, A., & Mehta, N. (2014, November 13). *United States Patent No. US 201400336807 A1*.

Spanish National Statistics Institute (INE). (2013). *National Index of Construction Wages (Base 1980, Data Collected from Spanish Ministry of Industry)*. (INE, Compiler) Madrid, Madrid, Spain. Retrieved August 13, 2016, from http://www.ine.es/jaxiT3/Tabla.htm?t=8377

Spanish National Statistics Institute (INE). (2016). *National Index of Prices of Commodities and Construction Labor (Base December 2011), Data collected from Spanish Ministry of Industry.* (INE, Compiler) Madrid, Madrid, Spain. Retrieved August 14, 2016, from http://www.ine.es/jaxiT3/Datos.htm?t=8381

Stratasys, Inc. (1992). Rapid Prototyping Using FDM: A Fast, Precise, Safe Technology. *Solid Freeform Fabrication Symposium*, August 3-5., (pp. pp. 1-8). Austin, Texas.

Strauss, H. (2013). *AM Envelope: The potential of Additive Manufacturing for façade construction*. Delft, The Netherlands: TU Delft. Retrieved from books.bk.tudelft.nl/index.php/press/catalog/download/25/30/38-1

Strauss, H. (2013). AM Envelope: The potential of Additive Manufacturing for façade construction. *Architecture and The Built Environment*, 3(1), pp. 1-19. doi:10.7480/abe.2013.1

Strauss, H., & Knaack, U. (2016). The Potential of 3D printed parts for the building envelope. *Journal of Façade Design and Engineering*, preprint, pp. 1-12. doi:10.3233/FDE-150042

Sung-Hoon, A., Montero, M., Odell, D., Roundy, S., & Wright, P. K. (2002). Anisotropic material properties of fused deposition modeling ABS. *Rapid Prototyping Journal*, 8(4), pp. 248-257. doi:10.1108-13552540210441166

Swanson, W. J. (2015, December 22). *Patent No. US 9216544 B2*.

Swanson, W. J., Batchedler, J., Johnson, K., Hjelsand, T., & Comb, J. W. (2015, October 27). *United States Patent No. US 9168685 B2*.

Swanson, W. J., Batchelder, J. S., & Johnson, K. C. (2014, March 4). *United States Patent No. US 8663533 B2*.

Swanson, W. J., Batchelder, J., Johnson, K., Hjelsand, T., & Comb, J. (2014, February 11). *United States Patent Patent No. US 8647102 B2*.

Takahashi, H., Yamaguchi, S., & Takeuchi, Y. (2008, March 5). *European Patent No. EP 1 895 375 A1 also published as WO02006137120A1*.

Technavio. (2016, July 27). *Global Research and Development Spending in the Robotics Industry 2016-2020*. Retrieved August 29, 2016, from http://www.technavio.com/report/global-robotics-r-and-d-spending-robotics-market

The Concrete Centre, Mineral Products Association (MPA). (2005). *High performance buildings: Using Tunnel Form Concrete Construction*. Camberly, Surrey, UK.

The OCCS Development Committee. (2017, 01 27). *OmniClass*. Retrieved from A Stretegy for Classifying the Built Environment: www.omniclass.org/contributors.asp

Tibaut, A., Rebolj, D., & Nekrep Perc, M. (2014, January 10). Interoperability Requirements for automated manufacturing systems in construction. *Journal of Intelligent Manufacturing*, 251-262. doi:doi: 10.1007/s10845-013-0862-7, JIMS -1976R2

Torres, R. (2016, April). D*iseño de Hormigón para Impresión 3D*. Masters Thesis. Valencia, Comunidad Valenciana, Spain: Polytechnic University of Valencia.

UK Cement Admixtures Association (CAA). (2016, February 2). Admixture Technical Sheet – ATS 2: Superplasticising / High range water reducing. *Cement Admixtures Association Technical Sheets*, pp. 1-6.

UK Intellectual Property Office. (2013, November). *3D Printing: A patent Overview*. United Kingdom. Retrieved August 18, 2016, from https://www.gov.uk/government/uploads/system/uploads/attachment_data/file/445232/3D_Printing_Report.pdf

Ultimaker. (2017, 01 27). *Cura Software*. Retrieved from https://ultimaker.com/en/products/cura-software

Unión General de Trabajadores (UGT) and Metal Construcción y Afines Federación de Industria. (2014). *Informe de Siniestralidad Laboral Año 2014*. Madrid. Retrieved March 23, 2016, from http://mcaugt.org/documentos/0/doc14072.pdf

University of Southern California. (2014). *Contour Crafting: Robotic Construction System*. Retrieved November 23, 2014, from http://www.contourcrafting.org

Vergnes, B., Vincent, M., & Haudin, J. M. (2012). Properties of Polymers. In O. S. Carneiro, & J. M. Nóbrega, *Design of Extrusion Forming Tools* (p. 292). Shawbury, Shrosphire, UK: Smithers Rapra Technology Ltd.

WASP World's Advanced Saving Project. (2015, June 9). *La BigDelta sperimenta con CasaClima: risultati e riflessioni*. Retrieved September 22, 2015, from http://www.wasproject.it/w/la-bigdelta-sperimenta-con-casaclima-risultati-e-riflessioni/

Wei Hsiang, L., & Chung-I, C. (2008, October 23). *United States Patent No. US 20080260918 A1*.

Werner, L. (1995, March 1). Experiences with the construction of a building assembly robot. *Automation in Construction*, 4(3), pp. 45-60. doi:10.1016/0926-5805(94)00034-K

Williams, R., Albus, J., & Bostelman, R. (2004, May). Self-contained automated construction deposition system. *Automation in Construction*, 13(3), pp. 393-407. doi:10.1016/j.autcon.2004.01.001

Wired. (2013, 11 07). *Wired*. Retrieved from A mind-blowing dome made of 6500 computer-guided silkworms: https://www.wired.com/2013/07/your-next-3-d-printer-might-be-filled-with-worms/

Wohlers, T. (2001). *Wohlers Report: Rapid Prototyping & Tooling State of the Industry Annual WorldWide Progress Report*. (W. Associates, Ed.) Retrieved February 21, 2012, from https://wohlersassociates.com/2001-Executive-Summary.pdf

Wohlers, T. (2009). *Wohlers Report 2009: Additive Manufacturing State of The Industry*. Retrieved from https://wohlersassociates.com/2009report.htm

Wohlers, T. (2016). *Wohlers Annual Worldwide Progress Report 2016: 3D Printing and Additive Manufacturing State of the Industry*. Fort Collins, Colorado, US: Wohlers Inc.

World Economic Forum (WEF) with The Boston Consulting Group. (2016, May). *Shaping the future of construction: a breakthrough in Mindset and Technology*. Industry Agenda, World Economic Forum. Retrieved June 3, 2016, from http://www3.weforum.org/docs/WEF_Shaping_the_Future_of_Construction_full_report__.pdf

Wright, P. (2001). *21st Century Manufacturing*. Upper Saddle River, NJ: Prentice Hall.

Wu, A. (2014, January 23). *United States Patent No. US 2014/0025190 A1*.

Wu, P., Wang, J., & Wang, X. (2016, April). A critical review of the use of 3-D printing in the construction industry. *Automation in Construction*, 68, pp. 21-31. doi:0.1016/1.autam.2016.04.005

Yamazakia, Y., & Maeda, J. (1998, February). The SMART system: an integrated application of automation and information technology in production process. *Computers in Industry*, 35(1), pp. 87-99. doi:10.1016/s0166-3615(97)00086-9

Zhang, Y., & Bernard, A. (2014). AM Feature and Knowledge Based Process Planning for Additive Manufacturing in Multiple Parts Production Context. *Proceedings of 25th Annual International Solid Freeform Fabrication Symposium*, (pp. pp. 1259–1276). Austin, Texas.

Zhang, Y., Bernard, A., Harik, R., & Kanunakaran, K. (2015, February 28). Build Orientation Optimization for Multi-Part Production in Additive Manufacturing. *Journal of Intelligent Manufacturing*, pp. 1-15. doi:10.1007/s10845-015-1057-1

Zimmerman, A., Walczyk, D., Crump, S., & Batchelder, J. (2015, December 22). *United States Patent No. US 9215882 B2*.